

**Some pages of this thesis may have been removed for copyright restrictions.**

If you have discovered material in Aston Research Explorer which is unlawful e.g. breaches copyright, (either yours or that of a third party) or any other law, including but not limited to those relating to patent, trademark, confidentiality, data protection, obscenity, defamation, libel, then please read our [Takedown policy](#) and contact the service immediately (openaccess@aston.ac.uk)

# The Role of Amyloid Precursor Protein in Neuronal and Non-neuronal Cell Lines

Miss Erin Hsueh Ying Tse

Doctor of Philosophy

ASTON UNIVERSITY

April 2015

© Miss Erin Hsueh Ying Tse, April 2015 asserts her moral right to be identified as the author of this thesis

The copy of the thesis has been supplied on condition that anyone who consults it is understood to recognise that its copyright rests with its author and that no quotation from the thesis and no information derived from it may be published without appropriate permission or acknowledgement.

## The Role of Amyloid Precursor Protein in Neuronal and Non-neuronal Cell Lines

Erin Hsueh Ying Tse

Doctor of Philosophy

April 2015

### **Thesis Summary**

Models of Alzheimer's disease (AD) have provided useful insights into the pathogenesis and mechanistic pathways that lead to its development. One emerging idea about AD is that it may be described as a hypometabolic disorder due to the reduction of glucose uptake in AD brains. Inappropriate processing of Amyloid Precursor Protein (APP) is considered central to the initiation and progression of the disease. Although the exact role of APP misprocessing is unclear, it may play a role in neuronal metabolism before the onset of neurodegeneration.

To investigate the potential role of APP in neuronal metabolism, the SHSY5Y neuroblastoma cell line was used to generate cell lines that stably overexpress wild type APP695 or express Swedish mutated-APP observed in familial AD (FAD), both under the control of the neuronal promoter, Synapsin I. The effects of APP on glucose uptake, cellular stress and energy homeostasis were studied extensively. It was found that APP-overexpressing cells exhibited decreased glucose uptake with changes in basal oxygen consumption in comparison to control cell lines.

Similar studies were also performed in fibroblasts taken from FAD patients compared with control fibroblasts. Previous studies found FAD-derived fibroblasts displayed altered metabolic profiles, calcium homeostasis and oxidative stress when compared to controls. As such, in this study fibroblasts were studied in terms of their ability to metabolise glucose and their mitochondrial function. Results show that FAD-derived fibroblasts demonstrate no differences in mitochondrial function, or response to oxidative stress compared to control fibroblasts. However, control fibroblasts treated with A $\beta$ 1-42 demonstrated changes in glucose uptake. This study highlights the importance of APP expression within non-neuronal cell lines, suggesting that whilst AD is considered a brain-associated disorder, peripheral effects in non-neuronal cell types should also be considered when studying the effects of A $\beta$  on metabolism.

Key words: Alzheimer's disease, glucose, mitochondria, SHSY5Y cells, human dermal fibroblasts

## **Acknowledgements**

I would first like to thank my supervisor Dr Eric Hill for his patience, kindness and sharing his enthusiasm for science, which has let me develop into an independent scientist. I am especially grateful to Dr David Nagel, for his expertise, friendship and wisdom. I would also like to thank Dr John O'Neil and Dr Marta Tarczyluk for her friendship and advice. Thanks also to Professor Michael Coleman and Dr Rhein Parri for their guidance.

I would like to thank Derek Wong, who has been considerate, kind, patient, knows how to make me laugh, and can calm me down when I feel anxious. He has shown me the world and how to appreciate good food and the little things in life. I also thank my friends, including Karan Rana and Saima Begum who understand all too well the hardships and stress that comes with a PhD.

I will always be thankful to my loving family, for their love and support. Most of all, I would like to thank my parents for supporting me during this PhD, being understanding and picking me up when I fall.

## List of Contents

Aston University.....	2
Thesis Summary.....	2
Acknowledgements.....	3
List of Contents.....	4
List of Abbreviations .....	9
List of Tables and Figures.....	12
Chapter 1: Introduction to Alzheimer’s disease .....	17
1.1 Overview of Alzheimer’s disease .....	17
1.2. Symptoms and disease pathology .....	18
1.2.1 Amyloidogenesis.....	22
1.2.1.2 APP processing .....	26
1.2.2 The non-amyloidogenic pathway.....	29
1.2.3 Neurofibrillary degeneration (NFD) .....	31
1.3 The Causes of AD .....	33
1.3.1 EOAD .....	35
1.3.2 Sporadic AD.....	35
1.3.3 The amyloid hypothesis .....	39
1.4 Pathogenic mechanisms of Amyloid .....	40
1.4.1 Calcium homeostasis.....	41
1.4.2 A $\beta$ -induced excitotoxicity .....	41
1.4.3 Mitoenergetics and oxidative stress .....	43
1.5 The physiological role of APP .....	47
1.6 The study of AD using models .....	50
1.6.1 Animal models .....	50
1.6.2 <i>In vitro</i> Models .....	51
1.7 Therapeutic targets.....	55
1.7.1 BACE Inhibitors .....	56
1.7.2 Anti-A $\beta$ targeting antibodies.....	56
1.7.3 Enzyme Inhibitors .....	57
1.7.4 Targeting Tau .....	58
1.8 Aims and objectives of the study.....	60
Chapter 2: Molecular cloning of APP constructs .....	62
2.1 Introduction to cloning.....	62
2.1.1 Molecular cloning.....	62
2.1.2 APP structure.....	62
2.1.3 Genetic mutations in APP .....	65
2.1.4 Aims and objectives .....	68
2.2 Methods and materials.....	70
2.2.1 General molecular biology procedures.....	70

2.2.1.1 Preparation of Competent Cells (Rubidium Chloride Method) .....	70
2.2.1.2 Plasmid sequencing .....	70
2.2.1.3 Bioinformatics analysis.....	71
2.2.1.4 PCR .....	71
2.2.1.5 PCR Tailing reactions .....	72
2.2.1.6 TOPO cloning .....	72
2.2.1.7 Transformation of Topo reactions .....	73
2.2.1.8 Recombination reaction of TOPO vectors .....	73
2.2.1.9 Agarose gel electrophoresis.....	73
2.2.1.10 Gel extraction.....	74
2.2.1.11 Restriction Digest.....	74
2.2.1.12 PCR clean up.....	75
2.2.1.13 Dephosphorylation of cDNA ends .....	75
2.2.1.14 Ligation .....	75
2.2.1.15 Agar preparation .....	76
2.2.1.16 Transformation.....	76
2.2.1.17 Colony PCR .....	77
2.2.1.18 Small scale plasmid isolation (miniprep).....	78
2.2.1.19 Large plasmid isolation (midiprep).....	78
2.2.2 Protein expression procedures.....	78
2.2.2.1 Cell lysis.....	78
2.2.2.2 The BCA Protein Assay .....	79
2.2.2.3 SDS-PAGE .....	79
2.2.2.4 Western Blot Transfer .....	79
2.2.2.5 Immunoblotting .....	80
2.2.3 Protein expression studies .....	81
2.2.3.1 COS-7 cell culture.....	81
2.2.3.2 Cell Quantification (Trypan Blue Exclusion) .....	81
2.2.3.3 Preparation of COS7 cells for transfection .....	81
2.2.3.4 COS7 transfection.....	82
2.2.3.5 Immunostaining.....	82
2.2.3.6 Fluorescence Microscopy .....	83
2.2.3.7 Protein expression from transfected COS7 cells .....	83
2.3 Results.....	85
2.3.1 Plasmid Construction .....	85
2.3.2 Generation of APP695 .....	87
2.3.2.1 Donor APP gene transfer into pcDNA3.1 .....	88
2.3.2.2 Construction of APP695 into pcDNA3/3.1 .....	91
2.3.3 Construction of the SweAPP695-pcDNA3.1.....	95
2.3.4 Immunocytochemistry (ICC) of COS7 .....	99
2.3.5 Western blot.....	102

2.3.6 Construction of pLenti6.4 Syn1 wtAPP695/ SweAPP695 lentiviral constructs	102
2.3.6.1 Construction of pCR8-wtAPP/SweAPP	104
2.3.6.2 Construction of the promoter entry vector	111
2.3.6.3 Construction of the pLenti6.4 SYN1- wtAPP695/ SweAPP695 V5 DEST	116
2.4 Discussion	120
Chapter 3: Creation and Characterisation of APP-expressing SHSY5Y cell lines	123
3.1 Introduction to AD modelling	123
3.1.1 APP and mitochondrial function	123
3.1.2 Mitochondria and oxidative stress	126
3.1.3 Antioxidant defences in the brain	130
3.1.4 Methods of probing mitochondrial function	131
3.1.5 The SHSY5Y cell line	134
3.1.6 Generation of stable cell lines	137
3.1.7 Aims and objectives	142
3.2 Methods and Materials	143
3.2.1 Lentiviral packaging of the pLenti6.4 wtAPP/SweAPP695 constructs	143
3.2.1.1 HEK 293FT cell culture	143
3.2.1.2 Viral packaging	143
3.2.1.3 Lenti-X GoStix protocol	145
3.2.1.4 Viral concentration	145
3.2.1.5 Determining Lentiviral Concentration	145
3.2.2 Testing the Syn1 wtAPP695/ SweAPP695 Lentiviruses	146
3.2.2.1 SH-SY5Y	146
3.2.2.2 Viral infection of GFP-expressing virus in the neuroblastoma cell line	146
3.2.2.3 Testing of the APP lentivirus	147
3.2.2.4 Blastocidin kill curve	148
3.2.3 Production of stable APP-expressing SH-SY5Y cell lines	148
3.2.3.1 Lentiviral transduction	148
3.2.3.2 Clone selection and expansion	148
3.2.3.3 Characterisation of clones	149
3.2.4 Determining changes in metabolism between the cell lines	152
3.3 Results	161
3.3.1 Optimization of transduction into SHSY5Y cell line	161
3.3.2 Testing of the lentiviral constructs	164
3.3.3 Generation of cell lines	166
3.3.4 Metabolic studies of wtAPP695/SweAPP695 expressing SHSY5Y cell lines	168
3.3.4.1 Cell proliferation	168
3.3.4.2 APP protein expression	169
3.3.4.3 Amyloid production in 7 day RA-differentiated cell lines	171
3.3.4.4 Glucose uptake	172
3.3.4.5 Seahorse experiments	174

3.3.4.6 Oxidative stress studies .....	180
3.4 Discussion .....	183
3.4.1 Lentiviral infection of SHSY5Y cells .....	183
3.4.2 Characterisation of APP-expressing cell lines .....	185
3.4.3 Changes in metabolism between cell lines.....	186
Chapter 4: Characterization of FAD patient–derived fibroblasts .....	194
4.1 Introduction to familial mutations.....	194
4.1.1 Presenilins structure .....	196
4.1.2 Localization of Presenilins.....	197
4.1.3 Presenilin 1 function.....	198
4.1.4 Presenilin mutations.....	198
4.1.5 APP expression outside the CNS.....	200
4.1.6 Aims and objectives .....	204
4.2 Methods and materials.....	206
4.2.1 Human Dermal Fibroblast culture (hDFa).....	206
4.2.2 Metabolic studies between FAD-derived and control fibroblast cell lines .....	206
4.2.2.1 Cell proliferation study.....	206
4.2.2.2 Glucose uptake .....	207
4.2.2.3 A $\beta$ ELISA .....	207
4.2.2.4 Analysing mitochondrial function .....	207
4.2.2.3 Oxidative stress response studies.....	208
4.2.2.4 Amyloid treatment studies.....	209
4.3 Results.....	211
4.3.1 Cell proliferation.....	211
4.3.2 Glucose uptake .....	212
4.3.3 A $\beta$ ELISA .....	213
4.3.4 Analysing mitochondrial function .....	213
4.3.5 Oxidative stress of human dermal fibroblasts.....	216
4.3.6 Amyloid treatment of hDF .....	218
4.3.6.1 Cell viability.....	218
4.3.6.2 Glucose uptake .....	219
4.4 Discussion .....	221
4.4.1 Characterizing FAD-derived fibroblast metabolism.....	221
4.4.2 Effects of exogenous A $\beta$ 1-42 on fibroblasts .....	223
Chapter 5: Conclusions and future work .....	226
6.0 Bibliography .....	231
7.0 Appendices .....	269
7.1 Sequencing for Pittsburgh/ jAPP695 in pcDNA3.1 .....	269
7.2 Gel extraction.....	270
7.3 PCR Purification .....	271
7.4 QIAGEN Miniprep protocol.....	272

7.5 Transfection of COS7 with Lipofectamine LTX.....	273
7.5 PierceNet BCA protein assay.....	274
7.6 Antibodies for Western blotting .....	275
7.7 Recipe for making buffers (Western blotting) .....	275
7.8 DNA/ Protein Ladder sizing.....	276
7.9 List of primers used.....	277
7.10 Recombination of TOPO vector into final destination vector.....	278
7.11 293FT resurrection and culture .....	278
7.12 Lenti-X GoStix.....	280
7.13 QuickTiter Lentivirus Titer test (Lentivirus-associated HIV p24) .....	281
7.14 A $\beta$ 1-42 ELISA.....	282

## List of Abbreviations

A $\beta$  Amyloid beta

AD Alzheimer's Disease

ADAM A Disintegrin and Metalloprotease

AICD Amyloid precursor protein intracellular domain

AMP Ampere

APOE Apolipoprotein E

APP Amyloid precursor protein

ATP Adenosine-5'-triphosphate

BACE1  $\beta$ -site APP cleaving enzyme-1

BDNF Brain-derived neurotrophic factor

BSA Bovine serum albumin

CMRglc Cerebral metabolic rates of glucose

CMV Cytomegalovirus

CSF Cerebrospinal fluid

DAPI 4', 6-diamidino-2- Phenylindole

DMSO Dimethylsulfoxide

DS Down syndrome

ECAR Extracellular acidification rate

EOAD Early onset Alzheimer's disease

ETC Electron transport chain

FAD Familial Alzheimer's disease

FBS Foetal bovine serum

FCCP Carbonyl cyanide 4-(trifluoromethoxy)phenylhydrazone

FITC Fluorescein isothiocyanate

GFP Green fluorescent protein

GFAP Glial fibrillary acidic protein

GLUT Glucose transporter

GSK3 $\beta$  Glycogen kinase 3 beta

GSSG Glutathione disulfide

GSH Glutathione

GWAS Genome wide association studies

HBD1/2 Heparin binding domain

HEPES 4-(2-hydroxyethyl)-1-piperazineethanesulfonic acid

IDE Insulin degrading enzyme

IRE Iron-Responsive Element

iPSC Induced pluripotent stem cells

KPI Kunitz type serine protease inhibitor

$\lambda$  wavelength

LB Luria-Bertani broth

LDH Lactate dehydrogenase

LEC Lateral entorhinal cortex

MAP Microtubule associate protein

MCI Mild cognitive impairment

MMSE Mini mental state exam

MTT 3-[4, 5-dimethylthiazol-2-yl]-2, 5- diphenyltetrazolium bromide; thiazolyl blue

NAD<sup>+</sup> Nicotinamide adenine dinucleotide

NADH Reduced nicotinamide adenine dinucleotide

NADPH Nicotaminade adenine dinucleotide phosphate

NFT Neurofibrillary tangle

NGF Nerve growth factor

NMR Nuclear magnetic resonance

OCR Oxygen consumption rate

OD Optical density

MOPS (3-(N-morpholino) propanesulfonic acid

NO Nitric oxide

NOS Nitric oxide synthase

NMDAR Anti-N-Methyl-D-Aspartate Receptor

PBS Phosphate buffered saline  
PIB Pittsburgh Compound B  
PCR Polymerase chain reaction  
PDAPP platelet-derived growth factor mini-promoter  
PHF Paired helical filament  
PS1/ PS2 Presenilin 1/ 2  
PTB Phosphotyrosine binding  
RA Retinoic acid  
RIPA Radioimmunoprecipitation assay  
SDS PAGE Sodium dodecyl sulfate polyacrylamide electrophoresis  
SOB Super optimal broth  
SYN1 Synapsin I  
ROS Reactive oxygen species  
SOD Superoxide dismutase  
ThT Thioflavin T  
TGN Trans Golgi Network  
V Volt  
VLDL Very low density lipoproteins  
WPRE Woodchuck posttranslational response element

## List of Tables and Figures

Figure 1.1	Image of the characteristic hallmarks of AD	18
Figure 1.2	Diagram of Pittsburgh Compound B uptake in the AD brain	20
Figure 1.3	Diagram of APP processing	26
Figure 1.4	Diagram of APP processing and the location of familial mutations	27
Figure 1.5	Diagram of the structure of APP primary sequence	48
Table 2.1	List of known APP mutations and the position of the mutations	67
Table 2.2	Table of PCR running conditions	72
Figure 2.1	Sequence alignment of FG695 plasmid and wtAPP695 gene	86
Figure 2.2	Sequence alignment of wtAPP695 gene against 695IL plasmid	87
Figure 2.3	Sequence of the 5' HindIII primer used for APP695 amplification	88
Figure 2.4	Sequence of 5' XbaI primer used for APP695 amplification	88
Figure 2.5	Agarose gel of amplification of APP insert from FG 695 plasmid	89
Figure 2.6	Agarose gel of PCR amplification of APP751 insert	89
Figure 2.7	Colony PCR analysis of clones transformed with JapAPP695-pcDNA3.1	90
Figure 2.8	Colony PCR analysis of bacterial transformed with APP71-pcDNA3.1	90
Figure 2.9	Diagram of fragments in JapAPP695-pcDNA3.1 to construct wtAPP695	92
Figure 2.10	Diagram of fragments in APP751-pcDNA31 used to construct wtAPP695	93
Figure 2.11	Gel extraction of JapAPP695-pcDNA3.1 digestion	94
Figure 2.12	Gel extraction of APP751-pcDNA3.1 digestion	94
Figure 2.13	Sequence alignment of wtAPP695-pcDNA3.1 showing corrected point mutation	95
Figure 2.14	Sequence of the APPSwe Rev primer used to introduce the TC mutation	96
Figure 2.15	Gradient PCR to determine optimal annealing temperature for APP Swe Rev primer and Ex Alt For primers	96
Figure 2.16	PCR amplification of APP695	97
Figure 2.17	Gel extraction of digested wtAPP695-pcDNA3.1	97

Figure 2.18 Colony PCR analysis of clones transformed with SweAPP695-pcDNA3.1	98
Figure 2.19 Sequence alignment of SweAPP695-pcDNA3.1	99
Table 2.3 Microscope settings for visualising immunostained COS7 cells	100
Figure 2.20 Immunostained COS7 for wtAPP695/ SweAPP695	101
Figure 2.21 Western blot of transfected COS7 cells	101
Figure 2.22 Schematic of the Virapower HiPerform Promoterless Gateway Expression system	104
Table 2.4 PCR amplification conditions using Phusion	105
Figure 2.23 Gradient PCR analysis using APPP8 TOPO and APP P8 2STOP primers	106
Figure 2.24 Gel extraction for SweAPP695	106
Figure 2.2.5 Gel extraction for wtAPP695	106
Table 2.4 Number of clones recovered after transformation with pCR8 wtAPP695/ SweAPP695.	107
Figure 2.26 Colony PCR analysis of clones transformed with pCR8-SweAPP695	108
Figure 2.27 Colony PCR analysis of clones transformed with pCR8-wtAPP695	108
Figure 2.28 Diagram of pCR8-APP695 with restriction sites for determining orientation	109
Figure 2.29 Agarose gel of EcoRV and BamHI digested SweAPP695 pCR8 clones	109
Figure 2.30 Agarose gel of EcoRV and BamHI digested wtAPP695 pCR8 clones	110
Table 2.5 Sequencing results of clones carrying wtAPP695/SweAPP pCR8	110
Table 2.6 PCR conditions to amplify the SYN1 gene	113
Figure 2.31 Gradient PCR using Syn 1 Pentr5 For g and Syn1 Pentr5 Rev primers	113
Figure 2.32 Agarose gel of PCR amplification of SYN1	113
Figure 2.33 Colony PCR analysis of clones transformed with pENTR5SYN1	114
Figure 2.34 Diagram of pENTR5SYN1 with restriction sites for determining orientation	115
Figure 2.35 Agarose gel of Pst1 digested pENTR5 SYN1 clones	115
Figure 2.36 Sequence alignment of the clone 12 with the SYN1 gene sequence	116

Table 2.7	Number of recovered clones transformed with pLenti6.4 SYN1 wtAPP695/ SweAPP695	117
Figure 2.37	Agarose gel of Pst1 digested pENTR5 SYN1 clones	117
Figure 2.38	Colony PCR analysis of clones transformed with pLenti6.4SYN1wtAPP695	117
Figure 2.39	Full sequence alignment of pLenti6.4 SYN1 wtAPP695	118
Figure 2.40	Full sequence alignment of pLenti6.4 SYN1 SweAPP695 against constructed plasmid map	119
Figure 3.1	Diagram of oxidative phosphorylation within the mitochondrion	128
Figure 3.2	Diagram showing the synthesis of GSH	130
Figure 3.3	Schematic of Seahorse XF microplate and sensors	132
Figure 3.4	Diagram showing the typical metabolic profile of mitochondrial function	133
Figure 3.5	Diagram of the three plasmids for second generation system	141
Table 3.1	Protocol to measure basal OCR on the Seahorse analyser	156
Figure 3.6	Images of SHSY5Y cells transduced with CMV- GFP lentivirus (48 hrs)	163
Figure 3.7	Images of SHSY5Y cells transduced with CMV- GFP lentivirus (10 days)	164
Figure 3.8	Image of SHSY5Y cells transduced with EIF1 $\alpha$ - RFP lentivirus	165
Figure 3.9	Image of SHSY5Y infected with pLenti6.4 SYN1-SweAPP695	166
Figure 3.10	Image of SHSY5Y infected with pLenti6.4 SYN1-wtAPP695	166
Figure 3.11	Western blot analysis of SHSY5Y transduced with wtAPP/ SweAPP695	167
Figure 3.12	Amyloid 1-42 ELISA of conditioned SHSY5Y media	167
Table 3.2	Table of APP-expressing SHSY5Y clones isolated	168
Figure 3.13	Images of SHSY5Y clones differentiated with RA and BDNF	169
Figure 3.14	Cell proliferation rates of the SHSY5Y cell lines	170
Figure 3.15	Percentage pixel density of APP protein expression in cell lysates	171
Figure 3.16	A $\beta$ 1-42 ELISA results from conditioned media	171
Figure 3.17	Percentage glucose remaining in media from proliferating SHSY5Y lines	172

Figure 3.18 Percentage glucose remaining in media from RA differentiated cell lines	173
Figure 3.19 Representative graph of basal OCR readings on the Seahorse analyser	174
Figure 3.20 Basal OCR readings of SHSY5Y cells at different seeding densities	175
Table 3.3 Optimal concentrations of mitochondrial inhibitors determined	176
Figure 3.21 % basal OCR data for proliferating SHSY5Y cell lines	176
Figure 3.22 Basal OCR and proton leakage of proliferating SHSY5Y cell lines	177
Figure 3.23 Max respiration and spare respiratory capacity of proliferating cell lines	178
Figure 3.24 Non-mito respiration and ATP production of proliferating cell lines	178
Figure 3.25 % basal OCR data for RA-differentiated SHSY5Y cell lines	179
Figure 3.26 Basal OCR and proton leakage from RA-differentiated cell lines	180
Figure 3.27 Max respiration and spare respiratory capacity of RA-differentiated cells	180
Figure 3.28 Non-mito respiration and ATP production of RA-differentiated cell lines	181
Figure 3.29 Dose response curve of SweAPP695 expressing cell lines to H <sub>2</sub> O <sub>2</sub>	182
Table 3.4 Student T test analysis of IC <sub>50</sub> s calculated for each SweAPP695 cell line	182
Figure 3.30 Dose response curve of wtAPP695-expressing cell lines to H <sub>2</sub> O <sub>2</sub>	183
Table 3.5 Student T test analysis of IC <sub>50</sub> s calculated for each wtAPP695 cell line	183
Figure 4.1 Diagram of presenilin structure	198
Table 4.1 Table of FAD-derived fibroblasts	212
Figure 4.2 Cell growth between the different FAD-derived fibroblast cell lines	213
Figure 4.3 Percentage amount of glucose in media taken from fibroblast cell lines	213
Figure 4.4 Basal OCR readings of dermal fibroblasts seeded at different seeding densities	215
Figure 4.5 Basal ECAR readings of dermal fibroblasts seeded at different seeding densities	215
Table 4.2 Table of determined optimal concentrations of mitochondrial inhibitors	216

Figure 4.6	Representative graph of one Mito Stress test run on AD fibroblasts	216
Figure 4.7	Metabolic measurements calculated from running the MitoStress Test	217
Figure 4.8	Dose response curve diseased fibroblasts to H <sub>2</sub> O <sub>2</sub>	218
Table 4.3	Student T test analysis of IC <sub>50</sub> s calculated from each fibroblast cell line	219
Figure 4.9	Cell viability of dermal fibroblasts treated with A $\beta$ 1-42	220
Figure 4.10	% of glucose in media taken from A $\beta$ 1-42 treated fibroblasts	221

## **Chapter 1: Introduction to Alzheimer's disease**

### **1.1 Overview of Alzheimer's disease**

Dementia is defined as a substantial loss in intellectual abilities such as memory that impedes everyday functions. Alzheimer's disease is the most common form of dementia, making up to between 50 to 70% of dementia cases. It is estimated that currently 44.4 million people suffer from AD worldwide, with this figure estimated to rise to 135.5 million by 2050 (International, 2013), if no effective treatments or cures are found.

AD was first described by Dr Alois Alzheimer in 1908, after observing the symptoms of a patient with progressive memory impairment, changes in behaviour (including paranoia, delusions) and progressive decline in the ability to use language. Post-mortem brain examination of the patient revealed protein aggregates, which he termed 'plaques' and 'tangles' (Hippius and Neundörfer, 2003). However, it was Fischer (Fischer, 1907) who is credited to be the first to report plaques. In the late 1960s, the work of Blessed, et al, (1968) led to AD becoming widely accepted as the most common basis for senile dementia (Blessed et al., 1968, Kang and Muller-Hill, 1990, Arai et al., 1991).

Studies have attempted to define the pathogenesis of AD by observing and describing the two major structural hallmarks of the plaques and tangles (see Figure 1.1). Kidd et al (1964) and Terry et al (1963) utilised electron microscopy to study the two types of lesions. A number of studies have noted significant degeneration of neurons responsible for synthesising acetylcholine, as well as irregularities in the dopaminergic, glutaminergic and the inhibitory  $\gamma$ -aminobutyric acid (GABA) systems (Ellison et al., 1986). These observations strongly suggested that AD is the consequence of highly heterogeneous cell degeneration. The study of the composition and origin of the plaques and tangles also became central to studies of AD. However, current research

suggests that these lesions may only serve as pathological hallmarks observed late in disease.

A

B



Figure 1.1 Image of the characteristic plaques (A) and neurofibrillary tangles (B) found in AD brain (Images attributed to Wikimedia Commons, <https://common.wikimedia.org>).

### **1.2. Symptoms and disease pathology**

AD patients experience a range of symptoms including cognitive changes, memory loss and behavioural changes (Selkoe, 2001a). The significant loss in memory function is largely attributed to massive neuronal cell and synapse loss in preferential brain regions. Cholinergic neurons are specifically affected (Mesulam, 2004), and are characterized initially by synaptic dysfunction that precedes neuronal death (Mattson, 2004). These symptoms represent the later stages of AD, in which behavioural changes become evident due to death of neurons in key regions.

It is believed the lateral entorhinal cortex (LEC) is implicated in early AD. LEC dysfunction in preclinical AD is detected by functional magnetic resonance imaging (fMRI) (Khan et al., 2014b). The LEC is considered a gateway to the hippocampus, which plays a vital role in learning and consolidation for long term memories. This makes the hippocampus especially susceptible to damage in early AD (Mu and Gage, 2011). AD has been shown to spread directly from the LEC to other areas of the cerebral cortex, especially the parietal cortex, which is responsible for spatial orientation and navigation. Cognitive impairment is associated with synaptic loss in the neocortex and the limbic system, which are responsible for higher brain functions such as sensory perception, spatial reasoning and learning and memory (McIntosh et al.,

1998, Miller and Cummings, 2007). The extensive cell death observed leads to extreme shrinkage of the hippocampus and cerebral cortex.

In the early and pre-symptomatic AD stages, degeneration of basal forebrain cholinergic nuclei takes place (Mann et al., 1984, Perry et al., 1978). Neuronal cell death is attributed to exposure of cells to abnormal levels of beta amyloid (A $\beta$ ) peptide, with specific vulnerability of cholinergic basal forebrain neurons (Boncristiano et al., 2002). AD brains show hallmarks of apoptosis (Kadowaki et al., 2005, Mattson, 2000, Cotman and Su, 1996), such as DNA fragmentation and the activation of Caspase-3, a key effector enzyme of the apoptotic cascade (Stadelmann et al., 1999).

Currently, diagnosis of AD is carried out using subjective aptitude exams, which test the ability of a person to identify objects and recall events. The most common test is the mini mental state examination MMSE, first established in the 1970's (Folstein et al., 1975). Clinicians can assess the severity of dementia based on the score attained and then recommend the appropriate treatment. However, problems arise from variations in test specificity, with the major disadvantage of being unable to distinguish mild cognitive impairment (MCI) reliably from dementia and the difficulty in recording changes in cases of severe dementia (Lancu and Olmer, 2006). In reality, 50% to 90% of dementia cases may be unrecognised due to the difficulty in distinguishing AD from normal aging (Ritchie and Lovestone, 2002).

At present, definitive diagnosis can be only be carried out by post mortem brain autopsy to confirm the presence of plaques and tangles. To date, there are no definitive biomarkers for diagnosing AD, but studies into levels of A $\beta$ , total tau and phosphorylated-tau 181 taken from cerebral spinal fluid (CSF) have been assessed. Samples taken from MCI patients have demonstrated an increase in the level of total tau and phosphorylated tau but decreased levels of neurotoxic A $\beta$ 1-42 species (Hansson et al., 2006). Sensitivity in these tests was estimated to be at 95% but

specificity was lower. These results are encouraging but still require further validation. A current major issue in AD diagnosis is that neuronal degeneration is probably advanced to a stage that some current drug treatments may be ineffective (Peterson and Goldman, 1986).

Advancements in brain imaging technology may prove useful to diagnose AD. Imaging of AD brains showed decreases in total brain mass (Teipel et al., 2014) with shrinkage of the cerebral cortex and hippocampus (Dubois et al., 2007) and severely enlarged ventricles, as shown in Figure 1.2).



Figure 1.2. Image showing Pittsburgh Compound B (PIB) uptake to visualise amyloid in the brain of non-demented patient compared to Alzheimer's patient brain. (Image attributed to Wikimedia Commons, [https://commons.wikimedia.org/wiki/File:PET\\_AD.jpg](https://commons.wikimedia.org/wiki/File:PET_AD.jpg)).

Amyloid deposition can be visualised in the brain with the use of Pittsburgh Compound B in PET scans (Klunk et al., 2004) (see Figure 1.2). This technique could aid early diagnosis. PIB is a radioactive thioflavin T analog which binds to beta sheets of amyloid, and is currently under development by GE Healthcare as a clinical diagnostic tool to assess brain amyloidosis (Landau et al., 2013). Higher PIB retention has been demonstrated in AD patients when compared to controls (Rowe et al., 2007); with PIB retention particularly pronounced in the striatum of AD mutation carriers compared to sporadic patients/controls (Klunk et al., 2004).

The other major protein involved in AD is tau, which can also be imaged with tau-specific radiotracers. This technique may provide accurate, reliable and reproducible quantitative measures of global and regional brain tau burden (Zhang et al., 2012c). Such detailed neuroimaging methods provide a good evaluation of disease progression, (as the spread of tangles is a good correlation of AD pathology). Most selective tau imaging tracers focus towards binding paired helical filaments (PHFs) (Villemagne et al., 2014). However, the running costs of using such techniques for routine AD screening would likely deter clinicians from frequent use.

Methods to detect early biomarkers for dementia could provide a more high throughput, non-invasive and inexpensive alternative. A blood test is in development, which detects peripheral blood lipids profiles, that are associated with the development of MCI or AD within 3 years (Mapstone et al., 2014). The researchers detected preclinical AD with 90% accuracy, which was comparable with published CSF studies. Therefore simple blood tests such as these could provide faster and reliable diagnosis of patients at risk of developing AD, as well as alleviating the costs of using alternative methods.

Fluorodeoxyglucose tracer positron emission tomography (FDG-PET) imaging detects glucose uptake in patients and has been used to study brain metabolism extensively in AD (see Figure 1.2). FDG-PET has been utilised to measure cerebral metabolic rates of glucose (CMR<sub>glc</sub>), an indicator of neuronal activity. In the AD brain, there are regional patterns of CMR<sub>glc</sub> reductions, with consistent deficits in parieto-temporal areas (Krystal, 1987), posterior cingulate cortex (Minoshima et al., 1997) and the medial temporal lobes, which encompasses the hippocampus, transentorhinal/entorhinal cortex and subiculum) (Mosconi, 2005). In contrast, fMRI scans of the LEC in young healthy individuals show signs of high metabolism (Khan et al., 2014a). Reductions in the activity of key mitochondrial enzyme complexes such as the  $\alpha$ -ketoglutarate dehydrogenase complex and decrease in the expression of glycolytic enzymes and pyruvate dehydrogenase (PDH) complex has also been

observed in AD (Yao et al., 2009a). Reductions in glucose utilisation in the brain as well as mitochondrial function appears decades before any symptoms or histopathological changes occur, making these metabolic changes useful biomarkers of risk of AD (Mosconi et al., 2008a, Reiman et al., 2004).

As discussed in section 3.1.2, there is gradual decline in the energetics of mitochondria (production of ATP) as well as increases in production of oxidants and oxidative stress in AD. A $\beta$  has also been shown to interact with mitochondrial proteins including ABAD (amyloid-binding alcohol dehydrogenase) and CypD (cyclophilin D), which results in altered homeostasis (Yao et al., 2007). Carbohydrates are the major respiratory substrates in aerobic respiration, with glucose being the predominant energy source. A shift toward the metabolism of ketone bodies away from glucose observed in AD could point to attempts by the cell to alleviate bioenergetic deficits and compensate for the decline in glucose-driven ATP generation (Hoyer, 1991, Blalock et al., 2004). Ketone bodies produced from fatty acids in the liver, can be converted to acetyl-Coenzyme A, which can be fed into the Krebs cycle, by its conversion to citrate, the first compound of the Tricarboxylic acid cycle (TCA).

These observations suggest that AD can be considered a result of hypometabolism (Mosconi et al., 2008b), with increasing evidence that AD is associated with type II diabetes. In fact, Type II diabetes has been shown to cause brain insulin resistance, oxidative stress and cognitive impairment (Zhao and Townsend, 2009). Indeed AD has recently been described as “type III diabetes” (de la Monte and Wands, 2008).

### **1.2.1 Amyloidogenesis**

One of the two major hallmarks of AD is the presence of intraneuronal plaques found throughout the brain, but particularly in the limbic and association cortices (Dickson, 1997). Such plaques are composed of an amyloid beta (A $\beta$ ) peptide core (Gouras et al., 2005, Gouras et al., 2000) surrounded by dystrophic neurites, reactive astrocytes

and other proteins. Structurally, these neurites appear dilated and twisted, with cellular abnormalities such as engorged lysosomes and numerous mitochondria (Selkoe, 2001b). Neurons are known to naturally produce amyloid and release the peptide into the intraneuronal space (Haass et al., 1992b), where it is speculated to have important physiological functions (see section 1.4). However, it should also be noted that plaque loads poorly correlate with cognitive impairment, which explains the incidence of non-demented individuals who were found to have plaques post-mortem (Price and Morris, 1999).

A $\beta$  is derived from a larger precursor protein called the Amyloid Precursor Protein (APP), which is cleaved in a complex pathway to generate peptides varying in length, ranging from 38 to 43 amino acids in length. The most neurotoxic peptide form A $\beta$ 1-42, has a higher propensity to aggregate due to the presence of two extra hydrophobic amino acids (Kim and Hecht, 2006) than its other forms (Snyder et al., 1994). A $\beta$ 1-42 and A $\beta$ 1-40 peptides found to make up the plaques seen in AD.

During the aggregation process, amyloid initially forms beta sheet structures, which then progress to oligomers, fibrils and then plaques (Powers and Powers, 2008). This increase in size can be detected when amyloid aggregates are separated by sodium dodecyl sulphate polyacrylamide gel electrophoresis. Non-fibrillar monomeric A $\beta$ 1-42 appears at 4kDa, increasing in size as it forms beta sheets (Glennner and Wong, 1984b, Masters et al., 1985). Amyloid plaques within tissue can also be positively stained with Congo red dye or Thioflavin T, which bind specifically to the beta sheet structures (Miura et al., 2002, Khurana et al., 2005).

APP is located within the cell membranes of neurons, where it is cleaved, allowing the release of A $\beta$  peptide into the extracellular space. The peptide can be internalised by neurons, where it is folded into beta sheet sheets that stack together to form fibrils, which aggregate to form plaques (Seeman and Seeman, 2011) under pathological

conditions. Three types of amyloid deposits have been identified in AD brains; diffuse plaques, senile plaques and cerebrovascular deposits (Morgan et al., 2004a). The development of amyloid deposits can be described in three stages, according to their distribution progressing from antero-basal to postero-lateral deposition (Braak and Braak, 1991).

Diffuse plaques are considered to occur early in plaque formation (Dickson, 1997). They are dispersed throughout the cerebral hemispheres and sparsely within the white matter, the striatum and cerebellar cortex. These plaques are more common than senile plaques, and appear as amorphous, spherical, diffuse amyloid deposits (Tagliavini et al., 1988). They are described as pre-amyloid deposits, where amyloid exists as non-amyloid aggregates, which do not stain with Congo Red or thioflavin-S, and can be found within 'normal' aged individuals. They also do not contain neurites or signs of neuronal injury (Serrano-Pozo et al., 2011). Senile plaques, on the other hand consist of a dense amyloid core (Iwatsubo et al., 1994), surrounded by dystrophic neurites, commonly containing paired helical filaments (PHFs, see section 1.2.2), closely associated to reactive astrocytes and microglia (Mandybur and Chuirazzi, 1990). A number of dystrophic neurites do contain tau but also stain positive for ubiquitin, which may be a sign of early plaque formation (Morgan et al., 2004a). Distinct hallmarks include the presence of butyrylcholinesterase (Guillozet et al., 1997), a protein associated with axonal growth cones and several neurotransmitters (Masliah et al., 1992). Axonal sprouting associated with senile plaques is also thought to trigger synaptic dysfunction (Arendt, 2001). Inflammation is evident in the vicinity of plaques, due to the presence of acute phase proteins such as antichymotrypsin, interleukin-1 and interleukin-6 (IL-6) positive activated microglia (Wegiel and Wisniewski, 1990, Eikelenboom and Veerhuis, 1996).

Amyloid angiopathy can accompany AD, whereby amyloid deposits in cerebral blood vessels, in association with senile plaques (Miyakawa and Uehara, 1979). However, cerebrovascular amyloid is also present in non-demented individuals who fail to possess the hallmarks of AD.

#### **1.2.1.1 APP Biosynthesis and trafficking**

The importance of amyloid and its precursor in AD has led to many studies on APP processing and whether upstream events may be future targets of therapeutic drugs. Amyloid Precursor Protein is encoded by the APP gene, which consists of 19 exons located on chromosome 21. There are three main isoforms produced through alternative splicing of exons 7 and 8 (Sandbrink et al., 1996); APP751, APP770 and APP695 (LaFerla, 2002, Price and Sisodia, 1998, Price et al., 1998). The two larger isoforms contain a 56-amino acid insert known as the Kunitz domain (KPI) (Fig 1.) within the extracellular domain, named as it shares homology to the Kunitz serine protease inhibitor domain (Price and Sisodia, 1998) but these isoforms when cleaved do not produce the amyloid peptide. Interestingly, increased levels of KPI containing APP isoforms have been reported in AD and to be associated with A $\beta$  (Zhang et al., 2011). The A $\beta$  peptide is derived from Amyloid Precursor Protein 695 (APP695) isoform (Haass and Selkoe, 2007, Vassar, 2005), expressed abundantly within neurons (Puig and Combs, 2013, Tanaka et al., 1989) and to a lesser degree within astrocytes (Sisodia et al., 1993).

Following transcription of the APP gene within the nucleus, full-length APP mRNA is directed to the endoplasmic reticulum for translation into protein by the action of ribosomes. From here, APP continues its journey through to the Golgi apparatus and trans-Golgi network (TGN), where APP undergoes post-translational modifications, acquiring N- and O-linked sugars quickly after biosynthesis (Annaert et al., 1999). Full length APP is a type I transmembrane protein, consisting of a large extracellular N-terminal domain, a hydrophobic transmembrane domain and a short C-terminus

intracellular domain (Reinhard et al., 2005). This protein quickly undergoes a series of proteolytic cleavages, resulting in a short half-life, estimated to be 20-30 minutes in most cell types tested. APP cleavage results in the secretion of products into vesicle lumens and the extracellular space (Kang et al., 1987, Bodovitz and Klein, 1996).

#### 1.2.1.2 APP processing

APP metabolism within the cell is complex, but has been particularly well-characterised for the APP695 isoform in the central nervous system. Once full length APP is formed, it can follow one of two processing pathways, as shown in Figure 1.3, leading to the production of fragments, which themselves can influence distinct signalling pathways.



Figure 1.3. Diagram showing the two processing pathways in which APP695 may be processed. Image attributed to Wikimedia Commons, [https://commons.wikimedia.org/wiki/File:P3\\_peptide\\_synthesis.jpg](https://commons.wikimedia.org/wiki/File:P3_peptide_synthesis.jpg).

##### 1.2.1.2.1 The amyloidogenic pathway

The amyloidogenic pathway (associated with AD) leads to sequential APP cleavage by two different enzymes,  $\beta$ -secretase-1 (BACE1) and  $\gamma$ -secretase, resulting in A $\beta$  peptide formation and the release of the C-terminal fragment, termed the Amyloid Precursor Intracellular Domain (AICD) (Zhang et al., 2012a). Mutations (in APP, Presenilin 1 (PSEN1), and Presenilin 2 (PSEN2)) have been identified, which influence APP metabolism (see Figure 1.4). Presenilins 1 and 2 encode for subunits that make up part of the  $\gamma$ -secretase enzyme complex. In particular, these pathogenic mutations preferentially increase the production of neurotoxic A $\beta$ 1-42 (Thinakaran and Koo, 2008,

Cole and Vassar, 2007b, Jankowsky et al., 2004) or increase the A $\beta$ 40/42 ratio (Haass et al., 1995, Selkoe and Wolfe, 2007).

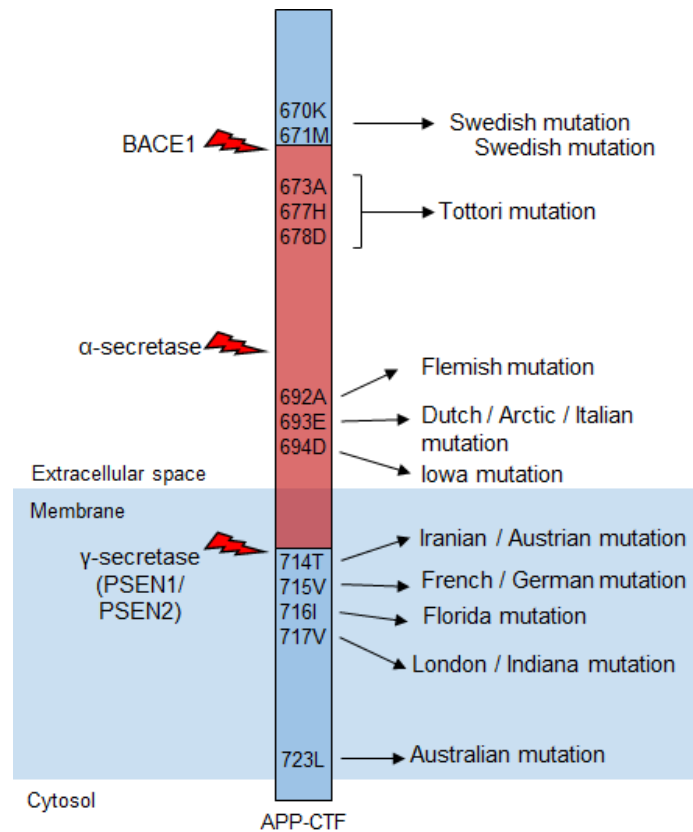


Figure 1.4. Diagram showing where enzymes act on APP, as well as some of the mutations that influence enzyme cleavage.

#### 1.2.1.2.2 Beta-site APP cleaving enzyme 1

BACE1 is widely expressed throughout the body but is highly active within neurons (Li et al., 2006, Czech et al., 2000). BACE1 is an aspartyl protease, with a single transmembrane domain close to the C-terminus and a palmitoylated cytoplasmic tail (Benjannet et al., 2001). It efficiently cleaves membrane bound substrates suggesting that the enzyme is likely to be membrane bound or closely associated with a membrane protein (Citron et al., 1995, Yu et al., 2000). BACE1 co-localises to the cell membrane of the Golgi Body, Trans Golgi Network and endosomes (Cole and Vassar, 2007a), where it functions optimally at acidic pH (Pastorino and Lu, 2006). This is further supported by the fact that endosomal dysfunction has been linked with Alzheimer's disease and neurodegeneration (Nixon, 2005). The cleavage of APP

occurs upon APP internalization, which also suggests that BACE1 may be active in other cellular compartments in addition to endosomes.

BACE1 acts at the Aspartate +1 residue of the A $\beta$  sequence of APP (Vassar et al., 1999) generating the amino terminus of A $\beta$  (Figure 1.4 shows the cleavage site in APP). This cleavage releases three fragments, sAPP $\alpha$ , a secreted APP ectodomain, and the membrane-bound carboxyl terminal fragment (CTF), C99. BACE can also cleave at Glutamine +11, at Valine-3 or at Isoleucine-6 (Haass et al., 1992b). The 501 amino acid sequence of BACE1 contains two aspartic protease active site motifs (DTGs). Mutation of either aspartic acid renders the enzyme inactive (Hussain et al., 1999, Bennett et al., 2000b). Site-directed mutagenesis of the amino acids close to the cleavage site of full length APP influences the sequence preference for BACE1 (Citron et al., 1995). Substitutions of the residues to larger hydrophobic amino acids (such as to leucine and asparagine; observed in Swedish APP) for the methionine or lysine residue enhance the efficiency of BACE1 cleavage.

This enzyme has broad substrate specificity, indicating it has other cellular functions. In addition to APP, BACE1 cleaves the APP-like proteins 1 and 2 (Eggert et al., 2004), low-density lipoprotein receptor LDLR related protein (LRP) (von Arnim et al., 2005), the  $\beta$ -subunits (VGSC $\beta$  and SCN2b) of sodium gated channels (Wong et al., 2005) and neuregulin (NRG1) (Willem et al., 2006). The study of BACE1 knock outs led to subtle side effects, most notably, being more timid and a less exploratory phenotype compared to controls (Harrison et al., 2003).

The only known mammalian homologue of BACE1 is BACE2, which is mapped to the DS critical region on chromosome 21. BACE2 shows only 75% sequence homology to BACE1, and is detected at low levels in peripheral tissues (Bennett et al., 2000a). With relevance to AD, it is expressed at low levels in the brain but can cleave APP at the  $\beta$ -site to produce A $\beta$  in vitro (Abdul-Hay et al., 2012). Interestingly, other studies have

reported BACE2 acting as an alternative  $\alpha$ -secretase (Yan et al., 2001) and serving as an antagonist to BACE1 (Basi et al., 2003). Furthermore, BACE2 expression is not up-regulated to compensate for a lack of BACE1 in knockout mice. BACE2 function has been associated with insulin expression in  $\beta$ -cells of the pancreas, where it modulates insulin receptor signalling

#### **1.2.1.2.3 $\gamma$ -secretase**

$\gamma$ -secretase is a multi-unit enzyme complex, consisting of: presenilin-1 or -2, nicastrin, anterior pharynx-defective 1 (APH-1), and presenilin enhancer-2 (PEN-2). Similarly to BACE-1,  $\gamma$ -secretase cleaves a range of substrates, preferentially processing type I integral membrane proteins such as Notch, E-cadherins and N-cadherins (Zhang et al., 2000, Marambaud et al., 2002, Marambaud et al., 2003, Haapasalo and Kovacs, 2011). With respect to APP,  $\gamma$ -secretase cleaves at several sites within the transmembrane domain of the C-terminal fragment, releasing A $\beta$  peptides ranging in length from 38 to 43 residues. Approximately 90% of secreted A $\beta$  ends in residue 40, whereas A $\beta$ 42 accounts for 10% under non-pathological physiological conditions. Minute amounts of shorter A $\beta$  peptides such as A $\beta$ 37 and A $\beta$ 38 have also been detected (Thinakaran and Koo, 2008).

#### **1.2.2 The non-amyloidogenic pathway**

Non-amyloidogenic processing of APP (see Figure 1.3) is not associated with pathogenic phenotypes, and occurs via the action of  $\alpha$ -secretase, which cleaves APP within the A $\beta$  domain (at the Lysine 16-Leucine 17 bond) thus precluding A $\beta$  peptide formation. Cleavage at this site leads to the generation of soluble APP fragments that are associated with a range physiological functions (Haass et al., 1992a). The second cleavage reaction is catalysed by  $\gamma$ -secretase.

#### **1.2.2.1 $\alpha$ -secretase**

$\alpha$ -secretase is a zinc metalloprotease (Roberts et al., 1994), and a type-1 transmembrane protein (Lammich et al., 1999). Enzyme activity principally occurs at

the plasma membrane (O'Brien and Wong, 2011) but some activity has also been observed in the trans-Golgi (Kuentzel et al., 1993, Epis et al., 2012). Activation of protein kinase C (PKC) causes an increase in  $\alpha$ -secretase cleavage of APP by promoting transport of APP to the cell surface (Mills and Reiner, 1999). Members of the A disintegrin and metalloprotease (ADAM) family were identified to have associated  $\alpha$ -secretase activity, specifically ADAM9, ADAM10 and ADAM17, all of which have been demonstrated to cleave APP.

The exact identity has been an area of intense research. ADAM9 knockout mice demonstrated no significant differences in A $\beta$  production or the  $\alpha$ -secretase cleavage product p3 (Weskamp et al., 2002), eliminating this ADAM as being responsible for amyloid production in the brain. Previously, ADAM17 was found to localise to plaques and tangles within the hippocampi of AD brains but its expression remains unchanged in AD (Skovronsky et al., 2001). Furthermore, the inhibition of ADAM17 leads to decreased production of sAPP $\alpha$ , one of the APP cleavage fragments. In addition, ADAM17-deficient cells retain  $\alpha$ -secretase activity (Buxbaum, 1998). Studies have strongly suggested that ADAM10 is the predominant  $\alpha$ -secretase produced within neurons (Kuhn et al., 2010). Overexpression of ADAM10 increases  $\alpha$ -cleavage whilst dominant-negative form of ADAM10 inhibited endogenous  $\alpha$ -cleavage activity (Lammich et al., 1999). ADAM10 RNA levels have been found to be significantly increased in AD brains (Gatta et al., 2002), strengthening the case of ADAM10 as the main candidate for  $\alpha$ -secretase activity. At present, the identity of  $\alpha$ -secretase is unclear, but may be due to the combined activities of both ADAM17 and ADAM10 (Nunan and Small, 2000).

Cleavage of APP by  $\alpha$ -secretase is similar to processing of the growth factors TGF- $\alpha$  and TNF- $\alpha$  and other integral membrane proteins (Werb and Yan, 1998). The mechanism involves a constitutive component and a modulated component, the latter of which is activated by PKC (Buxbaum et al., 1993) as well as other second

messengers. Generally, constitutive  $\alpha$ -secretase activity occurs in the brain arguably due to ADAM17, which is regulated by PKC. Under basal conditions,  $\alpha$ -secretase activity is estimated to outnumber  $\beta$ -secretase activity. Overexpression of ADAM10 within neurons of the cortex and hippocampus (Marcinkiewicz and Seidah, 2000) leads to reduced BACE1 processing of APP and a decrease in amyloid deposition (Postina et al., 2004). Studies such as these suggest that up-regulation of  $\alpha$ -secretase activity may potentially be of therapeutic value in AD (Postina et al., 2004).

### **1.2.3 Neurofibrillary degeneration (NFD)**

The second hallmark of AD is the neurofibrillary tangles (NFTs). NFTs are caused by intraneuronal aggregation of hyperphosphorylated protein into structures known as paired helical filaments (PHFs) (Kurt et al., 1997). PHF bundles are principally found within pyramidal cells of the entorhinal cortex, hippocampus and the supragranular (II-III) and infragranular (V-VI) layers of the association cortical areas (Braak and Braak, 1995).

PHFs are formed from phosphorylated tau (Grundke-Iqbal et al., 1986). Tau belongs to a family of neuronal microtubule-associated proteins (MAPs) whose physiological functions are to modulate microtubule network stability, as well as coordinating axonal plasma membrane and microtubule processes (Koechling et al., 2010). The human tau gene is found on chromosome 17q21, consisting of 16 exons, encoding for 6 tau isoforms as a consequence of alternative splicing of its mRNA. The relative proportions of the various tau isoforms have also been reported in other neurological disorders (Gong and Iqbal, 2008).

During neuronal development, tau stabilises microtubules in the axon. Site-specific phosphorylation of the C-terminal repeats of tau dictates its ability to bind and stabilise microtubules. Tau contains an exceptionally high number of putative phosphorylation sites (45 serines, 35 threonines and 4 tyrosines) but some sites appear to be

preferentially phosphorylated (Chen et al., 2004). It is understood that tau undergoes conformational changes to facilitate differential phosphorylation, resulting in dissociation of tau from microtubules (Gotz et al., 2011). Under pathological conditions, hyperphosphorylation at the C-terminal tail and proline-rich regions, located upstream of microtubule-binding domains (Liu et al., 2007), leads to tau dissociation from the microtubules, resulting in microtubule collapse and accumulation of tau in the dendrites.

To date, no tau mutations have been shown to directly lead to Alzheimer's disease. However neurofibrillary tangles appear independently of senile plaques in more than two dozen age-related disorders. Examples include Pick's Disease (Pickering-Brown et al., 2000), Frontotemporal dementia (Rademakers et al., 2004) and parkinsonism linked to chromosome 17 (Wray and Lewis, 2010). These disorders are termed as 'tauopathies', in which tau plays a central role in disease pathogenesis. It should also be noted that whilst tau is usually perceived as a neuronal protein, it is also expressed within non-neuronal cells such as glia and can lead to disorders such as progressive supranuclear palsy or corticobasal degeneration (Gotz, 2001).

The progression of tau pathology can be followed using Braak staging (Braak and Braak, 1991), which correlates well with disease progression (Archer et al., 2011) in relation to cognitive decline and neurodegeneration. The characteristic spread of tau tangles throughout the brain has led to the concept of the 'tau prion hypothesis'. This hypothesis centres around the idea that tau is an infectious agent capable of spreading from cell to cell, in a manner comparable to a prion protein (Reiniger et al., 2011). Prion proteins may be misfolded, leading to their aggregation as cellular prion protein in the central nervous system and can be removed from source and be injected into different tissues where they seed further aggregation and propagate pathology (Yanamandra et al., 2013). It has been shown that the transfer of tau and prion from a

mutated animal into another animal brain leads to the formation of tangles and infectious prions respectively (Morales et al., 2013).

There are six Braak stages each describing tau affected regions of the brain. Between stages I to II represent clinically silent cases, where no symptoms are exhibited by the AD sufferer. During these early stages, hyperphosphorylated tau is found in the cortex but confined to the transentorhinal region. The next stage of progression is stage II, in which there are numerous and denser neuropil threads (NT) in close proximity to the transentorhinal region. NFTs are detected within the *Cornu Ammonis* (CA) 1 regions, found within the hippocampus (Braak and Braak, 1991, Braak et al., 1993).

Stage III to IV represents incipient AD, where the presence of tau tangles and neuronal death begins to manifest as memory impairment. Neurons in the entorhinal and transentorhinal regions are affected with NFTs with hippocampal involvement. At stage V, the isocortex is severely burdened with tau tangles and by stage VI, all the changes in stages V are more prominent with neuronal death observed in the transentorhinal and entorhinal layers. In addition, many neurons of the substantia nigra stain positively for tau tangles (Braak and Braak, 1991).

In AD, tau aggregation is considered as a possible response to the disease process (Koechling et al., 2010). Cellular studies have demonstrated that A $\beta$  toxicity is dependent upon tau expression (Rapoport et al., 2002). Furthermore, studies have demonstrated the ability of tau to modulate A $\beta$  toxicity. Indeed, treatment of hippocampal slices with A $\beta$ 1-42 does not lead to the impairment of long term potentiation in Tau<sup>-/-</sup> mice (Shipton et al., 2011, Roberson et al., 2007).

### **1.3 The Causes of AD**

The presence of amyloid plaques and tau tangles in AD patient brains are important pathologically. However, as mentioned previously, the presence of plaques in non-

demented individuals (Price and Morris, 1999) suggests that the plaques themselves are not toxic to cells. Further studies have shown that oligomeric amyloid load is a better correlate of dementia symptoms. However, the presence of NFTs remains the best indicator of AD duration and severity (Arriagada et al., 1992).

Other than cases of FAD, a definitive cause for developing sporadic AD has not been established, however, a number of risk factors have been identified. Ageing is the principal factor to consider. Other factors include lifestyle, education (Hofman et al., 1997, Katzman, 1993, O'Carroll and Ebmeier, 1995, Zhang, 1990, Lindsay et al., 2002) and the inheritance of certain genes. Studies have revealed that more educated people or those who continued to learn into adulthood were less likely to develop dementia. This may reflect a compensation mechanism for neurodegeneration early in AD, however these individuals show rapid decline in cognitive function at the advanced stages of AD (Wilson et al., 2004). The importance of lifestyle choices such as diet and exercise have been demonstrated in providing protection against dementia (Daffner, 2010). Physical activity appears to slow down the decline associated with ageing and may ameliorate the rate of cognitive decline (Weuve et al., 2004, Larson et al., 2006). A Mediterranean diet has been associated with not only reducing the risk of developing cardiovascular disease and cancer but also dementia (Scarmeas et al., 2009, Scarmeas et al., 2006).

Generally, AD can be classified as being late onset (LOAD), occurring after the age of 65 or early onset (EAOD), before the age of 65. The majority of AD cases are described as late onset. In such cases, determination of common factors that lead to the development of Alzheimer's disease is problematic due to the apparent sporadic nature of the observed cases. In comparison, EOAD is associated with inheritance of autosomal dominant alleles. The contribution that genetic factors may play in sporadic cases is uncertain. However, both early and late onset AD are characterised by similar pathological phenotypes and may be clinically indistinguishable from one another.

### 1.3.1 EOAD

Early onset AD (also known as familial AD (FAD)) accounts for between 2 to 10% of all AD cases (Morgan, 2011, Selkoe, 2001b) and is genetically linked to genetic aberrations in chromosome 21, 14, and 1 where the genes encoding the Amyloid Precursor Protein (APP), Presenilins 1 (PSEN1) and 2 (PSEN2) reside respectively.

Subsets of families have been shown to carry point mutations in APP, which causes an imbalance in amyloid turnover (Haass et al., 1995), and leads to an increase in A $\beta$ 1-42 production. Mutations in the Presenilin 1 (PSEN1) and 2 (PSEN2) genes encoding for protein subunits that constitute part of the  $\gamma$ -secretase enzyme are responsible for the majority of FAD cases (Price and Sisodia, 1998, Berezovska et al., 2005) , some of which are shown in Figure 1.4. Furthermore, the cloning of the presenilin genes (Sherrington et al., 1995) has demonstrated that presenilin mutations increase the production of A $\beta$ 1-42 in humans (De Strooper et al., 1998, Scheuner et al., 1996a) and transgenic mice (Duff et al., 1996).

### 1.3.2 Sporadic AD

Late onset AD (LOAD) or sporadic AD afflicts patients late in life with incidence mainly occurring between the seventh and eight decades. It is the commonest form of AD, contributing to 95–99% of AD cases but has a weaker association with genes than FAD cases (Bali et al., 2012). However, there is speculation that genetic components could account for up to 60-70% of all LOAD cases (Hollingworth, 2011), hence identifying these genetic factors has proven to be a more challenging issue to tackle. This also complicates how to model sporadic AD *in vitro*.

Results of several large genome wide association studies (GWAS) have linked novel loci associated with LOAD. These include clusterin (CLU), phosphatidylinostol-binding clathrin assembly protein (PICALM) (Harold et al., 2009), amphiphysin II (BIN1), complement receptor 1 (CR1) (Lambert et al., 2009), bridging integrator 1, ATP-binding cassette transporter 7 (ABCA7), membrane-spanning 4-domains subfamily A, CD2AP-

CD2-associated protein (CD2AP), CD33 (sialic acid-binding immunoglobulin-like lectin) and ephrin receptor A1 (EPHA1) (Naj et al., 2011). Genetic variants in triggering receptor expressed on myeloid cells (TREM2), which encodes for the triggering receptor expressed on myeloid cells has also been linked with an autosomal recessive form of EOAD. Recently, genetic variants in the apolipoprotein E receptor (SORL1) have been found to have an increased risk of SAD (Young et al., 2015). Proteins expressed from these genes are involved in a variety of different processes shown to have some mechanistic relationship with APP/ A $\beta$ . These will be discussed in the following sections.

PICALM is involved in clathrin-mediated endocytosis, where it acts to recruit clathrin and adaptor protein complex 2 to regions of site assembly (Tebar et al., 1999). BIN1 is involved in many cellular processes, such as actin dynamics, membrane trafficking and clathrin-mediated endocytosis (Pant et al., 2009), which may affect the processing of APP and A $\beta$  production or A $\beta$  clearance from the brain.

The other genes appear to be associated with the immune system. CR1 forms part of the complement system, where it binds complement factor C3b and C4b to participate in clearing immune complexes. Amyloid can bind to C3b, which suggests CR1 may be involved with A $\beta$  clearance (Thambisetty et al., 2013). CR1 is also implicated in neuroinflammation, which occurs commonly in AD (Crehan et al., 2012). CD33 encodes for a cell surface immune receptor, which can bind sialylated glycans. Increased expression of CD33 in microglial cells has been observed in AD brain, with the number of CD33-immunoreactive microglia correlating with plaque burden (Griciuc et al., 2013).

EPHA1 encodes for cell surface receptors which bind to ephrin ligands to modulate cell adhesion, synapse formation and plasticity. EPHA1 is found on CD4-positive T cells and monocytes in the cerebrospinal fluid. Genetic variations in EPHA1 were found to

affect pathological changes in the hippocampus and the lateral occipitotemporal and inferior temporal gyri, leading to reduced risk of AD (Wang et al., 2015a). CD2AP encodes for a scaffolding adaptor protein, which regulates cytoskeletal organization. It is believed that CD2AP is associated with increased plaque burden (Liao et al., 2015).

*ABCA7* mediates the production of high-density lipoprotein with lipids and apolipoproteins. It binds APOA-I and functions in apolipoprotein-mediated phospholipid and cholesterol efflux from cells. In addition, *ABCA7* influences the transport of APP through the cell membrane and is involved in host defence. In relation to AD, loss-of-function in *ABCA7* is found increase the risk of AD in Caucasians (Steinberg et al., 2015).

Clusterin is of great interest as it is co-localised with amyloid plaques. It is an ATP-independent molecular chaperone, found to be increased in AD brains (May et al., 1990), specifically within the pyramidal neurons and non-pyramidal cells of the hippocampus and entorhinal cortex, two areas known not to be affected by AD (Lidstrom et al., 1998). Expression of clusterin is highest in the brain, particularly within astrocytes (Pasinetti et al., 1994).

Clusterin exhibits broad substrate specificity and can stabilize misfolded proteins (Poon et al., 2000), and is activated during endoplasmic stress, in what is known as the unfolded protein response (UPR). When unfolded/ misfolded protein accumulate within the ER, the UPR is activated to restore normal cellular function by stopping protein translation, degrading misfolded proteins and activating signalling pathways to recruit molecular chaperones, whose functions are to aid protein folding. Should the UPR fail to achieve this, UPR results in apoptosis, which may be involved in AD pathogenesis (Stutzbach et al., 2013, Cornejo and Hetz, 2013).

Astrocytes can secrete clusterin in response to excitatory neurotransmitter kainic acid treatment, and ischemic insults. Clusterin may improve recovery in the brain to such stresses (Imhof et al., 2006), thus explaining its co-localisation to amyloid plaques. This protein also plays a role in amyloid clearance by binding to megalin receptors (Hammad et al., 1997) on the neuronal cell membrane thus facilitating amyloid endocytosis (Nuutinen et al., 2009). It has higher affinity for the shorter A $\beta$ 1-40 peptides than for fibrils and acts to increase A $\beta$  solubility, whilst preventing its aggregation (Matsubara et al., 1995). Although it can prevent A $\beta$  oligomerization and enhance fibril formation, a balance in the ratio of clusterin and A $\beta$  peptide is required. In addition, clusterin may be found in lipoproteins and functions to regulate cholesterol and lipid metabolism, two processes that are perturbed in AD (Calero et al., 2005).

Other independent GWAS studies have identified putative genetic variants in death-associated protein kinase 1, sortilin-related receptor 1 and low density lipoprotein receptor-related protein 6 which are associated with neuronal apoptosis, APP trafficking and altered Wnt/ $\beta$ -catenin signalling respectively (Waring and Rosenberg, 2008). A large meta-analysis from the AlzGene database reported thirteen additional potential AD-susceptibility genes including Angiotensin I converting enzyme, oestrogen receptor 1, prion protein mitochondrial transcription factor A as well as tumour necrosis factor (Waring and Rosenberg, 2008).

The most influential genetic factor associated with sporadic AD is the apolipoprotein E4 (APOE4) genetic variant which is carried by 15% of the human population (Coon et al., 2007). The APOE4 gene mapped to chromosome 19, encodes for a plasma lipoprotein which functions to transport cholesterol (Mahley, 1988). There are 3 known alleles; ApoE2, ApoE3 and ApoE4, of which the E4 variant carries an increased risk of AD (He et al., 2007), but is not essential for AD to develop. ApoE is produced and secreted in the central nervous system by astrocytes (Ignatius et al., 1986), with levels highest in the brain and liver (Elshourbagy et al., 1985). Levels of ApoE are increased

after injury and are increased in neurodegenerative diseases. In AD, it is localised to extracellular senile plaques and intracellular neurofibrillary tangles (Namba et al., 1991), strongly supporting its role in AD.

The mechanism by which ApoE plays a role in AD pathogenesis is unclear but one theory is that APOE4 interacts with a receptor that leads to increase A $\beta$  production. Specifically, the receptor APOE2R, expressed in the brain has been shown to alter A $\beta$  levels presumably via an unknown binding interaction (Hoe et al., 2005). Neuro-2a cells transfected with the Swedish mutation of APP (SweAPP695) demonstrated a twofold increase in A $\beta$  production in the presence of human very low density lipoproteins (VLDLs)(where APOE4 is most abundant) but not with LDL and HDL (high density lipoproteins) (Huang et al., 2001). In these cells, the presence of APOE4 may stimulate APP internalization and translocation of BACE1 from the cell membrane to endosomes. Transgenic animal studies have demonstrated that APOE4 is linked to amyloid deposition (Bales et al., 2009, Hartman et al., 2002) but as yet, there is poor understanding of the mechanistic relationship between the two. ApoE has also been found to have avid affinity for amyloid (Strittmatter et al., 1993), a finding which was confirmed by ApoE immunoreactivity with cerebral and systemic amyloid taken from patients (Wisniewski and Frangione, 1992).

### **1.3.3 The amyloid hypothesis**

At present, the amyloid cascade hypothesis is the most commonly accepted process thought to lead to AD pathology. Indeed, several mutations involved in familial AD influence amyloid production. The conventional view of AD is that the majority of the pathology is driven by an increased burden of A $\beta$  in the brain, which can be influenced by APP mutations such as the Swedish, London, Indiana and Arctic (see Figure 1.4). These different point mutations occur in different regions of the APP gene but all lie within or close the A $\beta$  peptide region. At least 33 mutations within the APP gene have been identified to be associated with EOAD (Cruts et al., 2012) and a related disorder

of hereditary cerebral amyloid angiopathy (CAA) (Weggen and Beher, 2012). APP duplication can also cause early-onset AD with CAA, as demonstrated by the increased incidence AD in individuals with trisomy 21 (who suffer from Down syndrome) (Roizen and Patterson, 2003). Recently, one APP mutation found in the Icelandic population which is an A673T substitution affects  $\beta$ -secretase cleavage of APP leading to a fall of A $\beta$  by approximately 40% (Jonsson et al., 2012). This is the only known mutation shown provide life-long protection against age-related cognitive decline. Such mutations suggest that therapy directed against  $\beta$ -secretase cleavage need only reduce A $\beta$  levels by 40% rather than eliminate its production completely to be effective whilst extending lifespan.

The A $\beta$  hypothesis states that the A $\beta$  aggregates trigger a complex pathological cascade that results in neurodegeneration. Emphasis on the importance of the amyloid hypothesis has been performed in studies using transgenic mice which overexpress human APP and mutant tau (Gotz et al., 2001, Lewis et al., 2001). These mice develop plaques before developing neurofibrillar deposits (Selkoe, 2001a). Furthermore, expression of human BACE1 in mice led to cleavage of murine APP to A $\beta$  56 and A $\beta$  hexamers. Mice exhibited AD-like phenotypes from three months of age which progressively worsened over time (Plucinska et al., 2014). It must be noted that no human mutations in tau have been found in Alzheimer's disease. Furthermore, to simulate significant AD pathology in rodents, mutations in both APP and tau are necessary. The increased incidence of AD in Down syndrome humans caused by trisomy of chromosome 21 (Glennner and Wong, 1984a) further supports this hypothesis. Such evidence suggests that A $\beta$  is an integral part of the disease and may be a more important factor to consider in comparison to tau (Hardy and Selkoe, 2002).

#### **1.4 Pathogenic mechanisms of Amyloid**

The manner in which A $\beta$  aggregates and the particular species of peptide produced is vital to consider. In AD, APP is cleaved to form a range of peptides; of these the A $\beta$ 1-

42 form is strongly associated with neurotoxicity both *in vivo* and *in vitro*. These neurotoxic effects lead to gradual impairments in short-term memory and cognition due to neuronal dysfunction (Rönicke et al. 2011) and death in the hippocampus, limbic system and cerebral cortex (Jhoo et al. 2004). The mechanism by which neuronal death occurs may be due to a number of pathways, some of the key mechanisms will be outlined in the subsequent sections.

#### **1.4.1 Calcium homeostasis**

A $\beta$ 1-42 has been shown to cause changes in calcium ( $\text{Ca}^{2+}$ ) concentration signals when applied to primary cultures of hippocampus or cortex-derived neurons and astrocytes (Abramov et al., 2004). These intracellular signals were limited to astrocytes. A $\beta$ -induced hyperactivity in astrocytes has also been observed in AD mice models (Kuchibhotla et al., 2009). This observation and the lack of response using calcium channel inhibitors led to suggestions that A $\beta$  itself might form calcium permeant channels in the astrocyte membrane, as a possible pathogenic mechanism (Arispe et al., 1993, Bhatia et al., 2000, Abramov et al., 2003). The changes in intracellular calcium levels in astrocytes could impair the astrocyte's role in supporting neuronal viability, leading to neuronal death. Neuronal death has been confirmed by deficits in cholinergic transmission and loss of synaptophysin protein (Morgan et al., 2004b). These aberrations are believed to result partly from oxidative stress and damage to the membrane.

#### **1.4.2 A $\beta$ -induced excitotoxicity**

Excitotoxicity describes the phenomena in which over-activation of the glutamate N-methyl-D-aspartate (NMDA) receptor (NMDAR) leads to increases in intracellular calcium by directing opening channels and affecting calcium homeostasis. Elevated calcium levels can overactivate several enzymes, such as PKC, calcium/calmodulin-dependent protein kinase II, phospholipases, and nitric oxide synthase (NOS) (Mark et al., 2001). One of the consequences of excessive stimulation of glutamate receptors, is the generation of nitric oxide (NO) and superoxide ions via NOS activation leading to

neuronal death. The release of NO is detrimental to the cell as it can cause downstream misfolding, aggregation and mitochondrial fragmentation. This process is one mechanism that underlies A $\beta$ -mediated neurodegeneration with evidence to suggest that amyloid itself can bind to the NMDAR (Texido et al., 2011). In the absence of glutamate, A $\beta$  oligomers was found to activate recombinant NR1/NR2A and NR1/NR2B receptors (subunits of NMDARs). In the same study, A $\beta$  oligomers are also able to activated native NMDARs with preference to receptors lacking NR2B subunits. This observation identified a possible therapeutic target, using antagonists directed against NR1/ NR2B receptors (Farlow, 2004). Clinically, anti-glutamatergic drugs have previously been demonstrated to ameliorate symptom severity in cases of moderate-to-severe AD (Reisberg et al., 2003).

The activation of glutamate receptors mediates many downstream processes such as inducing calcium ion influx, calpain activation, and dynamin-1 degradation (Kelly and Ferreira, 2006). Synapses, are structures that are essential to allow the passing of electrical signals (in the form of neurotransmitters) between neuronal cells, and are highly enriched in calpains 1 and 2 (Perlmutter et al., 1988). Calpains are calcium-dependent cysteine proteases with poorly understood functions. It is known that dysregulation calpain activity is leads to tissue damage during ischaemia and brain trauma (Goll et al., 2003). Increased levels of Calpain 2 are found to be associated with an increased risk of developing NFTs (Grynspan et al., 1997). The overactivation of calpain is one consequence of high calcium levels (Nixon, 2003), and can indirectly modulate APP processing (Siman et al., 1990, Mathews et al., 2002) as well as tau phosphorylation (Huang and Wang, 2001).

Another key consequence of excessive activation of NMDARs by amyloid, is the inhibition of LTP (Li et al., 2011, Taylor et al., 2008b). This finding could explain the memory loss observed in AD. Glutamate receptors located at synapses are vital for LTP, and also lie upstream of signalling pathways that lead to cell death. The inhibition

of LTP involves a series of kinases, most notably p38 MAP kinase and Jun NH<sub>2</sub>-terminal kinase (JNK). Both enzymes are also associated with tau phosphorylation, but inhibitors of these targets do not appreciably reduce neuronal cell death. The activity of Fyn kinase is of great interest and may link both amyloid and tau (Haass and Mandelkow, 2010). Tau is localised to dendrites, where it acts to target Fyn to the dendrite, to phosphorylate NMDAR subunit, NR2B (Bhaskar et al., 2005). This allows Fyn to modulate synaptic activity and plasticity. FYN/hAPP mutant mice exhibit impaired neuronal induction of Arc (activity-regulated cytoskeleton-associated protein) and spatial memory (Chin et al., 2005). The importance of tau is illustrated by the fact that without tau, excitotoxic signalling does not occur (Hoyos Flight, 2007). Tau reduction (studied with tau<sup>-/-</sup> mice-derived hippocampal cultures) also prevents the inhibition of axonal transport of mitochondria induced by amyloid (Vossel et al., 2010).

#### **1.4.3 Mitochondria and oxidative stress**

Cellular metabolism can be described as the process by which cells produce and consume energy in the form of adenosine triphosphate (ATP) in order to carry out metabolic functions. There are two main methods by which ATP is generated, one is oxidative phosphorylation, which takes place in mitochondria and the other is glycolysis, which occurs in the cytosol. At times of high demand, cells may interchange between the two distinct processes to maintain energy homeostasis.

Oxidative phosphorylation is a multi-step process, which involves the co-operation of several complexes. Mitochondria are unique organelles, originating from the symbiotic association between a proto-eukaryotic cell and a bacterium (Thrash et al., 2011). They have double membranes, are self-replicative, and carry 16.5 kB of DNA, which encode for 13 polypeptides that form part of the electron transport chain involved in oxidative phosphorylation. Synapses are highly enriched with mitochondria, where they are dynamic and mobile. Transport of mitochondria from the neuronal body to the axon occurs by microtubule-assisted transport (MacAskill and Kittler, 2010) and is vital

for not only ATP production but also maintaining calcium homeostasis (Patergnani et al., 2011).

Mitochondria are the main source of oxidative stress, in form of free radicals (also known as reactive oxygen species (ROS)), such as O<sup>-</sup>, HO<sub>2</sub>, H<sub>2</sub>O<sub>2</sub> and RO<sub>2</sub> and have been implicated in a range of pathologies that include cardiovascular disease, diabetes, cancer and neurodegeneration (Raha and Robinson, 2000). This is due to their wide involvement in a range of cellular processes such as fatty acid-oxidation (Kunau et al., 1995), cellular signalling (Tait and Green, 2012), apoptosis (Gulbins et al., 2003) and heme biosynthesis (Atamna, 2004). However, it should also be noted that these free radicals also play an important roles molecules in cell proliferation and survival (Ray et al., 2012a).

#### **1.4.3.1 Mitochondria in AD**

Mitochondrial dysfunction is implicated to play a role in AD pathogenesis. Neurons have a high energy demand that is met predominantly through the electron transport chain (glycolysis can be used to provide ATP at a faster rate but is not sustainable). Mitochondria also play important roles in calcium homeostasis, signal transduction and apoptosis (Abramov et al., 2004, Rottenberg and Scarpa, 1974, Green and Reed, 1998, Babcock et al., 1997, Brookes et al., 2002). Therefore, aberrant mitochondrial function leads to adverse effects in alterations in energy metabolism, the generation of excess free radicals and calcium homeostasis (Davis et al., 1997a).

Amyloid mediated-activation of extrasynaptic glutamate receptors can have detrimental downstream effects on mitochondria (Ciani et al., 1996) (Weber, 1999) via the release of nitric oxide (NO). A $\beta$  can stimulate  $\alpha$ 7 nicotinic acetylcholine receptors to induce astrocytic glutamate release, which activates extrasynaptic NMDARs on neurons (Talanta et al., 2013). In response to NMDAR activation, intracellular Ca<sup>2+</sup> levels rise, which induce nitric oxide synthase activity to produce NO. NO can then act as a

signalling molecule (Garthwaite, 1991); one consequence of which is to activate guanylate cyclase to stimulate cGMP formation, eliciting the relaxation of blood vessels. However, excessive NMDAR activation can lead to excess NO, which is a potent inhibitor of mitochondrial respiration (Bolanos et al., 1997). In addition to promoting mitochondrial fragmentation, NO competes with oxygen to bind reversibly to cytochrome oxidase (Sarti et al., 2012), causing a fall in ATP production and sensitization to hypoxia (Brown and Bal-Price, 2003). NO can also be converted to reactive oxygen species such as peroxynitrite, NO<sub>2</sub>, N<sub>2</sub>O<sub>3</sub>, and S-nitrosothiols, which in turn interact with key enzymes of the mitochondrial respiratory chain and can activate mitochondrial permeability transition, leading to cell death (Le et al., 1995). The importance of free radicals was demonstrated by the delayed progression of cognitive impairment in AD patients treated with the antioxidant Vitamin E (Dysken et al., 2014, Sano et al., 1997).

Mitochondrial respiration itself is a major source of free radicals. Free radical production is believed to be vital in the initiation and progression of neurodegeneration in AD. These highly unstable molecules may also be generated in response to bacterial or viral infection and during the normal oxidative metabolism of substances. When levels of ROS exceed the antioxidant capacity of cells, this leads to toxicity and cause oxidative injury. Targets of ROS include mitochondria themselves, membrane lipids, proteins and nucleic acids. ROS is also implicated in other diseases in association with atherosclerosis, diabetes and aging (Ray et al., 2012b).

The association of oxidative injury and ROS generation to AD has been demonstrated by presence of iron (Fe), copper (Cu) and zinc (Zn) accumulating within the brains of AD patients (Exley et al., 2012), as well as elevated levels of peroxynitrite (Smith et al., 1997), increased expression of heme oxygenase (Smith et al., 1994, Barone et al., 2012), elevated lipid peroxidase activity (Montine et al., 2002) and high levels of hydroxynonenal (Sayre et al., 1997), a lipid peroxidation product. Metals have long

been implicated in A $\beta$  deposition *in vivo*, where zinc and copper participate in NMDA-induced activation, and react with A $\beta$  to form amyloid aggregates (Barnham and Bush, 2008). These complexes of amyloid: Fe/Cu are considered to be pathologically important in AD (Bishop and Robinson, 2004).

#### **1.4.3.2 APP accumulation within mitochondria**

Further evidence for the involvement of mitochondria in AD is that the N-terminal region of APP contains a mitochondrial targeting signal, with the positively charged residues at positions 40, 44 and 51 revealed as vital components. In human cortical neurons expressing either wild type APP or Swedish APP695, APP was found to be localized not only to the plasma membrane, but also to the mitochondria of these cells (Anandatheerthavarada et al., 2003). Furthermore, mammalian cells transfected with APP also demonstrate sub-localization of APP to the mitochondria. The effects of APP695 expression have been associated with decreased mitochondrial membrane potential, decline in ATP levels and cytochrome c oxidase activity (Anandatheerthavarada and Devi, 2007).

Recent studies have observed A $\beta$  accumulation within mitochondria (Lin and Beal, 2006, Lustbader et al., 2004). In AD patients and transgenic mice, amyloid accumulates gradually within brain mitochondria, causing mitochondrial dysfunction energy failure, altered mitochondrial properties and release of ROS. One particular mitochondrial enzyme found to bind A $\beta$  with high affinity is ABAD (A $\beta$ -binding alcohol dehydrogenase) (Yao et al., 2011). ABAD has broad substrate specificity and its levels are increased in the cerebral cortex and hippocampus of AD-affected brain regions of humans and rodents (Lustbader et al., 2004, Mei et al., 2010, Yan et al., 2010). Tau itself can affect the activity of Complex I of the mitochondrial respiratory chain (Swerdlow et al., 2000) and therefore both amyloid and tau can synergistically impair mitochondrial functions, contributing to oxidative stress leading and a reduction in

energy metabolism (Gotz et al., 2011). Mitochondrial function in AD will be discussed further in Chapter 3.

### **1.5 The physiological role of APP**

Despite many studies on AD, there is no definitive agreement on the physiological function of APP. APP is widely expressed throughout the body with the APP695 isoform, being the predominant form in the central nervous system and the peripheral nervous system (Golde et al., 1990, Arai et al., 1991, Kang and Muller-Hill, 1990). Deletion of the APP gene in mice produces viable offspring but the mice exhibit cerebral gliosis, impaired learning and memory and changes in locomotor behaviour. In the same study, APP KO mice showed reduced growth throughout adult life suggesting that APP plays a role in somatic growth and muscle development (Senechal et al., 2008). This was also reflected *in vitro*, where fibroblasts expressing an antisense APP construct to decrease APP levels exhibited slower growth, a finding which was reversed by treating the cultures with APP (Saitoh et al., 1989).

Proteins homologous to APP have been identified in *Drosophila*, *C.elegans* and mammals (Zheng and Koo, 2006a, Link, 2005, Zheng and Koo, 2006b) but these lack the A $\beta$  domain. Structural studies of APP (see Figure 1.5) have led to the identification of several domains such as the growth factor-like domain (Rossjohn et al., 1999) and the copper-binding domain, that form part of the E1 and E2 domains (Barnham et al., 2003). Indeed, studies have shown that amyloid binds to both Cu and Zn. (Stellato et al., 2006). Evidence of involvement in iron export has also been linked to APP (Duce et al., 2010b), as a functional Iron-Responsive Element (IRE) stem-loop exists within APP mRNA, which has sequence homology to IREs for ferritin and transferrin receptor mRNA (Rogers et al., 2002). Indeed, cytoplasmic free iron levels were found to influence APP translation, with APP<sup>-/-</sup> mice showing vulnerability to iron, leading to oxidative stress within cortical neurons (Duce et al., 2010a).

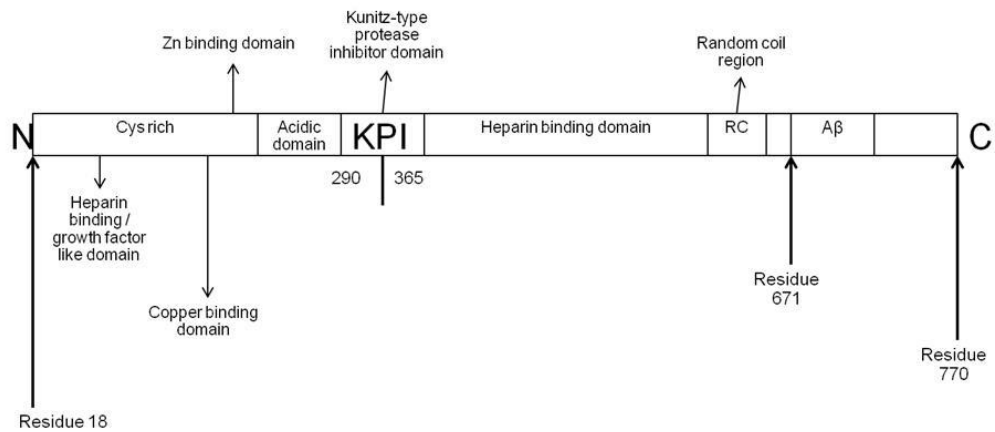


Figure 1.5 Diagrammatic overview of the primary sequence of full-length APP, its main domains and the residue positions.

Other studies have linked APP to roles in regulating synaptic formation and neural plasticity (Turner et al., 2003, Thinakaran and Koo, 2008). An increasing number of studies strongly suggest that Aβ plays a role in normal synaptic function. For example, in hippocampal slices, BACE1 activity is increased by synaptic activity but Aβ peptides were able to lower excitatory transmission through AMPA (non-NMDA type receptor for glutamate) and NMDA receptors, implying a role in homeostatic plasticity (Taylor et al., 2008a). Furthermore, Aβ release has been demonstrated to be activity-dependent. This has been shown for both Aβ1-40 and Aβ1-42 when APP was overexpressed following transfection and when produced endogenously (Kamenetz et al. 2003). Interestingly, patients with traumatic brain injury show an increase in cerebral amyloid as neuronal function and mental status recover (Brody et al., 2008). In addition, amyloid has been associated with neuronal survival and increasing LTP in the hippocampus (Giuffrida et al., 2009).

Full-length APP may function to facilitate cell adhesion and cell-cell interactions due to the presence of an RHDS motif (Ghiso et al., 1992). This region may act like an integrin and can be blocked by the RGDS peptide found from within the fibronectin-binding domain. APP has previously shown to co-localise with integrins on axonal surfaces and interact with laminin and collagen (Storey et al 1996, Breen 1992) via its heparin binding domain.

Analysis of the APP primary structure has identified the presence of a YENPTY sequence, which contains consensus sequences for a phosphotyrosine binding (PTB) domain interaction (Borg et al., 1996). Proteins like the neuronal X11 and the adaptor protein, Fe65 (which forms a complex with AICD) contain PTB domains and are found to bind to APP (Borg et al., 1996).

Other APP fragments also display physiological functions. The N-terminal sAPP $\alpha$  fragment has been shown to promote axonal outgrowth (Billnitzer et al., 2013) and appears to drive the neuronal differentiation of human embryonic stem cells (Freude et al., 2011). These findings suggest that it may play a neuroprotective role. Furthermore, APP $\alpha$  is involved in proliferation of neural stem cells and non-neuronal cells (Ohsawa et al., 1999, Pietrzik et al., 1998). In addition, sAPP $\alpha$  was found to increase glucose uptake in neurons (Mattson et al., 1999) and has memory-enhancing effects, by increasing LTP (Bour et al., 2004) and facilitates NMDA receptor-mediated currents (Taylor et al., 2008b). AICD fragment has been found to act as a transcription factor (Lee et al., 2008a), regulating cell death (Wang et al., 2014b), neprilysin-mediated A $\beta$  degradation (Belyaev et al., 2009), influencing calcium and ATP homeostasis (Hamid et al., 2007) and regulating intracellular trafficking and cytoskeletal dynamics (Muller et al., 2007).

Increasing evidence suggests that AD could be defined as a systemic disorder with the expression of abnormalities most evident in neuronal tissue. Several pathological changes have been observed outside of the brain, for example, increase in platelet membrane fluidity (Zubenko et al., 1987) and changes in membrane protein states erythrocytes (Markesbery et al., 1980, Bosman et al., 1991). Expression of APP outside the brain will be discussed in Chapter 4.

## **1.6 The study of AD using models**

AD is an increasingly complex disorder, in which the pathogenic mechanisms have been studied using a variety of different models. Each of these models has provided valuable insight into AD pathology as well as the physiological function of APP (section 1.5). Here, an outline of the commonly used AD models will be discussed.

### **1.6.1 Animal models**

Since the discovery of specific genetic mutations and the advancements in molecular genetics, scientists have generated a range of transgenic animal models. Such models have demonstrated behavioural effects due to mutant transgene expression, producing some of the pathological characteristics seen in human AD. However, massive neuronal cell loss has only been attained in a few mouse strains that express multiple transgenes.

The first mouse model to exhibit amyloid plaques was derived from expression of the pathogenic V717F APP mutation under a platelet-derived growth factor mini-promoter (PDAPP). These PDAPP mice present with extensive deposits of extracellular plaques, astrogliosis and neurite dystrophy (Games et al., 1995), all of which are associated with the pathological features of AD. Other researchers have demonstrated similar phenotypes in the Tg2576 strain and the APP23 strain, both of which utilised the Swedish APP695 mutation (Hsiao et al., 1996, Gotz and Ittner, 2008). The Tg2576 mouse remains the most widely used model of AD. However, these mice fail to demonstrate extensive neuronal death observed in humans (Richardson and Burns, 2002).

The triple transgenic (3xTg-AD) mouse, which carries the mutant PS1 (M146V), APP (Swe) and tau (P301L) transgenes (Oddo et al. 2003) develop plaques and tangles but also exhibit synaptic dysfunction including LTP deficits that precedes the appearance of plaques and tangles. These mice are useful to study pathogenic mechanisms and to develop therapeutic approaches (Blurton-Jones et al., 2009). Whilst this model is one

of the few to show the majority of pathologies associated with human AD, this is not truly reflective of human pathology in which a single mutation is able to induce AD.

Whilst animal models have been useful, AD is only found in humans and higher primates, and therefore the use of rodent models should be questioned. To date, there are no animal models which fully recapitulate the human AD pathology without the use of multiple mutant gene expression.

### **1.6.2 *In vitro* Models**

In addition to animal models, scientists have created a number of *in vitro* models to investigate specific aspects of the disease. Cultured models provide an easy platform to study cells under controlled conditions allowing the investigation of disease processes. Such models also allow for the screening of therapeutic drugs. However, the simplicity of these models do not reflect the complex cellular networks seen in tissues, and therefore the results obtained should be treated with caution when translating to complex tissues.

#### **1.6.2.1 Transformed cells**

As AD is a neurological disorder, it is natural to use neuronal cells to study such a disease. The SH-SY5Y neuroblastoma cell line, derived from the SK-NSH cell line is a common model used because it reaches confluency quickly, and can be easily transfected. In addition, researchers have developed protocols to enhance their neuronal differentiation by supplementation with retinoic acid and brain-derived neurotrophic factor (BDNF) (Jamsa et al., 2004). A number of studies carried out using this cell line have investigated the effects of mutant PSEN1 (Fang et al., 2006) and its effects of intracellular storage (Smith et al. 2002), tau phosphorylation (Löffler et al., 2012, Huang et al., 2014), the effects of mutant Swedish APP expression (Di et al., 2010) and the inhibition of A $\beta$  production by Zn (Lee et al. 2009). Additionally, the effects of amyloid on neuronal CRMP-2 phosphorylation (Petratos et al., 2008) and

how different APP isoforms lead to different APP metabolites (Belyaev et al., 2010) have been studied using this cell line.

Another neuroblastoma cell line that was previously used is the human IMR-32, derived from 13 month old male brain. IMR-32 cells were found to accumulate an intracellular fibrillary material which reacts positively for anti-paired helical filament antibodies when using *in situ* immunoelectron microscopy (Neill et al., 1994). This cell line has also been used to study expression and processing of APP. More recently, the protective role of S100b, against A $\beta$ -42-dependent toxicity has also been studied in this cell line (Clementi et al., 2013).

In addition, to neurons the brain also contains a number of other cell types such as astrocytic cells. Astrocytic cell lines such as the U373 astrocytoma are useful because of their fundamental role within the pathology of AD including protection of neurons from excitotoxicity and to allow the study of the effects of reactive gliosis (Beach et al., 1989).

To investigate toxic effects on heterogenous cultures, co-cultures of different cell types have also been used. For instance, THP-1 (a macrophage like) and SH-SY5Y (Messmer and Reynolds 2005) have been co-cultured together. In addition, co-cultures of THP-1 and U373 cells (Klegeris et al., 1997) as well as, SH-SY5Y and glioblastoma U251-MG cells have been studied (Fujiki et al. 2012). Whilst co-cultures of these cells are useful to investigate how they communicate with each other, they are hampered by the proliferative nature of the cells used, making these cultures unsuitable for chronic studies.

#### **1.6.2.2 Primary cultures**

Many early AD studies were based on primary cultures and brain slices. This requires careful extraction of animal tissue which is first dissociated and then plated onto either

a plastic surface or grown in suspension. The expression of cellular features and plating efficiency is greatly influenced by different factors, which include culture environment, tissue type and the dissociation technique utilised (Harry et al., 1998). Tissue taken from adult brains are fully differentiated and post-mitotic, which limits their effective lifespan in culture. However, the sources of embryonic rodent brains, which contain more neural progenitor cells has provided a solution to this issue. Whilst these tissues may provide useful insights into disease process, inherent species differences may impede the relevance of these models.

More valuable and relevant sources of tissue would be those taken from human brain biopsies. In the UK, resource centres have been set up with support from the Medical Research Council, Alzheimer's Research UK and the Alzheimer's Society. These cellular banks provide valuable yet limited sources of human AD brain tissue, revealing key information about late AD pathogenesis; but may be considered of limited use when investigating early AD development.

#### **1.6.2.3 Stem cell models of AD**

The issue of producing co-cultures of the different cell types required to simulate the complex environment of the brain could be solved by the use of stem cells. Undeniably, human embryonic stem cell (hESC)-derived neuronal cultures have become an attractive alternative model. They are human in origin, differentiate into multiple cell types found in the brain and can become truly postmitotic. Despite their potential, ES cell studies have been hampered by their inherent ethical issues (de Wert and Mummery, 2003). Such problems have forced researchers to look for alternative sources of stem cells. In 2006, Japanese scientists (Takahashi and Yamanaka, 2006b), used somatic fibroblasts to create ES-like pluripotent stem cells. These cells came to be known as induced pluripotent cells (iPSCs). Self-renewing iPSCs can be generated from somatic cells from any individual and as they are genetically identical to the donor, make them ideal as cell-based models for studying human disorders (Chen

and Xiao, 2011). Indeed, iPSCs have been derived from patients suffering from amyotrophic lateral sclerosis, spinal muscular atrophy and familial dysautonomia (Hu et al., 2010).

The reprogramming of somatic cells to iPSCs involves the expression of Yamanaka factors (Oct3/4, Sox2, Klf4, c-Myc) to induce pluripotency (Takahashi and Yamanaka, 2006a, Park et al., 2008b). Cell-to-cell variations do occur in different laboratories which can reflect the inefficiency and extensive procedure to produce iPSCs. Therefore, when proceeding to generating disease-specific iPSCs, several factors need to be considered. These include the source of somatic cells used, method of cellular reprogramming (retroviral or episomal) and the reliability of differentiation protocols to produce mature cell types (Mohamet et al., 2014).

With respect to the brain, the development of differentiation protocols to produce functional cortical neurons has recently been demonstrated successfully (Shi et al., 2012b). iPSCs derived from Down syndrome patient fibroblasts were successfully differentiated into neuronal networks (Shi et al., 2012a) to model AD. This model demonstrated detectable AD pathologies over a period of months, allowing the researchers to probe into AD development as the cultures age (Livesey, 2012). Detecting early changes in cellular responses that precede plaque and tangles would allow researchers to find therapeutic drugs to target AD earlier. This is particularly important as current drugs only treat symptoms and not the cause of the disease, which most likely lies upstream of amyloid deposition.

Other studies using iPSCs-based neurons have demonstrated the ability to recapitulate pathological features of AD *in vitro* (Israel et al., 2012, Shi et al., 2012a, Qiang et al., 2011, Sherer et al., 2003, Yagi et al., 2011). Indeed, iPSC-derived neurons from patients with either PSEN1 or PSEN2 mutations give rise to heterogenous neuron populations, with increases in A $\beta$ 42 secretion but variable expression of tau (Yagi et

al., 2011). These cultures were also responsive to  $\gamma$ -secretase inhibitors, which demonstrate the drug screening potential of using such cellular models.

Another cell line which has been used to study AD is the clonally derived, pluripotent human embryonal carcinoma NTERA-2 cl. D1 (NT2/D1) (Andrews et al., 1984). Retinoic acid treatment differentiates these cells into functional networks of neurons and astrocytes, providing a suitable model for human development (Andrews et al., 1984, Lee and Andrews, 1986, Pleasure et al., 1992). The neurons and astrocytes exhibited morphology and functional properties consistent with these cell types (Hill et al., 2012), allowing the use of such cultures for studying human toxicology/disease models (Hill et al., 2008, Woehrling et al., 2007, Hill et al., 2013). This cell line also highlights the importance of incorporating astrocytes into the cultures, which facilitate neuronal survival and maturation (Hartley et al., 1999). Recent work in our laboratory (Tarczyluk et al., 2015) demonstrated that NT2-derived neuronal and astrocytic co-cultures treated with A $\beta$ 1-42 display significant changes in metabolism, which is reflected in both human brain scans and some animal studies. In this study, hypometabolism was observed in relation to glucose, pyruvate, lactate and glycogen, all of which known to provide alternative fuel sources in the brain under different conditions. Such changes also led to a reduction in cellular ATP levels, suggesting energy deficiencies could prove detrimental to the brain which has a high energy expenditure to facilitate LTP, neurotransmission and combating oxidative stress. Other effects of A $\beta$ 1-42 observed was its ability to induce oxidative stress and calcium responses and decrease the availability of NAD<sup>+</sup>, potentially affecting antioxidant production, ATP generation and DNA repair.

### **1.7 Therapeutic targets**

Significant efforts have been made to develop treatments that reduce A $\beta$  production via enzyme inhibitors or the use of specific antibodies to target the neurotoxic A $\beta$  1-42 species. Whilst there are numerous avenues of research being investigated, it was

estimated that between 2002 and 2012, 99.6 % clinical trials aimed at preventing or reversing AD failed (Cummings et al., 2014). It was considered that this is mainly due to treating patients at a point when the disease is too advanced. As such there is a significant effort to improve diagnosis by identifying biomarkers to detect AD earlier.

### **1.7.1 BACE Inhibitors**

BACE1 is considered to be a therapeutic target for AD because it is the rate-limiting step in the A $\beta$  production process (Evin and Kenche, 2007). BACE inhibitors have been developed to inhibit A $\beta$  production, with animal experiments demonstrating a reduction in A $\beta$  production. More recently, a potent BACE inhibitor AZ-4217 was found to inhibit soluble amyloid deposition in the Tg2756 mice, with high target selectivity and no noticeable side effects (Eketjall et al., 2013). Currently, another inhibitor AZD3293, developed by AstraZeneca will be entering Phase II/III trials in patients with early onset AD, after it was found to dose-dependently reduce A $\beta$  levels in cerebrospinal fluid from AD and healthy volunteers in Phase I trials.

### **1.7.2 Anti-A $\beta$ targeting antibodies**

A more direct method of targeting A $\beta$  is to develop anti-A $\beta$  antibodies but success in this area has been limited. Results from clinical trials either failed to show sufficient clinical benefit in reducing the number of plaques or patients exhibited severe side effects associated with cerebral amyloid angiopathy (CAA, where amyloid is deposited in blood vessel walls) including oedema and haemorrhaging in the brain (Castello et al., 2014).

A newly developed antibody, mE8 which acts to specifically bind to pyroglutamate A $\beta$  (found in amyloid plaques) but not to soluble A $\beta$  has been used (Roh and Holtzman, 2012). Pyroglutamate A $\beta$  has its first two N-terminal amino acids of A $\beta$  truncated with the following posttranslational conversion of the third amino acid, glutamate to pyroglutamate. This form of A $\beta$  has a higher propensity to aggregate, forming oligomers and is more toxic than other amyloid forms. When mE8 was administered to

PDAPP mice (which express mutated APPV717F), it reduced insoluble A $\beta$  levels without side effects. This antibody was also effective in decreasing amyloid plaques and insoluble A $\beta$  when given as a preventative treatment. Better targeted drugs such as this antibody may one day prove useful as this approach considers that not all amyloid is toxic but may have more critical functions.

### **1.7.3 Enzyme Inhibitors**

Current treatments used to treat AD only help to ameliorate the symptoms. These treatments concentrate on modulating neurotransmitter levels (either by inhibiting acetylcholine release or preventing glutamate-associated excitotoxicity). Such treatments may improve quality of life, but may only be prescribed in those with moderate to severe AD.

In the AD brain, degeneration of cholinergic neurons leads to deficiency of the excitatory neurotransmitter acetylcholine (ACh), leading to adverse effects in cognitive function. Acetylcholinesterase, expressed predominantly in nervous tissue, neuromuscular junctions and plasma, plays a major role in cholinergic transmission. It is a serine-protease which hydrolyses the carboxylic ester of ACh, to produce choline and acetic acid, thereby reducing ACh levels. Therefore, acetylcholinesterase inhibitors were developed to reduce the rate at which ACh is degraded. Currently, only donepezil is approved to treat advanced AD, showing cognitive benefits in mild-to-severe AD (Howard et al., 2012). However, recently there have been some reports of severe side effects involving the breakdown of muscle tissue leading abnormal heart rhythms and kidney failure.

Targeting glutamate toxicity is also an approach that has been well-characterised in late dementia (Winblad et al., 2002). The use of the non-competitive NMDA receptor antagonist, memantine demonstrated moderate efficacy in treating moderate to severe AD (Reisberg et al., 2003). Memantine binds to the NMDA receptor to inhibit calcium

ion influx, thereby prevent the signalling cascade that leads to neuronal excitotoxicity. The decline in cognition, function and behaviour in these patients was ameliorated and justified its approved use for later stage AD treatment (Robinson and Keating, 2006).

Both of the drugs mentioned above show added benefits when given in combination (Lopez et al., 2009). In addition to these traditional treatments, AD patients can be treated with antipsychotic drugs, which are typically prescribed to treat agitation, aggression and psychosis. However, the adverse side effects of sedation and Parkinsonism accompanying drug use limit their usage (Ballard and Howard, 2006). Despite development of these inhibitors, the efficiency of these drugs was found to decrease over time. As these can only ameliorate the symptoms and not cure the patient, the outlook for dementia sufferers remains disappointing. Sadly there is a severe lack of reliable biomarkers that allow clinicians to detect AD symptoms to treat patients early in disease. A recent study investigated the health of cholinergic neurons in post mortem brains from people aged 20-95, of both AD patients and healthy controls. Investigators demonstrated the accumulation of A $\beta$  within neurons in patients as young as 20 years, decades before the onset of dementia (Baker-Nigh et al., 2015)

#### **1.7.4 Targeting Tau**

Numerous studies have demonstrated the requirement of tau for A $\beta$ -mediated neurotoxicity *in vitro* and *in vivo* (Roberson et al., 2007, Ittner et al., 2010, Park and Ferreira, 2005). Furthermore, the absence of tau confers some protection against excitotoxicity, where tau plays a key role in postsynaptic NMDAR signalling (Ke et al., 2012). Therefore therapeutic strategies against tau are currently being developed (Gotz et al., 2012). One approach is to inhibit tau aggregation with low-molecular mass compounds (Brunden et al., 2009). Phase II data showed that methylene blue (MB), was reported to inhibit tau aggregation (Wischnik and Staff, 2009), although later work in tau transgenic fish failed to show improvement (van Bebber et al., 2010). A study in 3xTG AD mice fed with MB ameliorated AD pathology by increasing proteasome

activity and promoting amyloid clearance (Medina et al., 2011). These encouraging studies provide further incentive to consider MB as a possible future treatment.

Another strategy for targeting tau would be to inhibit tau hyperphosphorylation using glycogen synthase kinase 3 beta (GSK-3 $\beta$ ) inhibitors. Two commonly used mood stabilizers; lithium and valproic acid (VPA) inhibit this enzyme and were shown to reduce tau phosphorylation in animal models. The anticonvulsant drug, VPA was shown to reverse AD pathology in mouse models by reducing amyloid plaques (Noh and Seo, 2014). VPA is a histone deacetylase (HDAC) inhibitor, with age-dependent effects on AD mice, by increasing nerve growth factor expression and improving cognitive function (Long et al., 2013). Furthermore, it was shown to inhibit GSK-3 $\beta$  *in vitro* and increase clusterin expression (Chen et al., 1999, Nuutinen et al., 2010). Despite showing promise, a long term study in AD patients found no improvement in cognitive function with accelerated hippocampal volume. The use of VPA in patients with moderate AD failed to delay behavioural symptoms of psychosis or agitation and also cognitive decline. Its associated side effects of weakness, diarrhoea and tremors have detracted clinicians from prescribing VPA routinely to dementia patients (Jahromi et al., 2011).

Trials using lithium have shown more potential, reducing tau concentration, phosphorylation and amyloid production. It also reduced axonal degeneration and enhance the release of TGF- $\beta$ 1 in cultured neurons and transgenic mice. Patients with bipolar disorder treated with lithium chronically, demonstrated a reduced risk of developing dementia (Kessing et al., 2008). A study carried out in patients with MCI found that long term lithium treatment, demonstrated benefits in cognition, with reduced levels of phosphorylated tau in CSF. However, patients with mild AD treated with lithium for 10 weeks showed no significant changes in cognitive function. The side effects associated chronic lithium treatment which include increased risk of kidney failure have detracted the use of lithium in AD treatment.

Despite the extensive efforts spent on understanding AD and its impact on the human brain, the drugs treatments discussed so far have not provided any fruitful benefits on reversing the brain damage caused by AD. The increase in life expectancy has led the number of dementia cases to increase steadily with no cure in sight. A suitable therapeutic approach that addresses the balance between normal and aberrant levels of amyloid is desperately needed. A key issue to note is at the time of AD diagnosis, drug treatments are most likely prescribed at a stage of the disease where the damage is irreversible. Therefore, studies into the events that precede amyloid deposition are imperative. One area of study would be to examine the effects of APP overexpression/mutant APP expression in order to study the earliest events that lead to cognitive decline.

### **1.8 Aims and objectives of the study**

The aim of this study was to investigate the role of APP in cellular metabolism. The human neuroblastoma SHSY5Y cell line was used to create stable cell lines that overexpressed either Wild type APP695 or APP695 carrying the Swedish mutation.

As APP695 is expressed abundantly in neurons *in vivo*, this gene was placed under the control of the Synapsin 1 promoter (SynI) ensuring neuronal specific expression in the stable cell lines. Synapsins are a group of neuronal phosphoproteins, which coat the cytoplasmic surface of synaptic vesicles and specifically SynI and SynII are only expressed in the nervous system, which established the synapsin genes as good candidates for an investigation of neuron-specific gene expression (Schoch et al., 1996). The advantage of using this neuronal promoter over a viral promoter, such as CMV provides increased APP expression at non-toxic levels and is found natively within human neurons. The use of viral promoters gives abnormally high protein expression, which would not occur *in vivo*.

The stable cell lines produced were used to study metabolic changes in the cells associated with overexpression SweAPP695/ wtAPP695 expression using the Seahorse analyser. Using this technique, measures of mitochondrial function as well as investigation of glucose uptake using simple enzymatic assays were performed. As oxidative stress is a common feature associated with AD the ability of cells to respond to oxidative insults was tested.

Additionally, in order to investigate the peripheral consequences of APP misprocessing, fibroblasts obtained from FAD-patients were studied in terms of their metabolic capacity using the Seahorse analyser as well as their ability to cope with oxidative stress.

The aims of these studies was to improve our understanding the consequences of APP overexpression and its role in not only AD but normal cellular metabolism. Such knowledge may inform the earliest changes that occur in AD and allow investigation of the pathways that are perturbed in order to develop novel treatments.

## **Chapter 2: Molecular cloning of APP constructs**

### **2.1 Introduction to cloning**

#### **2.1.1 Molecular cloning**

Advancements in molecular genetics have allowed researchers to clone genes of interest directly into cells in order to study the effects of gene expression. Since the 1940's, major discoveries in DNA structure and replication have allowed scientists to determine the specific sequence of genes. Following the invention of the Polymerase Chain Reaction (PCR) (Mullis et al., 1986), new opportunities for cloning and sequencing became available. Cloning of cDNA encoding for a specific protein allows researchers to manipulate DNA in order to allow expression in a variety of cell model systems. Furthermore, the identification of pathogenic mutations in humans and advances in gene editing have allowed researchers to replicate these mutations *in vitro*, and even produce animal models in which genes can either be knocked in or out.

#### **2.1.2 APP structure**

Determination of the genetic sequence and protein structure of APP has identified a number of possible cellular functions. The APP gene is comprised of approximately 400kb of DNA, and is spread across 19 exons (Yoshikai et al., 1990). The gene encodes for a number of alternatively spliced APP mRNA products (Price and Sisodia, 1998) that give rise to 8 known splice variants. Of the 8 isoforms identified, the APP695 isoform is expressed at highest levels in the central nervous system (Kang and Muller-Hill, 1990). This neuronal APP is 695 amino acids in length and is of particular relevance to AD. Nuclear magnetic resonance (NMR) and crystallization studies have been utilised to determine APP structure, however no full crystal structure has been produced (Gralle and Ferreira, 2007, Xue et al., 2011, Coburger et al., 2013).

APP is a type-I integral membrane glycoprotein, part of a family of proteins, that includes APLP1 and APLP2 (Wasco et al., 1992, Sprecher et al., 1993). The protein structure consists of several domains which include a large extracellular domain, a hydrophobic transmembrane domain and a short cytoplasmic carboxyl terminus, as

shown in Figure 1.5. Larger APP isoforms also contain the Kunitz-type serine protease inhibitor (KPI) domain, located in the middle of the extracellular domain (Ponte et al., 1988), and is 57 amino acids in length. APLP1 and APLP2 are the only known homologs of APP, sharing 38-51% amino acid homology (Walsh et al., 2007), undergoing proteolysis processing similarly to that of APP, but neither have the A $\beta$  domain (Cousins et al., 2015). Expression of APLP2 is found within neuronal and non-neuronal tissues like that of APP, but APLP1 is largely confined to the CNS (Lorent et al., 1995).

Identification of the primary sequence has led to possible functions of APP. The C-terminal cytoplasmic tail of APP contains a tetrapeptide sequence, NPXY, required for rapid endocytosis of the low density lipoprotein receptor (LDLR) (Chen et al., 1990). Deleting this cytoplasmic domain increases secretion of APP (Haass et al., 1993), suggesting this region plays some role in APP trafficking. The A $\beta$  peptide region is located near to the C-terminus, (amino acids 597-613) and sits partially outside the cell membrane. Adjacent to this small region is a domain where glycosylation can occur.

The N-terminal region of APP has been characterised substantially. It is 172 residues in length and is conserved amongst the APP isoforms and in its homologues in both humans and other species (Daigle and Li, 1993). This region is rich in cysteines, allowing disulphide bond formation, facilitating the formation of a rigid tertiary structure (Rossjohn et al., 1999). This region binds heparin (Clarris et al., 1997), to the extracellular matrix protein fibulin (Ohsawa et al., 2001) as well as to A $\beta$  itself (Van Nostrand et al., 2002) and is called the heparin binding domain 1 (HBD1).

The sequence adjacent to the HBD1 has been found to bind Cu<sup>2+</sup> and Zn<sup>2+</sup> ions *in vitro*. This domain is degraded *in vitro* possibly due to generation of reactive oxygen species (ROS) arbitrated by bound Cu<sup>2+</sup> ions. Three disulphide bonds are present within the copper binding site. Binding of Zn<sup>2+</sup> ions can increase APP's binding affinity to heparin.

However, the residues of this domain are not sufficient to fully chelate  $Zn^{2+}$  suggesting that amino acids from a different domain may contribute to metal binding. Therefore, it is likely that the N-terminal region relies on interactions from other APP domains to carry out its possible functions.

The central regions of APP contain another heparin binding domain, HBD2 which is well conserved and is 179-residues in length. This domain is followed by a 166-amino acid sized segment that is only found in vertebrate APP, and is quickly degraded by proteases (Daigle and Li, 1993). This fragile segment may be less compact in conformation whilst the HBD2 forms an  $\alpha$ -helical structure (Gralle et al., 2002, Wang and Ha, 2004). APP has also been shown to bind to laminin and collagen *in vitro* via this domain. F-spondin, a protein associated with differentiation of tissue growth, can also bind to these helical regions and can inhibit APP cleavage via BACE1. The central region is also where an N-glycosylation site is located. Post-translational modifications such as glycosylation are important in axonal sorting and secretion of APP. Changes in the glycosylation state of APP lead to decreased secretion of the neuroprotective sAPP $\alpha$  (a cleavage product of APP demonstrated to decrease A $\beta$  production), with a simultaneous increase in APP deposition within cells (Georgopoulou et al., 2001, Obregon et al., 2012).

The A $\beta$  region is where BACE1 and  $\alpha$ -secretase cleavage sites are found, and it is mutations within this region which influence APP cleavage by  $\beta$ -secretase (as shown in Figure 2.2). The activity of  $\gamma$ -secretase and BACE1 can influence the extent to which N-glycosylation and sialylation of APP can occur respectively (Schedin-Weiss et al., 2014). Furthermore, APP mutations have been shown to alter N-glycosylation, of this protein (Akasaka-Manya et al., 2008).

### 2.1.3 Genetic mutations in APP

Genetic mutations in the APP and the presenilin genes, that are associated with familial (early onset) AD influence the amyloidogenic processing of APP. Under physiological conditions, neurons produce picomolar levels of APP in a regulated manner, producing small amounts of A $\beta$ 40 that are postulated to modulate synaptic activity. However, familial mutations increase the concentration of A $\beta$ 1-40 and the toxic species A $\beta$ 1-42, which aggregates to form plaques. The effects of mutations that increase the production of A $\beta$ 42 are also reflected in sporadic AD (Lippa et al., 1996). Both familial and sporadic AD pathologies exhibit severe neuronal loss, as well as the presence of neuritic plaques and neurofibrillary tangles. Clinical features present in both forms of AD are also indistinguishable from each other when using PET or MRI scans, with the only difference being the age of onset (Duara et al., 1993).

As mentioned in Chapter 1, overexpression of the APP gene, as observed in Down Syndrome (DS) patients is sufficient to cause early onset of AD pathology. An increase in A $\beta$ 1-42 production leading to the development of plaques has not only been observed in DS patient brains, but also in iPSC-derived neurons, which were reprogrammed from DS fibroblast cells (Shi et al., 2012a). In other studies, fibroblasts taken from patients with either familial or sporadic AD, reprogrammed into iPSC-derived neurons, exhibited higher levels of A $\beta$ 1-40 (but not A $\beta$ 1-42, due to small numbers of neurons purified) when compared to non-demented controls. In addition, there was an increase in the phosphorylation of Thr231 (one of the key residues of tau), as well as an increase in the activity of glycogen kinase 3 $\beta$  (GSK3 $\beta$ , one kinase that phosphorylates tau) implying a direct association between APP processing and tau phosphorylation. This was corroborated by the fact that BACE1 inhibitors decrease phosphorylated tau and the activity of GSK3 $\beta$  (Israel et al., 2012). As the phenotypes of both sporadic and familial are similar it suggests that changes in APP processing may be very important in the pathology of the disease.

### **2.1.3.1 The Swedish mutation of APP**

The discovery of genetic mutations in the presenilin and APP genes has led to the generation of cellular and animal models of AD. In particular, at least thirty mutations in the APP gene have been identified (Table 2.1).

Overexpression of APP can lead to pathological changes as well as early changes in cellular metabolism, as shown by the prevalence of dementia in Down syndrome patients. Interestingly, while brain scans of patients with AD and those with preclinical AD have demonstrated reduced glucose uptake (Mosconi et al., 2008b) as well as mitochondrial dysfunction (Moreira et al., 2010, Wang et al., 2014a), DS brains exhibited increased glucose uptake (Lengyel et al., 2006, Balogh et al., 2002). Despite this, Down syndrome patients exhibit increased levels of oxidative stress, with decreased levels of mitochondrial components (Nagy et al., 1999, Conti et al., 2007). Abnormal mitochondrial activity is also found in DS fibroblasts (Valenti et al., 2011) and DS cortical neurons showing increased levels of ROS and lipid peroxidation (Busciglio and Yankner, 1995), as well as increased production of A $\beta$  (Shi et al., 2012a). Hence studying these metabolic pathways may reveal key changes in metabolic functions associated with APP misprocessing early in AD.

In this project, genetically stable cell lines were generated which express either wildtype APP (wtAPP695), to assess the effects of APP overexpression, or the Swedish APP mutation (SweAPP695) to assess the effects of increased A $\beta$ -1-42 production. These cell lines could then be used to study any changes in metabolism as a result of APP expression or misprocessing. This chapter discusses the steps taken to construct the genes and the targeting constructs.



Table 2.1. List of known APP mutations, including positions. Information taken from the online Alzheimer Disease and Frontotemporal Dementia Mutation Database (<http://www.molgen.ua.ac.be/ADMutations/>).

The Swedish mutation was originally identified in two families in Sweden (Mullan et al., 1992), where the average age of onset was 55 years. This is a double substitution mutation leading to a residue change from Lysine to Asparagine and Methionine to Leucine at positions 670 and 671 respectively in. The mutation locus precedes the A $\beta$  peptide region of APP, and results in increased production and secretion of A $\beta$  (Haass et al., 1995). Expression of this mutation *in vitro* leads to an increase in the production of A $\beta$  and sAPP $\beta$  secretion by 6-8 fold in comparison to wildtype APP expression (Citron et al., 1992). This occurs as the Swedish mutation of APP enhances BACE1

cleavage and therefore promotes amyloidogenic processing of APP (Vassar et al., 1999).

The Swedish mutation has been used to create the well characterised AD mouse model (Tg2576) (Elder et al., 2010). These mice demonstrate increased production of A $\beta$ 1-40 and A $\beta$ 1-42 peptides (Price and Sisodia, 1998) leading to age-dependent amyloid pathology, CAA and memory deficits (McGowan et al., 2006, Hsiao et al., 1996). In addition, these mice exhibit an increased oxidative phenotype, with an increase in the expression of superoxide dismutase 1 (SOD1) (Apelt et al., 2004), hemoxygenase-1 (Siedlak et al., 2009) and increased amounts of 4-hydroxynonenal compound (Takagane et al., 2015). *In vitro* studies using expression of the Swedish APP mutation in a neuronal cell line was found to lead to decreased ATP levels (Keil et al., 2004, Walls et al., 2012b). The 5xFAD mouse models which overexpresses the human APP695 Swedish, Florida (I716V), London (V717I) mutations and human PS1 carrying the M146L and L286V mutations exhibit early A $\beta$  deposition, cognitive impairment and early signs of significantly reduced levels of brain glucose uptake (Macdonald et al., 2014).

Introducing these familial mutations into the cellular genome has enabled researchers to create models of AD in order to study AD pathology and the cellular effects of wildtype APP overexpression/mutant APP expression on host cells. This has revealed possible mechanisms of APP neurotoxicity. For example, A $\beta$  peptide production has been associated with deficits in energy metabolism, reflecting effects observed in human AD patients brains. As the Swedish APP695 mutation has been well characterised in the literature, it was utilised in this study to simulate FAD.

#### **2.1.4 Aims and objectives**

The aims and objectives of this study were to create plasmids expressing APP and to test constructs for expression in transfected cell lines. After ensuring APP production

from the cloned sequence in a high level expression vector, stable cell lines were produced. To avoid the excessive production the target protein associated with viral promoters which can be toxic to cells, neuronal specific promoters were used. Initially, vectors with neuronal specific promoters and vectors carrying with the wtAPP695/SweAPP695 were constructed. These vectors were used to create stable cell lines using the human SHSY5Y cell line, whereby differentiation of the cells would lead to increased APP expression, and therefore increased production of amyloid peptide. The expression of mutated APP and overexpression of APP in these cell lines could then be compared with untransfected cells to observe whether any significant changes in metabolism were associated with increased APP overexpression/ production of A $\beta$ 1-42.

## **2.2 Methods and materials**

All chemicals were molecular biology grade and were obtained from Sigma–Aldrich (Poole, UK) unless otherwise stated.

### **2.2.1 General molecular biology procedures**

#### **2.2.1.1 Preparation of Competent Cells (Rubidium Chloride Method)**

Overnight bacterial cultures were prepared using a single colony of Mach1TR (general cloning) or Stbl3 (for cloning viral constructs) *E.coli* cells to inoculate 10ml of Super Optimal Broth (SOB) (2% Bacto Tryptone, 0.5% Bacto Yeast extract, 10mM NaCl, 2.5mM KCl, 10mM MgCl<sub>2</sub>, 10mM MgSO<sub>4</sub>). On the following day, 0.25% (v/v) inoculums were added to sterile SOB media and incubated at 37°C until the cells reached the logarithmic phase of growth (determined by an O.D reading of 0.4 at 550nm). At this point, the culture was chilled on ice for 30 minutes and then the cells pelleted by centrifugation (3000g for 10 minutes at 4°C). The supernatant was removed and the cells re-suspended in ice-cold RF1 Buffer (100mM RbCl, 50mM MnCl<sub>2</sub> 4H<sub>2</sub>O, 30mM CH<sub>3</sub>COOK, 10mM CaCl<sub>2</sub> 2H<sub>2</sub>O and 15% (w/v) glycerol) at 33% of the original volume of media and chilled on ice for 60 minutes. The cells were then pelleted again (3000g for 10 minutes) to allow removal of RF1 buffer. Cells were finally re-suspended in RF2 Buffer (10mM MOPS (3-(N-morpholino) propanesulfonic acid), 10mM RbCl, 75mM CaCl<sub>2</sub> 2H<sub>2</sub>O and 15% (w/v) Glycerol) to prepare for snap freezing in liquid nitrogen. Cells were aliquoted into sterile microcentrifuge tubes and snap frozen in liquid nitrogen. Cells were stored at -80°C until required.

#### **2.2.1.2 Plasmid sequencing**

Sequencing reactions were carried out at the Functional Genomic Facility, University of Birmingham (<http://www.birmingham.ac.uk/facilities/genomics/about/index.aspx>). As chain termination sequencing was used, primers were designed to split the target sequences into approximately 700bp sequencing runs. Typically two to four reactions were prepared containing 250ng of plasmid DNA and 3.2pmoles of primer (Eurofins

MWG Operon, Ebersberg, Germany) to ensure sequencing of the complete gene sequence.

#### **2.2.1.3 Bioinformatics analysis**

Sequencing data was converted into Fasta format and the raw data observed using Chromas Lite 2.01 software (Technelysium Pty Ltd, Australia). Alignments of the obtained sequences were made against reference sequences (obtained from the NCBI website). The online Multalin (<http://multalin.toulouse.inra.fr/multalin/>) and EMBOSS Matcher (NMBL) ([http://www.ebi.ac.uk/Tools/psa/emboss\\_matcher/nucleotide.html](http://www.ebi.ac.uk/Tools/psa/emboss_matcher/nucleotide.html)) programs were used to confirm the identity of recovered plasmids. Plasmid maps and theoretical cloning were created/carried out using Clone manager 5 (Sci Ed Central, NC, USA).

#### **2.2.1.4 PCR**

For PCR reactions using different primer pairs, the optimum annealing temperature of the primers was initially determined by gradient PCR. A PCR mastermix was set up containing: 1x Pfu buffer (Invitrogen, Paisley, UK), 200 $\mu$ M dNTPs (Invitrogen, Paisley, UK), 0.5pmole/ $\mu$ l of the appropriate forward primer and reverse primer (Eurofins MWG Operon, Ebersberg, Germany), 0.5ng/100 $\mu$ l of reaction of DNA template, Pfu enzyme (Invitrogen, Paisley, UK) and the remaining volume made up in DNase/RNase free sterile water.

30 $\mu$ l aliquots of mastermix were dispensed into 0.2ml sterile PCR tubes and the PCR reaction was carried out in a Thermocycler PCR machine (Techne). The primary annealing temperature was set to 60°C with a gradient of 20°C as most primers have a theoretical melting ( $T_m$ ) temperature of 55-58°C. The PCR samples were analysed by agarose gel electrophoresis (see section 2.2.1.9).

Once the optimal annealing temperature was established, large scale PCR reactions were set up containing 1 x Pfu buffer (Invitrogen, 10x), 200 $\mu$ M dNTPs (Invitrogen,

10mM), 0.5pmoles/ $\mu$ l of the appropriate forward primer and reverse primer (Eurofins, MWG Operon, Ebersberg, Germany), 0.5 ng of DNA template/100 $\mu$ l reaction, 1.25U of Pfu enzyme/100 $\mu$ l (Invitrogen, UK, 5U/ $\mu$ l) and the remaining volume made up with sterile water. 50 $\mu$ l aliquots of the mastermix were dispensed into 0.2ml PCR tubes.

The PCR reaction was then set up using the previously determined optimum annealing temperature for 30 cycles. Reaction conditions were generally set out as listed in Table 2.1. For cloning DNA a final extension of 5 minutes was added to the last cycle.

Step	Temperature	Duration
Initial denaturation	95°C	1 minute
30 cycles of the following steps:	95°C	30 seconds
Annealing	Optimal temperature	30 seconds
Extension	72°C	2 minutes per 1kb of template DNA

Table 2.2. Protocol to run PCR.

#### 2.2.1.5 PCR Tailing reactions

To ensure 3' adenine overhangs were present on PCR products amplified with proof reading polymerases, purified products were tailed using Taq polymerase. Tailing reactions were performed in GoTaq Flexi buffer (1x, Promega, Southampton, UK), MgCl<sub>2</sub> (1.5mM, Promega, Southampton, UK), dATPs (100 $\mu$ M, Bioline, London, UK), GoTaq (1U, Promega, Southampton, UK) and 13.6 $\mu$ l of the purified PCR product to make up to a total volume of 20 $\mu$ l. The mixture was then incubated at 72°C for 20 minutes.

#### 2.2.1.6 TOPO cloning

Inserts carrying 3' adenine overhangs were cloned into commercially available pre charged Topoisomerase vectors (pCR8 TOPO vector). TOPO reactions were prepared in accordance with the manufacturer's instructions.

### **2.2.1.7 Transformation of Topo reactions**

2.5µl of the Topoisomerase reaction was transformed into Mach1TR *E.Coli* (see section 2.2.1.16), plated onto spectinomycin agar plates (100µg/ml) using 50µl, 100µl and 150µl of inoculated broth to ensure that there was no overgrowth of colonies overnight at 37°C.

### **2.2.1.8 Recombination reaction of TOPO vectors**

To recombine TOPO vectors into the final destination vector, a recombination reaction was prepared as recommended in the ViraPower Promoterless lentiviral Gateway Kit manual (see appendix). Briefly, 2µl of LR Clonase II Plus was added to 10fmoles of pENTR5' Syn1 TOPO, 10fmoles of pCR8 wtAPP695/SweAPP695, 20fmoles of pLenti6.4 R4/R2 V5 Dest with an appropriate volume of Tris-HCl EDTA buffer (10mM Tris-HCl, 1mM EDTA, pH 8.0) added to make the total reaction volume up to 8µl. After the reaction was incubated overnight at room temperature, 1µl of Proteinase K solution was added and the reaction incubated at 37°C for a further 10 minutes and then the reaction was immediately transformed into Stbl3 *E.coli* cells (see section 2.2.1.16 for protocol). Transformed bacteria were plated onto LB agar plates containing ampicillin (50µg/ml) for selection. On the following day, colonies were counted and selected for further analysis.

### **2.2.1.9 Agarose gel electrophoresis**

Standard agarose gels were made with Hi-Res Standard Agarose (GeneFlow, Lichfield, UK) and 1xTAE buffer (0.04M Tris-acetate, 0.001M EDTA, pH 8.0). The agarose was heated until fully dissolved and once cool enough to pour; 0.5µg/ml of ethidium bromide (Sigma-Aldrich, Poole, UK) was added. The gel was poured into a caster with the appropriate sized comb. 5µl of each PCR sample was loaded into wells with 6x Mass Ruler loading dye (for large sized PCR products, Thermo Scientific, UK). (Xylene cyanol dye (Sigma-Aldrich, Poole, UK) was used for fragments less than 800bp). Mass Ruler High Range ladder (Fermentas, Thermo Scientific, UK) and MassRuler Low Range Ladder (Fermentas, Thermo Scientific, UK) were also loaded to

determine band size. The gel was run for 1 hour at 100V, after which time the DNA was visualised under UV transillumination (using the G: Box HR-16, GENE Sys, Syngene, UK).

#### **2.2.1.10 Gel extraction**

To purify PCR products of the appropriate size from low level contaminating bands and primers, PCR sample were pooled and then gel purified on 1% Seaplaque™GTG™ (Lonza SLS Nottingham, UK). PCR samples were prepared with 6x loading dye (Thermo Scientific, UK) and run in the same well and run for 1 hour at 100V.

Under UV transillumination, the appropriately sized band was excised from the gel using a sterile scalpel blade. Subsequent gel extraction was carried out using the QIAQUICK Gel Extraction Kit (QIAGEN, Manchester, UK) in accordance with the manufacturer's instructions (see appendix). DNA was concentrated through a single column and eluted in the minimal recommended volume of sterile water to increase DNA concentration.

DNA concentration and purity were determined using the NanoDrop spectrophotometer (Thermoscientific, UK). DNA concentration was determined from absorbance at 260nm, and the  $A_{260}$  and  $A_{280}$  were noted as an indication of its purity.

#### **2.2.1.11 Restriction Digest**

Restriction enzymes were used in conjunction with appropriate buffers as recommended by the manufacturer (NEB, New England, USA). Typical reactions consisted of 10µg vector in a 200µl reaction or 5µg of insert in a 100µl reaction with 2-4 units of restriction enzymes/µg DNA added. Reactions were typically carried out at 37°C for 3-4 hours before being heat-inactivated at 65°C/80°C (depending on the enzymes used, NEB double digest software was used to calculate optimal temperature and compatibility of enzymes in double restriction digests).

#### **2.2.1.12 PCR clean up**

Digested PCR products were purified using the QIAQUICK PCR Purification Kit (QIAGEN, Manchester, UK) in accordance with the manufacturer's instructions (see appendix for protocol).

#### **2.2.1.13 Dephosphorylation of cDNA ends**

Digested DNA vectors were dephosphorylated to remove 5' phosphates from the cohesive ends to prevent self-ligation or concatemerisation of the vector. Subsequent to restriction digest, dephosphorylation reactions were carried out in the appropriate restriction enzyme buffer with the addition of Antarctic Phosphatase Reaction Buffer (NEB, New England, USA, 10x) at 1/10th of the total digest reaction volume. Five units of Antarctic Phosphatase (NEB, New England, USA) were added and the reaction was mixed gently. The reaction was incubated for 50 minutes at 37°C and then heat-inactivated for 20 minutes at 65°C. The digested, dephosphorylated vectors were subsequently gel purified to remove both the excised fragment and enzymes (see section 2.2.1.10).

#### **2.2.1.14 Ligation**

A 3:1 molar ratio of insert to vector was used for ligation reactions unless otherwise stated. Molar concentrations of each purified DNA was calculated assuming the average mass of 1bp = 660 Daltons. Typically 100ng of vector was used for each ligation with 3:1 molar ratio of the respective insert.

Ligations were carried out in 20µl reactions containing 100ng of dephosphorylated vector, a 3x molar ratio of insert, 1x Ligase Buffer (Invitrogen, 5x), 1 unit of T4 DNA Ligase (Invitrogen), with the remaining volume made up with sterile water. Self-ligation reactions in which the insert was omitted were carried out with each ligation. Reactions were incubated at 16°C for 16 hours and subsequently heat-inactivated to stop further enzyme activity at 65°C for 20 minutes.

### 2.2.1.15 Agar preparation

20g of Luria-Bertani broth (LB) (Invitrogen, Paisley, UK) was dissolved in 1L of distilled water. Difco Bacto Agar (BD; Oxford, UK, 1.5%W/V) was added and the media was autoclaved at 121°C. Ampillicin sodium salt (Sigma-Aldrich, Poole, UK) stocks were prepared at 50mg/ml dissolved in sterile water and sterilised using a 0.2µm filter. After autoclaving, media was cooled to 50°C, and (where required) the respective antibiotic stock solution added to achieve the following final concentrations, Ampillicin (50µg/ml), Spectinomycin dihydrochloride pentahydrate (Sigma-Aldrich, Poole, UK, 50µg/ml), Kanamycin (Sigma-Aldrich, Poole, UK, 40 µg/ml). The media was then poured into sterile Petri dishes (Sarstedt, UK) to set. LB plates containing no antibiotics were also prepared in a similar manner.

### 2.2.1.16 Transformation

Ligation reactions were transformed into *E. Coli* strains Mach1™T1<sup>R</sup> (Genotype F<sup>-</sup> φ80(*lacZ*)ΔM15 Δ*lacX74* *hsdR*(r<sub>K</sub><sup>-</sup>m<sub>K</sub><sup>+</sup>) Δ*recA1398* *endA1* *tonA*) for the mammalian expression vectors (see section 2.2.4 and 2.2.5) whilst Stb13™ (Genotype F<sup>-</sup>*mcrB* *mrrhsdS20*(r<sub>B</sub><sup>-</sup>, m<sub>B</sub><sup>-</sup>) *recA13* *supE44* *ara-14* *galK2* *lacY1* *proA2* *rpsL20*(Str<sup>R</sup>) *xyI-5* λ<sup>-</sup> *leumtl-1*) were used for viral vectors (see section 2.2.7). Both bacterial strains were obtained from Life Technologies (Paisley, UK).

Ready competent *E.coli* strains were thawed on ice (15 minutes) whilst 100µl of the cells were pipetted into tubes (pre cooled on ice) containing 5µl of the respective ligation reaction. Reactions were mixed by flicking the tubes and were then incubated on ice for 30 minutes. A positive control using undigested plasmid was also carried out. A tube containing cells only was also incubated on ice to ensure cell viability. After 30 minutes, all tubes were heatshocked at 37°C for 1 minute and then immediately recovered on ice for 2 minutes. 500µl of LB media was added to each tube and the cultures were shaken at 200rpm at 37°C (30°C for 70 minutes for viral plasmids) for 50 minutes to allow expression of antibiotic resistance markers. During

this time, Ampicillin (or Kanamycin) containing agar plates were air dried by inverting them at 37°C to remove excess moisture.

For plating, 150-200µl of each cell suspension was pipetted onto Ampicillin plates and spread evenly with a sterile plate spreader. Tubes containing no vector were plated onto LB only plates to determine the growth of cells. All plates were then incubated overnight at 37°C (30°C for viral plasmids).

#### **2.2.1.17 Colony PCR**

Colonies of bacteria derived from transformed bacteria were screened for the correct gene insert using colony PCR (primers for each vector are contained in the appendix). Sterile universal tubes containing 6ml of LB media with the appropriate antibiotic were prepared. Ampicillin plates were divided into sections with each section labelled for the respective colony.

Each colony was picked with a sterile pipette tip and a small amount of bacteria scraped into a sterile PCR tube. The bacteria were then streaked onto a clean section of an antibiotic selection plate and the pipette tip was placed into the sterile universal tube which was incubated overnight with shaking (200rpm) at 37°C.

PCR mastermix (30µl) was added to each PCR tube, along with a negative control. The PCR conditions included an initial denaturation step of 95°C for 2 minutes to lyse the bacteria, followed by 30 cycles of, denaturation at 95°C for 1 minute, primer annealing at 54°C for 30 cycles and extension at 72°C for 1Kb/minute with a final extension of 72°C for 5 minutes. The PCR reactions were analysed by DNA gel electrophoresis (see section 2.2.1.9). Samples shown to contain the appropriate sized band were subject to small scale plasmid isolation (see section 2.2.1.18) using 3ml of the 5ml cultures for subsequent sequencing (see section 2.2.1.2).

#### **2.2.1.18 Small scale plasmid isolation (miniprep)**

The miniprep procedure was carried out using the QIAQUICK Miniprep Kit (QIAGEN, Manchester, UK). 3ml of bacterial culture was centrifuged at 17900 x g to pellet the cells. DNA was extracted in accordance with the manufacturer's instructions (see appendix) and the plasmid DNA was eluted into 50µl of sterile water. The plasmid DNA concentration was determined (see section 2.2.1.10) to prepare for sequencing (see section 2.2.1.2).

#### **2.2.1.19 Large plasmid isolation (midiprep)**

Colonies confirmed as containing the correct sequence were picked from the replica streak plates (see section 2.2.1.12) and used to inoculate small cultures (30ml LB) with the appropriate antibiotic. After incubation for 8 hours (200rpm) at 37°C, these cultures were used to inoculate a larger 200ml overnight culture. On the following day, the optical densities of the cultures were measured to determine the scale up of plasmid isolation. 200ml cultures which gave an OD reading of 2 were prepared using a midi prep kit whereas, cultures giving OD readings for 6 were prepared using a Maxiprep kit to account for the larger amount of bacterial cells and plasmid DNA. The Machery-Nagel Endotoxin-Free DNA Purification Kit (Fisher Scientific, Loughborough, UK) was used.

### **2.2.2 Protein expression procedures**

#### **2.2.2.1 Cell lysis**

Cells were washed three times with ice-cold PBS to remove any serum proteins. Protein samples were prepared in an appropriate volume of 1X Radio-Immunoprecipitation Assay (RIPA) buffer (Millipore, Watford, UK) containing Mini complete protease cocktail inhibitors (Roche Diagnostics Ltd, West Sussex, UK). The cells were detached with a sterile scraper and transferred into 1.5ml microcentrifuge tubes and incubated at 4°C for 30 minutes to ensure complete lysis. Cell debris was pelleted at 10,000rpm at 4°C for 10 minutes and the cell lysate collected. Cell lysates were stored at -80°C.

#### **2.2.2.2 The BCA Protein Assay**

To determine the total protein concentration, the Pierce BCA™ protein assay kit (Thermo Scientific, Paisley, UK) was used (for protocol see appendix). Briefly, 25µl of sample, BSA standard (ranging from 125-2000µg/ml) or assay diluent (BSA-free control) were incubated in a 96-well microplate with 200µl of working reagent (50:1, Reagent A: B) for 30 minutes at 37°C. The absorbance was then read at 562nm using the Multiscan GO plate reader (Thermo Scientific, Loughborough, UK), and the data obtained from Skan It 3.2 (Thermo Scientific, Loughborough, UK). The protein concentration was calculated using the absorbance of a known BSA standard (Pierce, Thermo Scientific Loughborough, UK) diluted in identical buffer to the sample tested.

#### **2.2.2.3 SDS-PAGE**

Polyacrylamide gel electrophoresis (PAGE) followed by Western Blotting was performed on the protein samples. SDS-PAGE was performed using the Mini Protean® 3 Cell (Bio-Rad Laboratories Ltd., Hemel Hempsted, UK). Sodium dodecyl sulphate polyacrylamide gels were prepared according to the manufacturer's guidelines. Stacking gels (4% polyacrylamide, made with final concentration of 0.125M Tris-HCl, pH6.8, 3.9% w/v acrylamide, 0.1% SDS in deionised water) and resolving gels (10% polyacrylamide) were prepared with 0.75mm thick glass plates. 5-10µg of cell lysates were denatured in sample buffer at 1x final concentration (deionized water, 5% glycerol, 12.5mM Tris-HCl pH 6.8, 0.4% SDS, 0.002% bromophenol blue and 1% β-mercaptoethanol) for 5 minutes at 95°C and were separated by electrophoresis for 45 minutes at 200V or until the bromophenol blue reached the bottom of the gel. PageRuler Plus Prestained Protein Ladder (Thermo Scientific, Northumberland, UK) was included as reference to determine sample protein size.

#### **2.2.2.4 Western Blot Transfer**

Following SDS-PAGE, plates were carefully separated, and the gels equilibrated in transfer buffer (25mM Tris, 192mM Glycine, 10% Methanol in deionised water) for 15 minutes before being transferred onto Nitrocellulose Hybond ECL membranes

(Amersham, GE Healthcare, Buckinghamshire, UK). The SDS gels and nitrocellulose membranes were then sandwiched between four pieces of Whatman cellulose chromatography paper and two pieces of sponge, pre-soaked in transfer buffer. Transfers were performed using the mini trans-blot electrophoretic transfer cell (Bio-Rad Laboratories Ltd., Hemel Hempsted, UK) at 30V, 90mA for 16 hours on ice.

#### **2.2.2.5 Immunoblotting**

Nitrocellulose membranes were equilibrated in Tris-buffered saline (TBS) (138mM NaCl, 2.68mM KCl, 24.8mM Tris-base in deionized water, pH 8.0) before being blocked in TBS-Tween (0.1% Tween)/ 5% powdered milk (Marvel Skimmed Milk, UK) for 2 hours at room temperature.

Membranes were then incubated in the appropriate primary antibody diluted in 3% (w/v) dried milk powder in TBS 0.1% (v/v) Tween on a rolling platform overnight at 4°C. On the following day, the membranes were washed six times (5 minutes/wash) in TBS-0.1% Tween, 3% powdered milk to eliminate excess unbound antibody. The blot was then incubated for 1 hour at room temperature in the appropriate secondary antibody to visualise bound primary antibody.

After incubation with secondary antibody, blots were washed a further six times in TBS 0.1% (v/v) Tween (5 minutes/wash). Protein-antibody binding was detected on X-ray film (CL-XPosure Film, Thermo Fisher Scientific, UK) using the enhanced chemiluminescence (EZ ECL Blotting analysis system, Geneflow, Lichfield, UK). EZ ECL was prepared and left to equilibrate for 5 minutes protected from light, before being applied to the blots for 1 minute. Blots were secured in an autoradiography cassette (Hypercassette, Amersham, GE Healthcare, Buckinghamshire, UK) between two pieces of acetate before exposing to X-Ray film. X-ray films were exposed to the blots until clear protein bands were visible. Films were developed between 30 seconds

to 1 minute (Kodak, Sigma-Aldrich, Dorset, UK), washed thoroughly in water (30 seconds), and then fixed for 3 minutes (Kodak, Sigma-Aldrich, Dorset, UK).

### **2.2.3 Protein expression studies**

#### **2.2.3.1 COS-7 cell culture**

Monkey kidney COS7 cells (ATCC) were cultured in DMEM with Glutamax (Gibco, Life Technologies, Paisley, UK) with 100U/ml Penicillin and 100µg/ml Streptomycin (Gibco, Life Technologies, Paisley, UK) and 10% Foetal Bovine Serum (FBS) (Invitrogen, Fisher Scientific, UK). When cells reached 90% confluence, they were washed once with Phosphate buffer saline (PBS) without MgCl<sub>2</sub>/CaCl<sub>2</sub> (Gibco, Life Technologies, Paisley, UK) and detached using 0.05% Trypsin-EDTA (Gibco, Life Technologies, Paisley, UK). Cells were pelleted at 200g for 5 minutes and the cells re-suspended in fresh media. Cells were split 1:5/1:4 twice a week depending on the rate of growth and maintained at 37°C, 5% CO<sub>2</sub>.

#### **2.2.3.2 Cell Quantification (Trypan Blue Exclusion)**

To quantify the number of living cells, cells were diluted 1:2 with Trypan Blue 0.4% solution (Sigma-Aldrich, Poole, UK). To prepare cells, they were trypsinised, cells, and the cells pelleted by centrifugation. Cells were re-suspended in fresh medium and then diluted 1:2 with Trypan Blue. Cells were counted using average counts from both sides of a haemocytometer slide.

#### **2.2.3.3 Preparation of COS7 cells for transfection**

For protein studies, COS7 cells from an 80% confluent flask were trypsinised and the trypsin neutralised with fresh media. Cells were pelleted and then re-suspended in fresh media and live cells enumerated using a haemocytometer (see section 2.2.3.2). Six-well plates (Corning, MA, USA), were seeded at a density of 2.5 x10<sup>5</sup> per well to ensure 60-90% confluence could be reached for transfection the following day. To perform immunocytochemistry, Poly-D-lysine/ Laminin coated coverslips (BD Biocoat, BD Biosciences, Oxford, UK) were placed into 6-well plates prior to seeding.

#### **2.2.3.4 COS7 transfection**

Transfections were carried out using Lipofectamine LTX Plus (Gibco, Life Technologies, Paisley, UK) in accordance with the manufacturer's instructions (see appendix). Plasmid DNA (2.5µg/well) was diluted with 500µl of Opti-MEM® I Reduced Serum Medium (Gibco, Life Technologies, Paisley, UK) and 2.5µl of Plus Reagent added directly to the DNA. The solution was mixed gently and incubated for 15 minutes at room temperature. After 15 minutes, 8.75µl of Lipofectamine LTX reagent (as recommended in the manufacturer's instructions, see appendix) was added to the DNA-Plus reagent mixture and the solution incubated for 30 minutes at room temperature to allow complexes to form.

As a positive control, cells were also transfected with the Green Fluorescent Protein (GFP) expressing plasmid (PAC-GFP-Nuc, Clontech, Saint-Germain-en-Laye France). For protein studies, COS7 cells were transfected in triplicate with either SweAPP695 or wtAPP695 expressing plasmids. As a negative control, untransfected COS7 cells were prepared in triplicate and incubated alongside transfected cells. Before transfection, the cells were refreshed with 500µl of complete media and 100µl of the DNA-lipofectamine complexes were added drop-wise to the wells, and incubated at 37°C, 5% CO<sub>2</sub> until the following day. The media was then replaced and the cells were incubated for a further 36 hours to allow for protein expression.

#### **2.2.3.5 Immunostaining**

48 hours post-transfection, COS7 cells were washed once in ice-cold PBS (Gibco, Life Technologies, Paisley, UK) and then fixed in 4% Paraformaldehyde (PFA, Sigma-Aldrich, Poole, UK) for 20 minutes on ice. Following fixation, cells were washed twice in PBS to remove PFA. Positive controls transfected with PAC- GFP Nuc were stored in PBS containing 0.2% sodium azide (Sigma-Aldrich, Poole, UK) at 4°C.

In wells containing coverslips, cells were permeabilised in 0.1% Triton X-100/PBS (Sigma-Aldrich, Poole, UK) for 5 minutes at room temperature, and then blocked in 5%

BSA, 4% Triton X-100/PBS solution for 1 hour to prevent non-specific antibody binding. Cells were incubated with mouse anti-APP695 antibody (Invitrogen, 1:500, diluted in 5% BSA, 1% Triton X-100/PBS) for 2 hours at room temperature to detect wtAPP695/ SweAPP695. After incubation with primary antibodies, cells were washed three times in 5% BSA, 0.2% Triton/PBS and then incubated with the secondary antibody, anti-mouse Fluorescein isothiocyanate (FITC) (Jackson Laboratories, Maine, USA, 1:500) in the absence of light for 2 hours at room temperature to visualise bound APP primary antibody.

The coverslips were washed for a further three times in 5% BSA, 0.2% Triton/PBS to remove unbound excess antibody. Excess washing solution was removed by dabbing edge of coverslip with tissue. The coverslips were then mounted by inverting them onto glass slides with HardSet Mounting Medium containing 4', 6-diamidino-2-Phenylindole (DAPI) (VectaShield, Vector Laboratories, Peterborough, UK) to stain the nuclei. The coverslips were left to dry overnight (protected from light) before examination by fluorescence microscopy (section 2.2.3.6).

#### **2.2.3.6 Fluorescence Microscopy**

Stained COS7 were examined using the Leica SP2 fluorescent microscope. Cells were imaged with the 10x/63x dry/oil objectives. Fluorescent images were taken using the green filter cubes (excitation  $\lambda$  of 495nm, emission  $\lambda$  of 519nm) for APP visualisation and blue filter cube (excitation  $\lambda$  of 345nm, emission  $\lambda$  of 455nm) for nuclear visualisation. The exposure and intensity were altered accordingly for optimal image capture. Microscope images were analysed using the LAS AF Lite software.

#### **2.2.3.7 Protein expression from transfected COS7 cells**

COS7 cells were lysed in 300 $\mu$ l of RIPA buffer and with replicate wells pooled together (see section 2.2.2.1) and the protein concentration of the lysate determined in accordance with section 2.2.2.2).

10µg of cell lysates were subjected to SDS PAGE analysis using a 10% resolving gel (see section 2.2.4) and then transferred onto nitrocellulose membranes (see section 2.2.5) overnight at 30V, 90mA on ice. Membranes were blocked in 5% powdered milk and probed with mouse anti-APP695 (Invitrogen, Camarillo, USA, 1:2000, diluted in 3% powdered milk) or mouse anti-A $\beta$  (1-42) (6E10, Covance, 1:2000, diluted in 3% powdered milk) antibodies to detect the wtAPP695/SweAPP695 and A $\beta$  (1-42) respectively (see sections 2.2.3 to 2.2.5). As a positive control, neuronal NT2.D1 lysate (known to express APP) was included when APP blotting and synthetic A $\beta$ 1-42 (AnaSpec, CA, USA, 20µM) made up in HEPES was used as a positive control for blotting A $\beta$ .

## 2.3 Results

### 2.3.1 Plasmid Construction

To generate stable cell lines over expressing wtAPP695 or APP containing the Swedish mutation (SweAPP695), initially this required the DNA sequence encoding wtAPP695 as well as the sequence of APP bearing the Swedish mutation (K595N/M596L). After identifying groups working with constructs containing APP or SweAPP plasmids, these constructs were requested in order to provide the base APP sequences for incorporation into new constructs. A wild type donor APP construct (Plasmid IL695) was obtained as a kind gift from Dr Illiya Letterov (Pittsburgh University, PA, USA) and the coding sequence of the APP bearing the Swedish mutation (FGSwe695) was obtained from Prof. Frank Gunn-Moore (St Andrews University, Fife, UK).

Constructs were initially sequenced using primers reading outwards from the human wild type APP695 DNA sequence (full primer sequences for each construct are contained in appendix). In order to do this, primers capable of checking the sequence integrity of the APP gene were designed. These primers were then used in sequencing reactions (section 2.2.1.2) to obtain the sequence of the APP genes in each construct. The sequence data was compared against the sequence of human APP695 (obtained from the NCBI nucleotide database, accession no. NM\_201414.2).

Sequence alignments showed that both plasmids contained sequence anomalies when compared to APP695. Full sequence alignments were carried out using Multalin (<http://multalin.toulouse.inra.fr/multalin/>). The sequence alignment of FGSwe695 and the wtAPP695 sequence are shown in Figure 2.1. The alignment shows that the sequence of the plasmid FG695 correctly aligned with the wild type sequence but did not contain the expected Swedish mutation (KM595/596NL). The sequence contained an additional point mutation at position 1924 (position 2124 in Figure 2.1) of the APP DNA sequence. This was identified as a rare Japanese mutation, which causes FAD.

This Japanese mutation corresponds to amino acid substitution V642F, valine to phenylalanine substitution at position 642 of primary sequence of APP695 (Hashimoto et al., 2000, Yamatsuji et al., 1996).

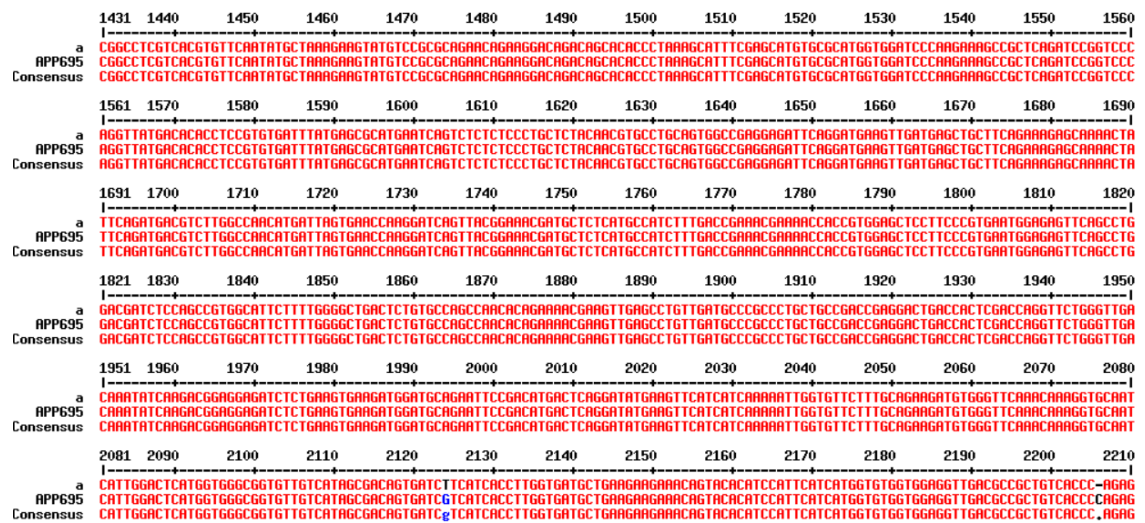


Figure 2.1. Alignment of the FGswe695 plasmid and the wtAPP695 gene using the Multialin software. The base change from G>T occurs at position 1924 of the APP gene sequence. This was detected in the sequencing reaction containing the APP1004 and that containing the APP1545 primer, demonstrating that this apparent base change is genuine, and not the result of inaccurate sequencing.

The sequence of the IL695 plasmid when aligned with the wild type sequence (NM\_201414.2) using Multialin did not produce a correct alignment, suggesting either no sequence similarity or a large number of inserted/deleted bases. The sequences were compared using the EMBOSS Matcher (EMBL-EBI) software ([http://www.ebi.ac.uk/Tools/psa/emboss\\_matcher/nucleotide.html](http://www.ebi.ac.uk/Tools/psa/emboss_matcher/nucleotide.html)), which highlighted an insertion of a 168bp fragment (Figure 2.2) in the derived sequence when compared with wtAPP695. The inserted sequence was identified as the region of DNA that encodes the KPI domain of APP using the Basic Local Alignment Search Tool (BLAST, NCBI, <http://blast.ncbi.nlm.nih.gov/Blast.cgi>) to compare the obtained sequence with all known sequences in the database. This suggested that the donor construct in fact contained a larger isoform of APP (APP751), which was confirmed by direct alignment of the inserted sequence with the reference sequence of APP751 (data not shown).

```

NM_201414.2      846 GACTATGCAGATGGGAGTGAAGACAAAGTAGTAGAAGTAGCAGAGGAGGA      895
a                8 GACTATGCAGATGGGAGTGA--GACAA--GTAGTAGAAGTAGCAGAGGAGGA      55
NM_201414.2      896 AGAAGTGGCTGAGGTTGGAAGAAGAAGAGCCGATGATGACGAGGACGATG      945
a                56 AGAAGTGGCTGAGGTTGGAAGAAGAAGAGCCGATGATGACGAGGACGATG      105
NM_201414.2      946 AGGATGGTGTAGAGGTAGAGGAAGAGGCTGAGGAACCCCTACGAAGAAGCC      995
a                106 AGGATGGTGTAGAGGTAGAGGAAGAGGCTGAGGAACCCCTACGAAGAAGCC      155
NM_201414.2      996 ACAGAGAGAACCACCAGCATTGCCACCACCACCACCACCACCACAGAGTC      1045
a                156 ACAGAGAGAACCACCAGCATTGCCACCACCACCACCACCACCACAGAGTC      205
NM_201414.2      1046 TGTGGAAGAGGTGGTTTCGAG-----                            1065
a                206 TGTGGAAGAGGTGGTTTCGAGAGTGTGCTCTGAACAAGCCGAGACGGGGC      255
NM_201414.2      1066 -----                            1065
a                256 CGTGCCGAGCAATGATCTCCCGCTGGTACTTTGATGTGACTGAAGGGAAG      305
NM_201414.2      1066 -----                            1065
a                306 TGTGCCCAATCTTTTACGGCGGATGTGGCGCAACCGGAACAACCTTTGA      355
NM_201414.2      1066 -----TTCTACAACAG-----                            1077
a                356 CACAGAAGAGTACTGCATGGCCGTGTGTGGCAGCGCCATTCTCTACAACAG      405
NM_201414.2      1078 CAGCCAGTACCCTGATGCCGTTGACAAGTATCTCGAGACACCTGGGGAT      1127
a                406 CAGCCAGTACCCTGATGCCGTTGACAAGTATCTCGAGACACCTGGGGAT      455
NM_201414.2      1128 GAGAATGAACATGCCCAATTCAGAAAAGCCAAAGAGAGGCTTGAGGCCAA      1177
a                456 GAGAATGAACATGCCCAATTCAGAAAAGCCAAAGAGAGGCTTGAGGCCAA      505
NM_201414.2      1178 GCACCGAGAGAGAATGTCCCAGGTGATGAGAGAATGGGARGAGGCAGAAC      1227
a                506 GCACCGAGAGAGAATGTCCCAGGTGATGAGAGAATGGGARGAGGCAGAAC      555
NM_201414.2      1228 GTC AAGCAAGAACTTGCCTAAAGCTGATAAAGAGGCAGTTATCCAGCAT      1277
a                556 GTC AAGCAAGAACTTGCCTAAAGCTGATAAAGAGGCAGTTATCCAGCAT      605

```

Figure 2.2. Sequence alignment (using the EMBOSS Matcher program) of the known wtAPP695 sequence (NM\_201414.2) compared against the sequencing data obtained for the IL695 plasmid. The highlighted area shows an extra length of sequence from the donor that is 168bp long located in the middle of APP.

In summary the obtained constructs contained APP695 with an unwanted mutation (FGSwe695) or in the case of IL695 a larger wild type APP751. For clarity, these plasmids were re-designated FG695 and IL751 respectively.

### 2.3.2 Generation of APP695

Sequencing of the donor constructs had demonstrated that neither of the obtained constructs contained the desired APP695 or SweAPP695 gene. However, this analysis also demonstrated that different areas of each of the donor genes were completely homologous to the APP695 reference gene. After careful analysis of the obtained sequences revealed that using the appropriate gene construction strategy, it was possible to ligate specific fragments of each construct together in order to create wild type APP695.



Amplicons were visualised by agarose gel electrophoresis (see section 2.2.1.4). Products corresponding to the expected size for APP from FG695 (Figure 2.5) and APP751 from IL751 (Figure 2.6) were then gel purified (see section 2.2.1.10).

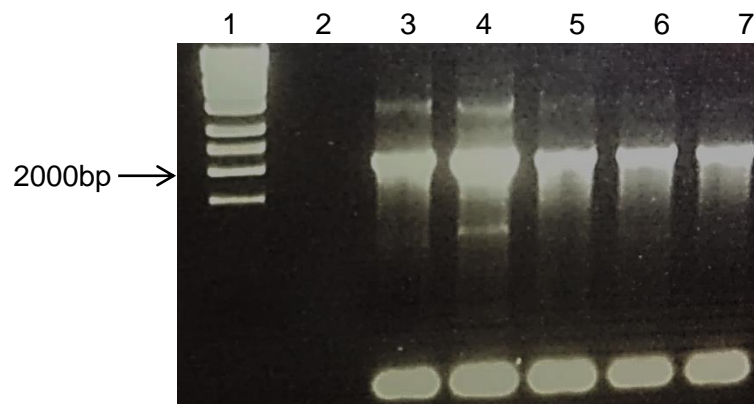


Figure 2.5. Agarose gel of PCR amplification of APP insert from FG695 plasmid using the primers ex alt APP695 and APP695rev (1% agarose gel). PCR products (lanes 3, 4, 5, 6, 7) were analysed alongside with Mass Ruler High (lane 1).

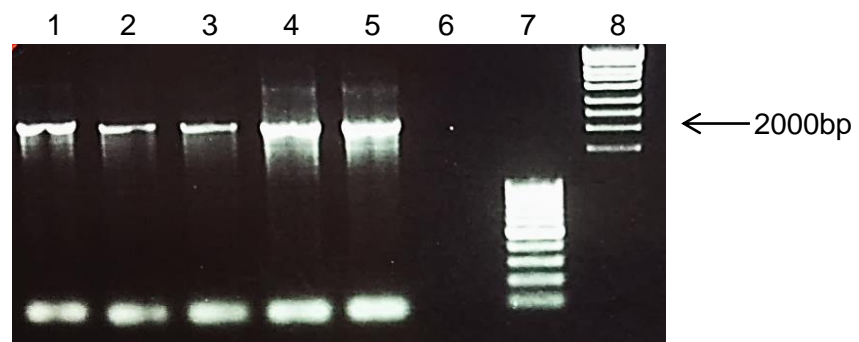


Figure 2.6. Agarose gel electrophoresis of PCR amplification of APP751 insert (lanes 1 to 5) using the primers ex alt APP695 and APP695rev (1% agarose gel). Lanes 7 and 8 Mass Ruler Low Range and Mass Ruler High Range respectively.

After quantifying the DNA concentrations, both APP amplicons were digested with 3 Units of HindIII and 3 Units of XbaI (section 2.2.1.11). The digested inserts were then subject to PCR purification (see section 2.2.1.12) to remove the small (<25bp) fragments and restriction enzymes. pcDNA3.1 was also digested with these enzymes (section 2.2.1.11), and dephosphorylated (section 2.2.1.13) to reduce the possibility of self-ligations, and gel extracted (section 2.2.1.10).

Both purified APP inserts were ligated into the digested vector (section 2.2.1.14). Ligations were then transformed (section 2.2.1.16) and the colonies screened (see section 2.2.1.17) for presence of the APP insert using the T7 forward and BGH Rev sequencing primers (see appendix for sequences). Figures 2.7 and 2.8 show the results of the screening of colonies for FG695 and IL751 respectively. Twelve JapAPP695 colonies and eleven IL751 colonies were chosen for screening.

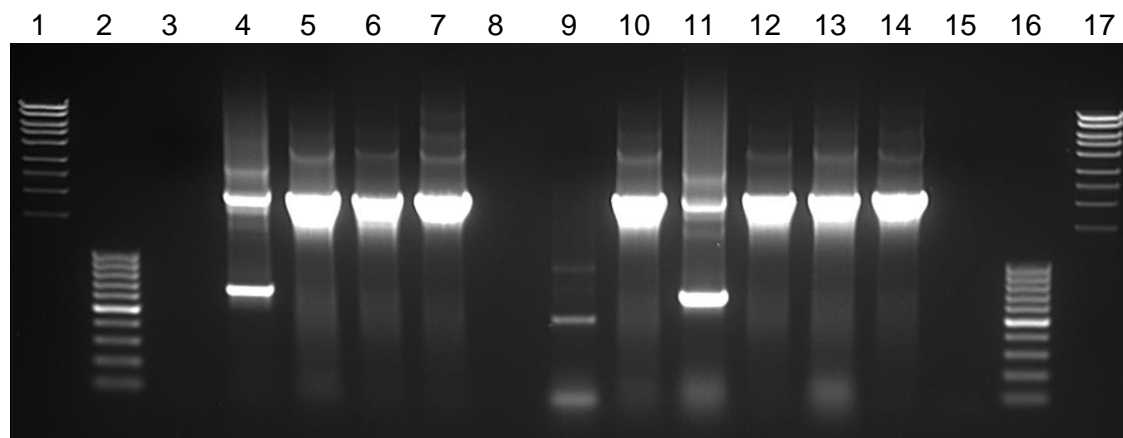


Figure 2.7. Agarose gel of colony PCR of bacterial clones transformed with JapAPP695-pcDNA3.1 (1% agarose gel). Lane 1, Mass Ruler High, lane 2, Mass Ruler Low Range, lane 3, negative control, lane 4, self-ligation reaction, lanes 5 to 7, bacterial clones designated EM1-3, lane 9, self-ligation reaction for size comparison, lanes 10 to 14, bacterial clones designated EM4 – 8, lane 15, negative control, lane 16, Mass Ruler Low Range, lane 17 Mass Ruler High Range. Clones EM1, 2, 3, 4, 6, 7 and 8 were confirmed positive for the presence of the 2000bp insert that corresponds to JapAPP695.

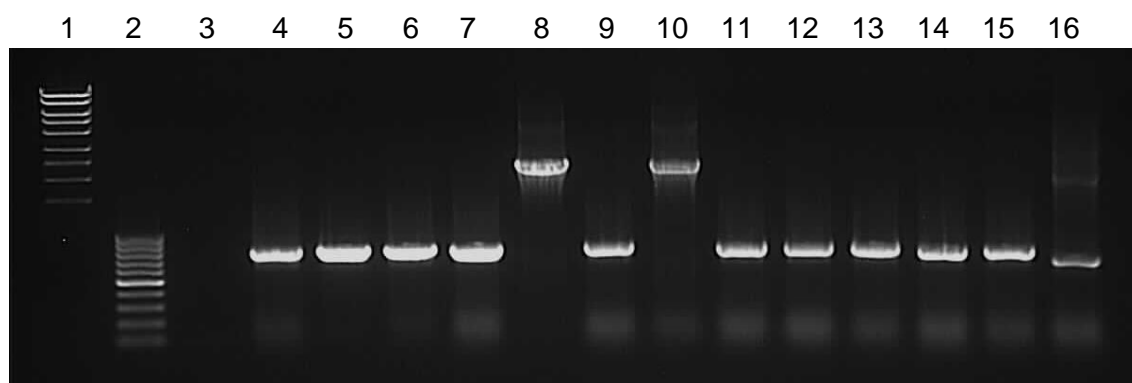


Figure 2.8. Agarose gel electrophoresis of colony PCR of bacterial clones transformed with APP751 pcDNA3.1 (1% agarose gel). Lane 1, Mass Ruler High, lane 2, Gene Ruler 100bp, lane 3, negative control, lane 4, self-ligation, lanes 5 and 6 bacterial clones designated EP1 and EP2, lane 7, self-ligation, lanes 8 to 16, bacterial clones designated EP3 to EP11 lane 17 negative control. Clones EP3 and EP5 were confirmed positive for the presence of the 2168bp insert that corresponds to APP751.

Analysis of the recovered colonies of cells transformed with JapAPP695-pcDNA3.1 revealed that of the screened clones, seven (EM1, 2, 3, 4, 6, 7 and 8) contained an

insert of the expected size generating a 2000bp amplicon, with 1 colony expected to be a self-ligation of the parental plasmid. Colonies designated EM3, EM4, EM7 were selected for small scale isolation (section 2.2.1.18) and prepared for sequencing (section 2.2.1.2). Analysis of the colonies generated after transformation with APP751-pcDNA3.1 showed that most of the colonies appeared to be the result of self-ligation of the parental vector. Two colonies designated EP3 and EP5 were selected for small scale isolation (section 2.2.1.18) and prepared for sequencing (section 2.2.1.2). Sequencing results were compared with the designed sequence using Multalin software and revealed that all sequenced clones contained the correct sequence. Clone EM3 (JapAPP695-pcDNA3.1) and clone EP3 (APP751-pcDNA3.1) were selected for large scale plasmid isolation (section 2.2.1.19). The sequencing results of this intermediate step are contained in Appendix 7.

#### **2.3.2.2 Construction of APP695 into pcDNA3/3.1**

Having obtained pcDNA3.1 constructs containing the FGJapAPP695 sequence/APP751, a strategy was devised to correct the sequence back into that of wild type APP695 using fragments of the APP genes. In both APP genes, an EcoRI site, is located upstream of the Japanese point mutation in FGJapAPP695 and also downstream of the KPI domain in APP751. This was used along with the 3'XbaI restriction site which flanks both APP genes to produce the essential fragments needed to reconstruct wtAPP695 (see Figure 2.9). The region of DNA following the EcoRI site of pcDNA3.1-APP751 is 294bp in size and is identical to the corresponding flanking region of wtAPP695, whilst the first ~1800bp of the FGJap695 gene is identical to the corresponding region of wtAPP695. Therefore, the complete sequence of wtAPP695 is contained in both plasmids, and could be generated by the excision and re-ligation of purified fragments to reconstruct the full wtAPP695 gene within pcDNA3.1.

Initially, the pcDNA3-JapAPP695 plasmid was digested with EcoRI HF and XbaI HF (3' end of APP, which was what was originally used to clone the donor genes into

pcDNA3.1). This produces two fragments; one that is approximately 7000bp in size which incorporates the first approximately 1800bp of wtAPP695, with the 5' end of the APP gene attached to the backbone of the pcDNA3.1 vector, and a small 294bp fragment, representing the 3' flanking region of APP695 containing the Japanese point mutation that was to be removed.

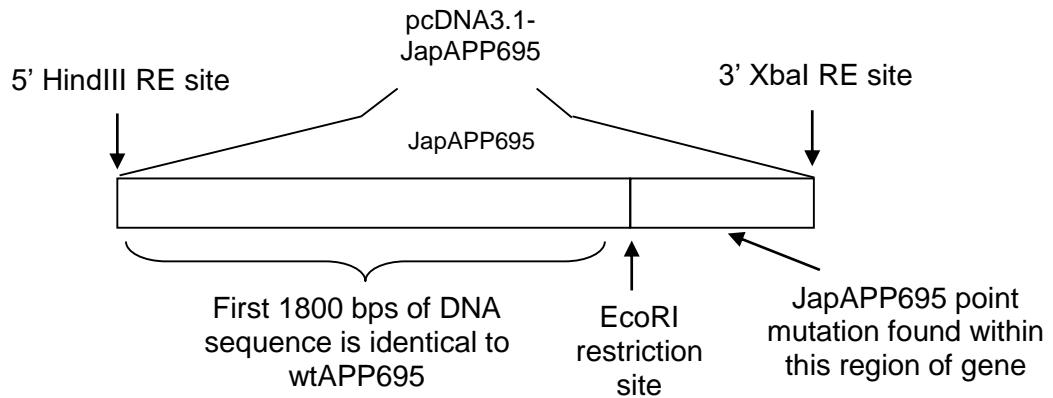


Figure 2.9. Diagram of the key fragments identified in pcDNA3-JapAPP695 which were used to construct the wtAPP695 gene.

The pcDNA3-APP751 plasmid was digested with EcoRI-HF and XbaI-HF, producing two fragments; one is a large unwanted fragment of the APP gene attached to the backbone of the plasmid (carrying the KPI domain and a smaller fragment homologous to the 3' region of wtAPP695 (see Figure 2.10 for restriction site location). Directional ligation of the excised 7158bp fragment from JapAPP695-pcDNA3.1 with the 294bp terminal sequence from pcDNA3-APP751 was used to create a wild type APP695 construct in a characterised mammalian expression vector.

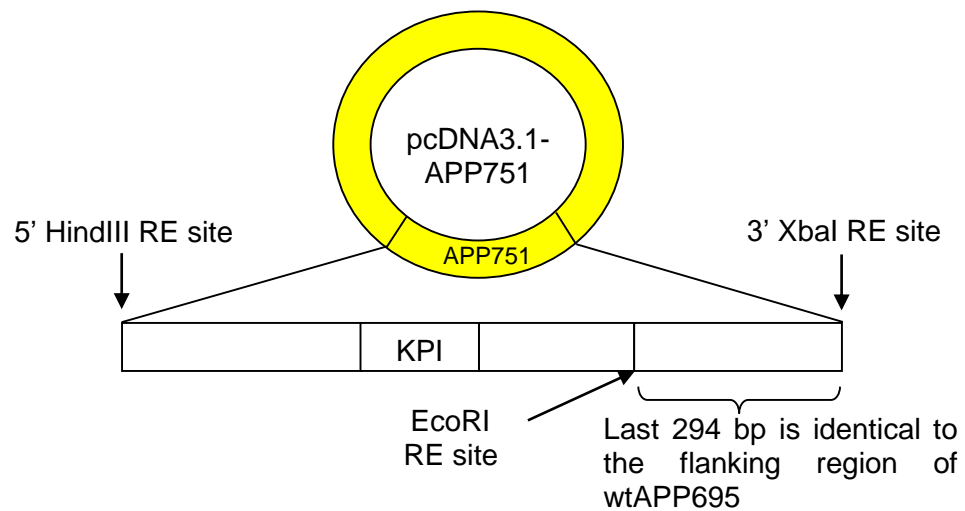


Figure 2.10. Diagram of the key fragments in APP751-pcDNA3.1 which were used to construct the wtAPP695 gene.

APP751-pcDNA3 was digested (with EcoRI-HF and XbaI-HF) and the products separated by agarose gel electrophoresis. Digestion APP751 led to the formation of two fragments; the large fragment (7158bp) represented the upstream region of the APP gene containing the unwanted KPI domain (found only in the larger APP isoforms) and the vector backbone and a small 294bp fragment which forms 3' end of the APP gene. The 294bp fragment was isolated from the gel in Figure 2.11. The JapAPP695-pcDNA3 plasmid was digested with XbaI-HF and EcoRI-HF) and the 7158bp fragment (Figure 2.11) consisting of the vector backbone and 5' end of the APP gene was excised and purified to remove 294bp (containing the unwanted Japanese mutation) from the end of JapAPP695.

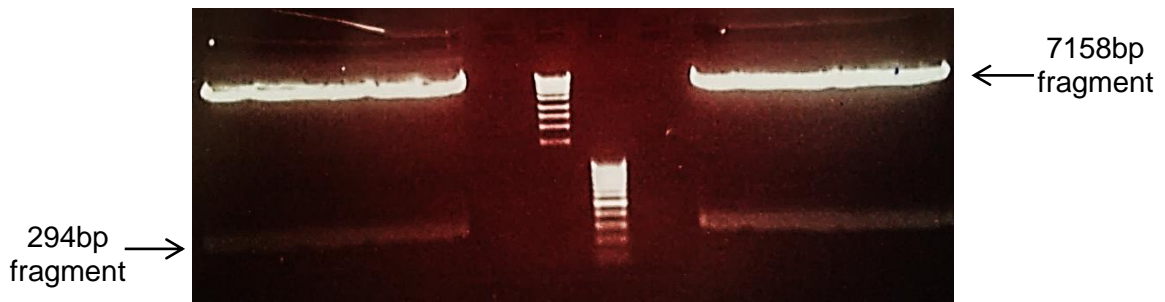


Figure 2.11. Purification gel (1% Seaplaque gel) APP751-pcDNA3.1 (lane 1) and FGJap695-pcDNA3.1 (Lane 4) digested with EcoRI and XbaI. The 294bp fragment excised from APP751 is highlighted and the 7158bp large fragment from JapAPP695 pcDNA 3.1 containing the first 1800bp of the wtAPP695 gene and the pcDNA3.1 backbone.

Ligation reactions (section 2.2.2.9) were performed to insert the purified 294bp fragment into the JapAPP695 pcDNA3.1 backbone. After transformation into *E.coli* only six colonies were recovered. All colonies were screened using colony PCR (section 2.2.1.17). The gel in Figure 2.12 shows that of the six colonies, three produced an amplicon of the expected size (2092bp).

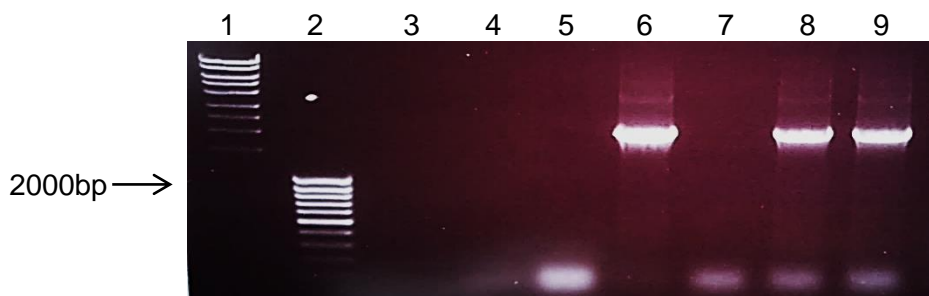


Figure 2.12. Colony PCR analysis of bacterial clones transformed with wtAPP695 pcDNA3.1 (1% agarose gel). Lane 1, Mass Ruler High, lane 2 Mass Ruler Low Range ladder, lane 3, negative control lanes 4 to 9 represent PCR products derived from bacterial clones designated EW1 to EW6, lane 7, negative control.

Plasmid DNA was recovered from the three positive clones designated EW3, EW5 and EW6 and sequenced (see section 2.2.1.2). The sequences were compared with that of the wtAPP695 DNA sequence (accession number, NM\_201414.2). The clones EW3 and EW5 contained the correct sequence. The sequence alignment of clone EW3 is shown in Figure 2.13.



Figure 2.13. Sequencing of wtAPP695-pcDNA3.1. Sequence alignment of clone EW3 with wtAPP695 gene confirmed the correct wildtype sequence had been generated (also confirmed by additional sequencing reactions). A section of the chromatogram obtained after sequencing with the (PCDNA+70 rev) primer demonstrating the corrected G->T base change at position 1923 of the APP gene sequence (enclosed within the black box).

### 2.3.3 Construction of the SweAPP695-pcDNA3.1

Once the wtAPP695-pcDNA3.1 had been successfully constructed, it was used as a DNA template to introduce the Swedish mutation by primer-induced mutagenesis. The Swedish mutation is a GA–TC mutation (Lysine–Methionine and Asparagine–Leucine (KM-NL)) that lies just upstream of the unique EcoRI restriction site within the APP695 cDNA sequence. The mutagenic APPSwe Rev primer (Figure 2.14), was designed to be complementary to the wtAPP695 sequence except in the region where it encodes the TC mutation which is stabilised during the PCR by the 14 complementary base pairs upstream and 11 base pairs downstream of the point mutation. The primer ends in an EcoRI recognition site (see appendix for sequence).



Figure 2.14. Sequence of the APPSwe Rev (reverse) primer used to introduce the TC mutation. Complementary base pairing is shown upstream and downstream of the two point mutations. The EcoRI recognition site is italicised for clarity.

The forward primer, Ex APP alt For was used with the mutagenic primer, APPSwe Rev in a PCR reaction (section 2.2.1.4) to produce an 1800bp product with the introduced Swedish mutation flanked by a 5' HindIII site and a 3' EcoRI site. This allowed the mutagenized fragment to be inserted into the wtAPP695-pcDNA3.1 construct by cassette mutagenesis. Initially a gradient PCR reaction (section 2.2.1.4) was performed to find the optimal annealing temperature. The resulting PCR products were analysed by agarose gel electrophoresis (section 2.2.1.9, Figure 2.15).

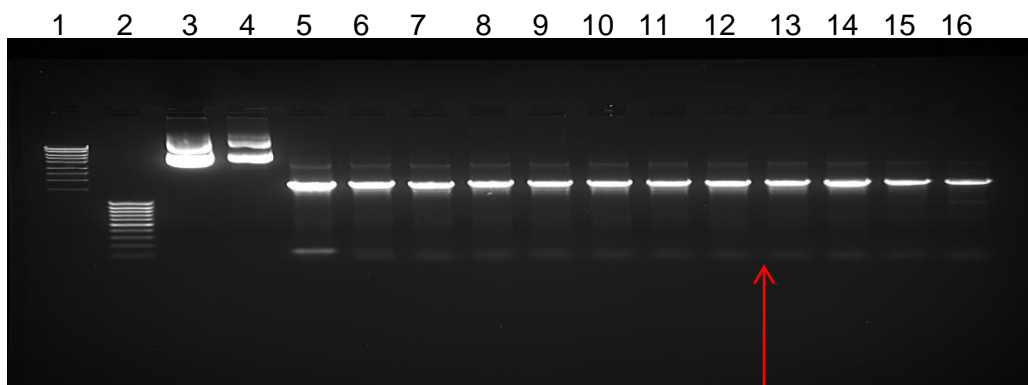


Figure 2.15. Agarose gel of gradient PCR (1% agarose gel). Lane 1, MassRuler High Range, lane 2, MassRuler Low Range, lanes 3 and 4 are plasmids EW3 and EW5 respectively, lanes 5 to 16, gradient PCR to determine optimal temperature for primer annealing in lanes 5 to 16. Temperatures ranged from 51.6 to 68.3°C.

The chosen temperature was 65°C, which is estimated to give a PCR product between lanes 13 and 14 (as indicated by the red arrow). This temperature gives maximal PCR product with relatively little primer dimer interaction (as shown by weak lower banding). A large scale PCR (section 2.2.1.4) was set up using 3ng of wtAPP695-pcDNA3.1 as template DNA and the resulting APP amplicons analysed by agarose gel electrophoresis (section 2.2.1.9) (see Figure 2.16.).

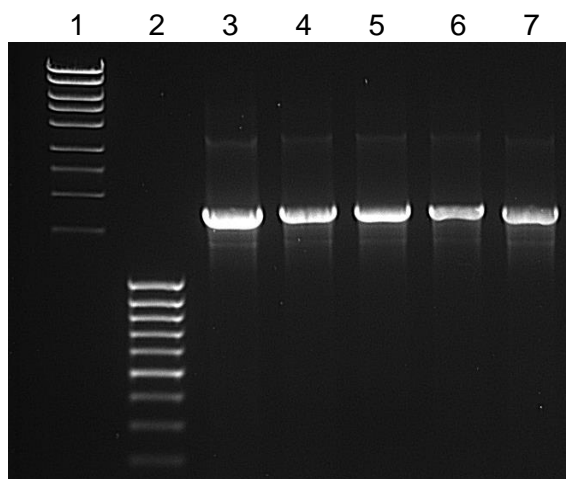


Figure 2.16. Agarose gel of PCR amplification of the 1800bp APP695 amplicon carrying the Swedish mutation (1% agarose gel). Lane 1, Mass Ruler High Range ladder, lane 2, Mass Ruler Low Range ladder, lanes 3 to 7 PCR products.

As only a single amplicon was visible in the SweAPP PCR products, the APP amplicon was PCR purified (see section 2.2.1.12) to remove unwanted small fragments along with the Pfu taq polymerase. The wtAPP695-pcDNA3.1 construct (10µg) and the purified APP amplicons (5µg) were digested with HindIII-XF and EcoRI-HF (4 hours at 37°C). After heat inactivation (80°C for 20 minutes), the digested plasmid was gel extracted (Figure 2.17, see section 2.2.1.10) and PCR purified (see section 2.2.1.12). Amplicons were PCR purified to remove unwanted small fragments removed in the digestion.

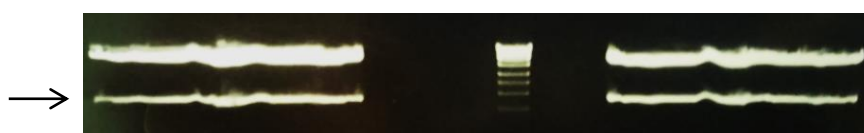


Figure 2.17. Agarose gel purification of the double digest (HindIII and EcoRI) of plasmid EW3 (1% Seaplaque gel). The large band corresponds to the pcDNA3.1 backbone attached to the 3' end of APP695. The lower target band of 1800bp (highlighted by the arrow) was excised and gel purified.

The purified plasmid was dephosphorylated (section 2.2.1.13) and a ligation reaction was set up with a 3:1 molar ratio of insert to vector (section 2.2.1.14) to insert the purified 1800bp APP amplicon carrying the Swedish mutation into the digested vector. A self-ligation was also performed in the presence of dephosphorylated vector. The ligation reactions were transformed into Mach1™T1R cells (section 2.2.1.16), and selected by plating on LB containing ampicillin (section 2.2.1.15).

Only two colonies were recovered from the transformation. Both colonies were screened by colony PCR (section 2.2.1.17) for the presence of the full length APP gene. Agarose gel electrophoresis of the colony PCR products (Figure 2.18) showed that only one of the two recovered clones contained the full length insert. This clone was designated ES1 and small scale plasmid isolation performed (section 2.2.1.18) and the DNA prepared for sequencing (section 2.2.1.2).

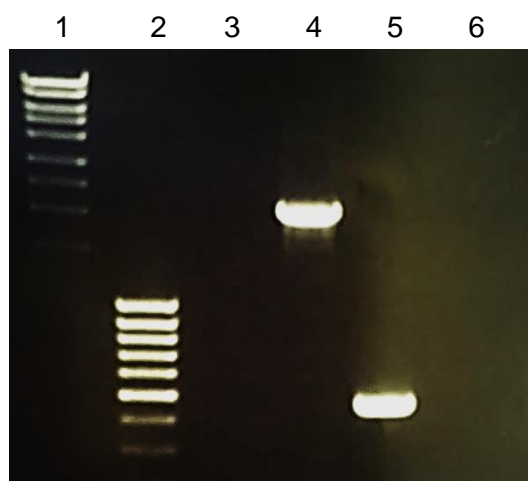


Figure 2.18. Agarose gel analysis (1% agarose gel) of clones transformed with SweAPP695-pcDNA3.1. Lane 1, Mass Ruler High Range ladder, lane 2, Mass Ruler Low Range ladder, lanes 3 and 6, negative controls, lane 4, clone ES1 and lane 5, clone ES2. Only ES1 was positive for the APP insert.

Sequence alignments between clone ES1 (Figure 2.19) and wtAPP695 in pCDNA3.1 showed complete homology with the inserted sequence except in the mutagenized region. One of the alignments obtained using the primer APP1004 is shown in Figure 2.19 with the 1985-1986bp region in the figure corresponding to the Swedish mutation at 1784-1785 of the APP gene. Alignments of multiple sequencing runs with differing forward and reverse primers spanning the entire construct confirmed the successful construction of SweAPP695-pcDNA3.1 (data not shown).

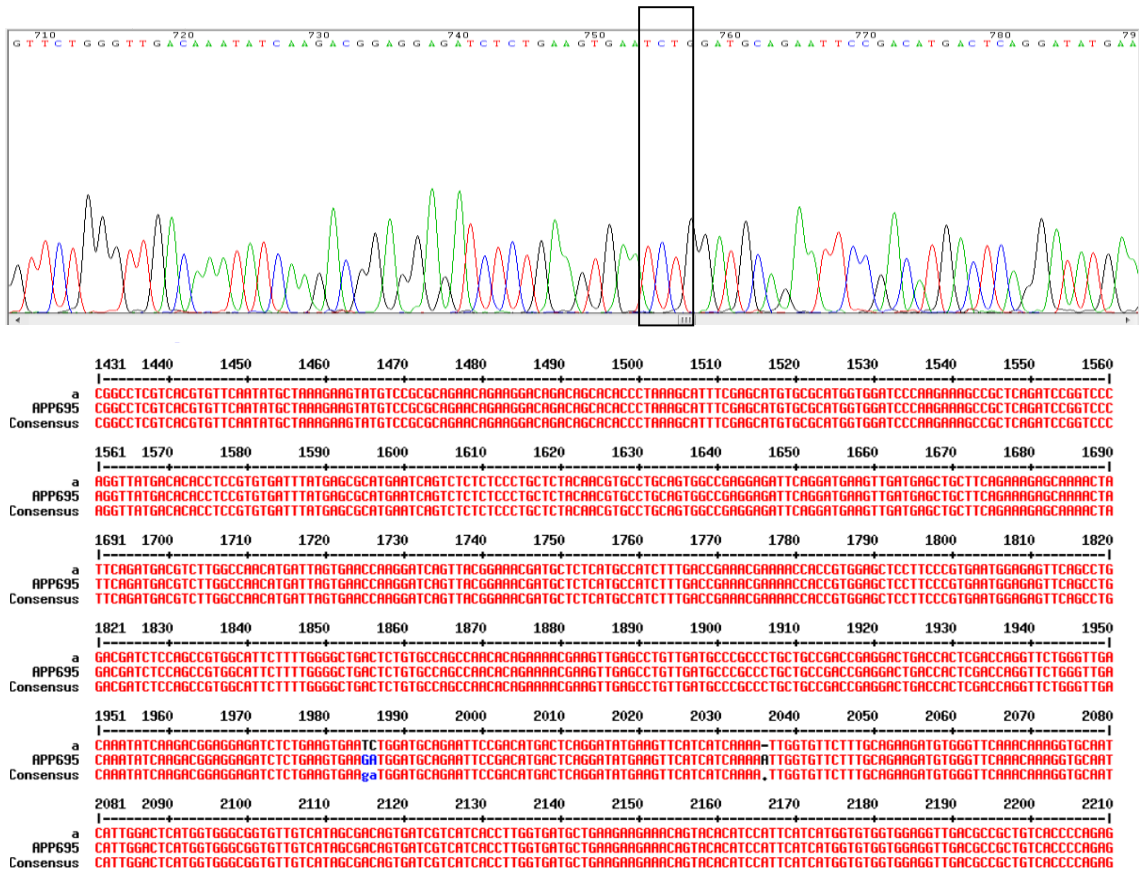


Figure 2.19. Alignment of APP gene sequence identified using the primer APP1004. The boxed area shows clearly the presence of the TC mutation, which when aligned with the wtAPP695 sequence in Multialin, shows its correct position at 1784-1785 of the APP gene. This mutation was also identified using the APP1545 primer, demonstrating that this apparent base change is genuine, and not the result of inaccurate sequencing.

### 2.3.4 Immunocytochemistry (ICC) of COS7

To ensure correct expression of the APP protein, the newly generated mammalian constructs were tested by transient transfection into COS7 cells in order to perform immunocytochemistry and protein expression studies. The African green monkey kidney fibroblast-like cell line, COS7 cell line was used to test expression of wtAPP695/SweAPP695-pcDNA3.1 created from the two donor plasmids.

To confirm expression of both wtAPP695 and SweAPP695, immunocytochemistry was employed, using antibodies directed against APP. Immunostaining is useful as it can be used to identify proteins in their native conformation and allows visualisation of cellular localisation. COS7 cells were transiently transfected (section 2.2.3.4) with the

SweAPP695 and wtAPP695 plasmids or the respective controls. After 48 hours, the transfected cells were fixed and permeabilised for ICC (section 2.2.3.5) using mouse anti-APP695 (Invitrogen, 1:500). The fixed cells were mounted on microscope slides and imaged using a Leica SP2 microscope (section 2.2.3.6), using the capture settings listed in Table 2.3.

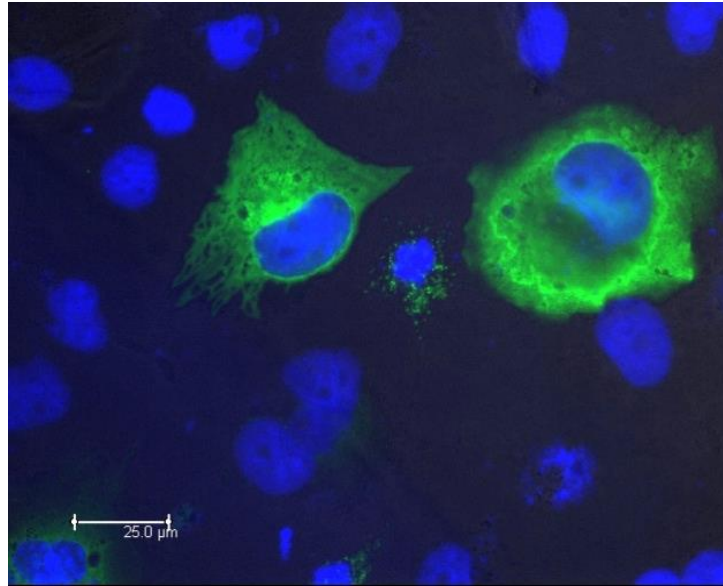
Component to view	Colour		Filter cube	UV Excitation $\lambda$ (nm)	UV Emission $\lambda$ (nm)
Cells	Greyscale	Phase bright	-	-	-
FITC (APP)	Green	Fluorescence	GFP	495	519
GFP-NLS	Green	Fluorescence	GFP	498	516
Nuclei (DAPI)	Blue	Fluorescence	A4	345	455/478

Table 2.3. Microscope settings used to view different fluorescent components of the cells.

The control cells (transfected with GFP-NLS) expressed GFP which was localised to the nucleus (data not shown). Negative controls (untransfected COS7 cells) did not express detectable APP that could be visualised via immunostaining (data not shown). This suggested any green fluorescence after staining of the APP transfected wells would be due to the presence of APP and not auto-fluorescence of the cells.

Results from SweAPP695- pcDNA3.1 and wtAPP695-pcDNA3.1 transfected cells (Figure 2.20) confirm that the APP was expressed within transfected cells and in most cases was diffusely located throughout the cytoplasm. APP expression which is normally found at the plasma membrane or within vesicles of the trans Golgi network was not confirmed by ICC. This non-organelle specific expression could suggest some loss of normal processing due to massively high levels of APP expression under the strong CMV promoter. In addition, the same primary antibody was able to recognise and bind to the SweAPP695 protein.

A



B

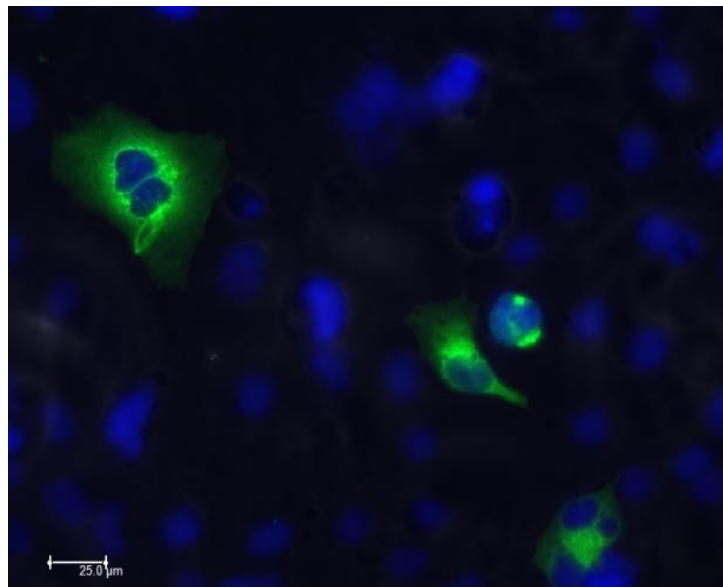


Figure 2.20. Representative fluorescent images of transfected COS7 cells (43 x oil objective). Mouse anti-APP695 antibody was used to visualise APP and FITC secondary antibody used to visualise the primary antibody. Figure A) shows the wtAPP695 transfection and Figure B) shows COS7 cells transfected with SweAPP695. Nuclei were visualised using Hard Mounting Medium containing DAPI (blue). Scale Bar 25μm.

### 2.3.5 Western blot

To further confirm the presence of APP, immunoblotting of the transfected COS7 cells was carried out. Immunoblotting using anti-APP695 antibody was able to detect bands in lanes containing COS7 cell lysate (Figure 2.21). The approximate molecular weight of APP695 is 115kDa and comparison to the molecular weight markers revealed protein bands detected between 100–130kDa in all 4 lanes. Weak APP protein expression was observed in untransfected COS-7 cells and in NT2.D1-derived neuronal cell lysates, which are known to express APP, and were used as a positive control. An increased level of APP expression was observed in wtAPP695 and SweAPP695 transfected cells, suggesting that the constructs were successfully overexpressing APP in these cells. Membranes were also blotted using anti-A $\beta$  antibodies, as a secondary conformation. These blots showed similar protein bands (data not shown) with the additional amyloid positive control at approximately 4kDa. It should be noted whilst increased APP expression seems apparent, it is unclear whether APP is processed accordingly.

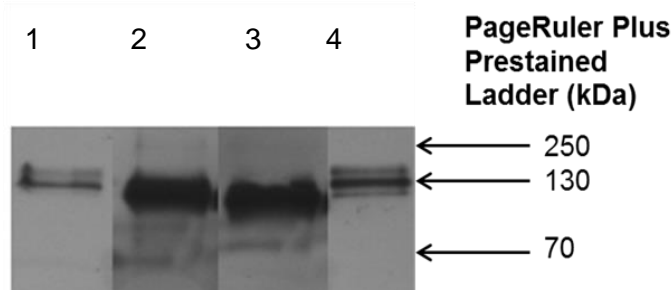


Figure 2.21. Western blot of APP695 expression in transfected cells. Lane 1, COS7 control lysate, lane 2, wtAPP695 transfected COS7 lysate, lane 3, SweAPP695 transfected COS7 lysate, lane 4, positive control of natural APP found within NT2 lysate (provided kindly by Dr Marta Tarczyluk).

### 2.3.6 Construction of pLenti6.4 Syn1 wtAPP695/ SweAPP695 lentiviral constructs

Transient transfection of both APP expressing constructs in pcDNA3.1 led to increased levels of detectable APP695 in COS7 cells suggesting both constructs are expressed effectively. The base plasmid pcDNA3.1 drives expression of these genes under the control of a cytomegalovirus enhancer (CMV) promoter. The high level expression of genes driven by the CMV promoter is beneficial for transient transfection, as results can be gained quickly. For the creation of a cell line, such high levels of expression

over long periods of time may however be detrimental to cell growth and metabolism. The CMV promoter is also active in all cell types, but in the brain, APP695 expression is predominantly limited to neurons. Prior to the creation of the cell lines, the tested coding sequence of APP695 and SweAPP695 were moved into a lentiviral vector and the promoter replaced with a neuronal specific promoter which drives low to medium level expression in neuronal cells.

Lentiviral vectors were used in the creation of the cell line as transduction with lentivirus results in stable integration of the cloned DNA into the host cell genome with better efficiency than spontaneous integration of plasmid DNA. The use of lentiviral vectors has the added advantage of being able to transduce differentiated cells for future studies. To construct the lentiviral vector, the ViraPower HiPerform Promoterless Gateway Expression System (Invitrogen Paisley UK) was used, as the included lentiviral destination vector already includes a blasticidin resistance marker, to enable the selection of transduced cells and thus create a cell line. This system allows for a high level of expression using any promoter to express a transgene of interest in a choice of cell types. The gateway system relies upon recombinase enzymes derived from bacteriophage Lambda, to catalyse the linking of separate strands of DNA contained in donor "entry" vectors into one continuous strand of DNA contained within the desired final expression construct. An outline of the technology is shown in Figure 2.22.

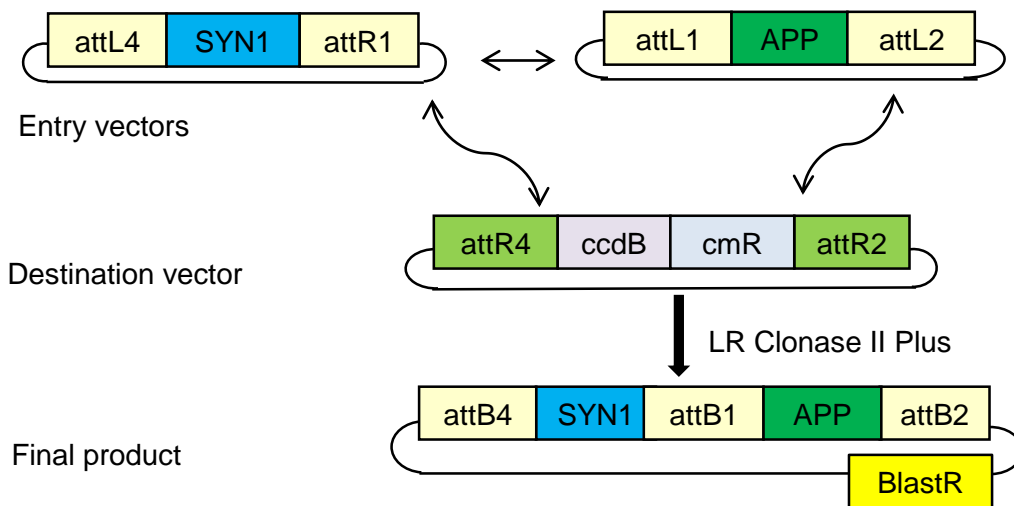


Figure 2.22. Schematic of the gateway<sup>®</sup> recombination reaction. During recombination *attL* and *attR* sites recombine to form an *attB* site (known as the LR reaction). The diagram represents the steps in the creation of lentiviral constructs expressing APP under the control of the Synapsin I (*SYN1*) promoter. The viral vector *ccdB* gene (essentially a “death gene”) is removed by the recombination allowing negative selection of non-recombined DNA. Note, after recombination, the *attB1* region which separates the promoter and transgene of interest is only 40-50bps in size.

As can be seen from Figure 2.22, by taking advantage of the specific recombination of the unique *attP* and *attB* sites allows directional recombination of multiple DNA coding sequences into the final expression construct. In the construction of the lentiviral viral vectors, the final expression plasmid was the lentiviral vector pLenti6.4/R4R2/V5-DEST. To produce these constructs the first step was the creation of donor “entry” vectors containing either the APP695 or SweAPP695 coding sequence, suitable for recombination into the final expression vector.

### 2.3.6.1 Construction of pCR8-wtAPP/SweAPP

An entry vector containing the correct *attL1* and *attL2* sites was selected for the cloning of human wtAPP695 and SweAPP695. The pCR8/GW/TOPO TA vector was selected as it is one of the few plasmids bearing the correct *attL1* and *attL2* sites for directional recombination into pLenti6.4/R4R2/V5-DEST. This plasmid forms part of a TA Cloning Kit (Invitrogen, Life Technologies, Paisley, UK). TA cloning is a subcloning technique which utilises topoisomerase to link PCR products into a topoisomerase charged vector utilising the additional 3’Adenine bases added by Taq polymerase during PCR

amplification. It is quicker than traditional subcloning but is non-directional. Thus the first step in the creation of the APP entry vectors was the amplification of the coding sequences (ensuring they contained the necessary 3'A overhangs), for their cloning into pCR8/GW/TOPO TA vector, and the identification of those plasmids in which the inserts were cloned in the correct orientation.

The wtAPP695/SweAPP695 genes were amplified with Phusion High-Fidelity DNA polymerase (NEB, New England, USA) in GC reaction buffer, using the wtAPP695/SweAPP695 pcDNA3.1 plasmids (described in section 2.2.4 and 2.2.5) as a template DNA. A gradient PCR was performed to determine the optimal annealing temperature for the primers; APP8 TOPO For G and APP FRAME STOP / APP P8 Rev 2STOP (sequences contained in appendix) using the cycling conditions in Table 2.3 for a total of 31 cycles.

Step	Task	Temperature	Duration
1	Initial denaturation	98°C	50 seconds
2	Primer annealing	60°C with gradient of 20°C	50 seconds
3	Extension	72°C	42 seconds (20 seconds per 1kb of template)
4	Final extension	72°C	10 minutes

Table 2.4. PCR amplification steps for Phusion amplification of template DNA.

Agarose gel analysis (Figure 2.23) of the amplicons showed a single specific band at most temperatures. An annealing temperature of 66°C was chosen for large scale amplification of the wtAPP695 and SweAPP695 genes.

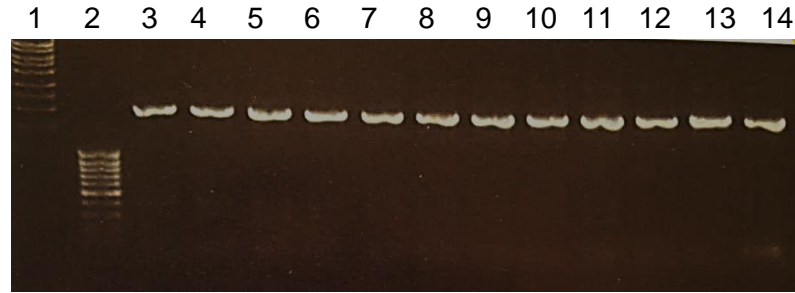


Figure 2.23. Agarose gel electrophoresis of gradient PCR with APP P8 TOPO and APP P8 2STOP primers (1% agarose gel). Lane 1, MassRuler High Range, lane 2, MassRuler Low Range, lanes 2 to 14 correspond to APP amplicons amplified at different annealing temperatures.

Both wtAPP695 and SweAPP695 were amplified in large scale PCR reactions using the primers and an annealing temperature of 66°C. The resulting PCR products were gel purified (see Figure 2.24 for SweAPP695 and Figure 2.25 for wtAPP695 gel purification, section 2.2.1.10) to remove the Phusion DNA polymerase and PCR purified (section 2.2.1.12) to remove any impurities carried through from the gel extraction.



Figure 2.24. Purification gel for SweAPP695 amplicons (1% Low melting point agarose gel).

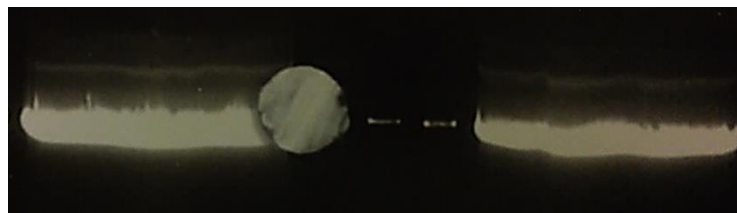


Figure 2.25. Purification of wtAPP695 amplicons DNA (1% low melting point agarose gel).

As the DNA polymerase Phusion has 3' to 5' proof-reading activity, it is capable of removing any overhanging adenine bases from the 3' end of amplified products. Prior to cloning the wtAPP695 and SweAPP695 genes into the TOPO vector (which is linearized and tagged with an overhanging Thymine) the 3'A overhangs were added to the purified products using a tailing reaction (section .2.2.1.5). The tailed products

were cloned into the pCR8/GW/TOPO TA using a Topo cloning reaction (section 2.2.1.6). Topo reactions were transformed (section 2.2.17) into *E.Coli* Mach1TR cells and selected using LB agar containing spectinomycin. The success of the Tailing/Topo reactions was confirmed by the recovery of large numbers of colonies (see Table 2.4).

Plasmid transformed	Volume of broth plated ( $\mu$ l)	Number of colonies
SweAPP695 FRAME pCR8	80	25
	160	68
SwAPP695 2STOP pCR8	80	45
	160	90
wtAPP695 FRAME pCR8	80	2
	160	7
wtAPP695 2STOP pCR8	80	4
	160	19
LB only		Confluent
Spectinomycin plate with TOPO vector only		0

Table 2.4. Colonies recovered after transformation with topoisomerase cloned PCR8-APP695 and PCR8SweAPP695 vectors.

No transformants were present as a result of transforming with the TOPO vector alone, but large numbers of colonies were recovered when insert was included which indicated high efficiency of ligation between the APP insert and pCR8 TOPO vector. There was a marked difference in colony recovery between vectors containing the SweAPP695 insert and the wtAPP695 insert with an approximately 7 fold greater total colony recovery in the SweAPP695. This difference in recovery was unexpected, as no protein expression would be expected to occur from the vector used. Furthermore, as the cloned DNA sequences were identical with the exception of the two base pairs encoding the Swedish mutation, it was considered unlikely that protein toxicity or changes in DNA structure of the insert would be the cause. It was considered that the difference in recovery most likely reflected differences between the quantitated and actual amounts of each insert after gel purification (where DNA is at a low concentration and difficult to quantitate) and therefore differences in the actual amount of each insert added into the Topo reactions. Twelve colonies expressing the SweAPP695/wtAPP695-pCR8 plasmid were picked for colony screening using colony

PCR (section 2.2.1.17). The results of the preliminary colony screen are shown in Figure 2.26 and Figure 2.27.

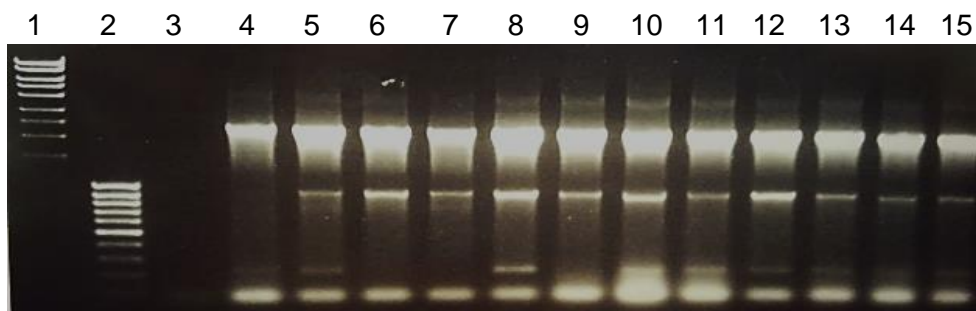


Figure 2.26. Agarose gel electrophoresis of clones transformed with SweAPP695-pCR8 (1% agarose gel); lane 1, MassRuler High Range, lane 2, MassRuler Low Range, lane 3 negative control, lanes 4 to 15 are clones designated SAP1 to SAP12.

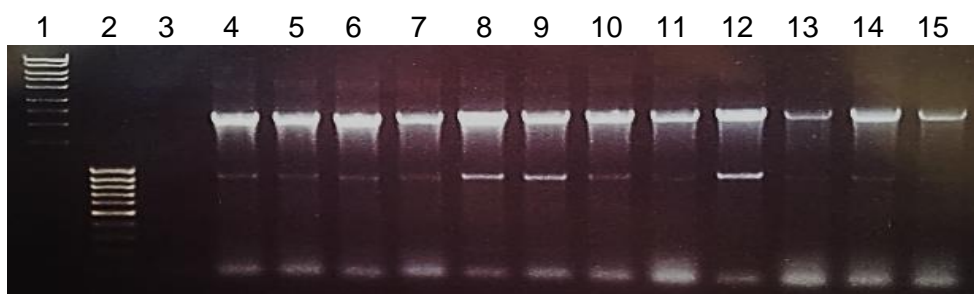


Figure 2.27. Agarose gel electrophoresis of clones transformed with wtAPP695-pCR8 (1% agarose gel); lane 1, MassRuler High Range, lane 2, MassRuler Low Range, lane 3 negative control, lanes 4 to 15 are bacterial clones designated WAP1 to WAP12.

The preliminary colony screen identified all the screened clones as containing an insert of approximately 2000bp, suggesting that topoisomerase mediated insertion of DNA occurred at high efficiency. Small scale plasmid isolation (section 2.2.1.18) was carried out for each of the twelve clones for SweAPP695-pCR8 and wtAPP695-pCR8 for further screening. As topoisomerase mediated cloning is non directional, a further screening strategy was devised to identify the clones in which the APP gene was contained in the correct forward orientation prior to sequence analysis. Plasmid maps of the desired constructs with APP in both orientations were analysed for suitable unique restriction sites in the vector backbone/ insert that could be used to clearly identify insert orientation. As shown in Figure 2.28, digestion with EcoRV (whose recognition sequence is in the plasmid backbone) and BamHI (approximately 1330bp into the clone APP gene), leads to the release of APP fragments of 891bp and 4028bp

if the insert is in the correct orientation, but fragment sizes of 1467bp and 3452bp if the insert is in the reverse orientation.

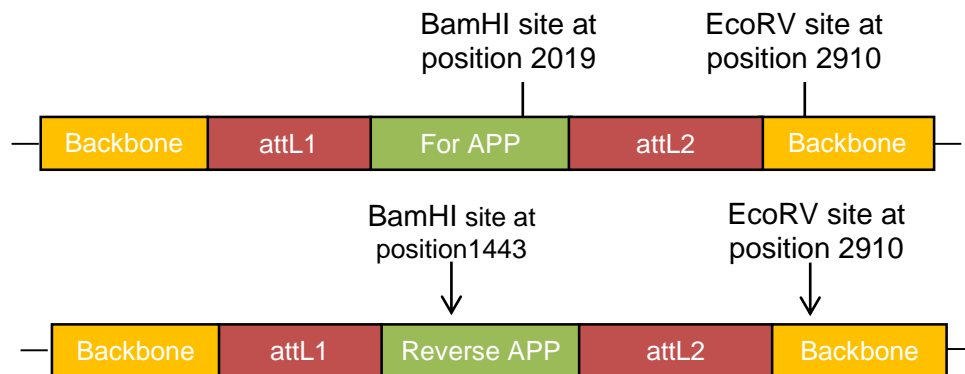


Figure 2.28. Diagrammatic representation of APP695 pCR8. The backbone is the pCR8 vector containing the EcoRV recognition site. If APP695 is in the correct orientation, the unique BamHI site lies at position 2019 of the vector (in the APP gene), but if APP695 is inserted in the reverse orientation, the *Bam*HI site lies at position 1443.

Six to eight clones of wildtype APP695 / SweAPP695 were digested and the resulting fragments analysed by agarose gel electrophoresis (Figure 2.29, Figure 2.30).

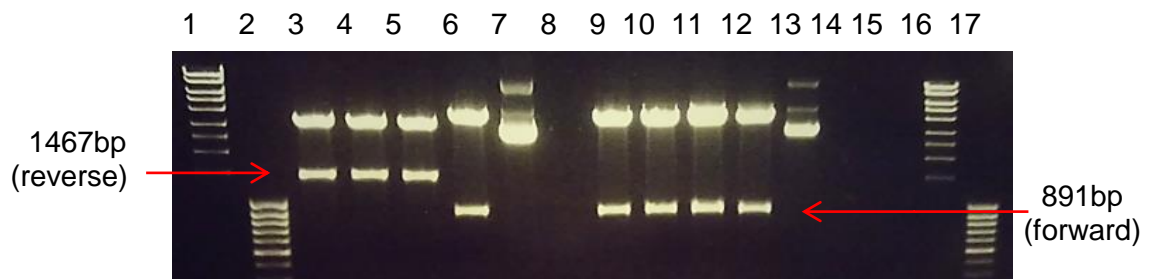


Figure 2.29. Agarose gel electrophoresis of orientation analysis from fragments excised from SweAPP695 plasmids (1% agarose gel); lane 1, MassRuler High, lane 2, MassRuler Low Range. Lanes 3 to 6 are from clones SAP1 to 4, lane 7, uncut SAP4 plasmid, lanes 9 to 13 clones SAP7, SAP 8, SAP10, SAP12, lane 14, uncut SAP8, lane 16 ,MassRuler High Range and lane 17, MassRuler Ruler Low Range.

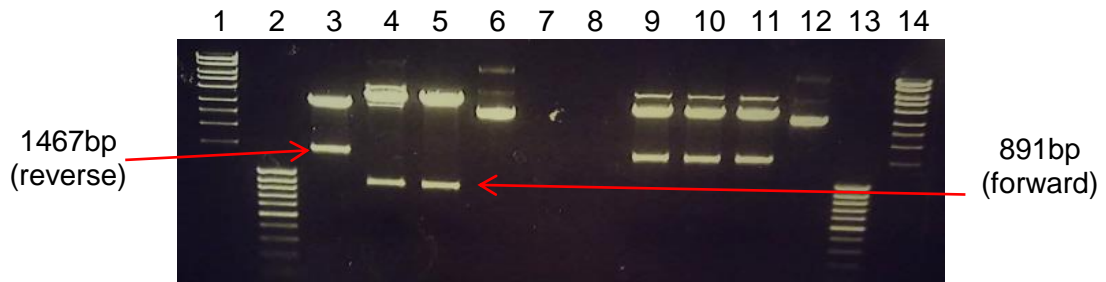


Figure 2.30. Agarose gel electrophoresis of orientation analysis from fragments excised from wtAPP695 pCR8 plasmids (1% agarose gel); lane 1, MassRuler High Range, lane 2, MassRuler Low Range, lanes 3 to 5, WAP1, WAP4, WAP6, lane 6, uncut plasmid, lanes 9 to 11, clones WAP10, WAP11 and WAP12, lane 12 uncut WAP11 plasmid, lane 13, MassRuler Low Range, lane 14, MassRuler High Range.

Clones SAP4, SAP10, WAP4 and WAP6 clones contained the 891bp and 4028bp fragment sizes confirming that the APP was in the correct orientation. These clones were selected for sequencing (section 2.2.1.2). Sequencing data was compared with the sequence of the designed APP constructs using MultiAlin software (<http://multalin.toulouse.inra.fr/multalin/>). Of the four clones sequenced (2 Swedish and 2 wildtype), all contained the correct SweAPP695/ wtAPP695 gene sequence inserted in the correct orientation, with the attL sites intact. However, one clone (SAP10) contained a point mutation (A > G) at position 1661, possibly due to a PCR-induced error. This clone was removed from further analysis. As each clone required four reactions to cover the complete APP sequence, a summary of sequencing results is tabulated (Table 2.5) for the remaining clones.

Sample	Primer	Construct	Comments
1	M13 FOR	SAP4	(start of attL1 site – 1545 (APP))
2	APP613	SAP4	1363-2197
3	APP1004	SAP4	1730 – 2716
4	M13 REV	SAP4	1920 – 2917 (into attL2)
9	M13 FOR	WAP4	575 – 1545
10	APP 613	WAP4	1406 – 2268
11	APP1004	WAP4	1802 – 2716
12	M13 REV	WAP4	1941 – 2916 (into attL2)
13	M13 FOR	WAP6	575 – 1579
14	APP 613	WAP6	1363 – 2268
15	APP1004	WAP6	1805 – 2670
16	M13 REV	WAP6	1915 – 2791 (end of APP)

Table 2.5. Sequencing results of successful clones confirming the correct sequence of APP and upstream and downstream of insert.

Once sequence analysis had confirmed that the SweAPP695/wtAPP695 gene sequence was correct, and that the attL recombination sites were intact, two clones SAP4 and WAP4 were taken forward for large scale plasmid isolation (see section 2.2.13).

#### **2.3.6.2 Construction of the promoter entry vector**

Many studies of APP expression have been based upon the use of viral-based promoters to achieve high level protein expression in all cell types. However, these levels may be considered abnormally high and in the case of neuronal expressed APP695, this approach is not appropriate. Therefore, a neuronal specific promoter was selected ensuring APP695 expression would be expressed in neuronal cells as would occur naturally in the brain. The chosen neuronal promoter for the viral construct was the Synapsin I promoter. Synapsins are a group of neuronal phosphoproteins, which coat the cytoplasmic surface of synaptic vesicles and specifically SynI and SynII are only expressed in the nervous system, which established the synapsin genes as good candidates for an investigation of neuron-specific gene expression (Schoch et al., 1996). Originally, APP expression was to be studied in the NT2.D1 embryocarcinoma cell line which differentiates into neuronal and astrocytic co-cultures, therefore placing APP expression under Synapsin I control would ensure APP expression within only neuronal cells. However, despite repeated attempts to create stable NT2.D1 cells expressing APP this line proved unsuitable for long term expression studies (data not shown). The project was redirected to use another available neuronal cell line in the laboratory, the neuroblastoma derived SHSY5Y line. SHSY5Y cells have been previously shown to express Syn1 (Goodall et al., 1997). The SYN1 promoter was chosen for physiological levels of APP expression after preliminary qPCR studies (data not shown) suggested an approximate ratio of 2:1 of APP to SYN1 mRNA. Therefore it was estimated (assuming that transcription from the incorporated SYN1 promoter is identical to that of the native promoter), that incorporation of a SYN1 driven APP

construct would result in an approximate 1.5 fold increase in APP in differentiated SHSY5Y cells.

An entry vector containing the correct attL4 and attR1 sites was selected for the cloning of human Synapsin I. The pENTR 5'-TOPO TA vector was selected as one of the few plasmids bearing the correct attL4 and attR1 site for directional recombination into pLenti6.4/R4R2/V5-DEST. This plasmid forms as part of a TA Cloning Kit (Invitrogen, Life Technologies, Paisley, UK).

The creation of the SYN1 entry vector followed a similar approach to that used to create the APP entry vectors. The SYN1 promoter was amplified from an existing plasmid construct (PZS-SYN1-eGFP, kindly provided by Dr David Nagel). This clone contains a truncated 495bp Syn1 promoter described in (Liu et al., 2008). The amplified products were tailed to ensure they contained the necessary 3'A overhangs for cloning into the pENTR5' TOPO TA vector, and then cloned using topoisomerase ligation before identifying those plasmids in which the SYN1 insert was cloned in the correct orientation.

The SYN1 gene was amplified with Phusion High-Fidelity DNA polymerase (NEB, New England, USA) in GC reaction buffer using the PZS-SYN1-eGFP plasmid as template DNA. A gradient PCR was performed to determine the optimal annealing temperature for the primers, SYN1 Pentr5 For G and Syn1 Pentr5 rev (complementary to the SYN1 promoter sequence) (see appendix for primer sequence and section 2.2.1.3). The cycling conditions are listed in Table 2.6. A total of 31 cycles was performed.

Step	Task	Temperature	Duration
1	Initial denaturation	98°C	50 seconds
2	Primer annealing	60°C with gradient of 20°C	50 seconds
3	Extension	72°C	15 seconds (20 seconds per 1kb of template)
4	Final extension	72°C	10 minutes

Table 2.6. PCR conditions set out to amplify the SYN1 gene.

After amplification, PCR products were analysed on a 2% agarose gel (section 2.2.1.9) (see Figure 2.31), for the presence of 495bp amplicons.

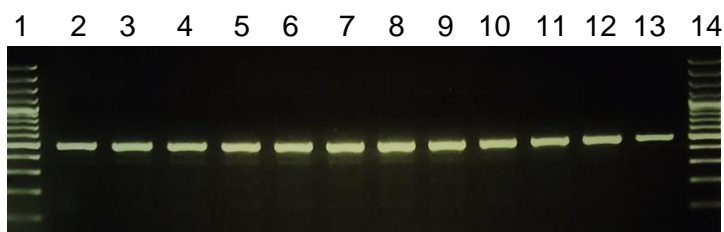


Figure 2.31. Agarose gel analysis of products from the gradient PCR of the SYN1 promoter using Syn 1 Pentr5 For g and Syn1 Pentr5 Rev primers (2% agarose gel). Lane 1, Mass Ruler High Range, lanes 2 to 13 correspond to products formed at increasing annealing temperatures, lane 14, Gene Ruler 100bp Plus.

The SYN1 promoter was subsequently amplified in large scale PCR reactions (section 2.2.1.4) using the primers Syn 1 Pentr5 For g and Syn1 Pentr5 Rev with an annealing temperature of 64.5°C. The resulting PCR products (Figure 2.32) showed predominantly a single band with minimal additional banding.

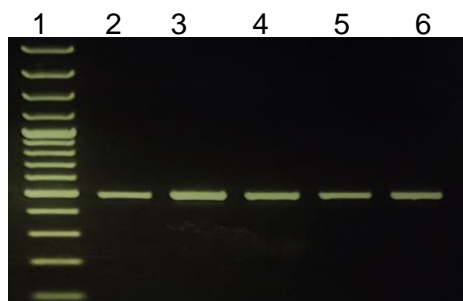


Figure 2.32. Agarose gel analysis of large scale PCR amplification of the SYN1 gene (1.75% agarose gel). Lane 1, Gene Ruler 100bp Plus, lanes 2 to 6, SYN1 amplicons of 495bp.

The amplicons were gel purified (section 2.2.1.10) and then PCR purified (section 2.2.1.12). Purified amplicons were tailed (section 2.2.1.5) and cloned into the pENTR5'

TOPO vector (section 2.2.1.6). Topo reactions were transformed (section 2.2.1.7) into *E.Coli* Mach1TR cells and selected using LB agar containing kanamycin. The success of the Tailing/Topo reactions was confirmed by the recovery of large numbers of colonies (data not shown, due high numbers of colonies recovered, estimated >2000/plate). Twelve colonies were picked and screened using M13 For and M13 Rev primers (section 2.2.1.17) and analysed on a 1.75% agarose gel (see Figure 2.33).

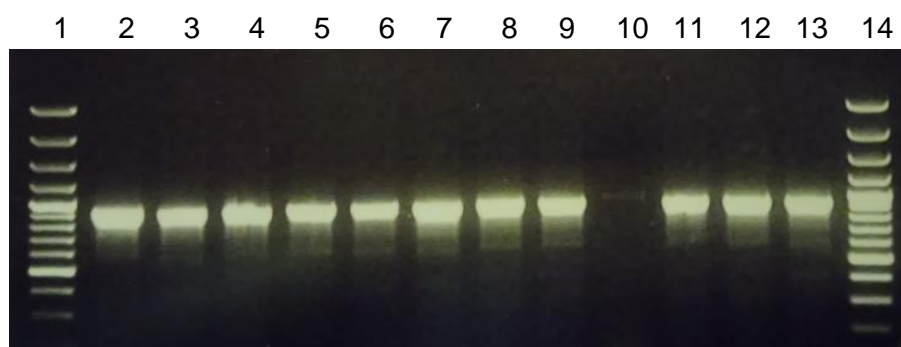


Figure 2.33. Agarose gel analysis of colony screening of the pENTR5 SYN1 TOPO clones (1.75% agarose gel). Lane 1, Gene Ruler 100bp Plus, lanes 2 to 13, G1 to G12 bacterial clones and lane 14, GeneRuler 100bp Plus.

The presence of the SYN1 gene and the two attL sites, which together produce amplicons approximately 800bp in size, was confirmed in all but clone G9. Small scale plasmid isolation (section 2.2.1.18) was carried out using the eight clones positive for the 495bp insert for analysis of insert orientation.

To identify the clones in which the SYN1 gene was contained in the correct forward orientation prior to sequence analysis, plasmid maps of the desired constructs with the SYN1 gene in both orientations were analysed for suitable unique restriction sites in the vector backbone and insert that could be used to clearly identify insert orientation (Figure 2.34). As shown in Figure 2.34, digestion with a single enzyme PST1 (whose recognition sequence is in both the plasmid backbone and cloned SYN1 gene), leads to the release of fragments of 668bp and 2477bp if the insert is in the correct orientation, but fragment sizes of 1211bp and 2934bp if the insert is in the reverse orientation.

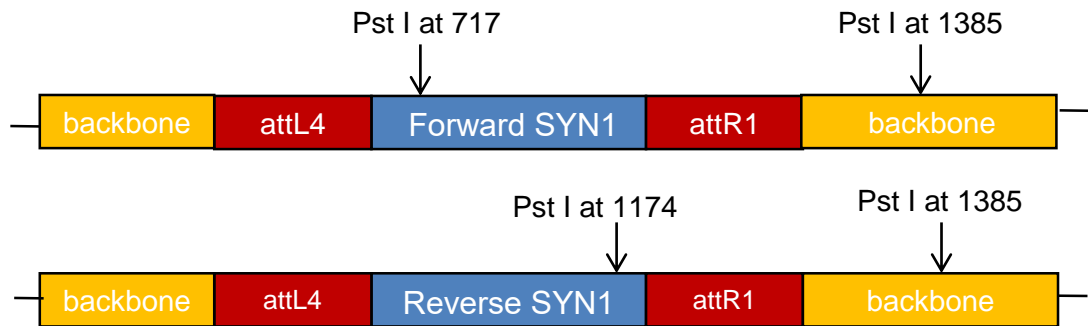


Figure 2.34. Diagrammatic representation of the PST1 sites in SYN1 pENTR5'. One site lies within the SYN1 promoter, whilst the other in the pENTR5' (backbone) vector. If SYN1 promoter is in the correct orientation, both PST1 sites are 668bp away from one another, but if SYN1 is in the reverse orientation, the PST1 sites lie closer to each other (209bp).

Eight bacterial clones of SYN1 were digested with Pst1 and the resulting fragments analysed by agarose gel electrophoresis (Figure 2.35).

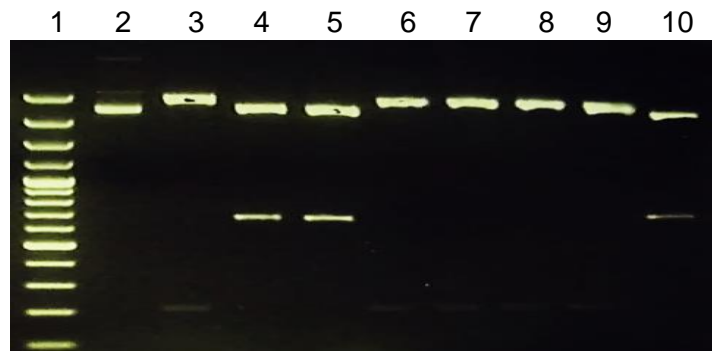


Figure 2.35. Agarose gel analysis of SYN1 pENTR5' clones digested with Pst 1 to determine SYN1 gene orientation (2% agarose gel). Lane 1, GeneRuler 100bp Plus, lane 2, uncut clone (G1), lanes 3 to 10, clones G1, G2, G6, G7, G8, G10, G11 and G12.

From the digest, clones G2 (lane 4), G6 (lane 5) and G12 (lane 10) were confirmed to carry SYN1 in the correct orientation. These were prepared for sequencing (section 2.2.1.2) using M13 For and M13 Rev primers. Sequencing data was analysed against the construct map of SYN1-pENTR5' created using the promoter sequence described in (Liu et al., 2008) using MultiAlin. Clone S12 for which the alignment is shown in Figure 2.36 contained the correct SYN1 promoter sequence and was chosen for large scale plasmid isolation to prepare for the final step of lentiviral plasmid construction.

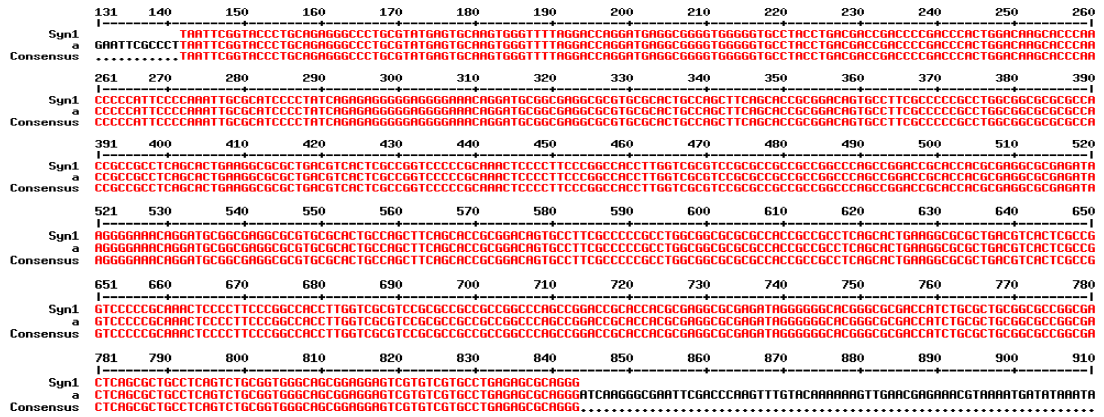


Figure 2.36. Alignment of pENTR5 SYN1 (clone S12) using M13 For and Rev primers aligned with the SYN1 gene sequence show complete alignment of the whole gene.

### 2.3.6.3 Construction of the pLenti6.4 SYN1- wtAPP695/ SweAPP695 V5 DEST

The final step in the construction of the lentiviral vectors was recombination of the Syn1 promoter and either the wtAPP695 or SweAPP695 coding sequence with the lentiviral destination vector. To recombine pCR8-wtAPP695 or pCR8-SweAPP695 with the pENTR5' Syn1 TOPO vector into the final destination vector (pLenti6.4 R4 R2 V5 Dest), a recombination reaction (section 2.2.1.8) was prepared according to the manufacturer's instructions. The reactions were immediately transformed into *Stb13 E.coli* and the recovery of colonies assessed (Table 2.7). Maps of the final vectors were constructed in Clone Manager 5 to approximate the insert size expected for sequencing.

	Volume of inoculated broth plated (µl)	Colonies
pLenti Syn1- SweAPP695	200	102
	300	152
pLenti Syn1-wtAPP695	200	76
	300	106
Negative control	200	1
	300	1

Table 2.7. Bacterial transformants recovered after transformation with pLenti6.4 SYN1- SweAPP695 or pLenti6.4 SYN1-wtAPP695. The high number of transformants reflects the high efficiency of the LR reaction.

Eight wtAPP695 and eight SweAPP695 clones were selected for colony screening using pLenti6.4 Forseq and WPRE Seq Rev seq primers (which read from beyond the attP sites and into the recombined region). Results of the colony screening were analysed by agarose gel electrophoresis (see Figures 2.37 and 2.38).

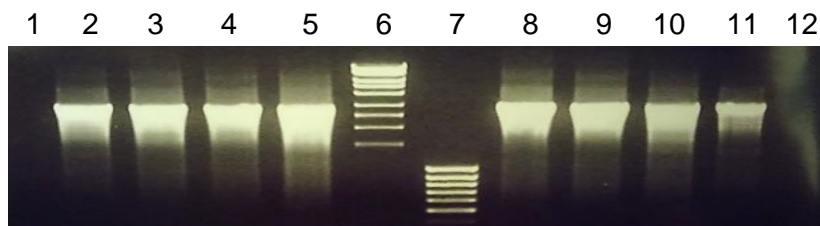


Figure 2.37. Agarose gel electrophoresis showing the colony PCR for pLenti6.4-SweAPP695 clones (1% agarose gel). Lane 1, negative control, lanes 2 to 5, clones WLR1 to WLR4, lane 6, MassRuler High Range, lane 7, MassRuler Low Range, lanes 8 to 11, clones WLR5 to WLR8, 12, negative control.

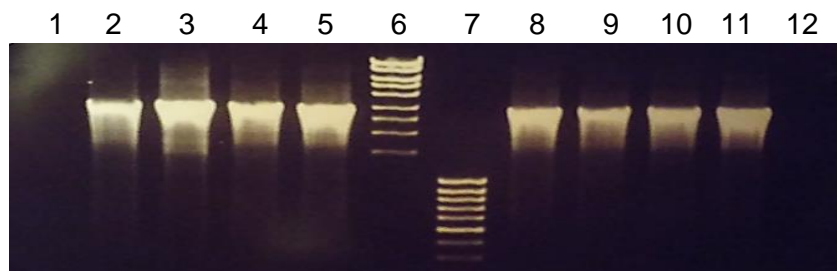


Figure 2.38. Agarose gel electrophoresis showing the colony PCR of pLenti6.4-wtAPP695 clones (1% agarose gel). Lane 1, negative control, lanes 2 to 5, clones SLR1 to SLR4, lane 6, MassRuler High Range, lane 7, MassRuler Low Range, lanes 8 to 11, clones SLR5 to SLR 8.

Of the clones screened, all appeared to produce the expected insert size of approximately 3000bp. This shows the 100% efficiency of recovery using this recombination technique. Only colonies containing the recombined vector would grow under ampicillin selection. Clones WLR 5, WLR7, SLR2 and SLR3 were prepared for sequencing (see appendix for list of primers). Sequencing data was analysed against pLenti-SYN1-wtAPP695/ SweAPP695 gene sequences (constructed using Clone Manager 5) using Multialin software. The complete sequence alignment of clone WLR7 (Figure 2.39) showed complete homology with the designed Syn1-wtAPP695 sequence. The alignment of clone SLR3 with the designed Syn1-SweAPP695 construct (Figure 2.40) again demonstrated complete homology and confirmed that, clones SLR3 and WLR7 represented the correct Syn1-SweAPP695 and Syn1-wtAPP695 promoter/gene constructs in plenti6.4 R4 R2 V5. These plasmids were re-transformed into Stbl3 *E.coli* for large scale isolation (section 2.2.1.19) to be kept as stocks to be used in lentiviral production.

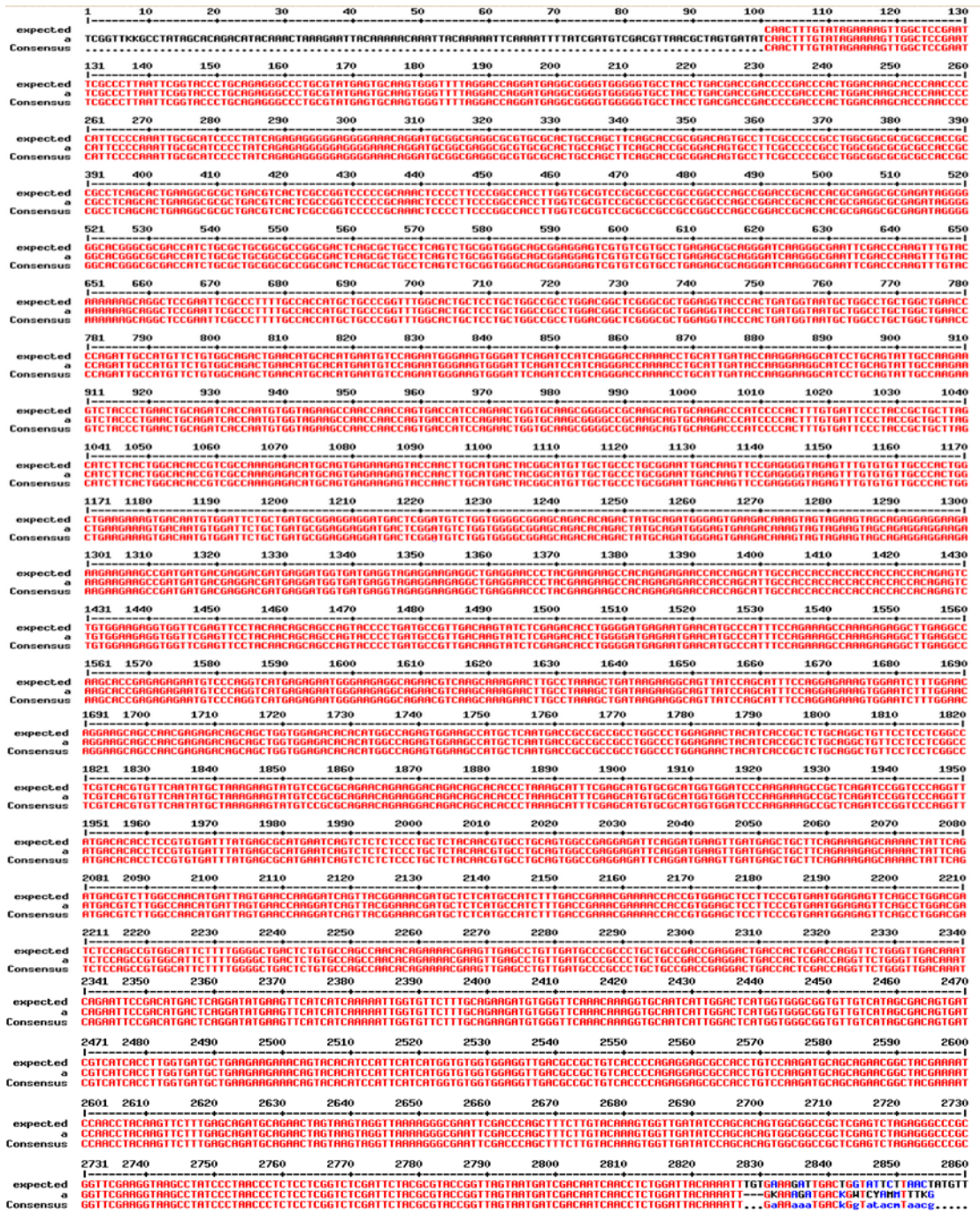


Figure 2.39. Final sequence alignment of the WLR7 (PLenti6.4 SYN1-wtAPP695) using the primers; pLenti6.4for seq, APP748 Rev, APP613 For, APP1004 For and WPRE Rev. Note SYN1 gene sequence begins at position 140 in Multalin. The end of the sequence finishes beyond the APP gene sequence and into the plasmid encoded WPRE (mismatching bases at the end of the sequence are in very close proximity to the 3' end of the WPRE Rev primer binding site and in a non-manipulated area of the plasmid

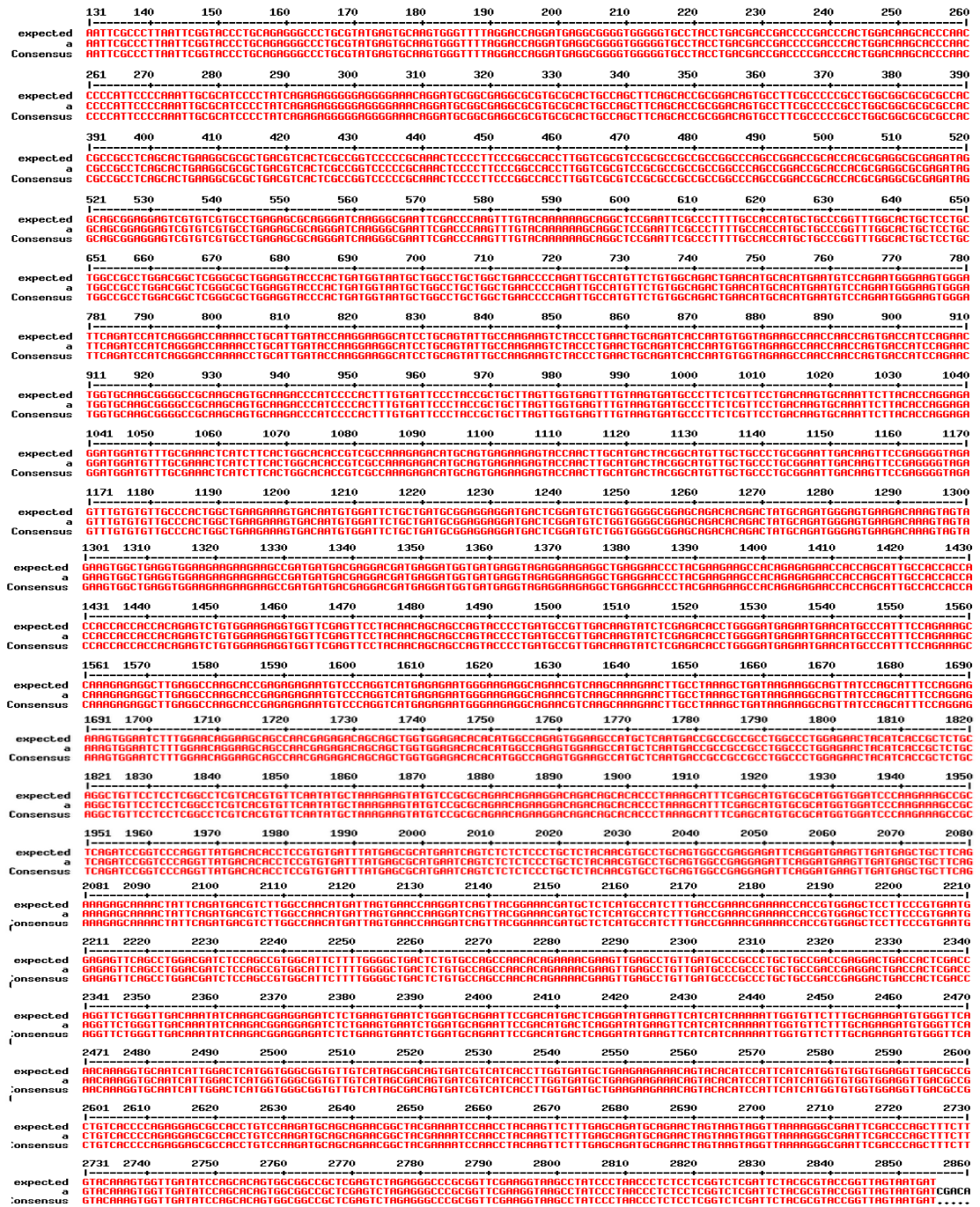


Figure 2.40. Complete sequence alignment of SLR3 (pLenti6.4 SYN1- SweAPP695) using the same primers (primer sequences can be found in appendix). Note the start of SYN1 gene is at position 140 in Multialin. The end of the sequence signifies the end of the V5 epitope, which lies beyond the APP695 gene sequence.

## 2.4 Discussion

The aim of the work described in this chapter was to construct lentiviral vectors to enable the long term expression of either wtAPP695 or SweAPP695. Sequencing of the donor plasmids revealed abnormalities in the gene sequence and therefore the aim of the initial molecular cloning described was to correct these abnormalities by excision and ligation of desired APP gene fragments to create the correct wtAPP695 gene sequence. Testing of the reconstructed wtAPP695 and SweAPP695 genes by expressing in the COS7 cell line demonstrated that APP695 could be expressed in a non-neuronal cell line, and that APP protein expression was recognised by antibodies.

Wildtype APP695 is the predominant isoform of APP expressed within the CNS. In AD, wtAPP695 is abnormally processed to form fragments, one of which is the A $\beta$ 1-42 peptide. Increased production of this peptide is associated with neuronal cell death seen within both AD patient brains and animal models. In particular, overexpression of wtAPP695 can lead to AD pathology as observed in many Down syndrome patients by the fourth decade of life (Lott and Head, 2001). In fact, there are many APP duplication mutations that lead to AD (as shown in Table 1). This was the basis of the decision to study overexpression of wtAPP695.

In addition to the wtAPP695 gene construction, an overexpression system containing a known familial mutation of APP695 was constructed using molecular cloning techniques. Familial mutations in the APP gene have long been associated with EOAD, by influencing APP processing towards the amyloidogenic pathway. The Swedish mutation is one of a number of APP695 mutations identified to cause FAD by increasing BACE cleavage of APP, thereby increasing A $\beta$ 1-42 production. This mutation was selected as it is used to create many AD transgenic mice models, most notably the Tg2576 mouse model, which exhibit age-dependent plaque formation, reflecting human brain pathology as well as showing signs of oxidative stress which is

one aspect considered important in affecting neuronal health. In addition, the expression of SweAPP695 within H4 cells was studied in terms of global gene expression, where as a result of SweAPP695 expression, 283 genes were found to be down-regulated and 384 genes were up-regulated (Shin et al., 2010).

Both the wtAPP695 and SweAPP695 genes were placed under the control of the Synapsin I promoter in a lentiviral construct. Previous studies have utilised viral promoters such as CMV which promote abnormally high expression of protein, in a non-cell specific manner that can also be transient (Moriyoshi et al., 1996). This may be due to the fact that viral CMV promoters may be more prone to being silenced in host cells than eukaryotic promoters (Akaaboune et al., 2000b, Choi et al., 2005). Expression of high levels of protein may also prove toxic to host cells. As APP695 expression is highest in neurons where AD pathology is found, the APP gene construct was designed for expression under the control of the neuronal Synapsin I promoter.

The original objective of this PhD project was based on expression of APP in which Synapsin I is expressed in neurons but not in the astrocytes derived from the NT2.D1 cell line (NT2 differentiation leads to development of neuronal-astrocytic co-cultures). However, preliminary studies performed in our laboratory found that infection of NT2 cells failed to give stable long term expression when using neuronal specific or even ubiquitous promoters. Therefore, the most suitable alternative neuronal cell line available was the SHSY5Y cell line. Lentiviral constructs were utilised as the method to generate stable cell lines, as they can transduce both actively proliferating and non-dividing cells, integrating genetic material into host cells for stable, long term transgene expression. In the future, this system could be used to transduce alternative cell lines for the study of AD.

Generation of cell lines expressing either wtAPP695/SweAPP695 will allow for the study of APP expression/ A $\beta$  production on the effects of cellular metabolism. AD

brains show metabolic changes, which include reductions in glucose consumption, correlating strongly with cognitive deterioration. Key changes are observed before the onset of AD. In fact, PET scans of people who carry familial AD mutations or those exhibiting MCI, which often develops into AD, found severe reductions in glucose consumption (Berti et al., 2010, Mosconi, 2005). These observations also extend to cognitively normal older persons (Mosconi et al., 2012) whose AD progression has been followed through MCI and then to AD, as well as middle-aged individuals carrying the ApoE4 genotype (Mosconi et al., 2004). The latter is particularly interesting, considering that the ApoE4 allele is a strong genetic risk factor for LOAD.

Furthermore, signs of oxidative stress are evident as observed by increased oxidation of proteins (Butterfield and Lauderback, 2002) and mitochondrial dysfunction in AD brains (Moreira et al., 2010). Mitochondrial dysfunction is widely associated with A $\beta$ , which can lead to the disruption of normal energy homeostasis. Mitochondrial aberrations involve reductions of enzymes, pyruvate dehydrogenase and ketoglutarate dehydrogenase (Gibson et al., 1998) This has been observed in the 3xTg AD model, shown by decreased mitochondrial respiration and pyruvate dehydrogenase, as early as 3 months. At this age, there is little brain A $\beta$  deposition, suggesting that mitochondrial abnormalities may occur before AD pathology sets in (Yao et al., 2009a). Mitochondrial dysfunction is discussed in further detail in section 3.1. With these early changes in metabolism which precede symptomatic AD, the generation of cell lines expressing wtAPP695/ SweAPP695 constructed in this chapter allow for the effects of APP expression and consequent early changes in metabolism to be monitored. This work is discussed further in chapter 3.

## **Chapter 3: Creation and Characterisation of APP-expressing SHYSY5Y cell lines**

### **3.1 Introduction to AD modelling**

Numerous models have been developed to investigate the pathogenesis of AD. Expression of familial AD mutations within cell lines is a common method used to simulate AD at the cellular level. In addition, overexpression of APP *in vitro* has been shown to lead to development of AD pathology. This is reflected in patients with Down syndrome, who carry three copies of chromosome 21 (where the APP gene is located) (Lott and Head, 2001). However, not all individuals with DS develop dementia, which highlights the complexity of this disease and therefore warrants the further investigation of the role of APP in AD. *In vivo* models which express mutated APP/overexpression of wild type APP, have consistently been shown to secrete increased levels of A $\beta$ . This leads to behavioural changes, similar to those associated with cognitive decline found in humans (Elder et al., 2010), further justifying use of the APP gene for studying AD pathology.

#### **3.1.1 APP and mitochondrial function**

As AD is increasingly considered to be a metabolic disorder with clear changes in glucose uptake and mitochondrial dysfunction associated with the disease, the study of energy homeostasis within the human brain in relation to neurodegenerative disorders is an important area of study. To understand how APP is involved in mitochondrial function, it is necessary to first understand the complex metabolic pathway oxidative phosphorylation, performed by most cells to release energy efficiently.



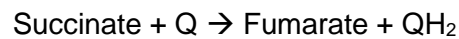
Figure 3.1. Diagram of oxidative phosphorylation within the mitochondrion. Oxidative phosphorylation involves five complexes embedded in the inner mitochondrial membrane which all have distinct but vital functions. Image attributed to Wikimedia Commons <https://commons.wikimedia.org/wiki/File:ETC.svg>,

Mitochondria are key organelles, with key roles in calcium homeostasis and ATP production (Brookes et al., 2004). The process by which ATP is generated is known as oxidative phosphorylation, as outlined in Figure 3.1. It involves the transfer of electrons along several complexes embedded in the inner mitochondrial membrane. The first protein complex, Complex I known as NADH (nicotinamide adenine dinucleotide) dehydrogenase acts to dehydrogenate/oxidise NADH to form  $\text{NAD}^+$ ; this provides the protons that are actively pumped into the outer mitochondrial membrane to establish an electrochemical gradient, whilst providing free electrons to Complex II. NADH is an energy-rich molecule which carries electrons that are fed into the system from the citric acid cycle and fatty acid oxidation. This first reaction is catalysed by coenzyme Q10 (CoQ)/ubiquinone (represented by Q in the equation below), a quinone found within the mitochondrial membrane:



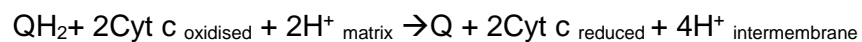
In the second reaction, Complex II (known as succinate-Q oxidoreductase) acts to oxidise succinate to fumarate, in the process transferring electrons to Coenzyme Q

(CoQ). The transfer of electrons to CoQ effectively reduces CoQ, which then acts to carries these electrons to Complex III. Complex II contains a bound flavin adenine dinucleotide (FAD) cofactor which facilitates conversion of succinate to fumarate reaction, by becoming hydrogenated itself. The reaction below summarises the key reaction:



No protons are produced in this reaction, and therefore no protons are transported across the mitochondrial membrane, and thus this reaction contributes less energy the overall reaction.

The transfer of electrons from CoQ to Complex III (known as Q-cytochrome c oxidoreductase) allows for the oxidation of one molecule of ubiquinol (the reduced form of Q in the reaction below) and the reduction of two molecules of cytochrome c (Cyt c). Cyt c is a water soluble heme protein, found within the intermembrane space, and is limited to carrying a single electron (as opposed to the two electrons carried by CoQ), which it transfers onto Complex IV. This limiting step causes the reaction mechanism within Complex III to take place in two steps, known as the Q cycle. The reaction is summarised as follows:



The protons released from the reaction are passed into the intermembrane space, further contributing to the electrochemical gradient.

The next complex in the pathway is Complex IV, known as Cytochrome c oxidase. It receives the electrons from Cyt c to mediate the reaction between protons and molecular oxygen to produce water. The oxygen is known as the terminal electron acceptor. Simultaneously, this complex pumps protons across the membrane, maximising the proton gradient. The reaction is summarised below:



The transport of electrons between the complexes within the mitochondria is known as the electron transport chain and it is these electrons that provide the energy required to actively transport protons across the mitochondrial membrane. This electrochemical gradient is utilised by the final complex V, ATP synthase, where the protons pass from the outer mitochondrial membrane, through the ATP synthase (via a proton channel) providing the energy needed to drive the synthesis of ATP from the reaction of ADP and phosphate ( $P_i$ ).

### **3.1.2 Mitochondria and oxidative stress**

Oxidative stress plays a role in early AD pathogenesis in which mitochondrial dysfunction plays a central role. AD patients exhibit a significant decrease in energy metabolism, correlated with an increase in oxidative damage and reduced activity of mitochondrial enzymes; cytochrome C oxidase, pyruvate dehydrogenase, and  $\alpha$ -ketoglurate dehydrogenase (Readnower et al., 2011). ATP production in mitochondria is a source of electron leakage (Orrenius et al., 2007). These negatively charged ions can reduce oxygen to form toxic reactive oxygen species (ROS) predominantly from the activity of Complex I, Complex II and Complex III. ROS can react with hydrogen ions to form toxic hydrogen peroxide. Cells possess defence systems against these reactive molecules, such as the release of glutathione (GSH) and superoxide dismutase activity to reduce ROS exposure. However, if there is a disturbance in the ROS-antioxidant balance that favours oxidation, oxidative damage occurs. Damage to mitochondria is detrimental to cell survival as mitochondria are key regulators of cellular metabolism and apoptosis.

Further evidence of mitochondrial involvement in AD is the presence of a mitochondrial targeting signal within APP. APP can be imported into this organelle by binding to the transporter outer membrane 40 (TOM40) and transporter inner membrane (TIM23) mitochondrial import proteins. However, complete transport is impeded by the acidic C-terminal sequence. Interestingly, previous studies have demonstrated the

localisation of  $\gamma$ -secretase to the mitochondria, where this enzyme can cleave APP to form A $\beta$  peptides (Hansson et al., 2004).

A $\beta$  can accumulate in mitochondria in AD patients. Indeed, intracellular and mitochondrial accumulation of A $\beta$  is likely to precede extracellular amyloid deposition. A $\beta$  was found to accumulate as early as 4 months in transgenic mice especially within synaptic mitochondria. Specifically, synaptic mitochondria contain a substantial amount of cyclophilin D (Cyp D), which functions to initiate opening of the mitochondrial permeability transition pore (mPTP). Mitochondrial A $\beta$  has been found to interact with CypD. In fact, a deficiency in CypD ameliorates A $\beta$ -induced mitochondrial stress and cognitive impairment in an AD mouse model (Guo et al., 2013). This key observation of the interaction between CypD and amyloid suggests a role of CypD in AD pathogenesis.

Opening of the mPTP allows the transport of calcium ions across the mitochondrial membrane, which dissipates the mitochondrial membrane potential and causes the release of pro-apoptotic molecules such as cytochrome C, Smac/Diablo and apoptosis-inducing factor (Martinou and Green, 2001, Zimmermann and Green, 2001). Collapse of the mitochondrial membrane potential not only leads to reduced mitochondrial calcium retention capacity, but also increases ROS production and ultimately cell death. Mitochondria within synapses regulate calcium homeostasis and therefore changes in calcium can perturb synaptic function (Du et al., 2012). As synaptic dysfunction is a prevalent feature of AD, this may be one possible effect of amyloid on neuronal cells.

Mitochondrial kinetics appears to be significantly affected in AD patients when compared to controls, with mitochondrial fission occurring more frequently than fusion in AD (Santos et al., 2010, Wang et al., 2009b). Mitochondrial fission is whereby mitochondrial can divide by binary fission whereas fusion occurs when two

mitochondria fuse together. The balance between fission and fusion is required to maintain functional mitochondria. The overexpression of APP, which influences increased A $\beta$  production, can increase fission-related protein levels such as dynamin-related protein 1 (Drp1) and Fis1 and inhibit levels of proteins that are associated with fusion, for example mitofusins 1 and 2 (Wang et al., 2009a). Increase of mitochondrial fission may occur during apoptosis or when mitochondria lose their mitochondrial potential (van der Bliek et al., 2013), therefore changes in mitochondrial dynamics may be a cellular response to alleviate mitochondrial stress before resorting to initiating cell death.

These cellular observations have also been reflected into animal AD models. The 3xTg AD mouse model displays impaired mitochondrial function, observed by decreases in state 3 and 4 respiration, lower COX IV activity and increased oxidative stress. Furthermore, it was reported that APP and A $\beta$  could be localised to the mitochondria, in which they have been shown to bind to HSP60, a molecular chaperone (Yao et al., 2009b, Walls et al., 2012a). This latter finding suggests a contribution of amyloid to the mitochondrial unfolded protein response (UPR). The UPR is a stress response pathway operating in higher eukaryotes, following the disruption of protein folding (Pellegrino et al., 2013). The molecular chaperones like HSP60 are important in transport and refolding of proteins from the cytoplasm into the mitochondrial matrix, therefore maintaining homeostasis and protecting against adverse effects of protein folding and aggregation (Haynes and Ron, 2010).

More interestingly, neural cells stably expressing the Swedish APP mutation or wildtype APP695, where APP exhibits a strong association with HSP60, demonstrated mitochondrial dysfunction (Walls et al., 2012a). Researchers in this study observed a decrease in ATP production with increased levels of oxidative stress. When comparing energy metabolism between the two cell lines, both were able to utilise oxidative phosphorylation and glycolysis equally. Surprisingly, maximal respiration (which is

defined as the maximal rate that oxygen is consumed to generate high levels of ATP in conditions of high energy demand) was higher in the Swedish APP-expressing cells. The authors suggested that this was a compensatory response to depleted ATP levels. Another key observation was that Swedish APP-expressing cells were more susceptible to secondary oxidative insults such as A $\beta$  oligomers.

One of the earliest signs of AD is the reduction in glucose uptake, which is a major energy substrate. Fluorodeoxyglucose Positron Emission Tomography (FDG-PET) scans have shown that AD brains exhibit reduced uptake of radiolabelled glucose, leading to some researchers to believe that AD is a hypometabolic disorder. This is also reflected in animal models, which express mutated genes (APP, PS1, Tau) to increase amyloid deposition and/ development of tau tangles. In these animals, researchers have found regional differences in cerebral glucose uptake (Nicholson et al., 2010). These mouse models include the PDAPP, PSAPP, TG2756 and the triple transgenic mice. Reductions in glucose uptake occur in an age dependent manner in areas of the brain that are responsible for the behavioural deficits. Epidemiological evidence has indicated that type 2 diabetes is a risk factor for AD. Insulin signalling is essential to brain glucose metabolism as insulin is able to cross the blood brain barrier and the neurons involved in cognitive function express insulin responsive glucose type 4 (GLUT4) and GLUT8 transporters receptors (Bingham et al., 2002, Blázquez et al., 2014, Membrez et al., 2006, El Messari et al., 1998, Apelt et al., 1999).

Oxidative stress in AD leads to the presence of advanced glycation end products, nitration, lipid peroxidation adduction products, carbonyl-modified neurofilaments and free carbonyls. These effects are observed in vulnerable neurons in AD with spatio-temporal distribution of different types of damage seen in the brain. The brain is particularly vulnerable to ROS, as it has a high metabolic demand, consuming 20% of the oxygen in the human body (Jain et al., 2010). This potentially generates high levels of ROS during oxidative phosphorylation. Furthermore, some brain areas contain high

levels of Fe, which can be used to catalyse the generation of ROS (Dixon and Stockwell, 2014). The brain is also enriched in lipids with unsaturated fatty acids, which are potential targets for lipid peroxidation (Bourre, 2010). Furthermore, the brain does not have substantial antioxidant defence systems, compared to other organs such as the liver and kidney, containing only moderate levels of superoxide dismutase (SOD), catalase and glutathione peroxidase.

### 3.1.3 Antioxidant defences in the brain

The most significant molecule used to defend against ROS in the brain is glutathione (GSH). GSH is a tripeptide, generated from glutamine, cysteine and glycine. Its synthesis requires ATP and occurs in two steps. Firstly,  $\gamma$ GluCys synthetase utilises glutamate and cysteine to generate  $\gamma$ GluCys. This forms the substrate for the enzyme glutathione synthetase that combines  $\gamma$ GluCys with glycine to generate GSH. The recycling of GSH is balanced by feedback inhibition of  $\gamma$ GluCys synthetase by GSH.

Figure 3.2. Diagram showing the synthesis of GSH.

GSH homeostasis in the brain is maintained by the recycling of GSH precursors. The synthesis of GSH is limited by cysteine, which can be provided to neurons by neighbouring astrocytes. Astrocytes also produce GSH, as they express both of the enzymes required for GSH synthesis. In response to oxidative stress, GSH is oxidised to GSSG (oxidised glutathione), which can be converted back to GSH by GSH reductase, and requires the cofactor NADPH (Pocernich and Butterfield, 2012).

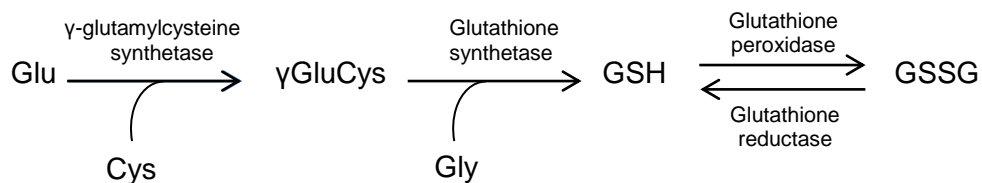


Figure 3.2 Diagram showing the synthesis of GSH.

Levels of GSH in the brain decrease with age (Saharan and Mandal, 2014). In AD, the level of GSH in peripheral lymphocytes is decreased whilst levels of GSSG are increased, in a manner that is consistent with an oxidative stress phenotype (Calabrese

et al., 2006). The ratio between GSSG and GSH is a marker of redox thiol status and oxidative stress, found to be significantly increased in AD (Owen and Butterfield, 2010). There is a correlation between increased GSSG levels and decreased cognitive function in AD patients (Lloret et al., 2009). Furthermore, individuals with MCI exhibit signs of oxidative stress, with the hippocampus showing decreased activity of SOD and glutathione S transferase (GST) (Sultana et al., 2008).

#### **3.1.4 Methods of probing mitochondrial function**

Evaluating mitochondrial functions and the influence of reactive species on this vital organelle is an important area of study. Such studies can be performed by measuring the oxygen consumption of intact isolated mitochondrion or by measuring the activity of mitochondrial enzymes. However, both methods do not measure mitochondrial function *in vitro* and therefore provide only a limited insight into organelle function in relation to its cellular environment.

##### **3.1.4.1 Clark Electrodes**

Clark electrodes have typically been used with cells suspended in stirred, buffered solutions in order to measure oxygen consumption (Chance and Williams, 1955). These electrodes are predominantly used to determine organelle function in isolated samples for clinical or animal studies. Taking oxygen consumption measurements from cultured cells requires the removal of cells from growth substrate and placing them in a stirred solution. However, this causes stress on many cells leading to cell death, especially in anchorage-dependent cells, accompanied by increased ROS production and mitochondrial damage (Li et al., 1999). In addition, stirring of the electrode causes non-laminar shear increasing oxidative stress (De Keulenaer et al., 1998).

##### **3.1.4.2 Fluorometric systems for cultured cells**

Recently, numerous studies across different fields of research have emphasized the application of the Seahorse XF24 flux analyser as an alternative to Clark Electrodes.

Results obtained using this instrument were found to be comparable to data obtained using electrodes and can be used to study both non-adherent and adherent cells in culture.

The Seahorse XF24 instrument utilises fluorometric technology to measure oxygen consumption and proton release, enabling the study of mitochondrial respiration and glycolysis respectively. Two sensors measuring either the oxygen consumption rate (OCR) or extracellular acidification rate (ECAR) are lowered into wells containing adherent cells and can be used to take multiple readings.

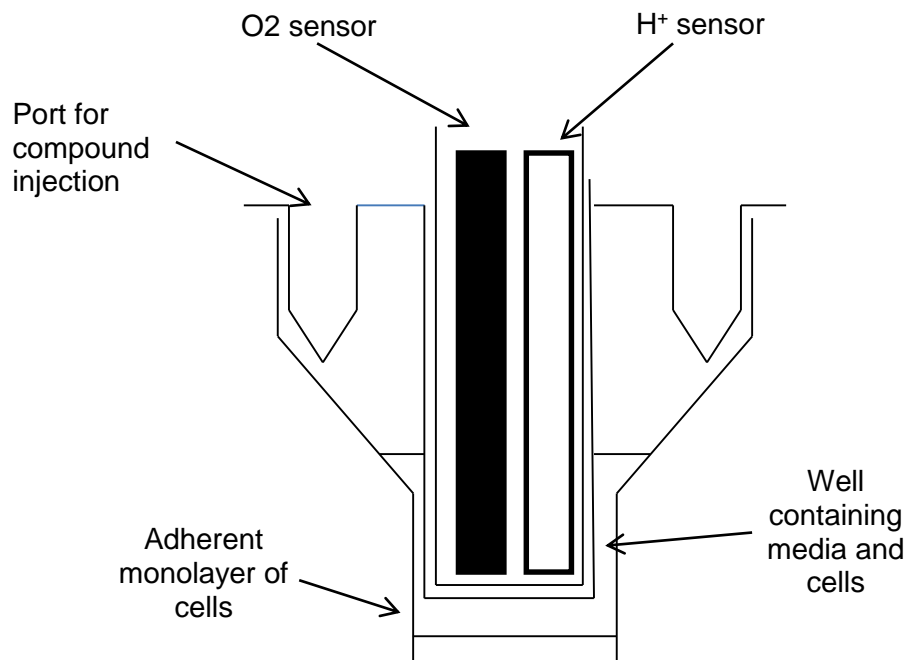


Figure 3.3. Schematic showing the side view of the layout of each well of a culture plate. A single tube containing two sensors is lowered in the pool of media to taking regular measurements. Compounds are stored in the ports over hanging the wells which the analyzer can be instructed to be inject into the well to elicit a metabolic response.

This system allows for highly sensitive and specific measurements of mitochondrial and glycolytic function with a greater output than that which can be achieved with traditional electrode-based systems. Compounds can be injected into the wells to stimulate a response in the cells, allowing the user to assess the ability of cells to respond under stress, whilst cells are maintained at 37°C. Experimental procedures can be tailored to

suit the needs of the user, allowing flexibility and even the potential study of novel therapeutic drugs targeting energy metabolism.

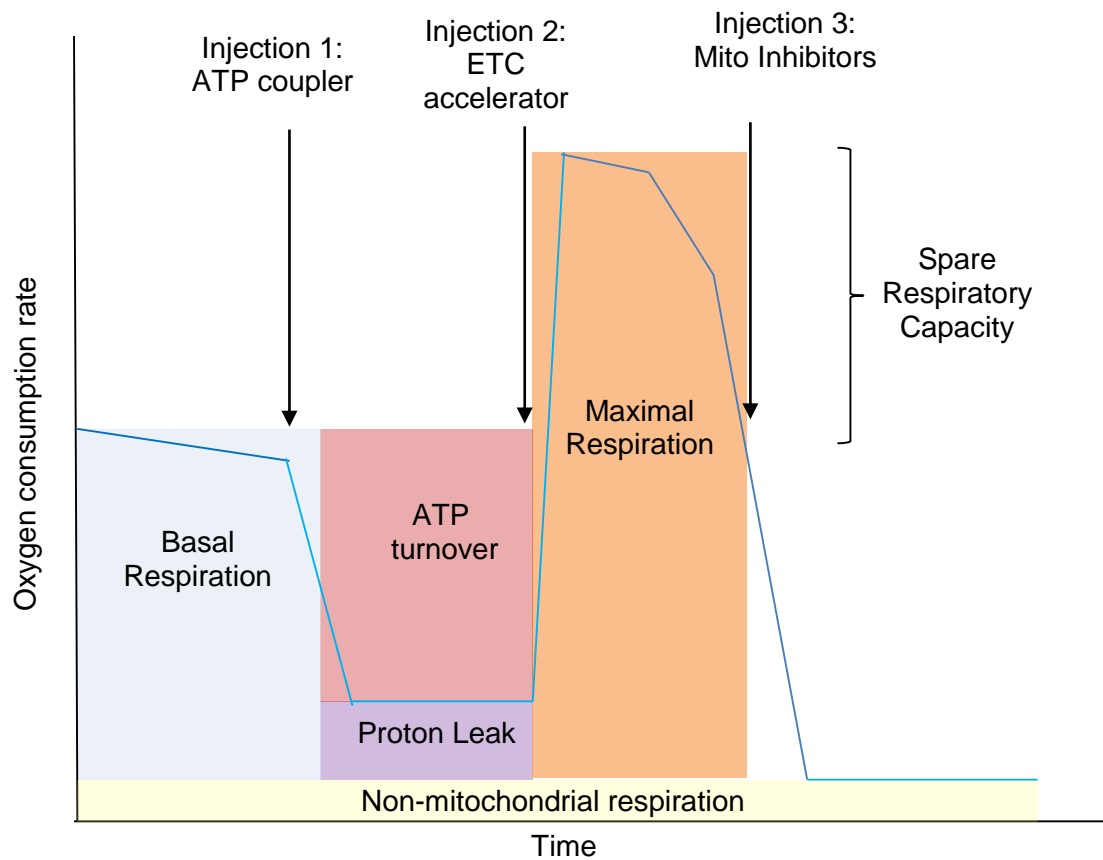


Figure 3.4. Diagram showing the typical metabolic profile of cells when studying mitochondrial function using the Seahorse analyser (taken from Seahorse Biosciences MitoStress Test manual).

By monitoring OCR, measurements of mitochondrial function can be performed. The analyser takes key readings to calculate mitochondrial parameters (Figure 3.4) after the injection of different mitochondrial inhibitors. The first measure is basal respiration defined as the cellular oxygen consumption whilst at rest. A decreased basal rate in treated or diseased cells versus controls can indicate a defect in the respiratory complexes. The first compound injected, Oligomycin (ATP coupler) blocks ATPase activity. This reduces OCR with the remaining respiration reflecting the natural proton leak of the mitochondria i.e the flow of protons across the inner mitochondrial membrane (which does not generate ATP). Injection of the ETC accelerator carbonyl cyanide 4-(trifluoromethoxy)phenylhydrazone (FCCP) dissipates the electrochemical

gradient, forcing the cells to increase the flow of electrons and oxygen consumption in an attempt to maintain the membrane potential leading to maximal respiration. The spare respiratory capacity gives an indication of the cell's ability to respond to increased ATP demand. It is considered that cells with reduced respiratory capacity are more vulnerable to changes in energy demand. Finally mitochondrial inhibitors, such as Rotenone and Antimycin A are added in the final injection to completely inhibit mitochondrial respiration. As shown in Figure 3.4, non-mitochondrial respiration may occur, whereby certain cell types consume oxygen for cellular processes. Examples include the activity of NADPH oxidases in macrophages during the respiratory burst, activated during an inflammatory response (Brand and Nicholls, 2011). Most cells have low non-mitochondrial oxygen consumption, due to the activity of desaturase/detoxification enzymes.

The Seahorse XF analyser offers great insight into both mitochondrial and glycolytic functions of any cell type. The ability to study a cell's mitochondrial response to toxic insults is particularly relevant to AD, with its close association with mitochondrial dysfunction. In this study, the Seahorse analyser was used to probe the mitochondrial responses of SHSY5Y cells expressing wtAPP695 and SweAPP695 in comparison to control cells.

### **3.1.5 The SHSY5Y cell line**

Cytotoxicity studies on neuronal cell types have been performed extensively in the SHSY5Y cell line because of the relative ease of culture and cost effectiveness of reagents. The neuroblastoma SHSY5Y cell line is a thrice cloned sub line of the neuroepithelioma cell line, SK-N-SH (Ross et al., 1983). The parental cell line was derived from a bone marrow biopsy in 1970 from a young girl with metastatic neuroblastoma, which when cultured, produces two distinct cell types (Ross et al., 1983). One is neuroblastic (known as N-type) in nature, whilst the other is substrate adherent (known as S-type) (Biedler et al., 1978). It is the former cell type from which

clones were selected and eventually gave rise to the following cell lines; SH-SY5, SH-SY5Y, MC-IIE and MC-IXC.

The SHSY5Y cell line possesses a neuroblast-like morphology (Biedler et al., 1978). This cell line has many advantages in the field of studying neuronal cultures. In addition to having a human neuronal lineage, the SHSY5Y cell line has a similar karyotype to that of human cells (with an extra copy of a fragment from 1q leading to a modal number of 47 chromosomes) (Yusuf et al., 2013). They can be rapidly cultured and express several neuronal markers most notably neuronal specific enolase (NSE) (Odelstad et al., 1981).

*In vitro* culture of SHSY5Y cells invariably leads to the growth of two cell types, one is adherent whilst the other are floating. The adherent population of cells has been the main subject of study (Kovalevich and Langford, 2013). The N-type cells are of particular interest as they can be differentiated into a more neuronal phenotype. Many methods are employed to differentiate these cells, with the use of retinoic acid (RA) being most common (Påhlman et al., 1984, Simpson et al., 2001, Sarkanen et al., 2007).

#### **3.1.5.1 SHSY5Y differentiation**

SHSY5Y cultures are commonly differentiated in the presence of the vitamin A derivative RA, which leads to differentiation into a more neuronal phenotype (Pahlman et al., 1984). Originally, the effect of RA was studied as a differentiation inducer in neuroblastoma therapy. Currently, RA is used to induce neuronal morphology in neuroblastomas as *in vitro* neuronal models for human diseases and neuroblastoma therapy. Therefore, studies into differential responses of proliferating and differentiated SHSY5Y cells to toxins have been extensively carried out (Hartley et al., 1996, Hong et al., 2003, Seoposengwe et al., 2013).

Treatment of RA on SHSY5Y cells leads to rapid withdrawal from the cell cycle, where cells arrest in G1-phase accompanied by DNA inhibition and gradual reduction in cellular proliferation detected within 48 hours (Melino et al., 1997). Morphologically, cells begin to extend neuritic processes. RA treatment was found to inhibit growth in the first 8-10 days of treatment (Encinas et al., 2000). The resulting neuronal phenotype exhibits increased expression of NSE, synaptophysin, synaptic associated protein-97 (Cheung et al., 2009), dopamine beta hydroxylase (Oyarce and Fleming, 1991) and tyrosine hydroxylase (Presgraves et al., 2003). This has attracted researchers in the field of Parkinson's disease who have used this cellular model (Lopes et al., 2010, Xie et al., 2010). In addition, this cell line has applications in AD research, for example, it has been used in the study of tau phosphorylation and potential screening of glycogen synthase kinase 3  $\beta$  inhibitors (Jamsa et al., 2004).

Following RA treatment, researchers have used growth factors, which promote the survival of neuronal subtypes. In particular, the neurotrophic factors which include nerve growth factor (NGF), brain-derived neurotrophic factor (BDNF), neurotrophin 3 and neurotrophin 4/5. Targeted knock down of the genes encoding neurotrophins or their specific tyrosine kinase receptors (TrkR) led to apoptosis of neuronal cell populations (Nguyen et al., 2010). Culture of neurons in the presence of growth factors is vital to ensure survival and protection from apoptosis following differentiation (Kristiansen and Ham, 2014, Misko et al., 1987). This dependence of neurons on neurotrophins has been also been demonstrated in the rat pheochromocytoma PC12 cell line (Takebayashi et al., 2002). The presence of NGF causes neurites to project from the cell bodies, forming neural networks. Neurite extension requires microtubule assembly (Drubin et al., 1985), which is driven by expression of microtubule-associated proteins (MAPs) that are up-regulated following NGF treatment.

Studies have shown that RA induces the expression of TrkB, allowing SHSY5Y cells to become responsive to BDNF (Kaplan et al., 1993) with BDNF enhancing the

differentiating effects of RA (Arcangeli et al., 1999). Neuronal basal medium supplemented with B27 and dibutyryl-cyclic AMP, potassium chloride (KCl), and L-glutamine has also been utilised to enhance differentiation. B-27 consists of a cocktail of growth factors, antioxidants, hormones and other chemicals known to improve cell survival and development (Brewer et al., 1993). Differentiation of SHSY5Y with 5 days of RA treatment followed by 5 days of BDNF treatment gives rise to a more morphologically neuronal phenotype (Gimenez-Cassina et al., 2006). Neuronal proteins such as MAP1B and neurofilament (NF) protein, MAP2 (Sanchez Martin et al., 1998), tau (Jamsa et al., 2004) and  $\beta$ -tubulin III are detectable within these cultures. Cultures also show decreased expression of cyclin-dependent kinase-1 (cdc2/ cdk1), evidence of withdrawal from the cell cycle.

### **3.1.6 Generation of stable cell lines**

Numerous studies have utilised transient transfection to study the effects of APP expression. Using this method, the transgene of interest is inserted in a plasmid that is introduced into the host cell, typically complexed with lipid reagents to mediate efficient delivery into cell's nucleus. Generally, transiently expressed transgenes can be detectable for up to seven days; however, transfected cells are usually harvested within 24 to 96 hours post-transfection. The transgene is not integrated into the genome, and following mitotic division is not passed from one generation to the next. Therefore over time with each mitotic division, the levels of protein expression decrease. In addition, transfection efficiencies can vary, meaning repeated experiments may be performed with cells expressing at different levels. This poses a problem when studying the effects of APP expression with relation to AD, a developmental ageing disorder. As such, in this project it was desirable to investigate methods to generate stably transfected SHSY5Y cell lines to study the chronic effects of APP expression.

Generating stable cell lines has major advantages over transient transfection as it permits long term protein expression studies without loss of transgene expression.

Typically, stable cell lines have a transgene of interest permanently incorporated into their cellular genome under a specified promoter as desired by the researcher. Stably transfected cells are selectable from a heterogeneous population as they also incorporate antibiotic resistance permanently into their genome. With antibiotics added into the culture media at the minimal concentration, non-transfected cells are eradicated from the culture, thus retaining a reduced number of stable cells which carry the transgene and antibiotic resistance marker. As the cultures grow, colonies arising from single cells develop which can be isolated and cultured as separate clones. Clones derived from a single cell, improve the consistency of protein expression over time, as all cells in the population have the same transgene, inserted in the same area of the chromosome. Several methods to achieve long term gene expression are available, but in this project lentiviruses were chosen of the preferred method of choice. The rationale for this method will be discussed in the following section.

#### **3.1.6.1 The lentiviral age**

Over the last twenty years, a number of viral delivery systems have been developed which include adenovirus, adeno-associated virus, retrovirus and lentivirus. Lentiviruses in particular, are known to infect a broad range of cell types (Kim et al., 2004), maintain chronic, sustainable transgene expression and have the major advantage of being able to stably integrate into quiescent, non-dividing cells (e.g. neurons) as well as actively dividing cells (Dissen et al., 2009). In addition, up to 100% transduction efficiency has been reported in some cell types (Li et al., 2004). Their use has also been extended to *in vivo*, where it is hoped they could form vehicles to deliver genes into the brain to treat neurodegenerative disorders (Bensadoun et al., 2000, de Almeida et al., 2001, Baekelandt et al., 2003). Traditionally, neuronal cultures have been extremely difficult to manipulate and stably express genes of interest. Since the sequencing of the HIV-1 retrovirus, significant advances in lentiviral technology have improved efficacy of infecting neuronal cultures to achieve stable and long term gene expression. Viral infection is generally a more efficient method of introducing genes

into cells than standard *in vitro* transfection and has also been used *in vivo* for gene therapy applications.

Lentiviral vectors are based upon HIV-1, which excel in host cell attachment, receptor mediated entry, viral mediated reverse transcription and genome integration (Zufferey et al., 1997). They can be manipulated to deliver complex expression elements including introns or large stretches of genomic DNA whilst exhibiting low toxicity and inducing minimal immune response in the host (Dissen et al., 2009). Lentiviral delivery systems have been modified, in that the pathogenic HIV genes have been removed and the remaining essential genes are spread over multiple plasmids. Another feature is that the viral particles can be pseudotyped with other envelope proteins, whilst the structural and enzymatic components of the virion are derived from HIV-1, the envelope glycoprotein used for this project originates from vesicular stomatitis virus (VSV) (Naldini et al., 1996). This was chosen due to its high stability and the broad tropism of its G protein (Zimmermann et al. 2011), which affords a vastly increased host cell range when compared to the natural limitations of the native HIV-1 trimeric envelope glycoprotein.

The sequencing of the lentivirus genome has allowed researchers to manipulate the genetic structure in order to produce different vector systems with which to infect host cells. There are three well established lentiviral systems; 'first generation', 'second generation' and 'third generation'. The main difference between these systems is the increase in biosafety due to the introduction of deletions in key genes and by partitioning genes involved in viral packaging onto separate vectors. In this project, the second generation lentiviral system was utilised due to its ability to package large inserts and also its relative simplicity in comparison to the third generation system, whilst still providing improved safety over the first generation systems.

Second generation vectors consist of the transfer vector, the packaging plasmid and the envelope plasmid. This split packaging system distributes key genes over several plasmids, as shown in Figure 3.5 and is one of several biosafety features.

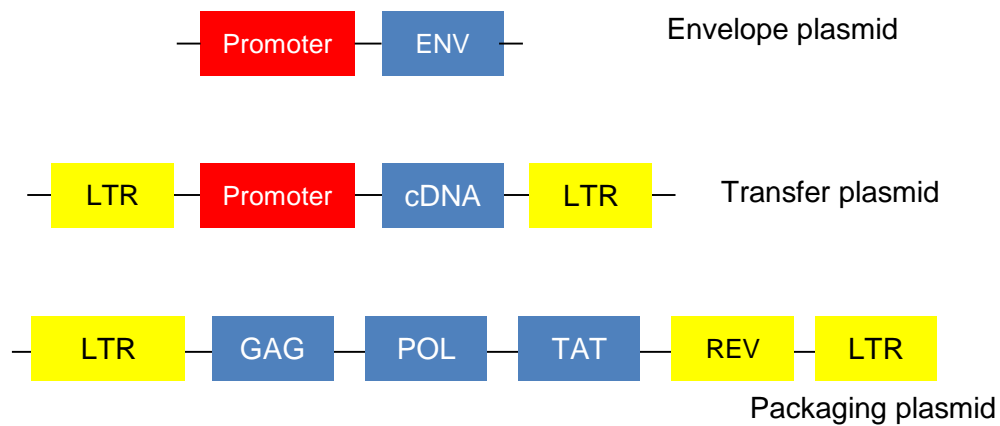


Figure 3.5. Diagram showing the three plasmids with the key genes.

The transfer vector has several lentiviral accessory genes deleted (*vif*, *vpr*, *vpu* and *nef*) as they are not essential for *in vitro* replication and are involved, to varying degrees, in HIV pathogenicity (Dull et al. 1998). This plasmid carries the cis-acting genetic sequences essential for the vector to infect the target cell, as well as the transgene of interest. Endonuclease restriction sites are also present to facilitate the insertion of transgenes of interest. A key feature of this vector is the presence of the PSI ( $\Psi$ ) packaging sequence, which ensures that only the transfer vector is packaged into infection competent virus. Expression of DNA from the transfer vector is limited to sites of infection in HIV-1 negative cells. Furthermore, the presence of promoter disabling mutations engineered into the U3 region of the 3' long terminal repeat (3'LTR) renders the virus self-inactivating (SIN), thereby reducing the risk of the virus generating full-length vector RNA after viral integration (Logan et al., 2002). Normally, when retroviral mRNA is reverse transcribed, the 3'LTR is copied to form the 5'LTR, acting as a promoter to direct expression of viral mRNA to be packaged into a new virus. Therefore, SIN vectors carrying deletions in the 3'LTR are transcriptionally inactive after transduction and cannot be converted into full length RNA and therefore do not replicate, ensuring no infectious virus is produced.

The packaging plasmid forms the backbone of the virus system, carrying the Gag, Pol, Rev, and Tat genes, which are essential for producing viral particles. The Gag gene encodes the capsid and matrix proteins which make up the structural elements of the virus, while the Pol gene encodes for the reverse transcriptase (reverse transcribes RNA to cDNA) and integrase (integrates double stranded cDNA into host genome), which is required to generate new viral particles (Amado and Chen, 1999). The Rev gene facilitates nuclear export of mRNA into the cytoplasm for translation of viral structural proteins. In third generation systems, the Rev gene is located on a separate packaging plasmid to maximise biosafety. Finally, the Tat gene encodes for a protein that significantly enhances viral transcription efficiency. This gene is completely omitted in the third generation system as a further biosafety feature (Logan et al., 2002). The second generation packaging vector used for this project was psPAX2, produced by the Trono laboratory (Prof Didier Trono Lab Packaging and Envelope Plasmids (<http://tronolab.epfl.ch/>)).

The envelope plasmid carries the viral envelope gene, which in this case encodes the VSV surface glycoprotein. This gene originates from a heterologous virus, which allows for pseudotyping of viral particles and the infection of a broad range of different cell types. The glycoprotein plasmid used for this this project was PMD2G (from the Trono Laboratory).

As previously stated, lentiviral based delivery systems have been shown to consistently infect non-dividing cells, such as neurons, with a high transduction efficiency (Klages et al., 2000). It was decided that lentiviral delivery of APP would most likely be the most appropriate method for successfully generating APP-expressing neuronal cell lines. The generation of these lines would provide consistently expressing wtAPP and SweAPP cell lines, allowing the investigation of the effect of APP expression on cellular metabolism.

### **3.1.7 Aims and objectives**

The aim of this study was to create wtAPP695/ SweAPP695 expressing SHSY5Y cell lines using lentiviral transduction. The cell lines generated were characterised by immunoblotting before and after differentiation. The levels of A $\beta$  release were assessed by determining concentrations of amyloid in the media taken from cell lines after 24hours/48hours after differentiation using ELISA. Differences in cell proliferation and glucose uptake were determined in transfected cells. Finally mitochondrial function was studied in comparison to untransfected SHSY5Y cells using the Seahorse analyser.

The hypothesis was that APP overexpression would cause metabolic dysfunction in cell lines and render cells more sensitive to oxidative stress. Experiments were performed in order to determine whether overexpression of mutant APP and wildtype APP could drive changes in energy metabolism. Identification of the relationship between APP overexpression or APP misprocessing and altered neuronal metabolism could yield important insights into the earliest stages of neuronal dysfunction in AD.

## **3.2 Methods and Materials**

### **3.2.1 Lentiviral packaging of the pLenti6.4 wtAPP/SweAPP695 constructs.**

The constructs, pLenti6.4 Syn1-wtAPP695/ SweAPP695 previously described (section 2.3.6.3), were packaged into active Lentivirus using the HEK293FT cell line (section 3.2.1.1). Another lentiviral construct (provided kindly by Dr John O'Neil), pGIPz (a CMV-driven GFP expression vector) was also packaged to test packaging and viral transduction into in the SHSY5Y cells.

#### **3.2.1.1 HEK 293FT cell culture**

The human embryonal kidney (HEK) 293FT cell line (Invitrogen, Paisley UK) was used as a host for lentiviral production. This cell line is fast-growing; easily transfectable and can generate high viral titers. It differs from HEK293 cells in that it carries the SV40 large antigen, which allows very high levels of protein to be expressed from vectors containing the SV40 origin of replication. All cell culture reagents were obtained from Gibco, Life Technologies, Paisley, UK, unless otherwise specified.

All sub-culturing was carried out according to the manufacturer's instructions (see appendix). Cells were cultured in DMEM High Glucose containing 6mM glutamine, 100U/ml Penicillin and 100µg/ml Streptomycin (PAA), 10% Foetal Bovine Serum, 0.1mM MEM Non-essential Amino Acids (NEAA) and 500µg/ml Geneticin.

Initially, cells frozen in 10% DMSO; 90% complete medium were resurrected in medium without Geneticin to allow recovery. After recovery and for all subsequent culturing, Geneticin was supplemented into the media. When cells reached 80-90% confluence, they were passaged 1:5 -1:10 using trypsin/EDTA with the media refreshed every alternate day.

#### **3.2.1.2 Viral packaging**

The manufacturer recommends passaging of HEK293FT cells two to three times before preparing for packaging. To prepare for packaging, HEK293FT cells were washed in

PBS and then detached with trypsin. Cells were pelleted (200g, for 5 minutes) and the pellet re-suspended in fresh medium. Live cells were counted using Trypan Blue exclusion dye on a haemocytometer (section 2.2.3.2). Cells were seeded at  $1.5 \times 10^5$  /flask into ten T25cm<sup>2</sup> flasks (Corning, MA, USA) and returned to the incubator.

After 24 hours, when the cells reached approximately 90% confluence, cells were refreshed with 5mls of fresh media without antibiotics and then returned to the incubator for 1 hour. After this period, cells were transfected using Lipofectamine 2000 (Invitrogen, Fisher Scientific, UK) according the manufacturer's instructions with either the wtAPP695 or SweAPP695 pLenti6.4 transfer vector together with the packaging plasmids psPAX2 and pMD2.G (purchased from Addgene, MA, USA) at a ratio (W/W) of 1:1:1 and returned to the incubator for 16 hours.

On the next day, medium was replaced with 5mls packaging media (DMEM High Glucose containing 6mM glutamine, 10% Heat inactivated Foetal Bovine Serum, 0.1mM MEM Non-essential Amino Acids) and the cells were returned to the incubator. After 72 hours, all media was removed from flasks and clarified by centrifugation at 2000g for 10 minutes. The resulting supernatant was then passed through a 0.4µM cellulose acetate or polyethersulfone (PES);(low protein binding) syringe filter to remove any remaining cellular debris. To test for the presence of p24 viral particles, which are indicative of active viral production, the clarified media was tested using the rapid Lenti GoStix (Clontech, Saint-Germain-en-Laye, France) (section 3.2.1.3).

All tubes, pipette tips, medium, flasks etc that came into contact with the virus were decontaminated in 1% high level laboratory disinfectant (Virkon) for at least 20 minutes in the tissue culture hood before autoclaving. Any equipment that was not in direct contact but opened in the tissue safety cabinet was decontaminated for 5 minutes with 1% Trigene (Fisher Scientific, UK). Surfaces were cleansed in 1% Trigene and the microbiological cabinet sterilised for 1 hour under UV illumination.

### **3.2.1.3 Lenti-X GoStix protocol**

To rapidly test for the presence of Lentiviral particles prior to purification, Lenti-X GoStix (Clontech, Saint-Germain-en-Laye, France) were used (for protocol see appendix). After lentiviral production was confirmed, the remaining viral supernatant was concentrated by sucrose cushion.

### **3.2.1.4 Viral concentration**

To concentrate viral particles sucrose cushion centrifugation was employed, based on a method, described by (al Yacoub et al., 2007). Briefly, a 20% sucrose (Sigma-Aldrich, Poole, UK) cushion was prepared in 15mls of TNE buffer (50mM Tris, 100mM NaCl, 0.5M EDTA) and 5ml added to a 50ml centrifuge tube, to which 20mls of virus was overlaid. The solution was centrifuged (6400g for two hours), with minimal acceleration. The viral pellet was then re-suspended in culture media and the lentiviral concentration determined (section 3.2.1.5). All lentivirus was aliquoted for single use aliquots into microcentrifuge tubes, frozen in crushed dry ice and stored in double ziplocked bags at -80°C to preserve viability.

### **3.2.1.5 Determining Lentiviral Concentration**

Concentrated lentivirus aliquots were titered using the QuickTiter™ Lentivirus Titer Kit (Lentivirus-Associated HIV p24)(CellBioLabs, Cambridge Bioscience Ltd, Cambridge, UK) (see appendix for protocol). Briefly, a series of lentiviral dilutions were prepared to ensure absorbance readings would fit within to the linear region of a p24 standard curve. Test samples and p24 standards were incubated in the anti-p24 antibody coated 96-well microplate overnight at 4°C. On the following day, the wells were washed in wash buffer to remove unbound sample and samples incubated sequentially in diluted FITC-Conjugated anti-p24 Monoclonal antibody and then diluted HRP-Conjugated Anti-FITC Monoclonal antibody for 1 hour at room temperature. When all wells reached a visible blue hue, stop solution was added to all wells and the absorbance at 450nm was measured on a spectrophotometer (Ascent MultiSkan, Thermo Scientific, UK).

### **3.2.2 Testing the Syn1 wtAPP695/ SweAPP695 Lentiviruses**

Once the viral titers of both viruses were determined, the next step was to test infectivity rates in the human neuroblastoma cell line.

#### **3.2.2.1 SH-SY5Y**

Human neuroblastoma SH-SY5Y cells were cultured in RPMI-1640 medium containing 100U/ml Penicillin and 100µg/ml Streptomycin), 10% Foetal Bovine Serum, 1% NEAA and 2mM L-Glutamine at 37°C, 5% CO<sub>2</sub>. During the initial resurrection procedure, cells were defrosted slowly at 37°C, before transferred into media for pelleting (200g for 5 minutes). The resulting pellet was re-suspended in fresh media and seeded into a T25 flask (Corning, MA, USA) for eventual expansion into T75 flasks. Cells were passaged in 0.05% Trypsin-EDTA and split 1:5/1:3 2-3 times a week when reaching 80% confluence.

#### **3.2.2.2 Viral infection of GFP-expressing virus in the neuroblastoma cell line**

For viral transfection studies, the cells were seeded at a density of  $5 \times 10^3$  cells in a 96-well plate (Corning, MA, USA). The numbers of cells were determined using a haemocytometer (section 2.2.3.2).

To determine the optimal viral transduction into this cell line, SHSY5Y cells were transduced with CMV-driven GFP virus (pGIPz) (provided kindly by Dr John O'Neil) at varying multiplies of transfection (MOI). Multiplities of infection refer to the number of virion particles infecting host cells. This can be approximately quantified by determining the active viral concentration (using the p24-associated ELISA). Different MOI's were tested to determine the effects of sub-lethal viral concentrations in the presence of a cationic polymer, polybrene (Sigma-Aldrich, Poole, UK) which acts to increase the efficiency of infection.

MOI's of 0, 5, 10, 25 and 50 were tested whereby 75µls of culture media were added to each well. The cells were incubated overnight and then the media refreshed before returning the cells to the incubator. After 3 changes of media, cultures were tested for the presence of p24 antigen to ensure that the safe removal of viral particles. Upon obtaining a negative result, cells were considered non-infectious to be imaged for GFP using the fluorescence microscopy (see section 2.2.3.6).

### **3.2.2.3 Testing of the APP lentivirus**

Once optimisation of viral transduction of SHSY5Y cells had been established, lentivirus carrying either SweAPP695 or wtAPP695 was transduced into SHSY5Y cells at an MOI of 5 and 10.

SHSY5Y cells were plated at a density of  $8 \times 10^4$  cells per well into a 12-wellplate (Corning, MA, USA) to achieve 50% confluence on the next day. The cells were then differentiated in RPMI media containing  $1 \times 10^{-5}$  M RA for five days. To prepare the cells for infection, specific volumes of concentrated virus, which equated to an MOI of 5 or 10 were prepared in media. 900µls of virus containing media was pipetted into wells in triplicate and the cells were incubated overnight to allow for viral transduction to take place. As a positive control, SHSY5Y cells were also infected with a virus expressing cherry red fluorescent protein under the control of the EIF1α promoter. Non-transduced cells were used as a negative control. After three changes of media, the positive control samples were visualised by fluorescence microscopy to determine the success of infection.

Three days post-infection, total cell lysates were obtained using RIPA buffer and pooling three wells (section 2.2.2.1). These were quantified (section 2.2.2.2) and assessed for APP expression by Western Blotting (section 2.2.2.3 to 2.2.2.5). Pure Aβ1-42 was also run on the SDS gel to confirm primary antibody binding. Mouse anti-

A $\beta$  (6E10, Covance, 1:1000) primary antibody was used to detect both full-length APP695 and A $\beta$  oligomers/monomers.

#### **3.2.2.4 Blastocidin kill curve**

SHSY5Y cells were seeded at  $4 \times 10^4$  cells per well of a 12-well plates and allowed to incubate overnight. On the following day, Blastocidin S HCl, (Life Technologies, Paisley, UK) was diluted in media from 0 to 10 $\mu$ g/ml. Cells were then grown in the presence of blastocidin with the media refreshed every alternate day for two weeks. The minimal concentration of Blastocidin that caused 100% of cell death was chosen for clone selection.

#### **3.2.3 Production of stable APP-expressing SH-SY5Y cell lines**

##### **3.2.3.1 Lentiviral transduction**

SHSY5Y cells were seeded into three T25 flasks to achieve approximately 90% confluence after 24 hours; cells were counted (section 2.2.3.2) in order to calculate multiplicities of infection (MOI). An MOI of 1 was used to infect one flask with either the wtAPP695 or SweAPP695 virus in 4.5ml of culture media. The flasks were then placed back into the incubator overnight.

On the following day, the cells were plated at a density of  $1 \times 10^4 / 5 \times 10^3$  cells per well of 6-well plates (Corning, MA, USA) in media and allowed to settle overnight. On the next day, media was replaced with media containing 2 $\mu$ g/ml of blastocidin to select for stably transduced cells. The blastocidin concentration was gradually increased to 3 $\mu$ g/ml which was determined to be the minimal concentration required to kill untransduced SHSY5Y cells.

##### **3.2.3.2 Clone selection and expansion**

Stable clones that formed colonies which grew to a sufficient size were washed with PBS and then isolated using glass cloning cylinders (Sigma-Aldrich, Poole, UK). Cells were detached with trypsin-EDTA, centrifuged (200g for 5 minutes) and re-plated into

12-wellplates (Corning, MA, USA). Upon reaching 90% confluence, clones were expanded into 6 well plates and then up scaled into T25 and subsequently T75 flasks. Once a sufficient number of cells were obtained, cells were frozen in FBS with 10% DMSO (Hybri-Max, Sigma-Aldrich, Poole UK) at -80C and then stored in liquid nitrogen.

### **3.2.3.3 Characterisation of clones**

Stable lines were characterised for increased APP expression and/or increased A $\beta$  production using Western blotting and A $\beta$  ELISA. Protein was extracted from APP-expressing cells at the proliferative stage and following differentiation with RA for 7 days. Clones were also assessed for their ability to differentiate in to a neuronal phenotype.

#### **3.2.3.3.1 Protein expression**

Total cell lysate was extracted using RIPA buffer (see section 2.2.2.1) and the protein concentration determined (section 2.2.2.2). To detect increases in APP expression in the stably selected cell lines, the protocol for SDS-PAGE (see section 2.2.2.3) was altered to maximise protein detection of APP in the lysates taken from the APP-expressing SHSY5Y cell lines. Resolving gels (12% polyacrylamide) were used for separation of 6.4 $\mu$ g of protein and the gels were electrophoresed for 40 minutes at 200V. 20 $\mu$ M of A $\beta$ 1-42 made up in HEPES (Sigma-Aldrich, Poole, UK) served as a positive control with the PageRuler Prestained Protein Ladder (Thermo Scientific, Northumberland, UK) used to determine protein band sizes.

The Western blotting procedure (section 2.2.2.4 and 2.2.2.5) was carried out but with several alterations. Transfer of protein from the polyacrylamide gel onto nitrocellulose membranes was performed for 2 hours at 80V in transfer buffer containing SDS (0.0005%). The membranes were then blocked overnight at 4°C in 5% powdered milk. On the following day, the nitrocellulose membranes were incubated overnight in mouse anti-human A $\beta$  (1-42) antibody (W0-2, Millipore, 1:1000) at 4°C. Secondary antibody

binding and developing of membranes using X-ray film was carried out as previously described.

For loading controls, membranes were stripped of all bound antibodies. The membranes were washed in stripping buffer (2% SDS, 100mM  $\beta$ -mercaptoethanol, 62.5mM Tris) for 30 minutes at 50°C with gentle agitation. Blots were then washed thoroughly in TBST six times (5 minutes each) before being blocked with 5% powdered milk for 2 hours. Membranes were then incubated using rabbit anti- $\beta$ -actin antibody (A5060, 1:1000, Sigma-Aldrich, Poole, UK) in 3% powdered milk at room temperature for 1 hour. Membranes were washed thoroughly in TBST six times (5 minutes each) and then incubated in goat anti-rabbit HRP secondary antibody (1:5000, Dako, Cambridgeshire, UK) for 1 hour. Membranes to be developed were processed as previously described (section 2.2.2.5).

Polyacrylamide gels were retained to be stained in Coomassie gel stain (1% Coomassie R250, 50% methanol, 10% glacial acetic acid) for 1 hour before being washed three times for 20 minutes in destaining solution (50% methanol, 10% glacial acetic acid) on a rocker. Gels were stained to confirm that protein had successfully transferred onto the membranes.

Protein bands were analysed using the GeneTools software (Syngene, Cambridge, UK), after initially capturing images of the X-ray films in the G:Box. Manual band quantification was performed by manually defining the protein bands, using automatic background correction. The raw volumes were corrected against  $\beta$ -actin protein bands, and then expressed as percentage of proliferating/7 day RA-differentiated SHSY5Y protein bands.

### 3.2.3.3.2 Amyloid ELISA

The amount of A $\beta$ 1-42 secreted into media was quantified using the Human A $\beta$ 1-42 ELISA kit (Invitrogen, Life Technologies, Paisley, UK).

For cell preparation, control SHSY5Y cells and clones expressing wtAPP695/SweAPP695 were seeded at  $2 \times 10^5$  cell per well of a six-wellplate. On the following day, the media was refreshed with RPMI media containing RA ( $1 \times 10^{-5}$  M). Cells were differentiated for 7 days in RA, with a final media change on the seventh day. After 24 and 48 hours, conditioned media was retained and clarified (10,000rpm for 3 minutes). Cells from which media was obtained were lysed for protein determination. Media samples were then treated with 4-(2-Aminoethyl)benzenesulfonyl fluoride hydrochloride (AEBSF) protease inhibitor (200mM, Melford, USA) and the media concentrated by vacuum evaporation to one fifth of the original volume.

The ELISA was performed in accordance with the manufacturer's instructions (see appendix). Briefly, media samples were incubated overnight in the coated ELISA plate at 4°C in human A $\beta$ 42 detection antibody. A $\beta$  standards were prepared in RPMI media. On the following day, the contents of each well was carefully aspirated and the well washed in wash buffer (4 times). 100 $\mu$ ls of anti-rabbit IgG HRP working solution was added to each well and the plate incubated at RT for 30 minutes with shaking at 200rpm. Wells were then washed again (4 times) and 100 $\mu$ l of stabilised chromogen added to the wells. The plate was incubated for 30 minutes in the dark with shaking at 200rpm. To stop the reaction, 100 $\mu$ ls stop solution was added to each well and the Abs<sub>450</sub> read on a spectrophotometer (MultiSkan, Ascent, Thermo Scientific, UK). Amyloid concentrations were determined by plotting the A $\beta$  standard against absorbance readings and performing linear regression analysis. Concentrations were then corrected to the number of cells by normalising against the total protein concentration from cellular lysates.

### **3.2.3.3 SHSY5Y differentiation and immunostaining**

Clones were seeded into 6-well plates at density of  $8 \times 10^4$  and then differentiated with 7 days of RA in RPMI, which was then followed by 11 days of BDNF (10ng/ml, Peprotech, UK) treatment in neuronal basal media (Gibco, Life Technologies, Paisley, UK), containing B27 supplement (Gibco, Life Technologies, Paisley, UK), l-glutamine (2mM) and Pen/Strep (100x, Gibco, Life Technologies, UK). To detect neuronal markers, immunostaining was carried out according to section 2.2.3.5. Cells were incubated in rabbit anti-Tubulin III (1: 500, Abcam, UK) for 1 hour and then to detect bound antibody, visualised with goat anti-rabbit FITC (1:200, Jackson ImmunoResearch, Europe). Fluorescent images were taken using red filter cubes using fluorescence microscopy.

### **3.2.4 Determining changes in metabolism between the cell lines**

#### **3.2.4.1 Cell proliferation/ cellular growth assay**

Cell proliferation/growth was measured using the Cell Titer-Blue Cell Viability Assay (Promega, Southampton, UK) which provides a homogenous method to monitor cell viability. The assay assesses the ability of viable cells to metabolise a redox dye, resazurin to resorufin. The rate of this reaction is directly proportional to the number of viable cells, and can be measured as a change in absorbance/ fluorescence. The absorbance maximum of resazurin is 605nm and that of resorufin is 573nm. The end product, resorufin also emits a fluorescence at 590nm giving the user flexibility in using reading absorbance or fluorescence. An additional advantage is that the cells remain viable after the removal of the assay reagent.

##### **3.2.4.1.1 Sample preparation**

To determine cellular growth rates, wtAPP695/ SweAPP695 expressing cell lines and control SHSY5Y cells (i.e untransfected cells) were plated at  $1.5 \times 10^4$  per well into 96-wellplates (Corning, MA, USA) in a triplicate. After 24 and 48 hours of seeding, culture media was aspirated from the wells. CellTiter-Blue reagent was diluted 1:6 in phenol-free DMEM (Gibco, Life Technologies, Paisley, UK) and then 100 $\mu$ ls of this solution

was added to each well. The well plate was then returned to the incubator for 3 hours, after which time, the absorbance readings were taken at 590nm with background absorbance readings taken at 690nm.

To calculate percentage cell viability, reference readings ( $A_{690}$ ) were subtracted from the  $A_{590}$ , and reciprocals of the averages were taken (to calculate the proportion of resazurin metabolised). All values were expressed as a percentage of the control (untransfected SHSY5Y cells).

#### **3.2.4.2 Glucose HK Assay**

The amount of total glucose levels remaining in conditioned media was detected using the Glucose HK assay (Sigma-Aldrich, Poole, UK). This assay relies on the phosphorylation of glucose by hexokinase to glucose-6-phosphate in the presence of ATP. The next step involving oxidation of glucose-6-phosphate to gluconate-6-phosphate by glucose-6-phosphate dehydrogenase, results in an equimolar amount of  $\text{NAD}^+$  being reduced to NADH.



The amount of NADH generated results in an increase in absorbance at 340nm which can be detected by a spectrophotometer, and is directly proportional to glucose concentration.

##### **3.2.4.2.1 Sample preparation**

Glucose uptake was measured in both proliferating SHSY5Y cells and seven day RA-differentiated SHSY5Y cells. Cell lines and control SHSY5Y cells were seeded at  $2 \times 10^5$  cells into six wells of a 6-wellplate (Corning, MA, USA). After 24 and 48 hours of incubation, media was removed from three wells and the cells washed three times in cold PBS. Total cell lysate was obtained using 1ml of RIPA buffer to lyse three wells, which were pooled. Total protein was quantified (see section 2.2.2.2). Meanwhile,

pooled media was clarified at 10,000rpm for 5 minutes to remove cellular debris and aliquoted into microcentrifuge tubes for storage at -20°C.

Differentiated cells were plated as described above but on the following day, the media was replaced with media containing  $1 \times 10^{-5}$  M RA (Sigma-Aldrich, Poole, UK). The media was then refreshed every alternate day for 7 days. On the seventh day, media was refreshed and the cultures incubated for 24 and 48 hours, after which time they were harvested as described above.

The assay was adapted to a 96-well microplate format. Media samples were diluted 1:10 in deionized water and glucose standards (1.0mg/ml Sigma-Aldrich, Poole, UK) were serially diluted 1:2 in deionised water with concentrations ranging from 500µg/ml to 15.6µg/ml, with water serving as a glucose-free control. 40µls of diluted media or standard were loaded into the microplate in duplicate and then 200µls of glucose HK reagent was added to each well. The reaction was incubated at RT (15 minutes) and then the absorbance read at 340nm on a spectrophotometer (Ascent Multiscan, Thermo Scientific, UK). The total glucose was then normalised to cellular protein levels, as determined using the BCA assay (see section 2.2.2.2).

### **3.2.4.3 Analysis of mitochondrial function**

Mitochondrial function was assessed using the Seahorse XF Analyzer (Seahorse Biosciences, Massachusetts, USA). To optimise conditions for each cell line, a series of optimization experiments were performed to achieve the best OCR readings (in accordance with the Seahorse MitoStress Test Manual). XF assay media and calibrant was purchased from Seahorse Biosciences.

#### **3.2.4.3.1 Cell titration**

Human SHSY5Y cells were plated at different cell densities into a Seahorse XF24 microplate in triplicate using the manufacturer's recommended seeding protocol and incubated overnight at 37°C, 5% CO<sub>2</sub> for 23 hours. The Seahorse XF analyser was

warmed to 37°C overnight. Assay cartridges were soaked in 1ml of XF Calibrant/well overnight (minimum of 16 hours) in a CO<sub>2</sub>-free incubator at 37°C. Four wells were randomly selected as negative controls for the analyser to account for background correction. After approximately 23 hours, XF assay media was prepared by supplementing with glucose (10mM, Sigma-Aldrich, Poole, UK) and sodium pyruvate (2mM, Gibco, Life Technologies, Paisley, UK). The pH of the media was adjusted to 7.4 with sodium hydroxide. One hour prior to the experiment, the cells were rinsed in 1ml XF assay media and then incubated in 1ml of fresh XF assay media in a CO<sub>2</sub> free incubator. Cell-free (negative control) wells were treated in a similar manner. Using the Seahorse software, a protocol was set up as instructed in Table 3.1. Following the protocol, OCR and ECAR readings were taken for each well and recorded.

Step	Instruction	Duration
1	Calibration	~30 minutes
2	Equilibrate	See below
Loop steps 2-4 six times		
2	Mix	4 minutes
3	Wait	4 minutes
4	Measure	4 minutes

Table 3.1. Table of experimental set up on the Seahorse software to record basal OCR readings.

#### **3.2.4.3.2 Protein normalisation**

OCR readings were normalised against protein. To do this, cells were washed in PBS and then lysed in 30µl of RIPA buffer (Millipore, UK) for 30 minutes for 4°C. The protein concentration was determined for each well (see section 2.2.2.2), using 10µl of lysate/BSA standard loaded in duplicate.

#### **3.2.4.3.3 Compound optimization**

The day before the assay, SHSY5Y cells were plated as at the optimal cell density (as determined in section 3.2.4.3.1). Background (cell-free) wells were assigned to wells A1, B4, C3 and D5. The cartridge was also soaked in Seahorse XF calibrant overnight.

On the following day, cells were washed in XF Assay Media and the wells incubated in 675µl of XF Assay media. The four compounds Oligomycin, FCCP, Rotenone and

Antimycin A (all obtained from Sigma-Aldrich, Poole, UK) were prepared as a stock in DMSO (Sigma-Aldrich, Poole, UK) and stored as single use aliquots at -20C. To perform the optimization experiments, each compound was diluted in XF Assay Media and 75µls of the compound was added to port A of the cartridge. For background wells, 75µls of media was added to those relevant ports. On the Seahorse XF software, the Mito Stress Test was selected and then optimization plate chosen from the list. The protocol corresponding to each compound for optimization was chosen. Key information such as seeding density, basal OCR levels and the test concentrations were specified.

After the experimental run was complete, the protein concentration for each was determined (see section 3.2.4.3.2). For analysis of data, the subsequent excel file, which accompanies each XF Seahorse file calculated the average OCR reading for each concentration of compound test. This is plotted as an OCR vs concentration curve, with values normalised to protein concentration.

#### **3.2.4.3.3.1 Oligomycin optimization**

Oligomycin is the first compound injected into the microplate wells to induce a rapid OCR response. Oligomycin is an ATP coupler that inhibits ATP synthesis by blocking the proton channel of the  $F_c$  protein ATP synthase. The software looks for the minimal concentration required to achieve the lowest OCR response.

#### **3.2.4.3.3.2 FCCP compound optimization**

Carbonyl cyanide 4-(trifluoromethoxy)phenylhydrazone (FCCP) is the second compound required for optimization. This compound is a protonophore, which acts as an uncoupler of oxidative phosphorylation by preferentially transporting protons across the mitochondrial membrane instead of through the ATP synthase complex, leading to a rapid consumption of energy and oxygen without the generation of ATP. OCR increases as a result of uncoupling and the ECAR will also increase as the cells revert

to glycolysis to generate ATP. The software looks for the maximal OCR response at the lowest FCCP concentration.

According to the literature (Schneider et al., 2011a, Xun et al., 2012), 7 day RA-differentiated SHSY5Y cells exhibit an increase in maximal OCR response compared to proliferating cells. Therefore, FCCP was also titrated across the plate containing 7 day RA-differentiated SHSY5Y cells.

#### **3.2.4.3.3.3 Rotenone and Antimycin concentration optimization**

The third compound titrated across the XF microplate was rotenone. Rotenone is a complex I inhibitor, inhibiting electron transfer from the iron-sulphur centre in complex I to ubiquinone. Inhibition of complex I prevents the potential energy in NADH from being converted to usable energy in the form of ATP. The fourth inhibitor optimized was antimycin A (which is a specific complex II inhibitor. This binds to the Qi site of cytochrome reductase to inhibit the oxidation of ubiquinol in the electron transport chain of oxidative phosphorylation. Inhibition of this reaction disrupts the formation of the proton gradient across the inner membrane, subsequently inhibiting ATP production. The software assesses the minimal concentration required to achieve the lowest OCR readings for both compounds.

#### **3.2.4.3.4 Performing the MitoStress test**

Once the optimization experiments were complete, the next step was to proceed to perform the MitoStress test to study mitochondrial responses. This assay measures OCR in response to the mitochondrial inhibitors to produce a unique metabolic profile.

To prepare the plate, three replicates of three SweAPP695-expressing cells, three wtAPP695-expressing cells and control uninfected SHSY5Y cells were plated at  $8 \times 10^4$  cells per well. The assay cartridge was soaked in XF Calibrant overnight. Control SHSY5Y and wtAPP695/SweAPP695 expressing cell lines were also tested after seven days of RA treatment. Initially,  $2 \times 10^5$  cells were seeded into three wells of a 6-

wellplate (Corning, MA, USA). On the following day media was replaced with RA ( $1 \times 10^{-5}$  M) and the media was refreshed every other day. On the seventh day, cells were washed in PBS and detached using Accutase (Gibco, UK). The cells were pelleted (200g for 5 minutes), re-suspended in media containing RA and counted (section 2.2.3.2).  $8 \times 10^4$  cells were seeded into the XF24 microplate in three replicate wells.

On the following day, the experiment was performed according to the manufacturer's instructions (XF Cell Mito Stress test kit manual). Briefly, Seahorse Assay media was supplemented with 10mM D-glucose (Sigma-Aldrich, Poole, UK) and 2mM sodium pyruvate (Gibco, Life Technologies, Paisley, UK). Compounds were diluted to previously determined optimal concentrations in XF Assay media. Cells were washed in 1ml of XF Assay media and then incubated in 500µl of fresh assay media 1 hour prior to the experiment in a CO<sub>2</sub>-free incubator at 37°C. After the experiment was run, protein concentration from each well was determined (see section 3.2.4.3.2).

#### **3.2.4.3.4.1 Seahorse Analysis**

The data file was analysed using the Seahorse Wave 2.0 software, which allows for normalization of OCR values against protein (or other means) and the removal of outlying values (determined by the standard deviation). The analysed data was then saved as a new Excel file. This file was then opened up in MitoStress Report Generator which automatically uses the raw values to calculate key measurements. Subsequent values were then analysed using two-way ANOVA using Graph Pad Prism 6.0.

#### **3.2.4.4 Oxidative stress response**

wtAPP695 and SweAPP695 expressing cells were treated with hydrogen peroxide (H<sub>2</sub>O<sub>2</sub>) to determine the stress response of cells.

#### **3.2.4.4.1 Optimization of seeding density and H<sub>2</sub>O<sub>2</sub> concentration**

The optimal seeding of SHSY5Y cells and the IC<sub>50</sub> of hydrogen peroxide was determined. The IC<sub>50</sub> for a given compound/ drug refers to the concentration at which the induced response is halfway between the baseline and maximum after a specified exposure period. In this case, the concentration of hydrogen peroxide required to kill 50% of the cells was determined. SHSY5Y cells were plated at 30 x 10<sup>5</sup> cells per well in duplicate and serially diluted 1:2 to 3.75 x 10<sup>3</sup> cells across the 96-wellplate in a total volume of 200µls per well. After 24 hours of incubation, the cells were treated with various concentrations of hydrogen peroxide to determine the minimum inhibitory concentration required to achieve 50% cell death. APP-expressing cell lines were also seeded in a similar manner to determine their responses to increasing hydrogen peroxide concentrations.

For cell treatments, fresh hydrogen peroxide (Sigma-Aldrich, Poole, UK) was diluted in phenol-free red media supplemented with 2mM l-glutamine to 6400µM. The stock was then serially diluted 1:2 to a final concentration of 25µM. Media was then removed from each well and replaced with 100µls of hydrogen peroxide solution in duplicate. Cells were incubated for 1 hour at 37°C after which time the hydrogen peroxide was replaced with 200µl of complete media to allow the cells to recover for 18 hours at 37°C. After 18 hours of recovery, cell toxicity was assessed by MTT assay (see section 3.2.4.4.2).

#### **3.2.4.4.2 MTT assay**

Cell viability was measured using the 3-[4,5-Dimethylthiazol-2-yl]-2, 5-diphenyltetrazolium bromide (MTT) assay. In this assay, the tetrazolium salt MTT, is reduced by dehydrogenase enzymes within metabolically active cells into insoluble formazan crystals. These intracellular crystals can then be solubilised and the absorbance determined as a direct measure of cell viability.

MTT (Sigma-Aldrich, Poole, UK) was dissolved in PBS to 2.5mg/ml and then filter sterilised using a 0.2µM filter. Stocks were stored in aliquots and protected from light at -20°C. To perform the assay, MTT stock was diluted 1:5 in phenol red-free DMEM and 100µl of the diluted stock was added to the wells. The microplate was incubated at 37°C for 3 hours. After incubation, all MTT solution was removed and 50µls of DMSO was added to each well to solubilise the formazan crystals. The microplate was mixed on a shaker (500rpm for 30 seconds) and then incubated at 37°C for a further 10 minutes to ensure complete crystal solubilisation. Finally, the absorbance at 570nm and reference absorbance at 690nm was read using a spectrophotometer (Ascent MultiScan FX, Thermo Scientific, Loughborough, UK). Cell viability was determined by subtracting the reference readings from the absorbencies from each hydrogen peroxide concentration tested. Results were expressed as a percentage of the untreated control (of that cell line).

#### **3.2.4.4.3 Statistical analysis**

When making comparisons between the control SHSY5Y cell lines and the APP-expressing cell lines at different time points, two way ANOVA was performed with Dunnetts multiple comparisons/student's T test as appropriate in Graph Pad Prism 6.0. A dose response curve was plotted for each cell line with increasing concentrations of hydrogen peroxide to determine the IC<sub>50</sub>.

### 3.3 Results

#### 3.3.1 Optimization of transduction into SHSY5Y cell line

Prior to infecting SHSY5Y cells with the APP lentiviruses, it was first important to establish a transduction protocol, with which lentiviral infection would be effective and cause minimal toxicity. To do this, a lentivirus expressing GFP, driven by the viral promoter CMV, pGIPz was packaged into active virus using psPAX2 and PMD2.G. SHSY5Y cells were seeded and differentiated with RA over five days. Different multiplicities of infection of pGIPz were determined by using the appropriate amount of virus (titre determined by p24 ELISA) to infect the cells. The efficiency of retrovirus-mediated gene transfer can be enhanced, most commonly with the use of cationic polymers, such as polybrene and protamine sulfate. Therefore, viral infection was tested in the presence or absence of Polybrene. 48-hours post infection, cells were visualised using fluorescence microscopy (section 2.2.3.6). Figure 3.6 shows GFP fluorescence detectable after 48 hours at all MOI's. As the MOI increases, the level of GFP fluorescence increases, as more cells have been infected and these cells may contain multiple viral copies. This effect was further enhanced in the presence of Polybrene.

Cells were also viewed 10 days post-infection (Figure 3.7). GFP fluorescence was still detectable at increased levels at lower MOI's in comparison with 48 hours imaging. Increasing the MOI resulted in fewer cells which were still expressing GFP expected to be due to toxicity. In the presence of Polybrene, there was significantly less GFP fluorescence due to cell death. Lower MOI's and infection without the use of Polybrene lead to potentially long term viable cells with stable protein expression. It should also be noted that the CMV promoter was utilised to maximise GFP expression for testing transduction efficiency. This promoter is noted to be prone to silencing and has associated toxic effects due to the high levels of protein expression.

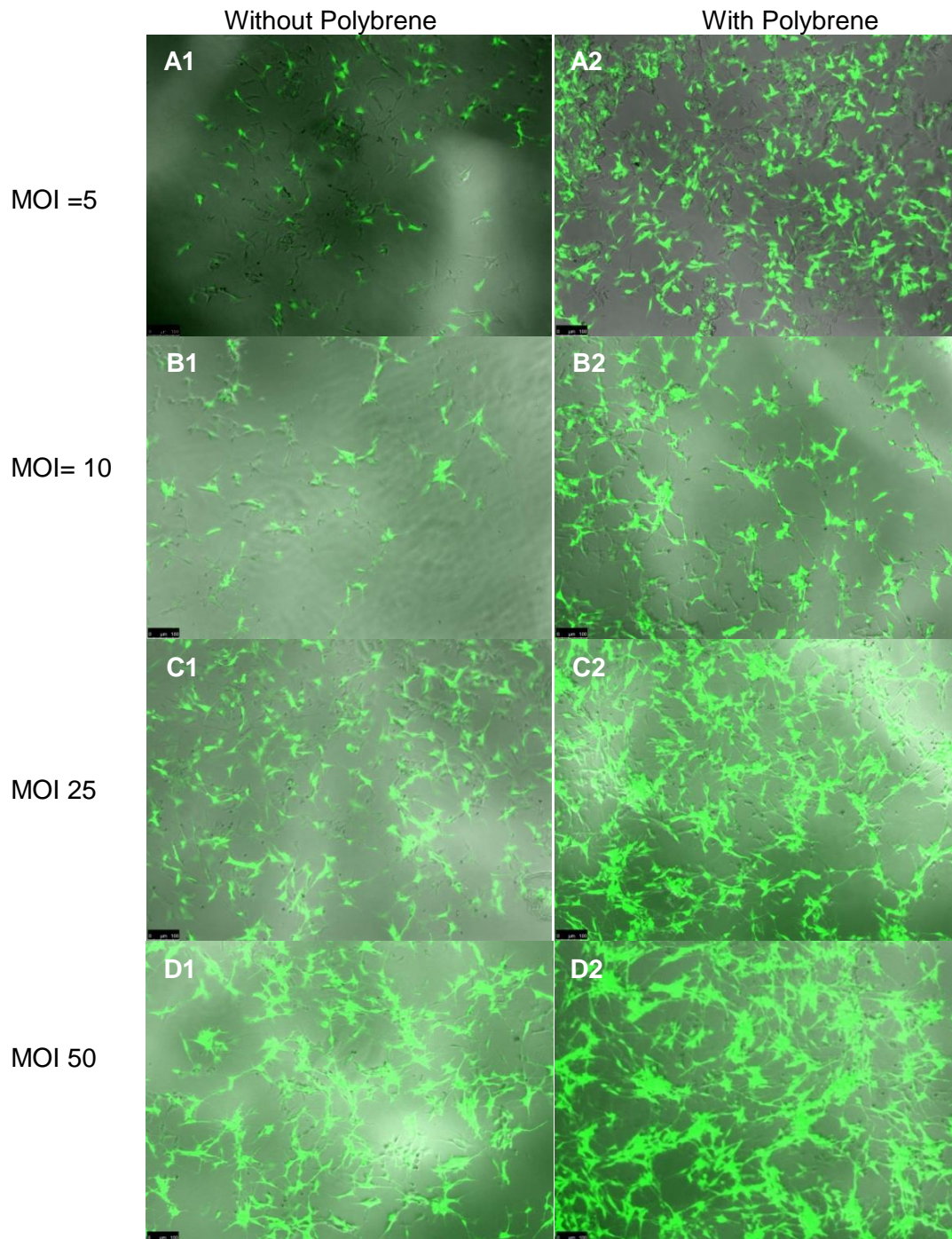


Figure 3.6. Fluorescent images of Lentiviral-GFP infected cells 48 hours following transduction. A1, MOI 5 without polybrene, A2, MOI 5 with polybrene, B1, MOI 10 without polybrene, B2, MOI 10 with polybrene, C1, MOI 25 without polybrene, C2, MOI 25 with polybrene, D1, MOI 50 without polybrene, D2, MOI 50 with polybrene. Scale Bar 100 $\mu$ m.

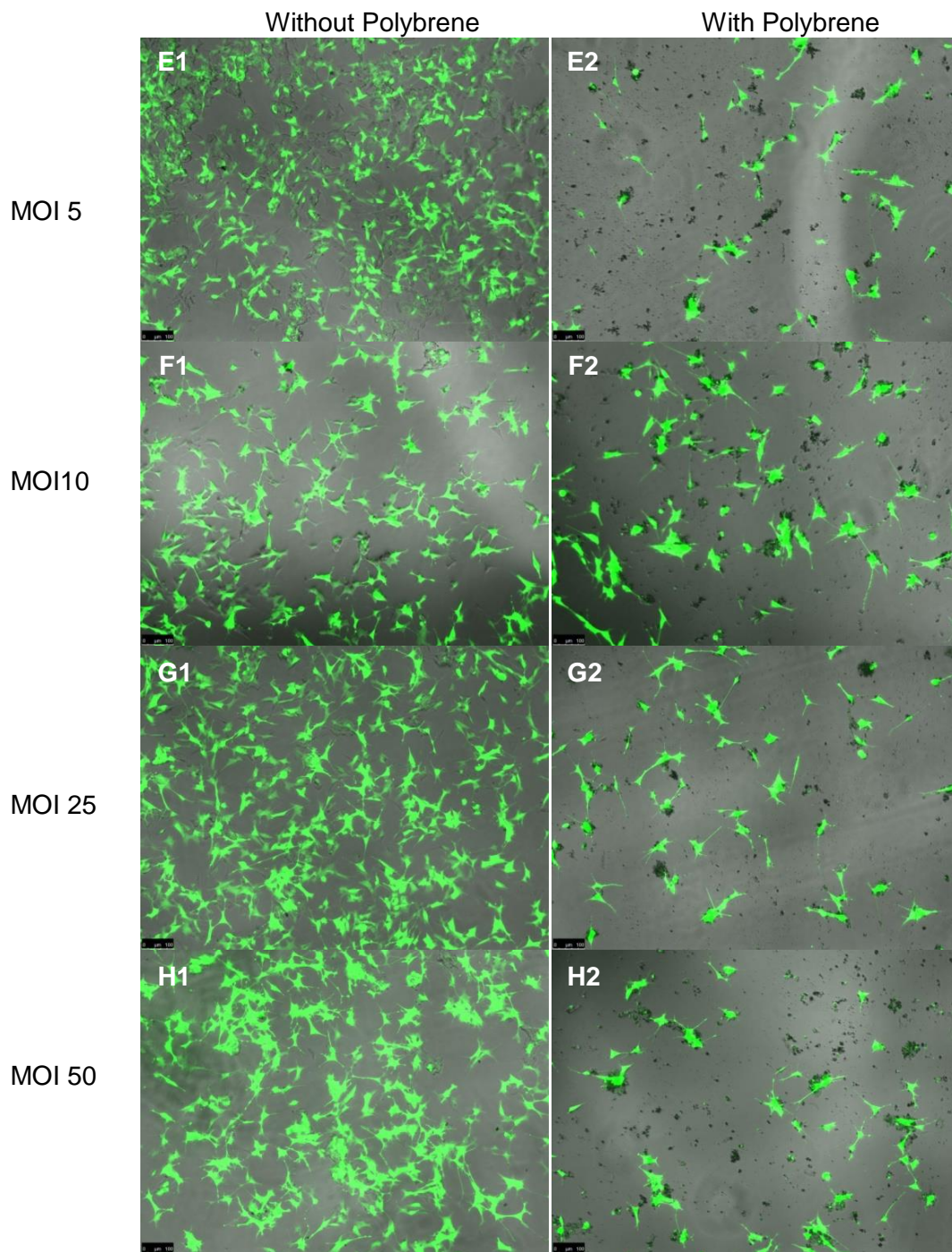
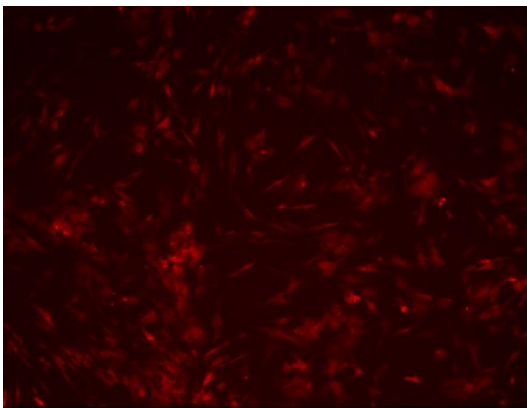


Figure 3.7. Fluorescent images of Lentiviral-GFP infected cells 10 days following transduction. E1, MOI 5 without polybrene, E2, MOI 5 with polybrene, F1, MOI 10 without polybrene, F2, MOI 10 with polybrene, G1, MOI 25 without polybrene, G2, MOI 25 with polybrene, H1, MOI 50 without polybrene, H2, MOI 50 with polybrene. Scale Bar 100 $\mu$ m.

### 3.3.2 Testing of the lentiviral constructs

The pLenti6.4 Syn1-wtAPP695/ SweAPP695 constructs were successfully packaged into lentivirus using the HEK293FT cell line. Packaging of p24-associated lentivirus was first confirmed using the Lenti GoStix (data not shown), and then the lentivirus was collected and concentrated using the sucrose gradient method (section 3.2.1.4). Both Lentiviruses were then diluted 1:500 / 1:1000 to obtain absorbance values within the p24-associated ELISA standard curve. The APP lentiviruses were tested at different MOI's. Using the results of the ELISA, the multiplicities of infection of 5 and 10 were determined from the viral titre of each virus. Five days post-RA differentiation, SHSY5Y cells were transduced with EIFa driven lentivirus expressing cherry red fluorescent protein (as a positive control) and with pLenti6.4SweAPP695 / wtAPP695 both at an MOI of 5 and 10. After three changes of media, the cells were viewed under the microscope to assess for RFP fluorescence (in the case of the positive control) and to assess for cell viability post infection (see Figure 3.8).

A



B

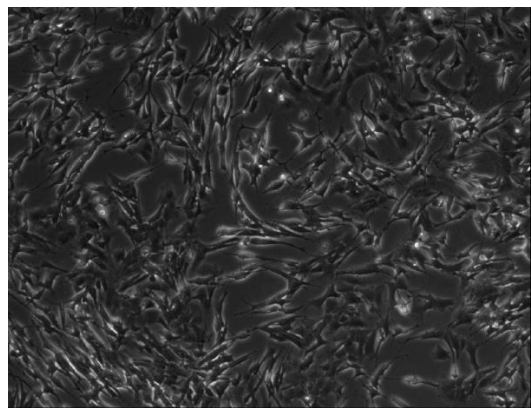


Figure 3.8. Fluorescence (A) and phase contrast image (B) of positive control for viral transduction testing with eIF1a-cherry red fluorescent protein.

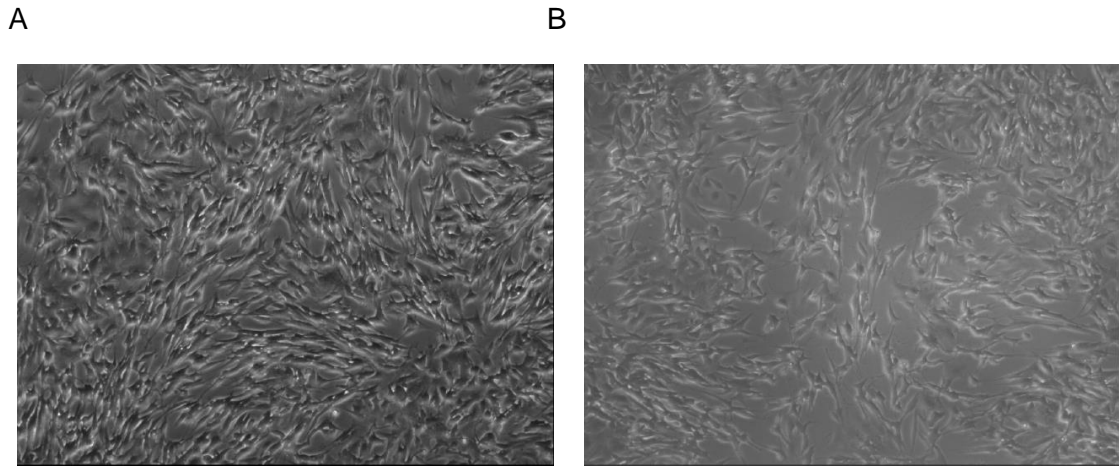


Figure 3.9. Phase contrast image of SHSY5Y cells infected with pLenti6.4 SYN-1 SweAPP695 lentivirus at MOI of 5 (A) and at MOI of 10 (B) 48 hours post-transduction.

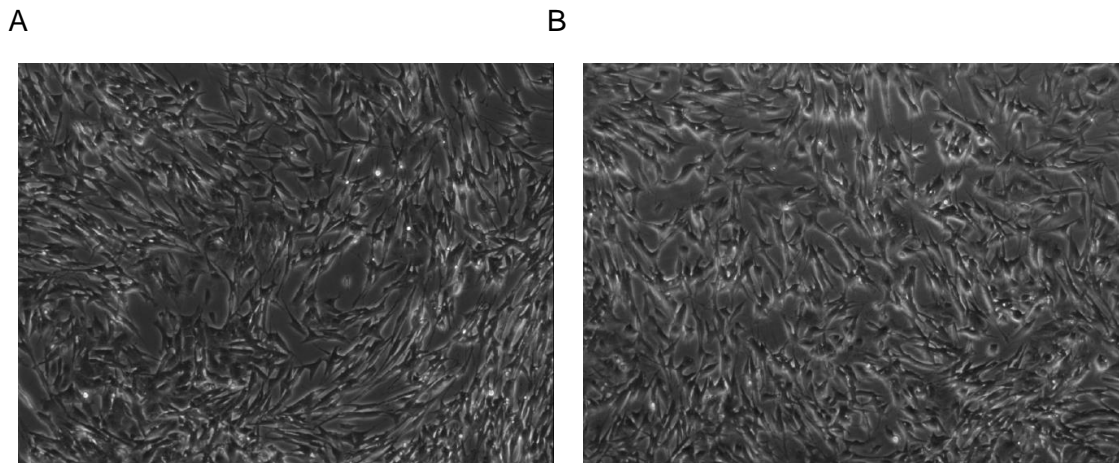


Figure 3.10. Phase contrast image of SHSY5Y cells infected with pLenti6.4 SYN-1 wtAPP695 lentivirus at MOI of 5 (A) and at MOI of 10 (B) 48 hours post-transduction.

Cell lysates from transduced wells were also collected and assessed for APP protein expression by Western blotting using anti-APP695 antibody (Figure 3.11). Results show a protein band that corresponds to 100-130kDa in size, which is the approximate size of APP695. Protein expression in the untransduced (control) SHY5Y cell line is comparatively weak compared to cells transduced with either SweAPP695 / wtAPP695. The results also show that anti-APP695 antibody can detect both forms of APP. Furthermore, the increase in MOI from 5 to 10 did not substantially increase APP protein expression.

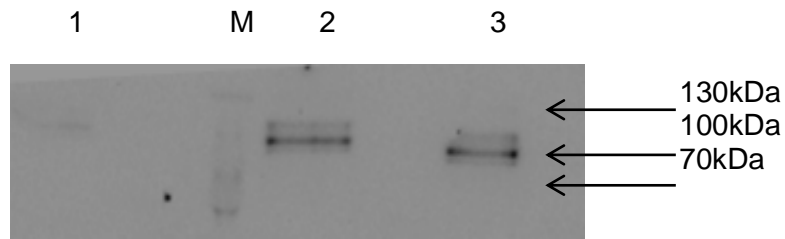


Figure 3.11. Western blot analysis of cell lysates from SHSY5Y cells transduced with SweAPP695 lentivirus. Lane 1, control cell lysate, lane M, Prestained Protein Ladder, lanes 2 and 3, cell lysates from SHSY5Y cells transduced with lentivirus at MOI of 5 and 10 respectively.

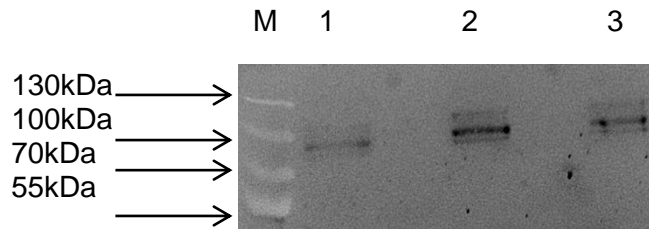


Figure 3.12. Western blot analysis of cell lysates from SHSY5Y cells transduced with wtAPP695 lentivirus. Lane M Protein Prestained Ladder, lane 1, control cell lysate, lanes 2 and 3, SHSY5Y cells lysates transduced at MOI of 5 and 10 respectively.

### 3.3.3 Generation of cell lines

SHSY5Y cell were seeded into flasks and transduced the next day with either pLenti6.4 wtAPP695 or SweAPP695 at an MOI of 1. Following transduction, cells were then re-plated into 6-wellplates and transduced cells were selected with Blastocidin-containing media (3 $\mu$ g/ml). Over next few weeks, well plates were assessed daily to detect the presence of clones derived from single cells. The clones were viewed under a light microscope (x10 objective), and when considered large enough, they were carefully isolated with a cloning cylinder from remainder of the well. Clones were then grown in separate wells of a 6-wellplate to be expanded into larger flasks. Clones were named in order of selection, with some clones unable to survive the isolation and re-plating step. This eventually led to the selection of potential clones (Table 3.2).

wtAPP695 expressing cell lines	SweAPP695 expressing cell lines
W1	S2
W2	S3
W3	S4
W4	S6
W5	S7
W7	S9
W9	S10
W11	S11
W13	S14
W14	S15
W17	S17
W18	

Table 3.2. Table of final clones isolated and expanded successfully.

After picking the clones that survived, the morphology and general growth rate of each clone was assessed by light microscopy. The ability of clones to differentiate into a more neuronal phenotype was assessed after RA and BDNF treatment. Clones were also immunostained for Tubulin, a marker of neurons (Figure 3.13). Clones were picked based on their ability to differentiate into neurons in comparison to differentiation of control SHSY5Y cells. After BDNF treatment, chosen clones (W17, W18, S7, S10) showed extensive neurite extension from small cell bodies. Over time the differentiation period, the number of cells decreases, influencing the density and distance between cells. In all cases, differentiated cells stained positively for the neuronal marker, tubulin, in particular highlighting the extensive neurite networks formed between cells. The level of differentiation between these different cell lines may be affected by the level of expressed APP695, as it is known that APP fragments are involved in cellular growth and neuronal differentiation. Therefore, levels of the APP fragments may differ between each cell line, due to different levels of BACE1.

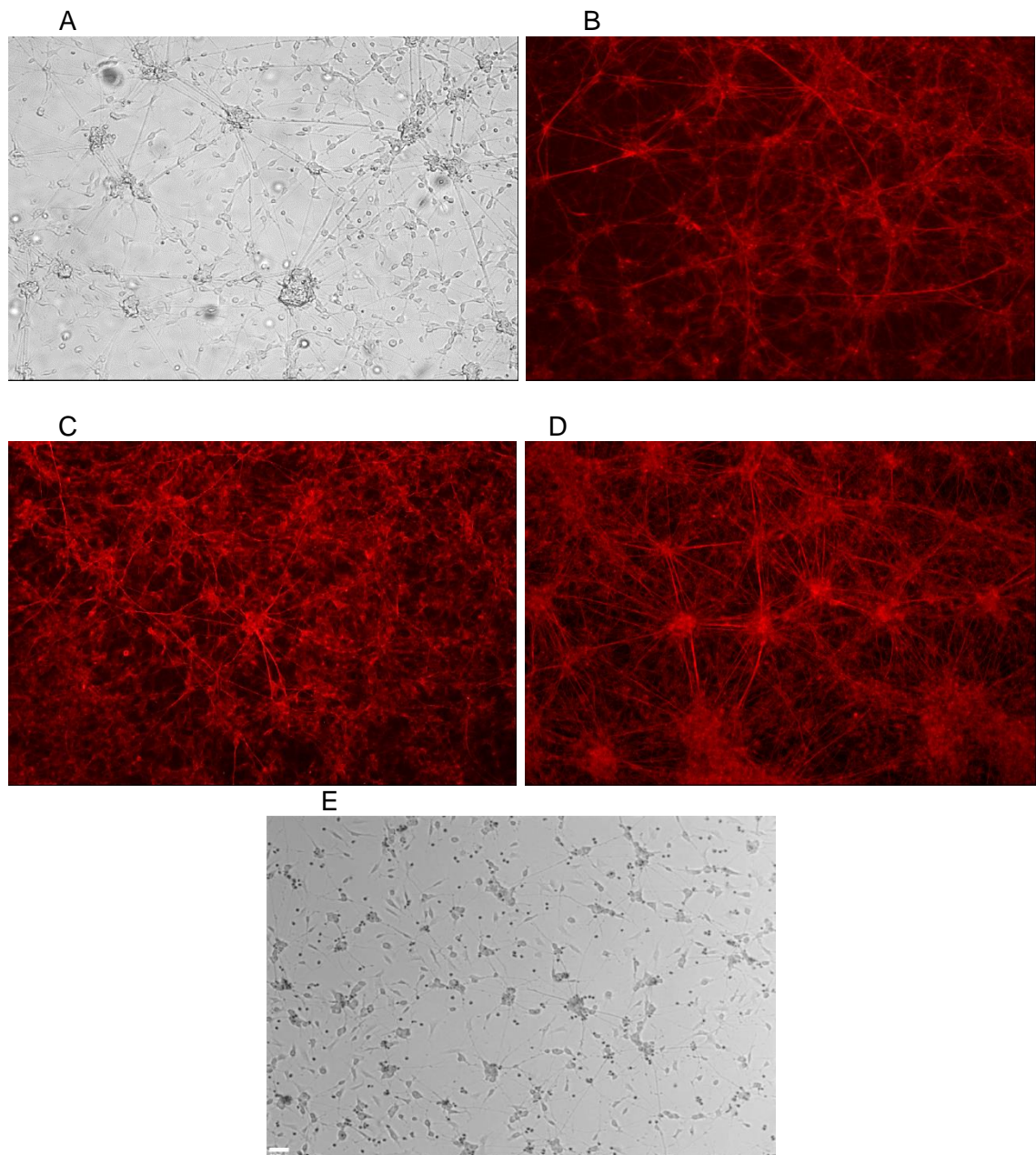


Figure 3.13. Fluorescence/ bright-field images of SHSY5Y clones post-BDNF treatment, immunostained for  $\beta$ -tubulin III (x10 objective). A, clone W17, B, clone W18, C, clone S7, D, clone S10, E, Bright-field image of differentiated of control SHSY5Y cells after RA and BDNF treatment (x10 objective, scale 100 $\mu$ M).

### 3.3.4 Metabolic studies of wtAPP695/SweAPP695 expressing SHSY5Y cell lines

#### 3.3.4.1 Cell proliferation

Chosen clones were assessed for their ability to proliferate over 24 and 48 hours following initial seeding using the Cell Titer Blue assay. Proliferation rates are presented as a percentage of the control SHSY5Y (untransfected) cell line (Figure 3.14). After 24 hours of growth, all cell lines exhibit slow growth, with none of the clones showing any significant changes in proliferation at 24 hours in comparison to the

control cell line. After 48 hours of incubation, proliferation increased slowly, clone S7 showed a significant increase in growth over the control of  $107.7 \pm 2.0 \%$  ( $p$  value = 0.0283). Proliferation was important to consider as any differences in growth/metabolic activity between clones could be due to differential processing of APP, leading to the production of different APP fragments. Furthermore, proliferation rate is important as experiments on the Seahorse analyzer a sufficient amount of cells to seed.

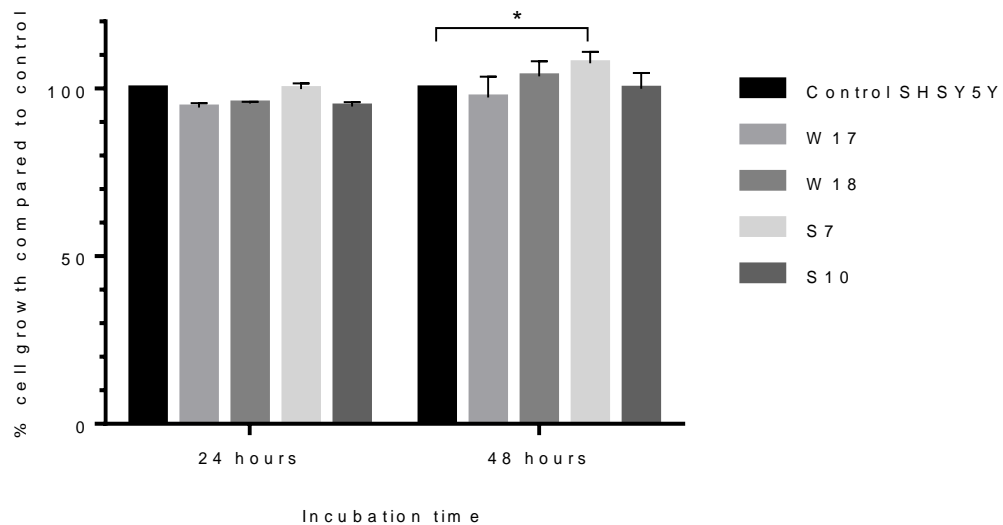


Figure 3.14. Cell proliferation rates of wtAPP695 and SweAPP695 clones using Cell Titer Blue. Results are expressed as a percentage of control SHSY5Y  $\pm$  SEM,  $n=3$ ,  $p < 0.05$ .

### 3.3.4.2 APP protein expression

Cell lines were assessed for altered APP protein expression. Total cell lysate was taken from proliferative SHSY5Y cells and 7 day RA-differentiated cells and the lysates assessed for APP protein expression by Western blotting using antibodies directed against A $\beta$  (6E10, Covance). Blots show that both SweAPP695/ wtAPP695 protein was detected by this antibody.  $\beta$ -actin was blotted as a reference control. Figure 3.15 shows one Western blot. Using manual band quantification in Gene Sys Tools, the pixels of each protein band were determined, corrected using automatic background. APP protein expression was normalized against  $\beta$ actin protein band for each cell lysate sample blotted.

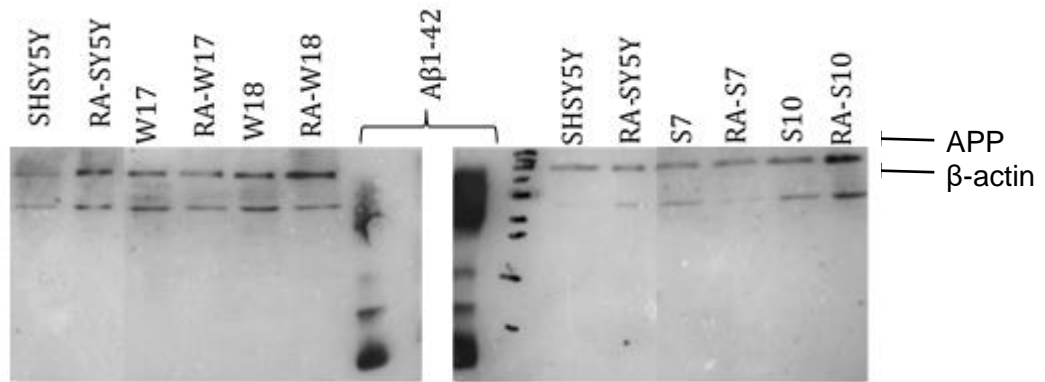


Figure 3.15. Representative Western blot analysis of total cell lysates taken from control SHSY5Y lines, wtAPP and SwedishAPP expressing cell lines.

Figure 3.16 shows the relative pixel density for APP protein detected from lysate from each cell line, normalized to  $\beta$ -actin. Results are presented as a percentage of APP expression from the control (untransduced) cell line. APP protein levels vary widely across all cell lines analysed. Lysate taken from proliferating wtAPP695 expressing cell lines generally contained more APP than the control, but levels appear to decrease after seven days of RA differentiation. By contrast, the SweAPP695 expressing cell lines appeared to contain less APP during the proliferative stages and after RA differentiation, with the exception of clone S7.

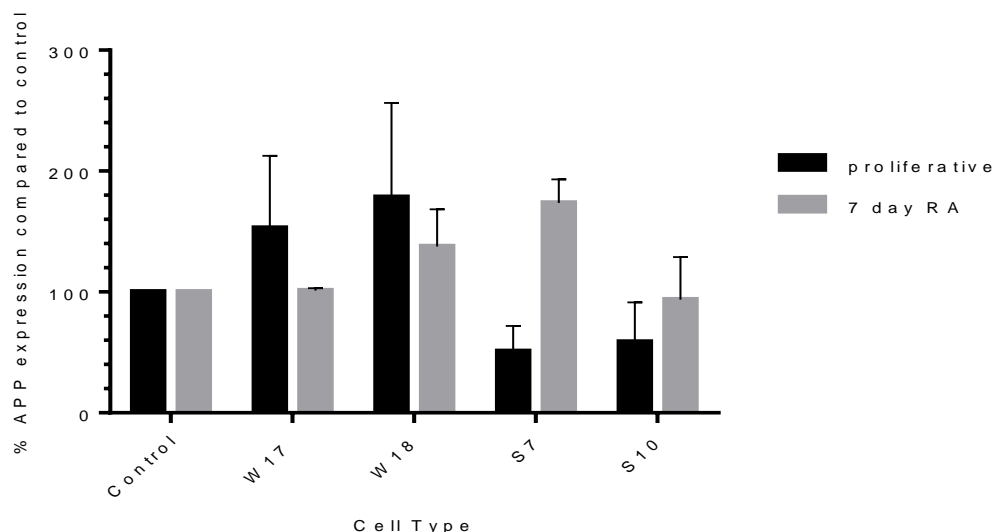


Figure 3.16. Percentage pixel density of APP protein detected in cell lysates. Results are presented as a percentage of the control SHSY5Y (proliferative/7 day RA differentiated)  $\pm$  SEM n=2.

### 3.3.4.3 Amyloid production in 7 day RA-differentiated cell lines

Amounts of A $\beta$ 1-42 secreted into the media were assessed after differentiation of the cell lines, at 24 and 48 hours of incubation following the seventh day of changing the media. SHSY5Y cells are reported to secrete amyloid from the cells (Zheng et al., 2013), in small amounts (Prasanthi et al., 2009). Media samples were vacuum evaporated five times the original volume and the concentration of A $\beta$ 1-42 was determined using the ELISA method. Figure 3.17 shows variable amounts of amyloid across the cell lines. After 24 hours, there was little amyloid or no amyloid detected, but after 48 hours, there was considerably more amyloid detected in the media. Clone S10 showed a significant increase in the amount of A $\beta$ 1-42 secreted when compared to control. After 24 hours, 0.008pg/ml/ mg of protein  $\pm$  0.002 SD was detected in conditioned media of clone S10 while the control media contained 0.00009  $\pm$  0.00002 pg/ml/ mg of protein (p value <0.0001). After 48 hours, S10 media contained 0.014  $\pm$  0.000152 pg/ml of amyloid compared to the control media, which contained 0.00104  $\pm$  0.00023 pg/ml (p value <0.0001). At 24 hours, the A $\beta$  ELISA detected more A $\beta$  in the conditioned media from the wtAPP-expressing cells compared to the control media, but this was not significant.

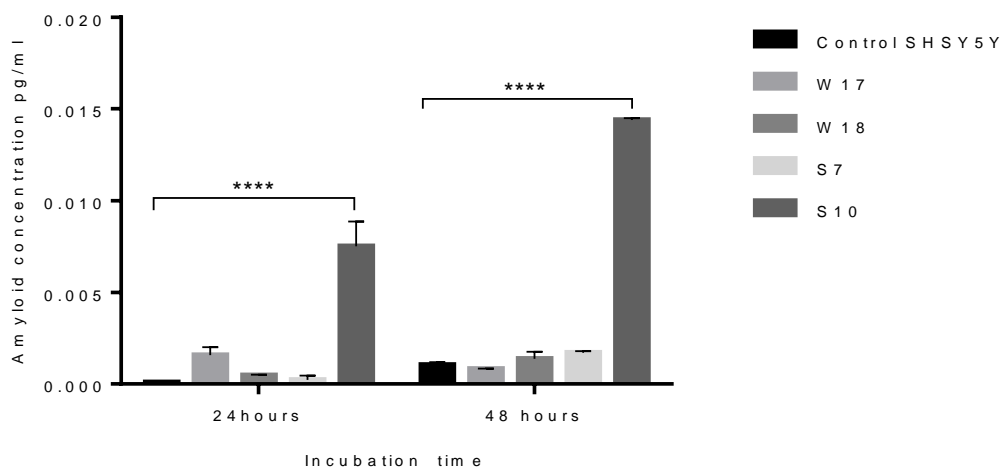


Figure 3.17. Graph showing concentration of A $\beta$ 1-42 secreted into media of 7 day RA-differentiated cell lines. Results are expressed as pg/ml, normalized to total cellular protein, n=2, p< 0.0001 (\*\*\*\*).

### 3.3.4.4 Glucose uptake

#### 3.3.4.4.1 Glucose uptake in the proliferating cell lines

Glucose uptake was measured by quantifying the concentration of glucose remaining in conditioned media taken from undifferentiated cell lines incubated after 24 and 48 hours. This was performed using the Glucose HK assay (Figure 3.18). The amount of glucose remaining in the media is expressed as a percentage of the control SHSY5Y cell line, after normalisation to total protein. At both incubation times, there is a general trend that there was more glucose remaining in the conditioned media compared to the control cell line, suggesting decreased glucose uptake by the proliferating cells. However, this was not found to be statistically significant most likely due to variations in glucose readings between replicate experiments. There was significant difference when comparing between the control cell line and the undifferentiated S10 clone, with the S10 clone showing an average of a 268.5 increase  $\pm$  68% over the control ( $p$  value = 0.03335).

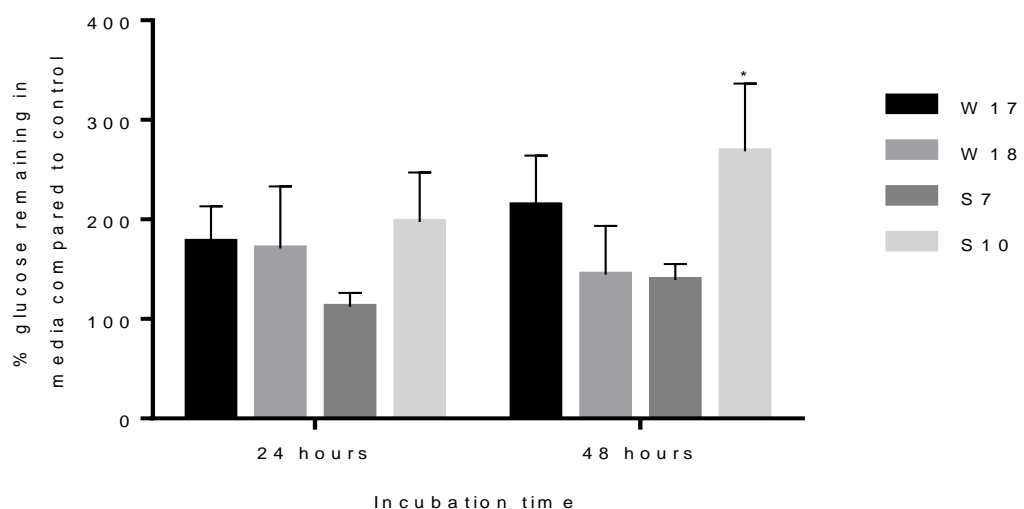


Figure 3.18. Graph the amount of glucose remaining in conditioned media after 24 and 48 hours of incubation of undifferentiated cell lines using the Glucose HK assay. Results are expressed as a percentage of the control  $\pm$  SEM,  $n=3$  ( $p<0.05$  (\*)).

### 3.3.4.4.2 Glucose uptake in 7 day RA-differentiated cell lines

Cell lines were also differentiated with RA for seven days, and on the seventh day, media was refreshed. Glucose remaining in the media was measured after 24 and 48 hours, and normalised to total protein (Figure 3.19). At both incubation times, there was a general trend that both wtAPP695 and SweAPP695 expressing cell lines demonstrated more glucose in the media, and hence decreased glucose uptake. However, this was only statistically significant in a number of the cell lines tested. At the 24 hours incubation time, differentiated W17 clones showed an average of a  $247.0 \pm 12.3$  % increase in remaining glucose over the differentiated control cell line ( $p$  value = 0.011). The differentiated W18 clone showed a significant increase in remaining glucose of  $286.3 \pm 72.8$ % over the control ( $p$  value = 0.0014). None of the differentiated SweAPP-expressing clones showed any significant differences. At the 48 hour time point, clone W17 showed a significant increase of  $221.7 \pm 46.0$ % SEM over the control ( $p$  value = 0.0386), whilst the W18 clone showed a significant increase of  $332.3 \pm 11.0$  SEM over the control ( $p$  value = 0.0001). These results between proliferative and the RA-differentiated SHSY5Y cell lines highlight differences in glucose uptake at both time points.

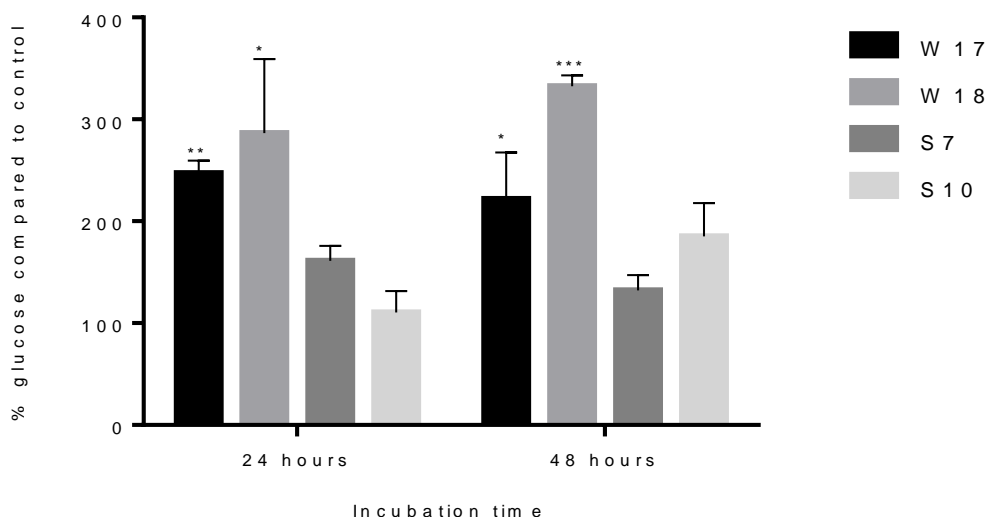


Figure 3.19. Graph of glucose remaining in conditioned media after 24 and 48 hours of incubation taken from 7 day RA-differentiated cell lines. Results are expressed as a percentage of the control  $\pm$  SEM,  $n=3$   $p<0.05$  (\*),  $p< 0.01$  (\*\*),  $p< 0.001$ ,  $p<0.0001$ .

### 3.3.4.5 Seahorse experiments

#### 3.3.4.5.1 Optimization of seeding cell density

For optimisation of conditions to establish a metabolic profile of mitochondrial function (see Figure 3.4 for a typical profile with the parameters obtained from such a profile) in SHSY5Y cells using the Seahorse analyser, cells were seeded between 20000 to 100000 cells per well in triplicate with six readings taken over a number of time points (Figure 3.20). 80000 cells was chosen as the optimal seeding density with an average basal OCR of 421pMoles/min. Basal OCR refers the oxygen consumed by cells at rest. Readings were consistent throughout and this in agreement with other studies using this cell line on the Seahorse analyser.

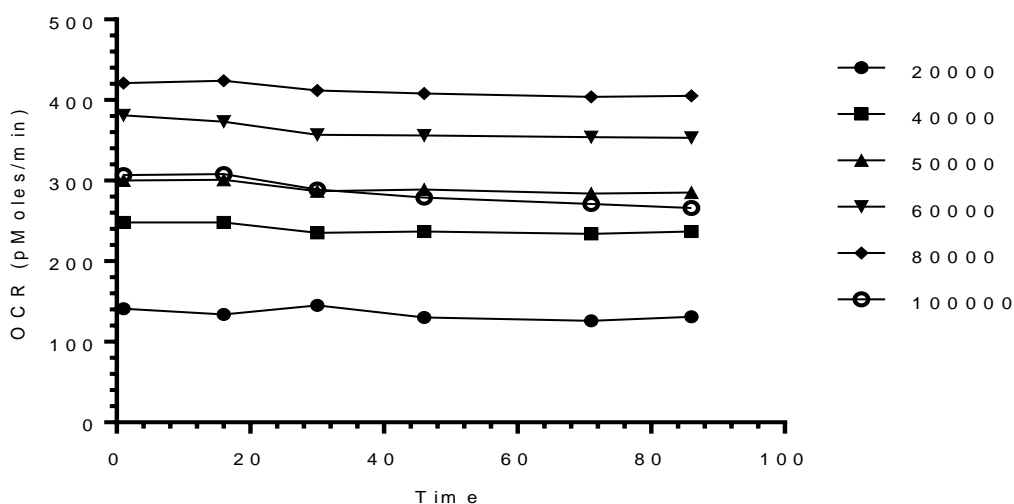


Figure 3.20. Representative graph of OCR readings over time of cells over a range of seeding densities.

#### 3.3.4.5.2 Optimization of mitochondrial inhibitor concentrations

Optimization of mitochondrial inhibitors was performed according to the Seahorse software. Subsequent OCR data is averaged by the software, and a graph is plotted of compound concentration against the average OCR reading. The last three measurements immediately following injection of each inhibitor into the well were measured and normalized against protein determined for each well. Replicate wells which produced outlying OCR values were excluded (determined by the large standard deviation), with the remaining replicate wells for each concentration tested averaged. The corrected values were plotted by the Seahorse Software into an Excel spreadsheet. Optimal concentrations determined are tabulated below (Table 3.3).

Additionally, FCCP titration was performed with SHSY5Y cells differentiated with RA for seven days. Past studies have suggest that the metabolic profiles between proliferative and differentiated SHSY5Y cells differ in that the spare respiratory capacity increases with differentiation (Schneider et al., 2011a). Therefore, it was necessary to perform FCCP titration on differentiated SHSY5Y cells. The effects of increasing glucose concentration and sodium pyruvate concentration were determined in order to maximise the OCR response to FCCP treatment (data not shown). Glucose concentrations of 2mM, 5mM, 10mM and 25mM and sodium pyruvate concentrations of 0.5mM, 1mM, 2mM and 4mMM were tested. It was found that 10mM glucose and 2mM sodium pyruvate gave the maximal OCR response to FCCP.

Mitochondrial inhibitor	Optimal concentration ( $\mu\text{M}$ )
Oligomycin	5 $\mu\text{M}$
FCCP	1 $\mu\text{M}$ for proliferative cells 2.5 $\mu\text{M}$ for RA-differentiated cells
Antimycin A	1 $\mu\text{M}$
Rotenone	2.5 $\mu\text{M}$

Table 3.3. Table of optimal concentrations determined after protein normalization.

### 3.3.4.5.3 Mitochondrial function of proliferative cell lines

The MitoStress test was then performed on cell lines at the proliferative cells. Results are presented as graphs detailing two measurements.

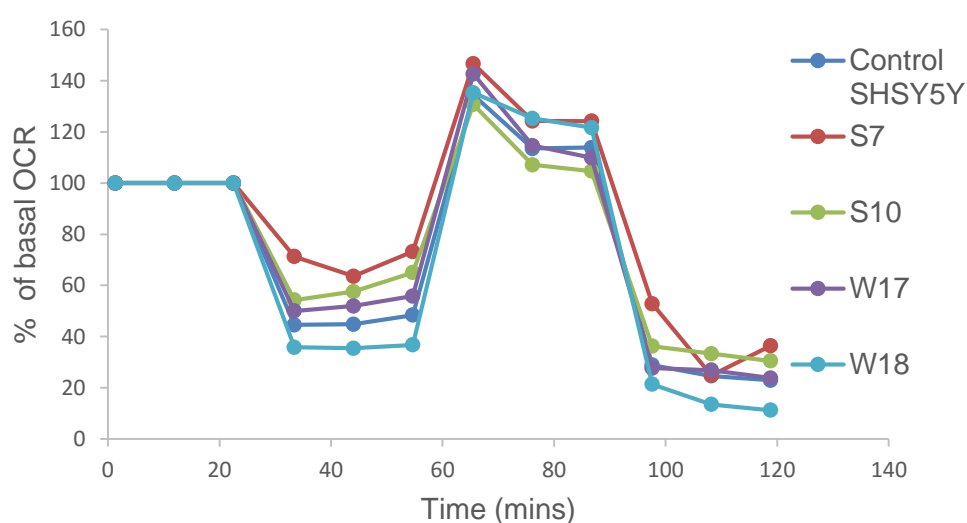


Figure 3.21. Percentage of basal OCR against time plotted for each cell line. Data shown is representative of one experiment.

Figure 3.21 shows raw data of OCR readings obtained over time for one experiment. The raw data was then analysed using the Seahorse MitoStress Report generator to calculate different parameters of mitochondrial function. When looking at the basal OCR readings for the proliferative cell lines (Figure 3.22), there was a statistical difference between the control which had an average basal OCR of  $0.315 \pm 0.053$  pMoles/min/mg protein and the proliferating clone S7, which an average basal OCR of  $0.125 \pm 0.030$  pMoles/min/mg protein ( $p$  value = 0.0046). There was also a difference between the control and clone S10, which had an average OCR of  $0.125 \pm 0.030$  pMoles/min/mg protein ( $p$  value = 0.0046).

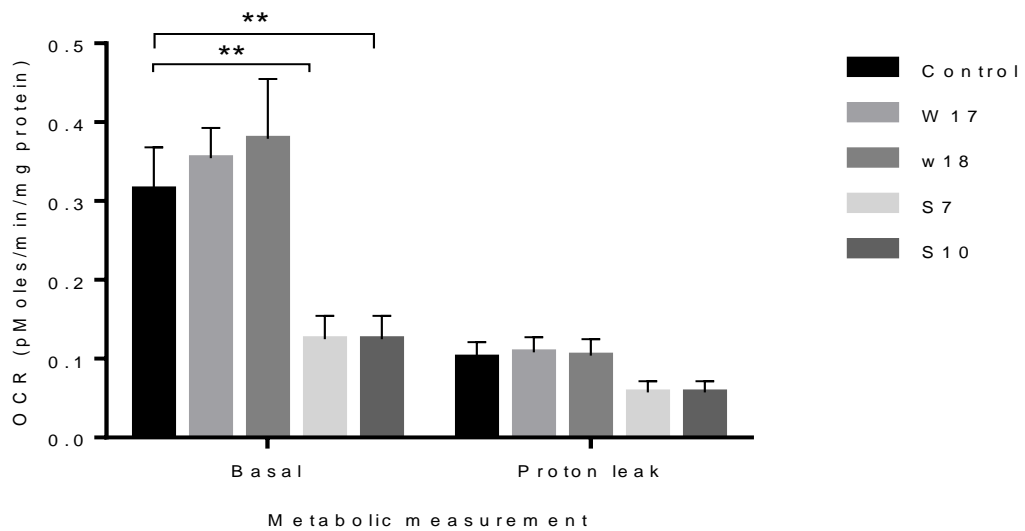


Figure 3.22. Graph of basal OCR and proton leak measurements for proliferating cell lines. Results presented as average OCR  $\pm$  SEM,  $n=3$ .  $P < 0.005$  (\*\*).

When comparing maximal respiration and the spare respiratory capacity between the proliferating different cell lines (Figure 3.23), there were no significant differences.

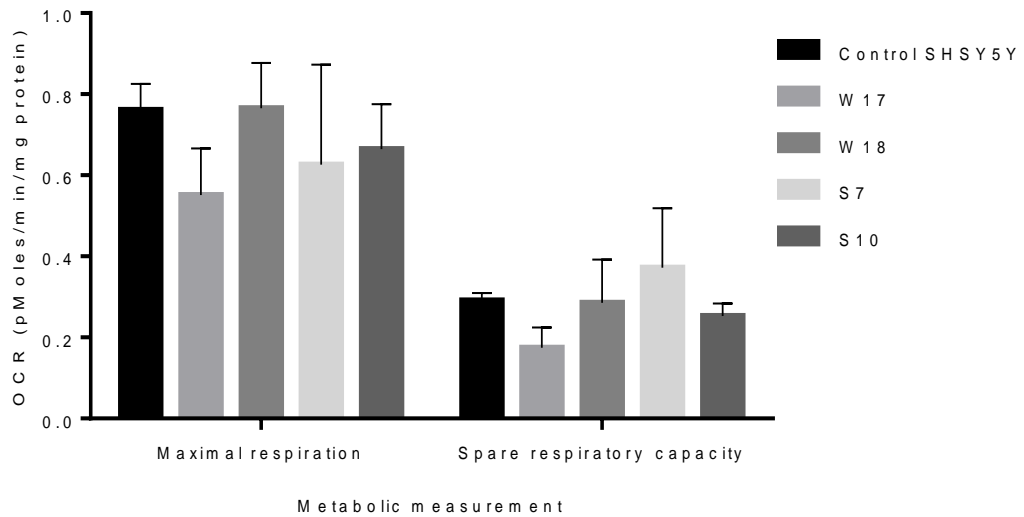


Figure 3.23. Graph of maximal respiration and spare respiratory capacity of proliferating SHSY5Y cell lines. Results are presented as average OCR  $\pm$  SEM, n=3.

There were no differences in non-mitochondrial respiration across any of the proliferating cell lines (Figure 3.24). ATP production did show some differences. There was a difference between the control, which had an average OCR of  $0.221 \pm 0.042$  pMoles/min/mg protein and the proliferating clone S7, which had an average OCR of  $0.096 \pm 0.013$  pMoles/min/mg protein (p value = 0.0377).

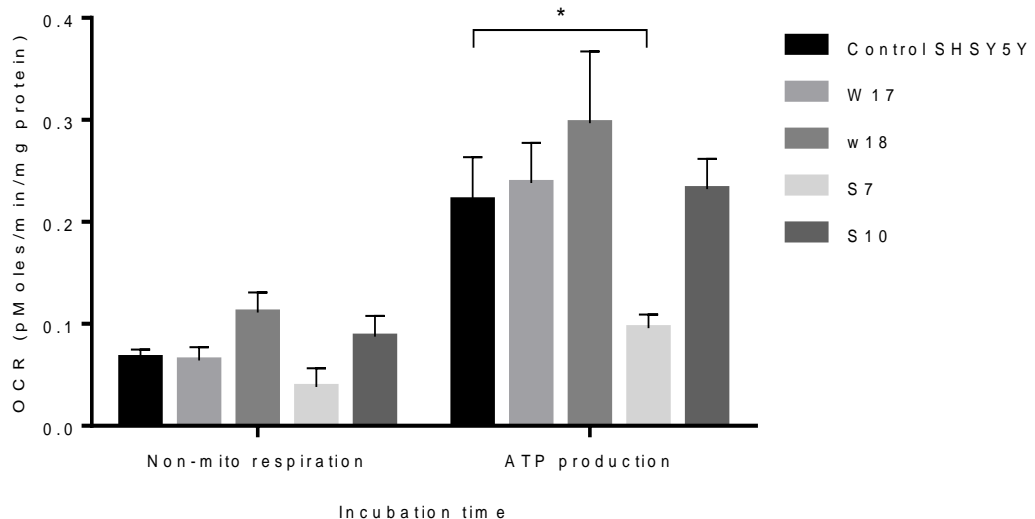


Figure 3.24. Graph showing measurements of non-mitochondrial respiration and ATP production in proliferating SHSY5Y cell lines. Results presented as OCR  $\pm$  SEM, n=3, p < 0.05 (\*).

### 3.3.4.5.2 Mitochondrial function in RA-differentiated cell lines

Mitochondrial function was also assessed for RA-differentiated cell lines. Figure 3.25

shows the OCR data plotted against time for one experiment.

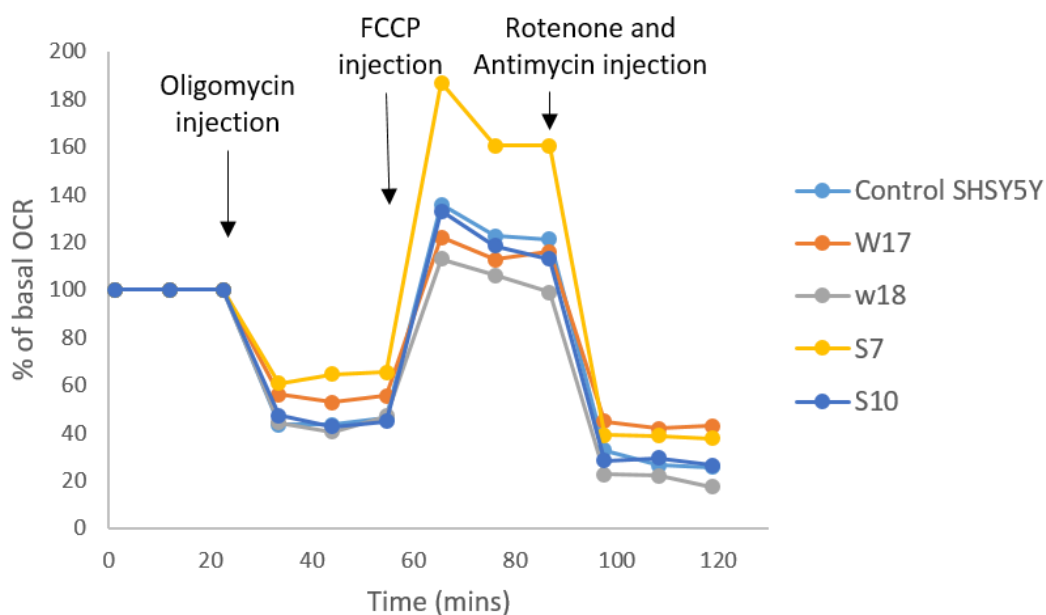


Figure 3.25. Percentage of basal OCR plotted against time for each RA-differentiated cell line. Data shown is representative of one experiment.

RA-differentiated cell lines showed no significant differences between the wtAPP695-expressing cell lines in terms of the resting (basal) OCR (Figure 3.26). However, there was a difference between the control, which had an average OCR of  $0.445 \pm 0.030$  pMoles/min/mg protein, and the S7 clone, which had an average OCR of  $0.254 \pm 0.102$  pMoles/min/mg protein ( $p=0.0337$ ). No differences in proton leak between the cell lines were observed.

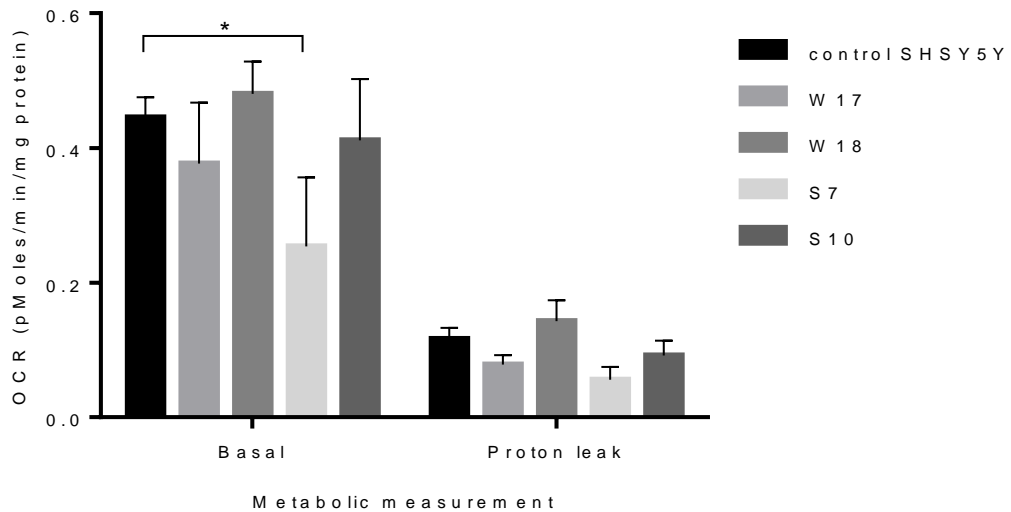


Figure 3.26. OCR measurements of basal respiration and proton leak of RA-differentiated cell lines, presented as average OCR  $\pm$  SEM, n=3.  $p < 0.05$  (\*).

Maximal respiration was measured in these cell lines (Figure 3.27) but no significant differences were found between the control cell line and the APP-expressing cell lines.

No differences in spare respiratory capacity were found between cell lines.

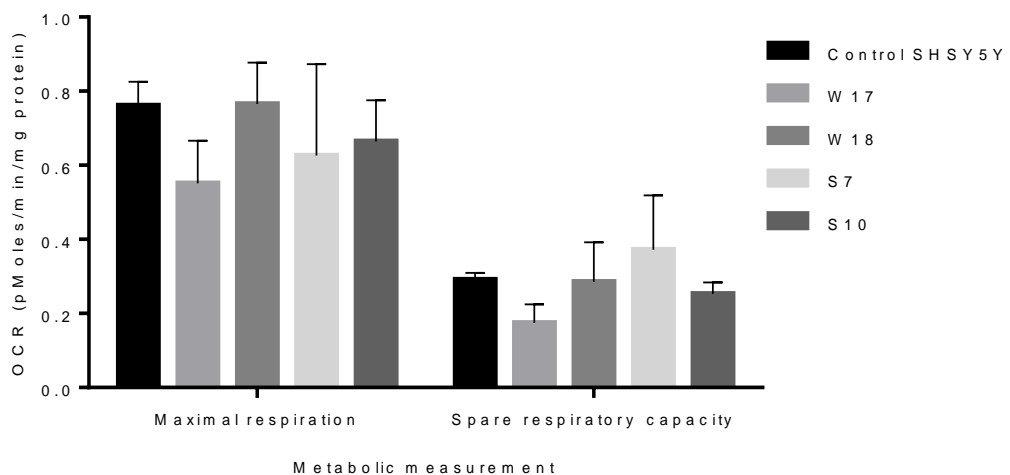


Figure 3.27. Graph of maximal respiration and spare respiratory capacity of RA-differentiated control, wtAPP695 and SweAPP695 expressing cell lines, presented as averaged OCR  $\pm$  SEM, n=3.

Non-mitochondrial respiration and ATP production was also studied in the differentiated cell lines (Figure 3.28). There were not differences between any of the cell lines. ATP production was found to vary in the S7 clone, which produced less ATP but there were no significant differences between this clone and the control cell line.

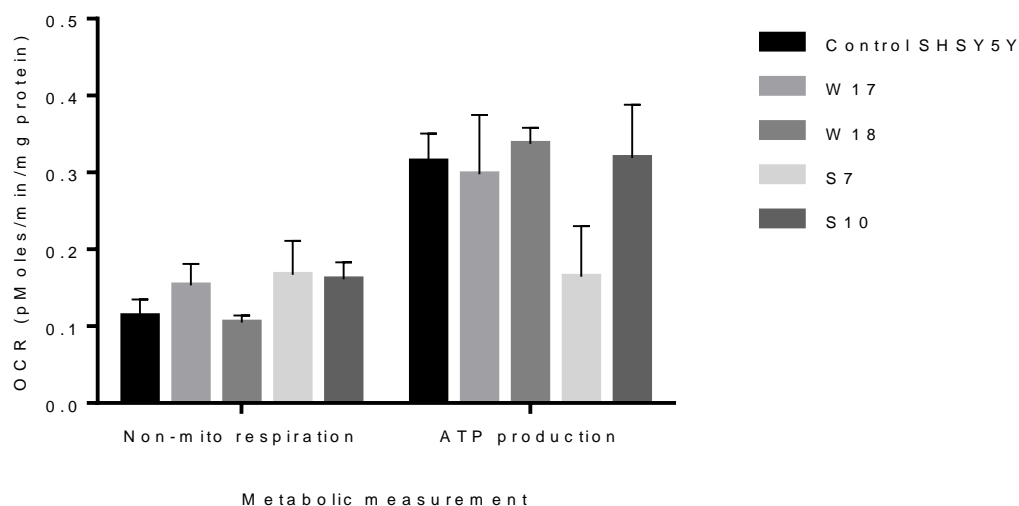


Figure 3.28. OCR readings for 7 day RA differentiated cell lines, showing non-mitochondrial respiration and ATP production, presented as averaged OCR  $\pm$  SEM, n=3.

### 3.3.4.6 Oxidative stress studies

As oxidative stress is strongly associated with AD, APP-expressing cell lines treated with hydrogen peroxide to determine their ability to withstand stress.

#### 3.3.4.6.1 Optimization of seeding density and hydrogen peroxide concentration

The optimal seeding density of proliferating SHSY5Y cells was found to be 15000 per well. The maximum concentration of hydrogen peroxide that killed 100% of cells was 3200 $\mu$ M whilst concentration of 25 $\mu$ M did not cause significant cell death. Therefore cells were treated with a range of concentrations from 3200 $\mu$ M to 25 $\mu$ M.

#### 3.3.4.6.2 Hydrogen peroxide treatment

Undifferentiated APP-expressing cell lines were seeded and treated with decreasing concentrations of hydrogen peroxide. Cell viability was assessed on the following day using the MTT assay. Results shows that all cell lines demonstrate susceptibility to hydrogen peroxide. A non-linear regression curve fit was plotted to produce a dose response curve for each cell line plotted against the control cell line (Figure 3.29 and

3.30) and  $IC_{50}$  values were calculated using Graph Pad prism. An unpaired Student's test was performed to determine significant differences between  $IC_{50}$  values for each cell line (Table 3.4 and 3.5). Results demonstrate that there were no significant differences between any of the SweAPP-expressing cell lines tested.

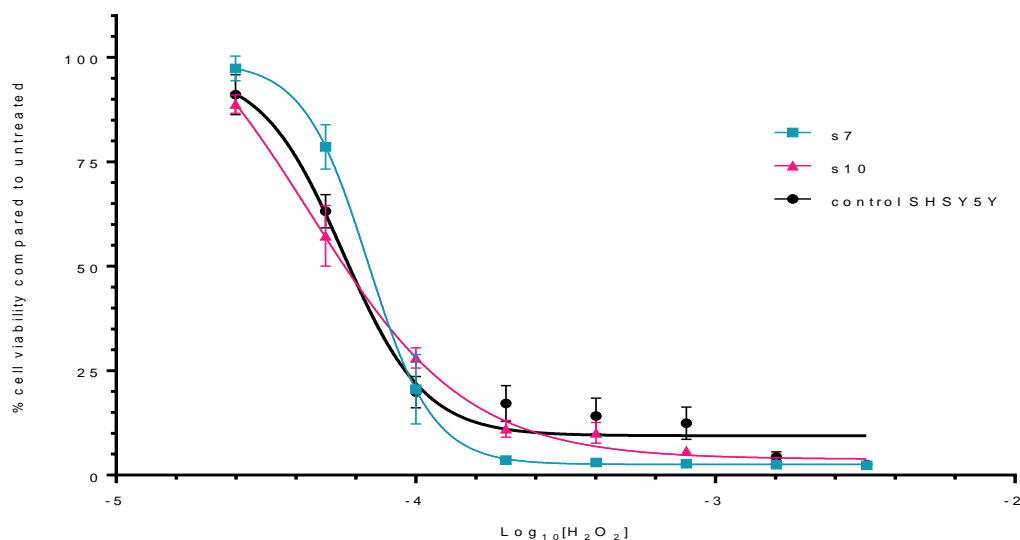


Figure 3.29. Dose response curve of SweAPP695-expressing cells to hydrogen peroxide using the MTT assay. Results expressed as a percentage of untreated  $\pm$  SEM,  $n=3$ .

Cell type	Average $IC_{50}$ (M)	T test analysis compared against control SHSY5Y	P value
Control SHSY5Y	$55.3 \pm 2.977$	-	-
S7	$70.2 \pm 5.22$	NS	0.0847
S10	$40 \pm 5.76$	NS	0.1031

Table 3.4. Table of the calculated  $IC_{50}$  calculated for each cell line. An unpaired Student's test (with Welch's correction) was performed between the  $IC_{50}$ 's of the control SHSY5Y versus each of the SweAPP695-expressing cell lines.

When comparing the dose response curves of the wtAPP695-expressing cell lines (Figure 3.30), Student's T test revealed that there no significant differences between the lines and the control cell line in the  $IC_{50}$  values (Table 3.5).

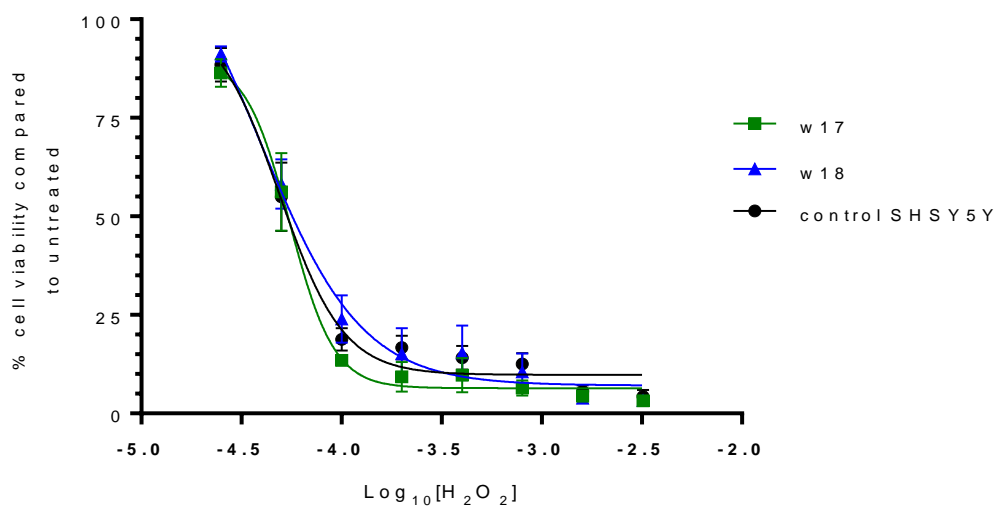


Figure 3.30. Dose response curve of wtAPP695-expressing cell lines using the MTT assay. Results are presented as a percentage of cell viability compared to untreated cell line  $\pm$  SEM, n=3.

Cell type	Average IC <sub>50</sub> (M)	Student T test analysis compared against Control SHSY5Y	P value
Control SHSY5Y	55.3 $\pm$ 2.977	-	-
W17	51.3 $\pm$ 2.98	NS	0.6209
W18	59.8 $\pm$ 2.56	NS	0.6224

Table 3.5. Students T test analysis (unpaired, two tailed with Welch's correction) of IC<sub>50</sub> for each cell line compared to control cell line. Results are expressed as molar concentration  $\pm$  SEM.

### 3.4 Discussion

#### 3.4.1 Lentiviral infection of SHSY5Y cells

Viral transduction of the SHSY5Y cells with CMV GFP demonstrated they could be readily transduced with lentivirus and maintain stable integration and expression of GFP over 10 days post-infection without the need for cationic polymers such as Polybrene to enhance lentiviral efficiency. High MOIs and the use of Polybrene elicited potential toxicity informing future transduction approaches using the SHSY5Y line. Using the lentiviral system to generate stable cells has many advantages, as the transgene is readily inserted into the host cell genome by viral integrases. In addition unlike plasmid transfection where integration is random, lentivirus tends to integrate in areas of active chromatin (Gierman *et al* 2007) which provides more comparable expression in clones formed from different insertions, than when using plasmid mediated techniques. The use of a lentiviral system also provides the opportunity to infect post-mitotic, non-dividing cells such as neurons which expands the potential future uses of these constructs.

The Swedish/wtAPP695 lentiviruses were tested in the SHSY5Y cell line at relatively high MOI's to ensure that expression of excess APP protein would not be toxic. The cells were initially differentiated for five days in RA to increase expression from the Synapsin I promoter that should drive APP expression within transduced cells. Whilst small amounts of toxicity were observed at MOI's of 10, most cells survived. Western blotting for APP protein expression however showed that increasing the MOI from 5 to 10 did not appear to lead to an observable increase in APP expression suggesting that the amount of expression was limited by the availability of the transcriptional machinery of the cells capable of interacting with the SYN1 promoter and not the copy number of the inserted transgene.

Many cellular models of AD have utilised a lentiviral mediated approach to generate cell lines. For example, expression of the amyloid precursor protein has been a

common avenue for studying the effects of APP expression on cellular activity. Indeed, an extra copy of the APP gene is sufficient to cause FAD in DS patients, therefore there is premise to overexpress the APP gene to study cellular effects. Furthermore the discovery of familial mutations such as the Swedish mutation of APP695 has allowed the effect of altered amyloid processing on cellular metabolism to be studied *in vitro* in terms of a human relevant model.

In this study, the effects of overexpression of both wildtype and APP695 containing the Swedish mutation were studied after stable transduction of the SHSY5Y cell line. Both APP genes are of great importance in relation to AD, as both have been demonstrated to cause AD pathology in human and AD models. The results of some of these studies should be taken with caution due to the use of viral promoters to drive APP expression. The CMV promoter has been used to drive high level expression of APP in many studies. However the level of APP driven by this promoter is not reflective of levels expected in the human brain. With relevance to AD, the purpose of this study was to determine the utility of using a neuronal-based promoter to drive APP expression within neuronal cells. Use of the Synapsin I promoter to simulate “physiological” levels of APP might lead to more physiologically relevant downstream effects similar to those observed in the human AD brain. Increases in APP695 expression were also achieved by differentiating the SHSY5Y cell line to become more neuronal in phenotype. As SHSY5Y cells possess a functional wtAPP695 gene, the inclusion of APP695 under the Syn1 promoter was expected to lead to overexpression of wtAPP695 which could be compared to cells expressing the Swedish APP695. wtAPP695 expression was expected to increase APP protein expression while, SweAPP695 expression was expected to increase APP cleavage via the amyloidogenic pathway, produce more amyloid 1-42.

### 3.4.2 Characterisation of APP-expressing cell lines

The clones were characterised by their ability to differentiate into a more neuronal cell type with RA and BDNF treatment. The clones tested produced extensive neurite networks at the end of BDNF treatment, with cultures staining positively for  $\beta$ -tubulin (a marker of neuronal differentiation). When differentiating cells with BDNF in the absence of serum, cell death often occurred, leading to differing densities of neuronal networks in these cultures. To overcome this problem further studies of these cell lines were carried out in RA differentiated cells to ensure similar cell numbers at the time of testing, which was especially important for the Seahorse studies.

APP protein expression was assessed before and after seven days of RA treatment. It was expected that RA treatment would increase APP expression by increasing expression from the Synapsin I promoter. Interestingly, Western blot analysis showed a trend toward larger amounts of APP in the proliferating wtAPP695-expressing SHY5Y cells compared to that of RA treated cells. All cells showed greater levels of APP than control. By contrast, after RA differentiation, SweAPP695-expressing cells contained more APP within differentiated cell than in proliferative cells, with a general trend toward these cells containing similar or lower levels of APP than the control cell line. This may have been due to increased cleavage of APP to the A $\beta$  peptide, which could be secreted out of the cell and into the media.

The conditioned media was assessed for A $\beta$ 1-42. ELISA results showed varying amounts of amyloid secreted from cell lines. The significant result was from clone S10 which showed less APP protein expression within the cell but the most amyloid secreted into the media. The variations in APP695 protein expression and A $\beta$  secretion may have been due to several reasons. Firstly, the manner in which the stable cell lines were made using lentiviral transduction. Lentivirus stably integrate the transgene of interest into the host genome in "hotspot" regions, however the number of insertions cannot be predicted, therefore multiple copies of the wtAPP695/

SweAPP695 gene may have integrated into the SHSY5Y cell line. Furthermore, the location in the genome where the transgene is integrated into the host genome may affect gene expression of native genes adjacent to the integration site. This could be addressed in future studies by determining how many copies of the APP gene may have integrated by Southern blotting, and characterising the integration sites by sequencing.

The production of cells that overexpress APP is an important step in the determination of this protein's function within cells. The results obtained in this chapter demonstrate that lentiviral transduction can be used to generate stable cell lines that overexpress both wild-type and APP carrying the Swedish mutation under the control of a neuronal promoter. Interestingly, overexpression of wtAPP695 increases the level of APP in proliferative cells whereas the overexpression of SweAPP695 results in lower levels of APP present in cell lysates. This could be a result of an increase in APP processing leading to the release of APP fragments including A $\beta$  in cells carrying the Swedish APP mutation, which influence BACE cleavage of APP to produce amyloid, leading to decreased amounts of APP detectable by Western blotting. Furthermore, production of sAPP $\alpha$  or sAPP $\beta$  into media cannot be ruled out. Results of the A $\beta$  ELISA agree with this interpretation with clones demonstrating a general increase in the secretion of A $\beta$  1-42. Results between clones were variable which may reflect differences in APP expression or APP processing. A more detailed analysis should be performed in order to determine the levels of multiple APP fragments including soluble APP (sAPP $\alpha$ ), as well as the ratio of A $\beta$ 1-42/40.

### **3.4.3 Changes in metabolism between cell lines**

*In vivo* studies of AD patient brains show consistent reductions in glucose utilisation in areas of the brain known to be affected by amyloid (Chen and Zhong, 2013, Mosconi, 2005). Further analysis of the glucose utilisation of proliferating clones in this study suggested a general trend for increased glucose levels in the media suggesting a

reduction in glucose uptake. However, only 1 clone expressing Swedish APP demonstrated any significance. Interestingly this clone (S10) was also the only clone to demonstrate a significant increase in A $\beta$ 1-42 production. Analysis of differentiated clones revealed a significant reduction in glucose uptake in all of wild type clones, with a similar but insignificant profile in SweAPP expressing clones. These results could suggest a difference in the metabolism of differentiated cells, which potentially renders them more sensitive to increased APP or A $\beta$  production. Production of sAPP $\alpha$  in these cells is important to consider as it is known to have potent neuroprotective effects against amyloid-induced oxidative injury (Goodman and Mattson, 1994) and glucose deprivation (Mattson et al., 1999, Barger and Mattson, 1995), the latter of which showed the ability of sAPP $\alpha$  to increase glucose transport through activation of guanylate cyclase.

Previous studies have demonstrated a difference in the metabolism of proliferating and differentiated SHSY5Y cells (Swerdlow et al 2013, (Schneider et al., 2011 ). Specifically, glucose uptake studies show a general trend that the APP-expressing cell lines utilise less glucose than the control cell line once differentiated. The differences in glucose uptake between proliferative and RA-differentiated SHSY5Y cells may also reflect the change in metabolism from glycolysis to oxidative phosphorylation. Cancerous cell lines such as SHSY5Y cell lines typically utilise glycolysis to sustain their energy needs (Swerdlow et al 2013), whereas RA-differentiated SHSY5Y cells predominantly rely on oxidative phosphorylation (Schneider et al., 2011b).

Schneider *et al.* (2011) demonstrated that SHSY5Y cells differentiated with RA exhibit increased mitochondrial membrane potential compared to proliferating cells. They also noted greater stimulation of mitochondrial respiration and increased bioenergetic energetic capacity. This trend was reflected in the RA-differentiated cell lines tested in this chapter. Comparison of the responses between the wtAPP695 and the SweAPP695 lines demonstrated a significant increase in basal oxygen consumption

compared to the control, yet only clone S10 showed significantly higher amount of A $\beta$ 1-42 secreted into the media. Interestingly, wtAPP695 expressing cells exhibited increased maximal respiration, which could be explained by increased number of mitochondria or an altered substrate supply.

There were no other correlations between SweAPP695, wtAPP695 and controls for any of the other Seahorse analyses carried out. There was no clear changes in ATP turnover or maximal respiration/ spare respiratory as either proliferative or RA-differentiated cell lines which suggests that the electron transport chain may be unaffected. This may reflect effects of differential APP processing between the cell lines leading to different responses in the MitoStress test.

Interestingly, previous studies have shown that wtAPP695 and SweAPP695 expressing cells were able to utilise both oxidative phosphorylation and glycolysis equally, and that these cells were healthy (Yang et al., 2009). In other studies stable transduction of pre-mitotic C17.2 cells with SweAPP695 found that these cells were more vulnerable to secondary insults such as A $\beta$  oligomers. This suggests that whilst the expression of APP/SweAPP695 in the cell lines may have had some effect on metabolism, the cells may have been able to compensate for this. Future work could employ a secondary insult such as the introduction of A $\beta$  oligomers to help identify the metabolic impact on the overexpressing cell lines.

A study performed in embryonic neurons derived from 3-x-Tg-AD mice demonstrated decreased mitochondrial respiration and an increase in glycolysis (Yao et al., 2009b). However in this study, there were no significant changes in maximal respiration which suggest that to observe any changes between the cell lines, further studies using the glycolysis stress test may be appropriate. The glycolysis stress test allows for the measure of basal glycolysis, that being the conversion of glucose to pyruvate, which produces ATP. Pyruvate may either be converted to lactate in the cytoplasm or to

carbon and water in the mitochondria. In the test, glycolysis is measured by the rate of protons released into the media after the addition of glucose. The second compound injection is oligomycin, which acts to inhibit oxidative phosphorylation and thereby forcing cells to rely on glycolysis to maintain ATP production. Elevated rates of glycolysis is known as the glycolytic capacity of the cell. It is also important to note the mutant genes expressed in the triple transgenic mouse model are under the control of the mouse Thy1.2 regulatory element, whereas the cell lines studied in this chapter are under the control of the Synapsin I promoter. Therefore APP/A $\beta$  expression within the SHSY5Y cell lines may be insufficient to observe any change in mitochondrial function.

Results suggest that RA-differentiated cell lines, which increase APP expression due to up-regulation of SYN1 may lead to decreased glucose uptake, with respect to the wtAPP-expressing cell lines. There were generally no significant differences between the proliferative cell lines and the control in terms of glucose uptake, with the exception of the S10 clone which produced the most A $\beta$ . A decrease in glucose uptake could be explained by negative feedback of glucose-6-phosphate accumulation within the cell, which leads decrease in flow of glucose through the hexokinase pathway. However further studies are needed to be able to draw any meaningful conclusions. Such studies will investigate the use of tritiated glucose to determine the efficiency of glucose uptake, as well assessing the effects of glycolysis in these cultures.

Mitochondrial function in AD is clearly perturbed and has been considered as an underlying mechanism in the early stage of AD, as deficits in energy metabolism are a fundamental characteristic of the AD brain. The fact that both full length APP and A $\beta$  are found to accumulate within mitochondria in the brains of AD patients strengthens this hypothesis. Mitochondrial enzyme activity is decreased in AD brains and animals, in particular PDH and  $\alpha$ -ketoglutarate activity. Decreased activity of these enzymes was found to correlate with the cholinergic deficits associated with AD.

These observations are also reflected in animal models, where mitochondria of presymptomatic Tg2576 mice were shown to be defective, particularly in mitochondria taken from areas of the brain important in cognition (Varghese et al., 2011). However, the authors could not fully ascertain whether the increased production of A $\beta$ 1-42 and not other fragments was responsible for these abnormalities. In another study, mitochondria taken from platelets of MCI and sporadic AD patients were transferred into mitochondria-depleted SHSY5Y cells (Silva et al., 2013). Analysis of mitochondrial function and glucose utilisation of these cells revealed changes in OCR, respiratory capacity and glucose utilisation. In particular, less ATP and increased NADH levels were observed in the diseased cybrids compared to controls. However, the patients from which the platelets were taken from were assessed by cognitive testing with no measurements in A $\beta$  levels in platelets made. Therefore whilst mitochondrial deficits did occur, it could not be conclusively attributed to amyloid, as other APP cleavage products are present in AD derived platelets (see Chapter 4).

Past studies have investigated the therapeutic of compounds including lipoic acid, nicotinamide mononucleotide (NMN) and hydroxybutyrate, which may help to improve mitochondrial function and could be tested in cell lines developed in this project in the future. Lipoic acid supplemented to AD mice increased brain glucose uptake and reversed impairments in synaptic function (Sancheti et al., 2013). Furthermore, lipoic acid improved memory and cognition in SAMP8 mice, Tg2576 transgenic mice and aged NMRI mice (Quinn et al., 2007, Farr et al., 2003, Stoll et al., 1993). Lipoic acid is a cofactor for acyltransferase activity PDH and  $\alpha$ -ketoglutarate dehydrogenase, acting to boost enzyme activity for both (Walgren et al., 2004, Tretter and Adam-Vizi, 2005). This leads to increased substrate delivery to the electron transport chain, ultimately driving glucose uptake. NMN is a NAD precursor which is shown to ameliorate mitochondrial dysfunction in mice (Long et al., 2015). Repletion of NAD is essential as it is a cofactor in metabolic reactions such as the conversion of pyruvate to acetyl CoA, which forms the first substrate in the Krebs's cycle, as well as being involved in other

steps of the Krebs cycle. Hydroxybutyrate is a ketone body, which provides an alternative energy source for the brain, by being converted to acetyl CoA, effectively bypassing the requirement of glucose. Increased levels of ketones were demonstrated to rescue mitochondrial enzyme activity, the mitochondrial membrane potential and improved memory in mice (Zhang et al., 2013).

Oxidative stress plays an important role in AD and other diseases. Previous models of AD show signs of oxidative stress (Morley et al., 2012, Butterfield et al., 1999, Oikawa et al., 2012), which provides an intriguing premise to study oxidative stress responses in these manipulated cell lines. All proliferating cell lines tested were susceptible to hydrogen peroxide, but there were no significant differences between wtAPP or SweAPP-expressing cell lines and the control SHSY5Y cell line. This may be due to the fact that as proliferative cells, APP expression was not upregulated (as it is driven by a neuronal promoter, whose expression is low in proliferative SHSY5Y cell lines). Further work should assess the stress responses of these cell lines in a differentiated state, where they are more neuronal in nature and may be more susceptible to hydrogen peroxide with increased APP expression/ A $\beta$  production.

There are potential issues with the methodology employed in this project, which may have resulted in inconsistent or insignificant results. The lack of control over levels of expression between clones is a potential issue. The mitochondrial deficits and glucose changes observed in other models may be due to the use of stronger promoters than the Synapsin I promoter utilised in this project. Therefore the level of expression of APP695 may be insufficient to observe any short term negative effects on cell metabolism. More importantly, the lack of significance in many of the studies conducted could be attributed to the use of RA to differentiate the SHSY5Y cell lines. Retinoic acid was found to down-regulate BACE1 expression in the brains of Tg2576 mice (Wang et al., 2015b), via NF $\kappa$ B, thereby providing an anti-inflammatory effect (Koryakina et al., 2009). Down-regulation of BACE1 would prevent the production of

A $\beta$ 1-42. Further work should assess for the levels of BACE1 protein expression before and after RA-induced differentiation of SHSY5Y cell lines to address this issue.

An alternative method of expressing APP at controllable levels would be to use a TET-based system (as described in Long et al., 2015). In this system, cells grown in the presence of different concentrations of Doxycycline would produce varying amounts of APP and therefore A $\beta$ . It should also be noted that many *in vivo* studies use powerful promoters to drive expression of APP/ PSEN1 protein expression. Animal models such as the TG2576 mice (which express the SweAPP595 mutation) express 8 times the normal level of amyloid (compared to the brain) and do not experience all of the symptoms of AD such as cell death. As such the results from these systems should be considered carefully, if they are overexpressing these proteins at abnormally high levels to observe cellular deficits.

The use of the Glucose HK assay to study glucose uptake has a drawback that it will also incorporate glucose oxidation/ usage in addition to glucose uptake, therefore may not be the ideal method to analyse glucose uptake. Alternative methods could be to utilise <sup>3</sup>H 2deoxyglucose or 2-NBDG (2-(*N*-(7-Nitrobenz-2-oxa-1,3-diazol-4-yl)Amino)-2-Deoxyglucose). Both forms of glucose are readily taken up by cells but cannot be metabolised and therefore accumulate within the cell. In terms of the Seahorse studies, cells are supplemented with 10mM D-glucose, which is relatively high compared with physiological concentrations of 2.5mM in the human brain. Supplementation of high levels of glucose may hamper the ability to observe any small differences in mitochondrial function due to the different clones.

The benefits of using SHSY5Y are that they are cheap and provide a high throughput model. However, as they are derived from cancer cells they have an abnormal karyotype and their metabolism does not model that of neuronal cells unless they are differentiated. Once differentiated cells demonstrate an enhanced sensitivity to APP

therefore highlighting the need to carefully consider the metabolic state of the cell used. However, differentiated cultures of SHSY5Y have a limited lifespan which precludes their use for long term studies.

In conclusion, issues with the phenotype of this cell line and the difficulties associated with overexpressing exogenous proteins complicate the analysis of the metabolic pathways perturbed in AD. Ideally, large subsets of clones should be analysed individually and then grouped according to levels of either APP or A $\beta$  expression in order to determine any significant differences. Additionally, each clone should be characterised to determine how APP is processed, as the variation in the OCR readings from the Seahorse experiments may reflect differential APP processing into other APP fragments, some of which are known to be neuroprotective (sAPP $\alpha$ ). Expression of these soluble APP fragments could help to explain the lack of metabolic dysfunction in some of the cell lines as APP processing can still occur via the non-amyloidogenic pathway in these cells. It would also help to address any potential changes in cell proliferation between the different clones.

A better model of AD would naturally develop AD in culture and produce natural levels of APP/amyloid and therefore avoid insertion related effects on other genes. Also, such models would not overstress cellular systems produced abnormal levels of protein or sequester cellular factors due to the use of viral promoters. The results presented here do not provide a conclusive argument as to the effects of APP overexpression on cellular metabolism that have been reported elsewhere. Perhaps a viral promoter would have produced much larger amount of APP and therefore more A $\beta$ 1-42 and provide more significant results. As models that produce natural levels of APP may provide much clearer results, AD patient derived fibroblasts were used in order to determine the effects of APP misprocessing in an unmodified cellular system. The results will be discussed in Chapter 4.

## **Chapter 4: Characterization of FAD patient–derived fibroblasts**

Alzheimer's disease has long been considered a disease that is limited to the brain. However, a number of studies have described differences in the phenotypes of numerous cell types around the body in FAD patients. These differences may be due to the genetic mutations that are associated with AD (especially in FAD cases) and therefore suggest that AD pathology is not merely limited to the human brain, and that pathways perturbed in the brain may also be disrupted in peripheral tissues. As such, studies into the pathways perturbed in these cells that may provide an insight into the earliest stages of AD. In this chapter FAD patient fibroblasts were studied. The metabolic profile of these cells was measured using the Seahorse analyser. In addition, glucose uptake and responses to oxidative stress were studied in these lines along with the effect of the addition of the AD associated peptide A $\beta$  1-42 to fibroblasts.

### **4.1 Introduction to familial mutations**

Whilst familial forms of AD constitute a small fraction of AD cases, cells taken from these patients provide a useful model of AD. As discussed in Chapter 3, duplications of the APP gene (Rovelet-Lecrux et al., 2006), mutations in the APP coding sequence and presenilin genes are the major genetic mutations associated with FAD, with the latter being more predominant. At least 10 pathogenic APP mutations have been discovered, all of which cluster near the proteolytic cleavage sites of APP (Figure 1.3 in Chapter 1) (De Jonghe et al., 2001), leading to increased A $\beta$  production (Feng et al., 2006). In this study, patient derived fibroblasts carrying the London V717I mutation in APP as well as the presenilin mutations M146I and Intron 4 were studied.

The London mutation was the first FAD mutation to be recognised (Goate et al., 1991) and is the most frequent APP mutation observed (Cruts et al., 2012). This mutation has been reported in several families suffering from FAD and causes a missense mutation at position 717, resulting in the transition from a Valine to Isoleucine base

substitution. This region of the APP gene appears to be a hotspot for mutation with several allelic variants identified to be pathogenic (Chartier-Harlin et al., 1991). Approximately 30 families identified from different countries were found to carry this mutation, affecting both Caucasian and Asian populations.

Variations of sequence at this position may increase amyloid deposition due to changes in APP processing, or that there may be increased APP mRNA translation (Tanzi and Hyman, 1991). Mouse models carrying this mutation display increases in A $\beta$ 42/ A $\beta$ 40 ratio, due to increased levels of A $\beta$ 42 production (Herl et al., 2009, Theuns et al., 2006, Moechars et al., 1999). More recently, studies using iPSC-derived neurons carrying the APPV717I mutation demonstrated increased BACE1 cleavage of APP, altered the initial cleavage site of  $\gamma$ -secretase, leading to increased amyloid peptide 1-42 and 1-38 production. Increased levels of total tau and phosphorylated tau were also observed (Muratore et al., 2014).

PS1 and PS2 proteins are encoded by the PSEN1 and PSEN2 genes, which are localized to chromosome 14q24.3 (Sherrington et al., 1995) and 1q42.1 (Rogaev et al., 1995, Takano et al., 1997) respectively. Both genes are similar in structure and consist of 13 exons, where 10 exons make up the coding sequences (Hutton and Hardy, 1997). The PS1 gene consists of 13 exons, of which exons 3-12 code for a protein, 467 amino acids in length (Prihar et al., 1996, Clark et al., 1995). Alternative splicing of a 12bp sequence in exon 3 and exon 8 (Sherrington et al., 1995) has been reported to give rise to different transcripts (Rogaev et al., 1997, Clark et al., 1995), with these transcripts leading to mutations associated with FAD. There are at least 180 mutations in the PS1 gene, which may account for up to 25-30% of early-onset AD, making this the most common genetic aberration to cause FAD. Interestingly de novo PS1 mutations have been reported in clinically sporadic, EOAD cases (Dumanchin et al., 1998, Levy-Lahad et al., 1995). Many of these mutations lie with the transmembrane

domains or adjacent to predicted loop domains, with most PS mutations reported to be missense mutations (Singleton et al., 2000).

#### **4.1.1 Presenilins structure**

PS1 and PS2 are homologous intracellular aspartyl proteases (Li et al., 2013). They are a transmembrane spanning protein (see Figure 4.1), having six to eight transmembrane domains with the N terminus, the large sixth hydrophilic loop (HL-VI) and the C-terminal hydrophobic regions associated with the cytosolic face (Price and Sisodia, 1998). Two putative catalytic residues, Asp162 and Asp220 are found on loops six and seven. During protein maturation, they are endoproteolytically processed within the HL-VI region, producing a 30kDa N-terminal fragment and a 20kDa C-terminal fragment (Thinakaran et al., 1996). The production of both products is tightly regulated ensuring equal amounts of both fragments are produced.

The function of PS1/PS2 was discovered through studies of the *C.elegans* homologue Sel-12, that functions to mediate LIN-12/ Notch signalling during cellular development (Wong et al., 1997). Wildtype PS1 can rescue mutant SEL-12 induced phenotypes in *C.elegans* but PS1 containing FAD-associated mutations only led to partial recovery (Qian et al., 1998). Both presenilins have some sequence similarity to SPE-4, found within *C.elegans* spermatocytes (L'Hernault and Arduengo, 1992). It is now understood that PS1 is involved in APP processing, as demonstrated by gain-of-function phenotype in PSEN1 mutations. PSEN1 mutations result in an increase in the production of A $\beta$ 42 in plasma and fibroblasts of mutation carriers (Scheuner et al., 1996b), in media of transfected cells (Citron et al., 1997) and in the brains of transgenic mice (Duff et al., 1996). PSEN1 knockout mice are embryonic lethal, exhibiting axial skeleton malformation and CNS defects.(Qian et al., 1998, Shen et al., 1997). However, PSEN2 null mice do not show these defects (Parent and Thinakaran, 2010).

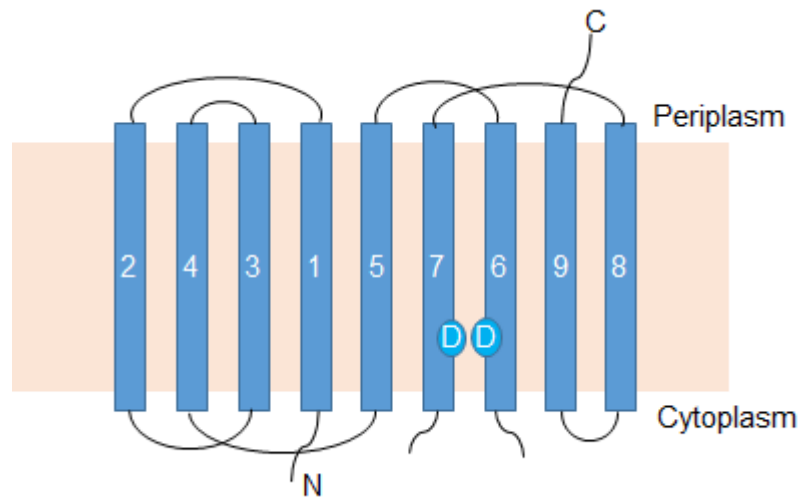


Figure 4.1. Diagram showing the structure of presenilins embed within the cell membrane.

PS1 and PS2 exhibit significant structural differences in their cytosolic domains, sharing less than 10% homology in the N-terminal 70 residues and between amino acids 305-375 in the loop. These regions are suggested to mediate cell- or PS-specific functions by interacting differently with cytosolic proteins. Biochemical studies suggest that presenilins are not subject to sulfation, glycosylation or acylation. However, serine residues in the cytosolic domain of PS1 and in the N terminal region of PS2 are sites for phosphorylation. PS1 phosphorylation is mediated by protein kinase C and cMAP-dependent protein kinase or inhibition of protein phosphatase 1 or 2A (De Strooper et al., 1997).

#### 4.1.2 Localization of Presenilins

Presenilins are expressed in many tissues and detectable at low levels in the brain. Full length PS1 and PS2 is localized to membranous compartments such as the ER and Golgi network, where they undergo endoproteolysis to yield stable N- and C-terminal fragments (Selkoe, 1998). The fragments appear to be highly regulated as mice overexpressing PS1 fail to increase fragment production, suggesting degradation of the presenilins via a nonspecific proteolytic pathway (Thinakaran et al., 1996). The PS1 fragments are transported to Golgi vesicles where they assemble together to form

heterodimers, which are considered to be their primary form (Steiner et al., 1998, Farquhar et al., 2003).

#### **4.1.3 Presenilin 1 function**

PS1 plays a role in a number of processes such as protein processing and cell signalling. Most notably, it is known to form part of the enzyme complex,  $\gamma$ -secretase which cleaves APP to yield the A $\beta$  peptide. Indeed, mice lacking PS1 demonstrated 70-80% decrease in A $\beta$ 40 and A $\beta$ 42 levels and a corresponding increase in their precursors, C99 and C-terminal fragment. Two hypotheses may explain how presenilins regulate APP proteolysis at the  $\gamma$ -secretase cleavage site. Presenilins may complex with C99 and C83 and modulate protease access to the peptide bond at A $\beta$ 40 and A $\beta$ 42. PS1 and PS2 have in fact been found to co-precipitate with the N-glycosylated form of APP. When the cytoplasmic domain of APP was deleted, this did not prevent co-precipitation with presenilins which suggests that its interaction could involve the transmembrane domains of the proteins, regions which may enable APP proteolysis.

#### **4.1.4 Presenilin mutations**

Mutations in PSEN1 are the most common cause of FAD (Sherrington et al., 1995) many of which occur in single-kindred families. The majority of these missense mutations are located within transmembrane II or immediately adjacent to the predicted loop domain, accounting for at least 50% of the known PS1 mutations. These mutations cause an early AD phenotype where the average age of onset is about 40 years, with one of the youngest ages of onset being 28 years. The location of the point mutations appears to influence age of onset, for instance, individuals with mutations in exon 8, have an average of onset of 43 years whilst other mutations outside this region lead to an average of onset of 48 years. Exon 8 encodes for a region of a predicted TM domain 6 (TM-6) and the largest cytoplasmic loop of PS1. Other mutations have also been localised to exon 5 which encodes the second predicted TM domain (TM-2) and the largest luminal loops of PS1. In addition, exon 9 is another location of interest,

which encodes for a region of HL-6. These so-called "hotspots" are found in critical functional or conformational domains in PS1, which may affect interactions with other proteins. Interestingly fewer PS2 mutations have been discovered, (Rogaev et al., 1995, Levy-Lahad et al., 1995).

One particular presenilin 1 mutation that occurs in intron 4, leads to the production of truncated deletion transcripts, and an in-frame insertion transcript due to alternative splicing using a cryptic splice site in intron 4 (De Jonghe et al., 1999). This mutation is common in the British population, who were found to develop AD in their mid-thirties and died in their mid-forties. A genotype analysis of polymorphic dinucleotide repeat markers found that many of the patients carrying this mutations share one common allele at one of these markers.

Individuals presenting with the PSEN1 point mutation at position 278 suffer from spastic paraparesis (Assini et al., 2003), speech production deficits and frontal behavioural disturbances (Kennedy et al., 1995), without the cognitive dysfunction usually associated with AD (Kwok et al., 1997). Indeed, a study of 2 AD cases with the R278I mutation, under the age of 55 years experienced no significant loss of episodic memory but exhibited symptoms of early language impairment (Godbolt et al., 2004), while individuals with R278K mutations showed increased A $\beta$ 40/A $\beta$ 42 ratio in cultured fibroblasts, implying that mutations at position 278 encourages amyloidogenesis (Assini et al., 2003).

Another hotspot for mutation is found in PS1 where Methionine 146 is commonly substituted with another hydrophobic residue, such as Valine, Leucine and Isoleucine, which corresponds to any nucleotide change at the first or third position of the codon (Jorgensen et al., 1996).

Much if not all the research of AD involving these familial mutations has been carried out in the brain, as traditionally, AD is considered a brain-related disorder because the production of amyloid is considered to be a neuronal phenomenon. In AD, the brain appears to be most vulnerable to the effects of these mutations which leads to adverse effects on mental functions. However several studies have since detected amyloid deposition or APP695 expression outside of the CNS. These studies and their relevance will be outlined in the following sections.

#### **4.1.5 APP expression outside the CNS**

Expression of the APP695 isoform is not restricted to the brain but is also widely expressed in other tissues, such as thymus, heart, muscle, kidney, adipose tissue, skin and intestine. This widespread expression suggests that APP may not only effect neurons but also other somatic cell types, expanding its potential physiological functions beyond that of neuronal networks (Puig and Combs, 2013). Aberrant deposition of amyloid is not only associated with dementia but also a series of diseases termed amyloidosis, in which amyloid-like peptides can be abnormally deposited in organs or tissue as fine fibrils (Kazmi, 2013). At least twenty-eight different kinds of human proteins in addition to APP, are found to be amyloidogenic *in vivo* and are associated with pathological disorders such as prion diseases, type II diabetes and familial, systemic and sporadic amyloidosis (Westermarck et al., 2007).

##### **4.1.5.1 APP function in adipose and intestine**

APP and its cleavage products are detectable in human adipocytes and macrophages (Lee et al., 2008b, Puig et al., 2012a). Obesity has been shown to influence APP levels *in vivo* in human adipose tissue, in correlation with hyperinsulinemia, insulin resistance and increase expression of pro-inflammatory genes, such as macrophage inflammatory protein-1 $\alpha$  and IL-6 (Lee et al., 2008b, Puig et al., 2012a). Inflammatory TNF $\alpha$  increases APP levels in 3T3 adipocytes corroborating *in vivo* studies carried out in a rodent model of diet-induced obesity (Sommer et al., 2009, Puig et al., 2012a).

#### **4.1.5.2 APP function in muscle**

APP has also been shown to localise to the synaptic compartments of mouse skeletal muscle and cultured murine myogenic cells (Akaaboune et al., 2000a). APP expression is detectable early in muscle fibre development, accumulating at neuromuscular junctions (NMJs). NMJs which lack APP exhibit abnormal localization of pre- and postsynaptic proteins with few synaptic vesicles at presynaptic junctions, resulting in increased synaptic dysfunction (Wang et al., 2005). In murine intestine, APP is localized in enterocytes, neurons and smooth muscle. Dietary cholesterol and saturated fats have been shown to increase APP and amyloid in columnar epithelial cells in mice (Galloway et al., 2007).

A $\beta$  peptide is also detectable within the Golgi and rough endoplasmic reticulum of enterocytes. Within the intestine, APP appears to modulate motility, barrier integrity and nutrient absorption within neurons, macrophages and epithelial cells. APP knockout mice demonstrate a weakened intestinal inflammatory profile, which suggests that APP may regulate host-microbe interactions or vulnerability to gastrointestinal inflammatory disease (Puig et al., 2012b). From a pathological viewpoint, aberrant amyloid aggregation is also present in Inclusion Body Myositis (IBM), which is a common myopathy affecting skeletal muscle cells (Askanas and Engel, 2002). IBM patients exhibit gradual muscle weakness, impaired innervation of muscle and muscle fibre degeneration (Minniti et al., 2009).

#### **4.1.5.3 APP function in skin**

APP expression is abundant in basal keratinocytes of the epidermis, melanocytes and melanoma cells (Herzog et al., 2004). A $\beta$  deposits have been detected under the epidermal/ dermal junction and adjacent to small blood vessels (Joachim et al., 1989). Here, APP may influence cell adhesion to components of the extracellular matrix and may function as a membrane receptor to regulate kinesin-1, an axonal transport protein (Lazarov et al., 2005). In addition, APP has been shown to regulate copper

homeostasis, and is associated with oxidative stress and apoptosis in human keratinocytes via its ability to reduce  $\text{Cu}^{2+}$  to  $\text{Cu}^+$  *in vitro* (Kagan et al., 2002).

In addition to AD pathogenesis, APP has been associated with skin disorders. For example, APP is upregulated in keratinocytes in psoriasis (Siemes et al., 2004), in which aberrant keratinocyte proliferation and differentiation are observed (Romanowska et al., 2009). Increased production of  $\text{A}\beta$  in the keratinocytes of psoriasis patients increases transcription of the pro-inflammatory enzyme kynureninase. Increased APP expression has also been reported in advanced melanoma, whilst down-regulation of APP leads to the terminal differentiation of human melanoma cell lines (Botelho et al., 2010).

#### **4.1.5.4 APP expression within fibroblasts**

APP processing has been observed in cultured skin fibroblasts, regulated by PKC activity. Phorbol ester-induced PKC activation of FAD-derived skin fibroblasts increased levels of  $\text{sAPP}\alpha$  and decreased levels of  $\text{A}\beta$  (Vestling et al., 1999). PKC can up-regulate ADAM10/17 (which has  $\alpha$ -secretase activity) thereby influencing the non-amyloidogenic pathway, increasing levels of  $\text{sAPP}\alpha$  and subsequently decreasing  $\text{A}\beta$  production (Ebsen et al., 2013). Basal amyloid levels were elevated in these fibroblasts, possibly due to reduced PKC activity. FAD-derived fibroblasts also show distinct metabolic profiles when compared to non-AD controls; including increased lactate production and abnormal glucose uptake (Gasparini et al., 1998).

Patient-derived fibroblasts have provided a great source of information concerning the role of APP outside of the CNS. Studies dating from the 1980's, have observed physiological differences in FAD-derived fibroblasts when compared against aged matched controls. These fibroblasts show abnormalities in energy metabolism (Sims et al., 1987), alterations in calcium content (Peterson and Goldman, 1986) and increased sensitivity to free radicals (Tesco et al., 1992). Interestingly, fibroblasts taken from DS

patients showed decreased growth rate and increased protein content (Segal and McCoy, 1974). In addition, SAD and FAD-derived fibroblasts exhibit reduced adhesiveness to plastic when compared to non-disease fibroblasts (Ueda et al., 1989). This finding is supported by other studies that have demonstrated abnormal cytoskeletal proteins, vimentin fibres, aberrant degradation of fodrin and aberrant calcium responses (Takeda et al., 1990, Takeda et al., 1991, Tatebayashi et al., 1995).

Oxidative stress within diseased fibroblasts is of particular relevance to AD. ROS generation is known to cause tissue damage, however cells possess mechanisms to scavenge these free radicals, such as the expression of manganese superoxide dismutase (MnSOD) (Tesco et al., 1992). The gene encoding MnSOD is located on chromosome 21 and is overexpressed in DS due to trisomy 21. Pathological changes common to both AD and DS strongly imply a possible role of free radicals in disease pathogenesis. Furthermore, fibroblasts taken from SAD patients showed impaired oxidative metabolism (Gasparini et al., 1998, Gibson et al., 1996). Cultured skin fibroblasts taken from SAD and FAD have previously been subjected to oxidative stress in order to observe their responses. SOD activity was higher in FAD than SAD fibroblasts, resulting in increased conversion of superoxide to hydrogen peroxide. Deficiency of cytochrome oxidase complex IV has also been reported in AD platelet mitochondria (Parker et al., 1990) suggesting that the scavenging system may be involved in increased ROS vulnerability. Decreased Cox activity was also observed in SAD-derived fibroblasts (Curti et al., 1997), which may lead to an increase in ROS leakage from the respiratory chain (Benzi et al., 1992). Decreased Cox activity in AD cybrids (SHSY5Y and AD platelets) was found to lead to increased ROS generation (Davis et al., 1997b).

More recently, genetic profiles of SAD-derived fibroblasts were compared with stressed healthy fibroblasts controls. AD cells experienced elevated unrepaired 8-oxo-guanine (8-OdG), a type of DNA base modification, providing evidence of chronic oxidative

stress. (Ramamoorthy et al., 2012). Altered gene expression was also detected between the two cell lines, with a number of genes previously associated with AD found to be altered. For example, IL-6 is differentially expressed amongst different ethnic groups reflecting varied AD risk amongst these ethnicities. A specific polymorphism in 3' flanking region of the IL-6 gene correlates negatively with AD in some populations (Papassotiropoulos et al., 1999). However, in Caucasians, this polymorphism is associated with an increased risk of developing sporadic AD (Bhojak et al., 2000). Another gene associated with AD is the PRKAA1 gene which encodes for the  $\alpha$ 1 subunit of the mammalian (adenosine monophosphate-activated protein kinase (AMPK). AMPK regulates cholesterol and glucose metabolism, and is also activated in response to DNA damage, regulates ROS autophagy and mitochondrial function (Wang et al., 2012). The exact relationship between AMPK and AD is unclear, but APP processing occurs in the membrane where changes in the cholesterol component may exert an effect. Furthermore, there is an association of high serum cholesterol in midlife and where there is increased incidence of AD (Wollmer, 2010).

These studies suggest that fibroblasts from both familial and sporadic AD patients exhibit metabolic differences when compared to age-matched controls. As some of these changes are also observed in sporadic AD-derived fibroblasts this finding suggests that there may be common changes in metabolic pathways shared between both forms of AD. Moreover, differences observed in both in culture and tissues outside of the CNS suggest that the effects of APP misprocessing are not limited to the brain but may also involve metabolic dysregulation in multiple peripheral tissues.

#### **4.1.6 Aims and objectives**

The aim of this study was to examine whether dermal fibroblasts taken from AD patients with confirmed familial mutations exhibit perturbed energy metabolism. Studies described in section 4.1.5.4 have previously demonstrated significant differences in patient derived fibroblasts in cellular metabolism, increased production of

A $\beta$  *in vitro* and most interestingly, oxidative stress in comparison to controls. In order to determine the metabolic changes present in FAD-derived fibroblasts (carrying the London V717I, PS1 mutations M146I and PS1 mutation Intron 4), glucose uptake from the media was measured. In addition, AD-derived fibroblasts were assessed for any changes in mitochondrial function, which may contribute to their susceptibility to oxidative stress using the Seahorse analyzer. They were also subjected to oxidative stress to study their responses in terms of cellular toxicity. Changes observed in fibroblasts could inform research into AD as this study will highlight the consequences of altered APP processing, not only in neuronal cultures but also in cells from the periphery. In addition, normal dermal fibroblast cells were treated with A $\beta$  1-42 to determine whether amyloid has any effects on healthy non-neuronal cell lines.

## **4.2 Methods and materials**

### **4.2.1 Human Dermal Fibroblast culture (hDFa)**

Human dermal fibroblasts (Gibco,, Thermo Fisher Scientific, Paisley, UK) and FAD-derived fibroblasts (a kind gift from UCL Institute of Neurology) were cultured in Dulbecco's minimal essential medium (DMEM) containing 4.5g/l glucose with Glutamax (Gibco, Invitrogen, Paisley, UK), with 100U/ml Penicillin and 100µg/ml Streptomycin and 10% FBS.

Cells were initially resurrected from liquid nitrogen by warming them at 37°C until the cells had thawed. The cell suspension was then mixed in pre-warmed media and pelleted at 180g for 7 minutes, after which point, the media was removed and the cell pellet re-suspended in 1ml media and then were seeded at 5000 cells/cm<sup>2</sup> of surface area of culture vessel. Fibroblasts were left to grow undisturbed at 37°C, 5% CO<sub>2</sub> for 3 days after which point media was refreshed every 2 days. When cells reached approximately 90% confluence they were passaged.

For passaging cells, media was decanted and cells washed twice in PBS. Cells were detached in Trypsin-EDTA (0.01%) with any remaining attached cells detached by gentle agitation of the flask. Fibroblasts were then pelleted and passaged at a ratio of 1:4/ 1:6. Media was refreshed every two days, and then when cells approached 80% confluence, media was refreshed every day. Cells were grown at 37°C, 5% CO<sub>2</sub>. For freezing, cells were pelleted and then re-suspended in 10% DMSO made in FCS, before being stored at -80°C overnight. Cells were then stored in liquid nitrogen for long term storage.

### **4.2.2 Metabolic studies between FAD-derived and control fibroblast cell lines**

#### **4.2.2.1 Cell proliferation study**

FAD-derived fibroblasts and control fibroblast cell lines were plated at  $7.5 \times 10^5$  cells/well into a 96-wellplate and incubated for 24, 48 and 72 hours at 37°C, after which time

the media was replaced with Cell Titer Blue reagent. The cells were incubated for 2 hours and the Abs<sub>620</sub> and background Abs<sub>690</sub> read on a platereader. Once the background readings were subtracted from the Abs<sub>590</sub> readings, proliferation of patient derived cells was determined as a percentage of the control cell line.

#### **4.2.2.2 Glucose uptake**

To study glucose uptake from the media, both diseased and control fibroblasts were seeded into 12 well plates at a seeding density of  $5.5 \times 10^4$  per well. After 24 and 48 hours, media was collected from three wells and pooled to be clarified by centrifugation (10000rpm for 5 minutes). Cells from the three wells were pooled and cell lysates obtained (section 2.2.2.1). The glucose in the conditioned media was quantified using the Glucose HK assay (section 3.3.4.4) and normalised to total cellular protein. Media samples were diluted 1:20 in deionized water to obtain absorbance readings that lay within the linear range of the glucose standard curve.

#### **4.2.2.3 A $\beta$ ELISA**

Extracellular amyloid 1-42 production was determined as described in section 3.2.3.3.2. Media samples (24 and 48 hours) obtained for glucose studies was vacuum evaporated to one fifth of the original volume. A $\beta$  standards were diluted in fibroblast culture media and samples and standards incubated overnight in A $\beta$ 1-42 detection antibody. A $\beta$  concentrations were corrected to total cellular protein.

#### **4.2.2.4 Analysing mitochondrial function**

##### **4.2.2.4.1 Optimization of seeding density**

Optimization of hDF cells on the Seahorse analyzer was carried out as discussed in Chapter 3 with some modifications. Fibroblasts were plated from  $2 \times 10^4$  to  $7 \times 10^4$  cells/well into XF 24 microplates. These ranges of cell numbers were chosen as recommended in the literature (Zhang et al., 2012b). Assay media was prepared containing 25mM glucose and 1mM sodium pyruvate (as recommended in the manufacturer's protocol).

#### **4.2.2.4.2 Optimization of mitochondrial inhibitors**

Control dermal fibroblasts were seeded at the optimal density across the XF microplate for titration of compounds. Optimisation was carried out as described in section 3.2.7. OCR readings were normalized using protein concentration (see section 2.2.2.1) and the average OCR plotted against increasing concentration of compound.

#### **4.2.2.4.3 Performing the MitoStress Test**

The Mito Stress test was performed as described in section 3.2.4.3.4. The three FAD-derived fibroblasts cell lines and control hDF cells were seeded across the plate in five replicate wells. Mitochondrial inhibitors were prepared (at the optimized concentrations) in the assay media and loaded into the cartridge. After the experimental run was complete, the protein concentration (see section 2.2.2.1) was determined.

Results were analysed using the Seahorse Wave 2.0 software, protein concentrations were used to normalize OCR readings for each well. The data was used to generate a MitoStress report (MitoStress report generator software, Seahorse Biosciences, Massachusetts, USA). The data from repeat experiments was collated and analysed using Graph Pad Prism 6.0 (La Jolla, CA, USA).

#### **4.2.2.3 Oxidative stress response studies**

Fibroblasts were treated with hydrogen peroxide ( $\text{H}_2\text{O}_2$ ) in order to induce oxidative stress. Previous studies have suggested that FAD-derived fibroblasts cells exhibit an oxidative phenotype as well as sensitivity to oxidative stress. Therefore, these cells were tested for their responses to  $\text{H}_2\text{O}_2$  in terms of cell survival.

##### **4.2.2.3.1 Optimization of seeding density and hydrogen peroxide concentration**

Initially control dermal fibroblasts were seeded at 5000 cells/well into a 96-wellplate. On the following day, fresh hydrogen peroxide (Sigma-Aldrich, Poole UK) was diluted in different media to determine dose response curve.  $\text{H}_2\text{O}_2$  was diluted in phenol red-free DMEM with 2mM l-glutamine to the following concentrations: 6400 $\mu\text{M}$ , 3200 $\mu\text{M}$ ,

1600 $\mu$ M, 800 $\mu$ M, 400 $\mu$ M, 200 $\mu$ M, 100 $\mu$ M 50 $\mu$ m and 25 $\mu$ M. Cells were treated for 1 hour after which time, media was replaced with complete growth media. The 96-wellplate was placed into the incubator for 18 hours.

#### **4.2.2.3.2 MTT assay**

After this period, cell viability was assessed using the MTT assay (see section 3.2.4.4.2). A dose response curve was constructed by plotting log<sub>10</sub> of H<sub>2</sub>O<sub>2</sub> concentrations against percentage cell viability compared to untreated fibroblasts.

#### **4.2.2.3.3 Statistical analysis**

Statistical analysis was performed using Graph Pad Prism 6.0 (La Jolla, CA, USA). When comparing amyloid treated cells to untreated controls, two-way analysis of variance (ANOVA) was performed with post hoc Bonferroni's/Dunnett's comparisons. Studies involving comparisons between different cell lines, a two way ANOVA was performed with Dunnett's multiple comparisons/ Students T test. Dose response curves of cell lines with hydrogen peroxide were constructed using nonlinear regression with a variable slope, from which the IC<sub>50</sub> of each cell line was calculated. IC<sub>50</sub> values were compared to the control cell line using a two tailed, unpaired Student's T test.

#### **4.2.2.4 Amyloid treatment studies**

Previous studies have examined the effects of exogenous A $\beta$ 1-42 on cell lines. Studies have shown metabolic effects (discussed in section 4.4) in response to amyloid treatment. Therefore it was of interest to investigate the effects of amyloid on normal dermal fibroblasts.

##### **4.2.2.4.1 Optimization of cell seeding density**

Control fibroblasts were initially plated at 2x10<sup>5</sup> cells/ well in triplicate and then serially diluted 1:2 to 3.125 x 10<sup>3</sup> cells/ well into two 96 well plates. The cells were incubated for 24 and 48 hours after which time; cell proliferation was measured using Cell Titer Blue reagent (see section 3.2.4.1). The fibroblasts were then placed back into the

incubator for 3 hours after which time the  $A_{620}$  and  $A_{690}$  readings were measured. The optimal seeding density was selected as the density at which the absorbance changed gradually over time without saturation.

#### **4.2.2.4.2 Amyloid treatment of hDF**

Human dermal fibroblasts were seeded into 96-wellplates (Corning) at  $7.5 \times 10^4$  cell/well. On the following day, human  $A\beta 1-42$ , pre-treated with hexafluoroisopropanol (to induced amyloid aggregation, forming oligomers was prepared in HEPES at a stock concentration of  $100 \mu\text{M}$ . This stock was diluted 1:10 to  $10 \mu\text{M}$ , which was then serially diluted 1:2 in culture media to the following concentrations,  $10 \mu\text{M}$ ,  $5 \mu\text{M}$ ,  $2.5 \mu\text{M}$ ,  $1.25 \mu\text{M}$ ,  $625 \text{nM}$ ,  $312.5 \text{nM}$ ,  $156 \text{nM}$  and finally  $78 \text{nM}$ .  $100 \mu\text{l}$  of each amyloid preparation was applied in triplicate to the fibroblasts and the cells incubated for 48 hours.

#### **4.2.2.4.3 Cell viability**

After 48 hours, the media was aspirated and clarified whilst cells were briefly washed in fresh PBS before being incubated in  $100 \mu\text{l}$  of Cell Titer Blue reagent (see section 3.2.4.1) for 2 hours to determine cell viability.

#### **4.2.2.4.4 Glucose uptake**

Media clarified from section 4.2.4.3 was assessed for glucose concentration using the Glucose HK assay kit (section 3.2.4.2). Samples were diluted 1:20 in deionized to fit within the linear region of the glucose standard curve.

### 4.3 Results

FAD-derived dermal fibroblasts were obtained from UCL Institute of Neurology carrying familial mutations in either PSEN1 or APP (Table 4.1), of which the mutations M146I, V717I and Intron 4 were picked for study.

Gene	Mutation	Passage received	Mutation description	Mean age of onset	Average age of death
PSEN1	R278I	P6	AGA -> ATA	49.5	-
PSEN1	Y115H	P6	TAT -> CAT	38.5	41.5
PSEN1	M139V	P4	ATG-> GTG	40.7	48.6
PSEN1	Y115C	P4	TAT -> TGT	44.2	55.0
PSEN1	Intron 4	P4	Point mutation leading to 3 transcripts *	35.6	42.0
PSEN1	M146I	P2	ATG -> ATA	46.7	55.4
APP	V717I	P4	London mutation, GTC -> ATC	53.2	63.2

Table 4.1. Table of patient mutations available for study. \*point mutation which can lead to 3 different transcripts which encode for either two truncated PS1 proteins or full length PS1 with extra Threonine residue.

#### 4.3.1 Cell proliferation

Cell lines were initially assessed for cell proliferation rate using the MTT assay, compared to the control cell line (see Figure 4.2). Cells were seeded for 24, 48 and 72 hours to determine if there were any significant differences in growth rates at these time points. No significant differences were observed at 24 or 48 hours. However, at the 72 hour time point, there was an increase in the proliferation of cells containing fibroblasts carrying the APP717I mutation ( $140 \pm 16.5\%$ ,  $p$  value = 0.0291) compared to control and an increase in growth of M146I cell line ( $139.2 \pm 12.4\%$ ,  $p$  value = 0.0366) when compared to control dermal fibroblasts.

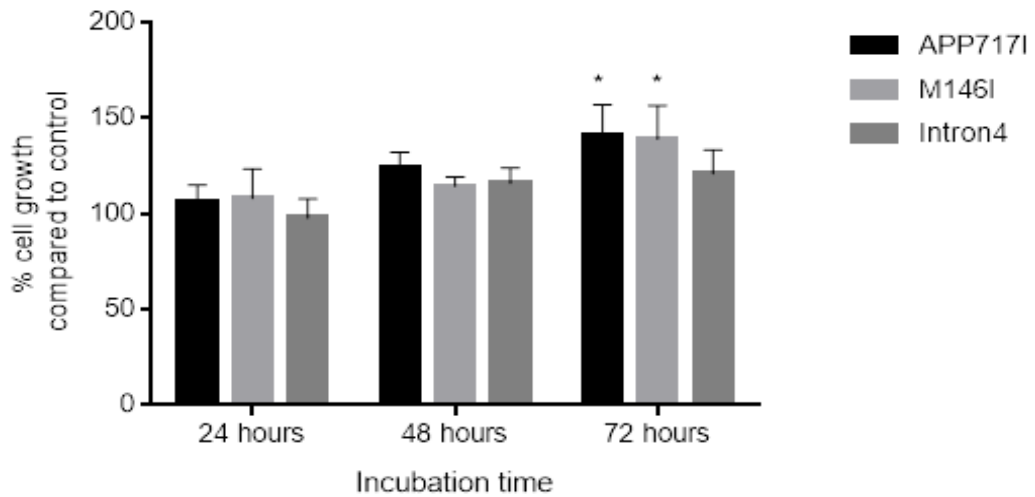


Figure 4.2. Graph of cell growth of fibroblast cell lines using the MTT assay. Viability was measured using MTT/Cell Titer blue. Results are expressed as a percentage cell growth compared with control fibroblasts  $\pm$  SEM, (n=3). P values <0.05 (\*).

#### 4.3.2 Glucose uptake

AD-derived fibroblasts were also tested for their ability to take up glucose from the media after 24 and 48 hours (see Figure 4.3), using the Glucose HK assay. Glucose levels in the media were normalised to total levels of protein/well to account for any differences in the proliferation of cells. There was a general trend of mutant cell lines utilising less glucose than the control cell line but no significant changes in glucose uptake were observed.

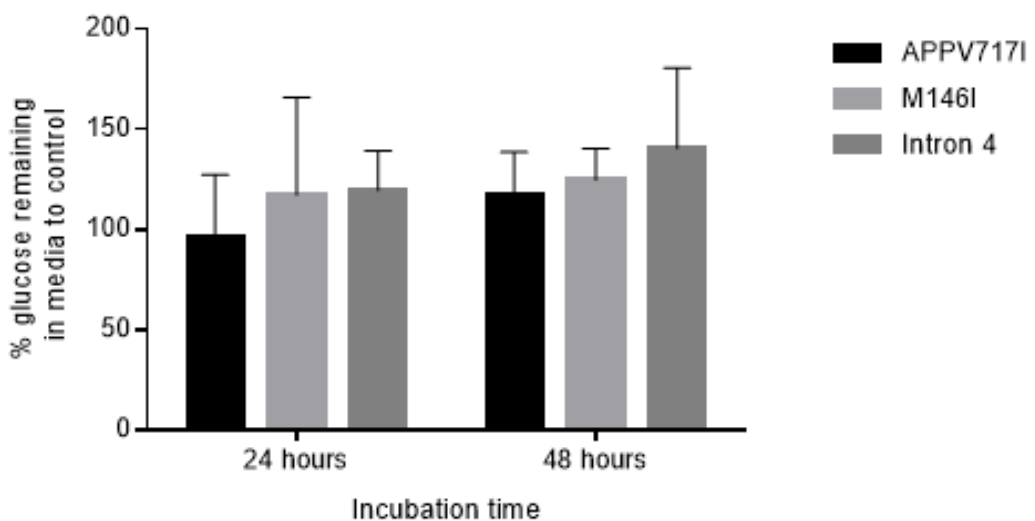


Figure 4.3. Graph showing the amount of glucose remaining in media after 24 and 48 hours using the Glucose HK assay. Results are presented as a percentage of the control cell line,  $\pm$  SEM (n=3), normalised to total cellular protein.

#### **4.3.3 A $\beta$ ELISA**

Amounts of A $\beta$ 1-42 secreted into the media were assessed for fibroblast cell lines after 24 and 48 hours of incubation. FAD-derived fibroblasts have been reported to secrete amounts of amyloid than compared to control cell lines (Citron et al., 1994). It was expected they would secrete small amounts of the peptide, so media samples were vacuum evaporated five times the original volume. Results from the amyloid ELISA showed non-detectable amounts of peptide (concentrations were below the limit of the assay, data not shown).

#### **4.3.4 Analysing mitochondrial function**

Optimization experiments were carried out using control dermal fibroblast cell lines. Cells were seeded to study mitochondrial function using the Seahorse Mito Stress Kit. Protocols provided by the manufacturer, recommend assay media to supplementation with 25mM glucose and 1mM sodium pyruvate, which is essential to be able to record a maximal OCR response.

Optimization of compounds on the Seahorse analyser with fibroblasts seeded at 20000 to 70000 cells per well across the plate. Basal OCR (Figure 4.4) and ECAR readings (Figure 4.5) were measured four times after setting up a looped protocol of mixing, waiting and measuring. The OCR measurements over time were constant throughout the experiment but ECAR readings were higher at the higher seeding densities. Generally, all OCR readings were stable, with increasing cell density leading to increases in OCR readings as expected. The ECAR readings (Figure 4.5) showed differences between the different seeding densities. ECAR readings for cells seeded at 20000 cells showed the lowest ECAR along with the lowest OCR measurements. Seeding 30000 cells gave an abnormal response in ECAR which was unexpected. Ideally, the optimal seeding density of any cell line should exhibit consistently low ECAR values at rest, with OCR readings expected to be between 100 to 500pmoles/min. The chosen seeding density for fibroblasts was 50000 cells, which gives an average

OCR of  $144 \pm 6.4$  and average ECAR of  $12.9 \pm 2.6$  mpH/ min. This low OCR indicates a cell type of low metabolic activity, which was evident by slow growth.

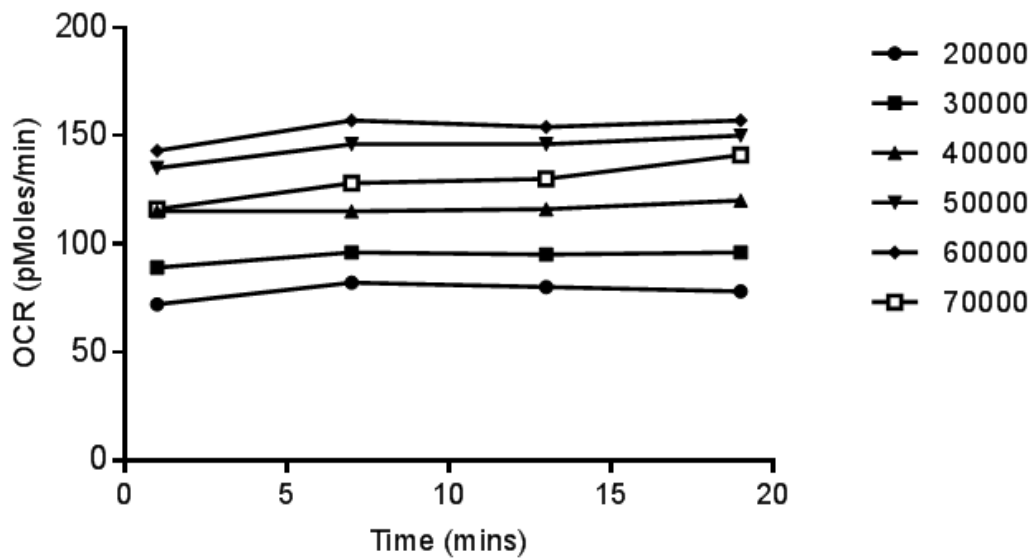


Figure 4.4. Basal OCR measurements of control hDF seeded at different densities.

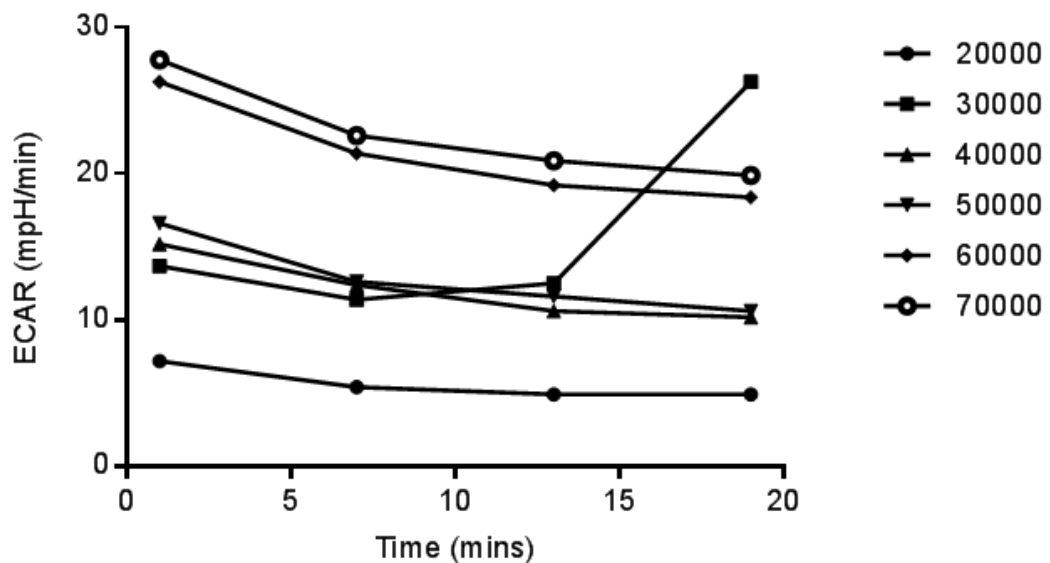


Figure 4.5. ECAR readings of the same cells seeded over time.

Following optimisation of the seeding density, the concentration of mitochondrial inhibitors was optimised. Optimized concentrations are tabulated in Table 4.2.

Mitochondrial inhibitor	Optimal concentration ( $\mu\text{M}$ )
Oligomycin	1
FCCP	5
Antimycin A	0.5
Rotenone	0.5

Table 4.2. Table of the optimal concentrations of inhibitors calculated.

The Mito Stress assay was performed in accordance with the manufacturer's instructions. After the run was complete, all readings were normalized to protein concentrations and measurements of OCR were analysed using the Seahorse MitoStress Report to determine the metabolic profiles of each cell line. Data was analysed in Graph Pad 6.0 using one way ANOVA and unpaired Students T test to compare the metabolic measurements of each cell line to each other.

Figure 4.6 shows a typical metabolic profile of the hDF cell line produced from the MitoStress test. The readings are presented as percentage of the basal OCR for each cell line. These cell lines respond to oligomycin by reducing OCR and demonstrate an increased OCR in response to FCCP. The following rotenone and antimycin A injection a modest fall in OCR is observed.

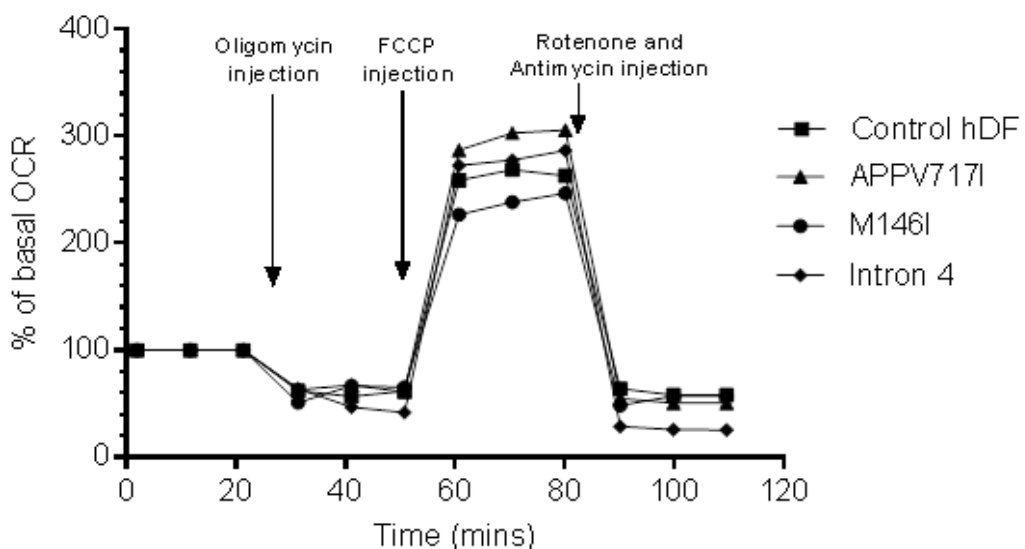


Figure 4.6. Graph of one MitoStress experiment of the hDF cell lines. Results are represented as percentage of basal OCR readings for each cell line.

Figure 4.7 shows the metabolic measurements calculated by analyzing the OCR readings in the MitoStress report V2. Results are presented as average OCR

readings, normalised against protein. Multiple Student's Tests with post hoc Holm-Sidak method ( $p < 0.05$ ) was performed between the different cell lines for the different metabolic measurements calculated, which revealed no significance between any of the cell lines. Results also show some variation between experimental runs, despite protein normalization.

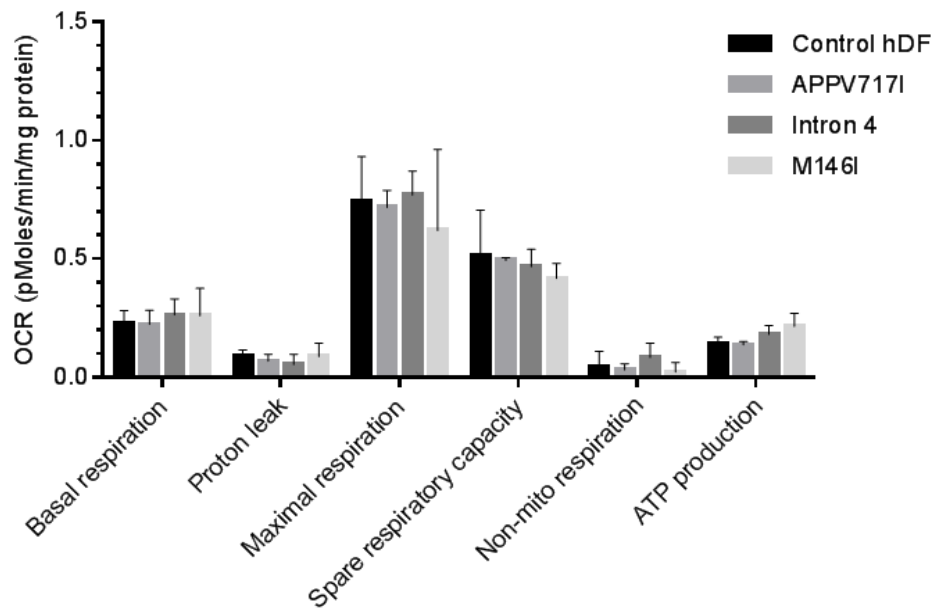


Figure 4.7. Graph of the metabolic parameter calculated OCR readings recorded from the MitoStress test. Results are presented as OCR readings, normalised to total protein per well  $\pm$  SEM, (n=3).

#### 4.3.5 Oxidative stress of human dermal fibroblasts

As oxidative stress is associated with AD and other neurodegenerative disorders, the next step was to determine the responses of dermal fibroblasts (both control and AD-derived) to oxidative stress. One common method to induce oxidative stress is to treat cells with hydrogen peroxide ( $H_2O_2$ ).  $H_2O_2$  is a strong oxidizing agent, which is highly unstable. When applied to organic material, it can break down to form highly reactive OH- radicals, which can interact with proteins and DNA. Therefore, the effects of hydrogen peroxide on fibroblasts were assessed using the MTT assay to study cell growth. Previous studies have shown that the effects of hydrogen peroxide on fibroblasts are both dose-dependent and cell density-dependent. To this end, fibroblast cells were seeded at 5000 cells/well across a 96-well plate. Decreasing concentrations of hydrogen peroxide diluted in, phenol-red free DMEM with 2mM l-glutamine. Cells

were incubated for 1 hour in H<sub>2</sub>O<sub>2</sub> and then cells allowed to recover after 18 hours to assess for cell viability in normal medium. To calculate the IC<sub>50</sub>, one point had to be excluded as this was distorting the data. Interestingly, at all densities tested, cell viability does not decrease at 800μM, but increases slightly. This variation occurs during all experiments suggesting that this is not due to technical error, but may reflect a positive response in fibroblasts.

For the analysis of stress responses in patient derived cells, cell viability was measured using the MTT assay, and calculated as a percentage of the untreated control (Figure 4.8). IC<sub>50</sub> values were calculated for each patient derived line and compared to the control (Table 4.2). Statistical analyses of the IC<sub>50</sub> values suggest that there was no significant difference in the IC<sub>50</sub> values between the control and patient derived fibroblasts. There was also considerable variation between repeat experiments.

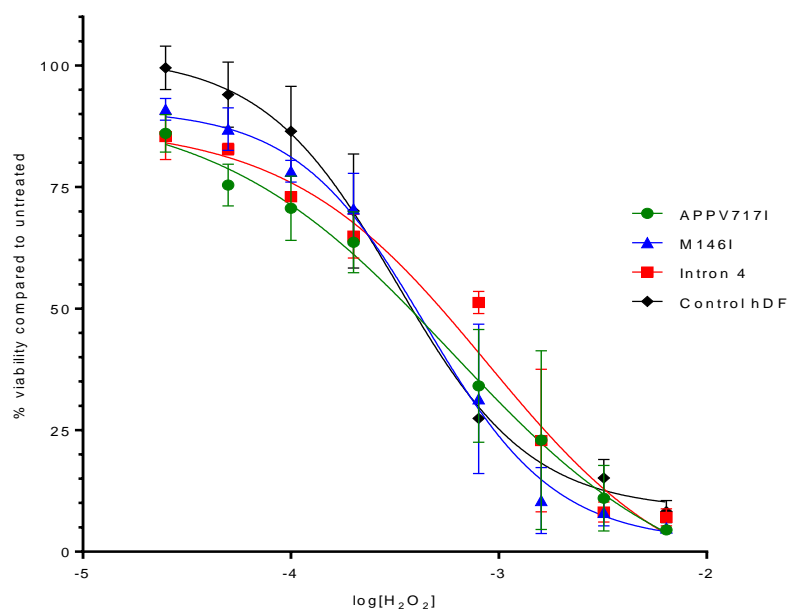


Figure 4.8. Non-linear regression curve fit demonstrating the dose response of AD-derived fibroblasts treated with increasing concentrations of H<sub>2</sub>O<sub>2</sub> (n=3). Cell viability was measured using the MTT assay. IC<sub>50</sub> values were calculated using GraphPad Prism 6.0 (see Table 4.3). Results are displayed as a percentage of the untreated cell line ± SEM, (n=3).

Cell type	Average IC <sub>50</sub> (μM)	T test analysis compared against Control HDF	P value
Control HDF	584.9 ± 122.6	-	-
APPV717I	583.9 ± 223.9	NS	0.4612
M146I	714.6 ± 330.3	NS	0.7412
Intron 4	669.7 ± 40	NS	0.5679

Table 4.3. Table of the average IC<sub>50</sub> calculated using Graph Pad Prism 6.0. A two tailed, unpaired T- test (with Welch's correction) showed no significant differences between mutations and control HDF.

#### 4.3.6 Amyloid treatment of hDF

Normal dermal fibroblasts were treated with a range of oligomeric Aβ<sub>1-42</sub> concentrations to determine its effects on this non-neuronal cell type.

##### 4.3.6.1 Cell viability

Human dermal fibroblasts were treated with increasing concentrations of Aβ<sub>1-42</sub> for 48 hours, after which time cell viability was assessed by Cell Titer Blue (Figure 4.9). At all concentrations, no cellular toxicity was observed. At the lower concentrations of 78nM and 156nM, there were no significant changes in viability. However at 312.5nM of amyloid, there was a significant increase of 109.6 ± 4.9%, (P<0.05) in resazurin absorbance. Significant increases in resazurin absorbance were also observed at 62.5nm (112.5 ± 1.4 %, (P<0.05) 125nM (109.8 ± 2.1, (P<0.05). 5μM 112 ± 3.6% (P<0.05) 10μM and 121.6% ±0.634% (P<0.05).

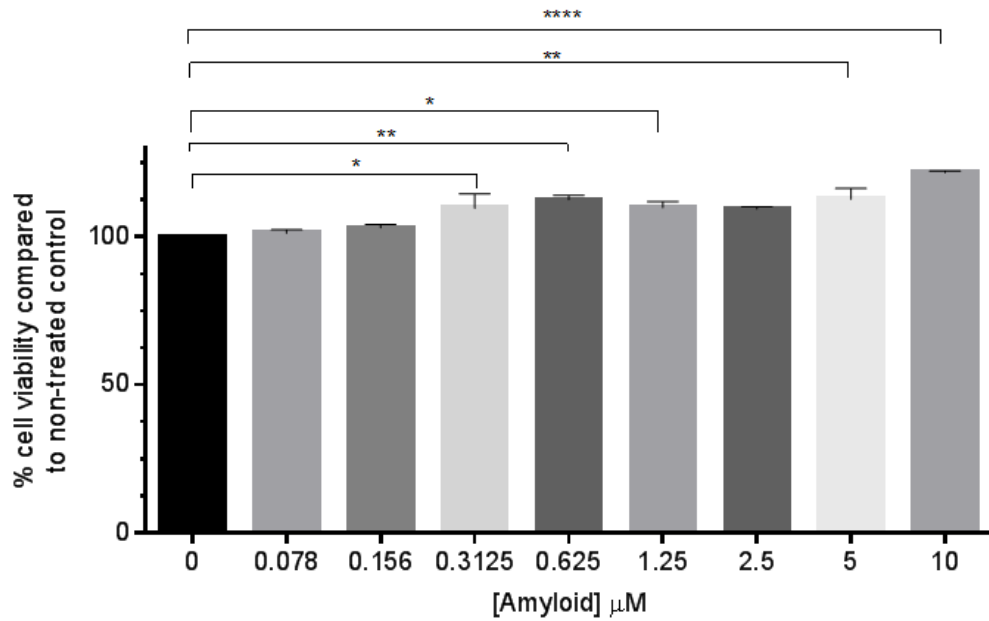


Figure 4.9. Graph showing the cell viability of dermal fibroblasts treated with increasing concentrations of A $\beta$ 1-42, represented as a percentage of control ( $\pm$  SEM n=3).  $p < 0.05$  (\*),  $p < 0.005$  (\*\*),  $p < 0.0001$  (\*\*\*\*).

#### 4.3.6.2 Glucose uptake

The glucose remaining in the media from dermal fibroblasts treated with A $\beta$ 1-42 was determined using the Glucose HK assay after 48 hours (Figure 4.10). There was a significant reduction in glucose uptake at 312.5nm, where there was  $113.3 \pm 2.0$  % ( $p < 0.05$ ) more glucose in the media, when compared to untreated controls. However, there was no significant difference at any of the other concentrations tested.

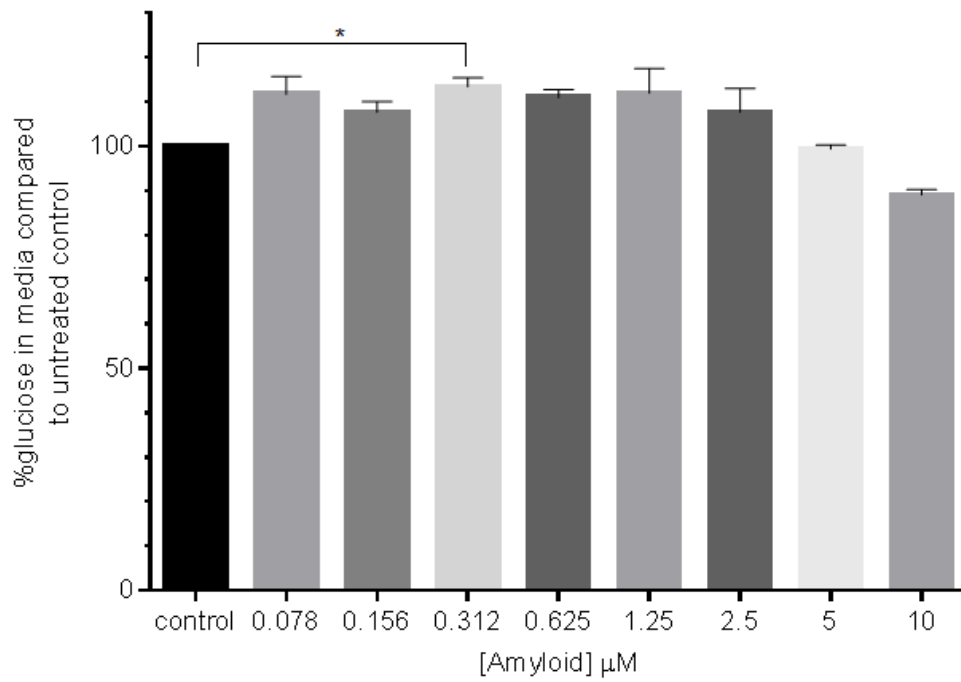


Figure 4.10. Graph showing the amount of glucose remaining in the media in A $\beta$ 1-42 – treated dermal fibroblasts compared to untreated controls. Cell viability was measured using Cell Titer Blue. Results are presented as a percentage  $\pm$  SEM compared to non-treated controls (n=3),  $p < 0.05$ (\*).

## **4.4 Discussion**

Since the emergence of iPSCs technology in 2006, researchers have used these cells to create cellular models of genetic disorders by taking patient somatic cells and reprogramming them back into induced pluripotent stem cells. Several studies have utilised FAD and SAD derived fibroblasts to create neuronal cultures and to study early AD development (Israel et al., 2012, Kondo et al., 2013, Qiang et al., 2011, Yagi et al., 2011). All of these studies have focussed on characterising iPSC-derived neurons. However, a recent study analysing neural precursor cells (hNPCs) prior to differentiation (Sproul et al., 2014) found significant differences in amyloid processing between AD and control NPCs. As NPCs are also a more homogenous population, this study suggested that hNPCs could provide a better system to identify novel molecules, potentially important for early events in AD and might allow better cross comparisons between control and FAD cells. This study demonstrated that FAD derived fibroblasts and their reprogrammed NPCs counterparts have a higher A $\beta$ 42/A $\beta$ 40 ratio than equivalent control cells, suggesting pathogenic proteolytic processing of endogenous APP in these cells. As patient derived fibroblasts represent an unadulterated patient cell line, these cells may provide useful tools for identification of novel molecules for the treatment of AD as well as pathways that may lead to the development of disease.

### **4.4.1 Characterizing FAD-derived fibroblast metabolism**

The above study provides an interesting rationale for studying alterations observed in FAD-derived fibroblasts in terms of their metabolism. Previous studies have observed changes in cell adhesion, vimentin distribution (Takeda et al., 1990) calcium regulation (Peterson et al., 1985), oxidative metabolism (Peterson and Goldman, 1986), potassium channel activity (Etcheberrigaray et al., 1993) and the phosphatidylinositol cascade including PKC (Bruehl et al., 1991, Govoni et al., 1993). Initial observations here in this study suggested that there were significant differences in the proliferation of some fibroblast lines. In addition, whilst results were insignificant, there was a trend for

reduced glucose uptake in these cells and a trend for increased sensitivity to oxidative stress which again was not significant. The reduction in glucose uptake has been observed in proliferating APP-expressing SHSY5Y cell lines which suggests some common mechanism of the effects of amyloid on both these cell lines. As such, the amount of secreted A $\beta$ 1-42 from these fibroblasts was assessed. Unfortunately, no amyloid could be detected as concentrations were below the limit of detection even after vacuum evaporation of the media. This contradicts previous studies which found FAD- derived fibroblasts secreting low levels of amyloid, which were more than that of control fibroblasts (Scheuner et al., 1996b, Scheuner et al., 1996a, Duff et al., 1996, Citron et al., 1994). DS derived fibroblasts were reported to secrete low levels of A $\beta$ 1-40 but A $\beta$ 1-42 levels were undetectable (Shi et al., 2012a). Future experiments will therefore assess A $\beta$ 1-40 secretion from fibroblasts, as well as the secretion of sAPP $\alpha$  and sAPP $\beta$  fragments. Investigating A $\beta$ 1-42 release after stressing fibroblasts with hydrogen peroxide may also be an option to consider studying.

Mitochondrial dysfunction has been observed in the brains of AD patients as well as AD transgenic mice. As metabolic dysfunction has previously been described within patient derived fibroblasts, this would suggest that either APP/ PSEN1 mutations are able to drive dysfunction within these cells or that bodies of AD patients due to chronic stress. To this end, mitochondrial function was studied extensively in AD-derived fibroblasts using the Seahorse analyser. However, no significant differences were observed suggesting that these cells are not suffering from mitochondrial stress. A previous study has shown that mitochondria isolated from AD-derived fibroblasts are more susceptible to free radicals (Kumar et al., 1994). Therefore, future experiments will determine the responses of patient derived cells in response to oxidative stress, (by using hydrogen peroxide treatment) on the Seahorse analyser. It should also be noted that the Mito Stress test was conducted in high glucose media (25mM). Future experiments will be performed using a range of glucose concentrations to determine its effects on mitochondrial function. Further kits available from Seahorse Biosciences

would also allow the determination of glycolysis stress as well as lipid metabolism. Interestingly, skin fibroblasts from AD patients have been demonstrated to show changes in cholesterol metabolism (Pani et al., 2009). To fully rule out metabolic dysfunction in these cells other pathways should also be determined.

#### **4.4.2 Effects of exogenous A $\beta$ 1-42 on fibroblasts**

As a number of studies have demonstrated increases in the secretion and ratio of A $\beta$ 1-42/40 in FAD-derived fibroblasts (Sproul et al., 2014, Duff et al., 1996, Scheuner et al., 1996a, Tamaoka et al., 1994), it was of great interest to determine the effects of exogenous A $\beta$ 1-42 on these cells. The secretion of A $\beta$  from platelets and leukocytes following their activation, led to autocrine or paracrine effects on cells throughout the body (Li et al., 1999, Chen et al., 1995). Aberrant A $\beta$  metabolism is consistently detected in plasma of AD mutation carriers, where platelets are suggested to be the major source of APP. Studies of patients with platelets with low  $\alpha$ -granule content demonstrate a reduction in APP expression, which led to a reduction in plasma APP levels (Li et al., 1994) supports this theory. The physiological role of this secreted APP from platelets is poorly characterised, but in AD, it is hypothesised to be deposited into the brain. The mechanism by which amyloid may be delivered into the brain may involve complexes containing HDL and VHDL in association with ApoJ (Koudinov et al., 1994). With respect to the immune system, lymphocytes, monocytes, neutrophils, macrophage and microglia have been confirmed to express and secrete APP (Konig et al., 1992). Stimulated T-lymphocytes secrete the larger APP isoforms as well as APP695, which may be associated with non-adherence and adherence in the immune system. Microglia produce APP, which can interact with different extracellular matrix components, and may influence APP secretion as well as intracellular APP metabolism, implying a role in microglial mobility (Monning et al., 1995). FAD-derived lymphocytes are also reported to secrete A $\beta$  (and other APP cleavage products) suggesting that these cells could be another source of A $\beta$  found in blood. Changes in calcium homeostasis are considered to play a role in AD pathology, in fact in stimulated

lymphocytes, A $\beta$  amplifies intracellular calcium signalling, although this effect was ameliorated in sporadic and FAD –derived lymphocytes (Eckert et al., 1994).

Recent studies in our laboratory have also investigated the effect of exogenous amyloid on a range of cells. Tarczykuk *et al.* (2015) demonstrated that human stem cell-derived neuron and astrocyte cultures treated with oligomeric A $\beta$ 1-42 display hypometabolism, with regards to the utilisation of substrates such as glucose, pyruvate, lactate and glutamate. In addition, astrocytes within these cultures stored significantly higher levels of glycogen in comparison to controls. Significant changes in NAD<sup>+</sup>/NADH, ATP and GSH levels were observed, suggesting a disturbance in the energy redox axis. Other studies in our laboratory (Dr Eric Hill, Personal communication) have demonstrated that following treatment of the mouse myoblast cell line C<sub>2</sub>C<sub>12</sub> cell line with amyloid, these cells exhibited increased cell viability, decreased glucose uptake and increased glycogen storage.

Treatment of normal dermal fibroblasts with A $\beta$ 1-42 at the low concentrations tested did not cause cell death but led to a significant decrease in glucose uptake within these cells. This suggests some metabolic effect which in line with previous studies discussed above. In contrary, at high concentrations of A $\beta$ 1-42 cells exhibited increased growth and increased glucose usage. A $\beta$  monomers are known to exert neurotrophic and neuroprotective effects (Giuffrida et al., 2009, Yankner et al., 1990, Chen and Dong, 2009). Therefore, the form of A $\beta$ 1-42 used in this study should be verified to identify which form of amyloid could be affecting fibroblast metabolism. Such observations strongly imply that the metabolic and proliferative effects of amyloid are not neuronal-specific and that AD is possibly one consequence of pathological APP misprocessing. Use of the Seahorse analyzer to study mitochondrial function and glycolysis in response to amyloid treatment would be ideal to further study fibroblast responses.

As numerous studies have demonstrated the production of APP and its cleavage products in skeletal muscle, skin cells, blood and gut, this further supports the idea that APP is expressed, metabolised and secreted by cells outside of the brain where its cleavage products may play physiological roles under non-pathological conditions that become perturbed in AD. As such, future studies should further investigate the utility of patient derived cells in order to study the biological roles of APP within tissues.

## Chapter 5: Conclusions and future work

The cell lines used for the study of endogenous APP expression in this thesis provide an interesting insight into the effects of APP on cellular metabolism. This study is novel in that it attempts to establish a link between APP overexpression/ mutant APP expression with reduced glucose uptake and mitochondrial function. APP overexpression has been a common route of generating AD models by transfecting the APP gene under the control of a non-native / viral promoter into host cells. This has led to the production of a plethora of AD *in vivo* and *in vitro* models, which has increased our knowledge of AD pathology, but their relevance to human disease has been questioned. For example, the use of rodents to induce AD-like symptoms by expressing multiple human genes has yielded results which may not relate to the natural development of dementia. A further point to note is that mouse amyloid does not aggregate as it does in humans, and so the effects of amyloid deposition may lead to responses that are rodent-specific. The promoter used is also of great importance, as the use of viral promoters can lead to unnaturally high levels of protein expression, which could exaggerate the pathology of AD. Taking these findings into account, the human synapsin I promoter which is native to neuronal phenotypes was used to control APP expression. This promoter is relatively weak in comparison to viral promoters such as CMV and may more naturally represent more mildly elevated levels of APP. However, the lack of significance in many of the assays used to assess clones suggests that the level of APP expression may not have been sufficient to drive significant pathology.

The use of patient fibroblasts provides an interesting opportunity to identify changes associated with mutations in APP expressed at natural levels. It also allows for the identification of early changes that may occur in non-neuronal cell lines that may be relevant to AD. However, the study of these cell lines did not reveal any overt pathological phenotypes in comparison to control cell lines.

The approaches used in this study are potentially hampered by a number of issues with the methodology used. Alternative strategies could be employed to investigate metabolism in AD. Future work will further aim to characterise the SHSY5Y lines in terms of the number and location of APP genes inserted into the cell line. Techniques such as inverse PCR sequencing and Southern blotting could be used to determine where and how many copies of the APP gene had integrated into the cellular genome of each clone. Using the SHSY5Y cell line to express a mutant form of APP may be an over simplification of studying APP metabolism in neuronal cell lines. In the SweAPP-expressing cell lines, the native wtAPP695 gene are still expressed by the cell, which may affect processing of the exogenous protein. Therefore, future work should consider knocking out the native wtAPP695 expression prior to integrating the SweAPP695 mutation.

As there is little control of the level of APP expression a useful tool would be to develop an inducible model such as the Tet-on system to control both the timing and level of APP expression in response to an exogenous additives such as doxycycline. As such, changes in APP expression and metabolism could be simultaneously monitored. Alternatively, knocking in the BACE1 gene or even knockdown of the  $\alpha$ -secretase activity could be considered to drive amyloid production.

In addition, cell lines should be fully characterised in terms of their APP metabolism, including analysis of the forms of soluble APP as well as A $\beta$ 1-40/42 ratios and crucially, levels of BACE1 activity. The levels of A $\beta$ 1-42 produced by the cell may be limited by the expression levels of BACE1. This could then be used to gain a better understanding of the effects of APP processing on cellular metabolism. Pharmacological inhibition of BACE or  $\gamma$  secretases could also be used to modulate APP processing and the effects on metabolism determined.

Future work with the cell lines developed will utilise the Glycolysis stress kit available from Seahorse Biosciences in order to investigate glycolytic pathways, which may operate within these cells and be affected by APP processing. The use of cellular stressors such as A $\beta$  or oxidative stress could also be used in combination with the Seahorse bioanalyser, could also be used to monitor the subtle effects of stress on cellular metabolism. Conversely potential neuroprotective agents such as hydroxybutyrate or NMN could also be analysed using this system.

iPS cells are increasingly used as tools to model AD. These stem cells can be generated from 'normal' controls as well as from people who carry genotypes associated with AD making them highly attractive models. They also overcome the ethical issues faced with hESCs and have already been used to study ALS, spinal muscular atrophy and familial dysautonomia (Hu et al., 2010). Since their discovery, iPSC lines have been successfully generated independently in different laboratories and are comparable to hESCs in their morphology and gene-expression profiles (Park et al., 2008a).

These cells can be differentiated into neuronal cell types but it was reported that the neural differentiation of iPSCs is variable and less efficient when compared to hESC differentiation. A number of groups have also suggested that there is large variability and unpredictability in the differentiation such cell lines (Hu et al. (2010). More recently, studies have successfully cultured neurons from DS patient fibroblasts, which produce more amyloid 1-42 and form amyloid plaques (Shi et al., 2012a). These cells also demonstrate network functionality and can therefore provide a system to model the functional effects of APP overexpression/misprocessing. In addition, phosphorylated tau was found to aberrantly accumulate in the dendrites and cell bodies of DS-derived neurons compared to control neurons (Shi et al., 2012a).

Emergence of iPSC cells derived from AD patients has rendered the use of cell lines such as the SHSY5Y cell lines almost obsolete in terms of studying AD development. Current studies already show both tau and amyloid pathology in cells derived from AD patients. This would not be possible to replicate naturally in SHSY5Y cells. Furthermore, neuronal cultures derived from patient cells do not need to be genetically manipulated in terms of molecular cloning as they already carry a specific mutation, and have been thoroughly genotyped and karyotyped to ensure that they represent a 'normal' cell line.

Caution should be taken when using iPSCs as numerous studies have described differences in the fibroblasts taken from AD patients (Chapter 4). These have the potential to be carried through to subsequent iPSC clones. A number of studies have suggested that iPSCs have a 'phenotypic memory' of their previous cell line and may continue to express genes associated with their previous state (Ohi et al., 2011). Therefore, epigenetic changes present in patient cells may contribute to the phenotypes observed in the cells after differentiation and need to be considered. Questions also remain over when AD begins. FAD patients probably express APP inappropriately during development and may therefore suffer the effects of AD before birth. In this way the effects of APP misprocessing on development should also be considered (Sproul *et al.* 2014). Alzheimer's disease is considered to develop over a number of decades. As such short term cultures may not reveal changes in cells at physiological levels of expression. However, experiments in our laboratory have demonstrated that iPSC derived neurons can be maintained in culture for over a year (Dr David Nagel; personal communication). As such long term effects of APP misprocessing could be studied during which time the low levels of expression may elicit changes in metabolism.

There are no easy answers as to how best to model AD. Instead a range of models should be considered and their translation into humans should be treated with caution.

However, it is clear that AD cannot be considered a brain specific phenomenon and future research should attempt to understand the role of APP in a range of tissues. This may eventually reveal its natural functions within the body and how it is changes in its processing lead to disease.

## 6.0 Bibliography

- Abdul-Hay, S. O., Sahara, T., McBride, M., Kang, D. and Leissring, M. A. (2012) 'Identification of BACE2 as an avid  $\beta$ -amyloid-degrading protease', *Mol Neurodegener*, 7, pp. 46.
- Abramov, A. Y., Canevari, L. and Duchen, M. R. (2003) 'Changes in intracellular calcium and glutathione in astrocytes as the primary mechanism of amyloid neurotoxicity', *Journal of Neuroscience*, 23(12), pp. 5088-95.
- Abramov, A. Y., Canevari, L. and Duchen, M. R. (2004) 'Beta-amyloid peptides induce mitochondrial dysfunction and oxidative stress in astrocytes and death of neurons through activation of NADPH oxidase', *Journal of Neuroscience*, 24(2), pp. 565-75.
- Akaaboune, M., Allinquant, B., Farza, H., Roy, K., Magoul, R., Fiszman, M., Festoff, B. W. and Hantai, D. (2000a) 'Developmental regulation of amyloid precursor protein at the neuromuscular junction in mouse skeletal muscle', *Mol Cell Neurosci*, 15(4), pp. 355-67.
- Akaaboune, M., Allinquant, B., Farza, H., Roy, K., Magoul, R., Fiszman, M., Festoff, B. W. and Hantai, D. (2000b) 'Developmental regulation of amyloid precursor protein at the neuromuscular junction in mouse skeletal', *Molecular and Cellular Neurosciences*, 15(4), pp. 355-367.
- Akasaka-Manyá, K., Manyá, H., Sakurai, Y., Wojczyk, B., Spitalnik, S. and Endo, T. (2008) 'Increased bisecting and core-fucosylated N-glycans on mutant human amyloid precursor proteins', *Glycoconjugate Journal*, 25(8), pp. 775-786.
- al Yacoub, N., Romanowska, M., Haritonova, N. and Foerster, J. (2007) 'Optimized production and concentration of lentiviral vectors containing large inserts', *J Gene Med*, 9(7), pp. 579-84.
- Amado, R. G. and Chen, I. S. (1999) 'Lentiviral vectors--the promise of gene therapy within reach?', *Science*, 285(5428), pp. 674-6.
- Anandatheerthavarada, H. K., Biswas, G., Robin, M. A. and Avadhani, N. G. (2003) 'Mitochondrial targeting and a novel transmembrane arrest of Alzheimer's amyloid precursor protein impairs mitochondrial function in neuronal cells', *Journal of Cell Biology*, 161(1), pp. 41-54.
- Anandatheerthavarada, H. K. and Devi, L. (2007) 'Amyloid precursor protein and mitochondrial dysfunction in Alzheimer's disease', *Neuroscientist*, 13(6), pp. 626-38.
- Andrews, P. W., Damjanov, I., Simon, D., Banting, G. S., Carlin, C., Dracopoli, N. C. and Fogh, J. (1984) 'Pluripotent embryonal carcinoma clones derived from the human teratocarcinoma cell line Tera-2. Differentiation in vivo and in vitro', *Laboratory Investigation*, 50(2), pp. 147-62.
- Annaert, W. G., Levesque, L., Craessaerts, K., Dierinck, I., Snellings, G., Westaway, D., George-Hyslop, P. S., Cordell, B., Fraser, P. and De Strooper, B. (1999) 'Presenilin 1 controls gamma-secretase processing of amyloid precursor protein in pre-golgi compartments of hippocampal neurons', *J Cell Biol*, 147(2), pp. 277-94.
- Apelt, J., Bigl, M., Wunderlich, P. and Schliebs, R. (2004) 'Aging-related increase in oxidative stress correlates with developmental pattern of beta-secretase activity and beta-amyloid plaque formation in transgenic Tg2576 mice with Alzheimer-like pathology', *International Journal of Developmental Neuroscience*, 22(7), pp. 475-484.
- Apelt, J., Mehlhorn, G. and Schliebs, R. (1999) 'Insulin-sensitive GLUT4 glucose transporters are colocalized with GLUT3-expressing cells and demonstrate a chemically distinct neuron-specific localization in rat brain', *J Neurosci Res*, 57(5), pp. 693-705.
- Arai, H., Lee, V. M., Messinger, M. L., Greenberg, B. D., Lowery, D. E. and Trojanowski, J. Q. (1991) 'Expression patterns of beta-amyloid precursor protein (beta-APP) in neural and nonneural human tissues from Alzheimer's disease and control subjects', *Ann Neurol*, 30(5), pp. 686-93.
- Arcangeli, A., Rosati, B., Crociani, O., Cherubini, A., Fontana, L., Passani, B., Wanke, E. and Olivetto, M. (1999) 'Modulation of HERG current and herg gene expression during retinoic acid treatment of human neuroblastoma cells: Potentiating effects of BDNF', *Journal of Neurobiology*, 40(2), pp. 214-225.

- Archer, T., Kostrzewa, R. M., Beninger, R. J. and Palomo, T. (2011) 'Staging Neurodegenerative Disorders: Structural, Regional, Biomarker, and Functional Progressions', *Neurotoxicity Research*, 19(2), pp. 211-234.
- Arendt, T. (2001) 'Alzheimer's disease as a disorder of mechanisms underlying structural brain self-organization', *Neuroscience*, 102(4), pp. 723-65.
- Arispe, N., Pollard, H. B. and Rojas, E. (1993) 'Giant multilevel cation channels formed by Alzheimer disease amyloid beta-protein [A beta P-(1-40)] in bilayer membranes', *Proc Natl Acad Sci U S A*, 90(22), pp. 10573-7.
- Arriagada, P. V., Growdon, J. H., Hedley-Whyte, E. T. and Hyman, B. T. (1992) 'Neurofibrillary tangles but not senile plaques parallel duration and severity of Alzheimer's disease', *Neurology*, 42(3), pp. 631-639.
- Askanas, V. and Engel, W. K. (2002) 'Inclusion-body myositis and myopathies: different etiologies, possibly similar pathogenic mechanisms', *Curr Opin Neurol*, 15(5), pp. 525-31.
- Assini, A., Terreni, L., Borghi, R., Giliberto, L., Piccini, A., Loqui, D., Fogliarino, S., Forloni, G. and Tabaton, M. (2003) 'Pure spastic paraparesis associated with a novel presenilin 1 R278K mutation', *Neurology*, 60(1), pp. 150.
- Atamna, H. (2004) 'Heme, iron, and the mitochondrial decay of ageing', *Ageing Res Rev*, 3(3), pp. 303-18.
- Babcock, D. F., Herrington, J., Goodwin, P. C., Park, Y. B. and Hille, B. (1997) 'Mitochondrial participation in the intracellular Ca<sup>2+</sup> network', *J Cell Biol*, 136(4), pp. 833-44.
- Baekelandt, V., Eggermont, K., Michiels, M., Nuttin, B. and Debyser, Z. (2003) 'Optimized lentiviral vector production and purification procedure prevents immune response after transduction of mouse brain', *Gene Ther*, 10(23), pp. 1933-1940.
- Baker-Nigh, A., Vahedi, S., Davis, E. G., Weintraub, S., Bigio, E. H., Klein, W. L. and Geula, C. (2015) 'Neuronal amyloid- $\beta$  accumulation within cholinergic basal forebrain in ageing and Alzheimer's disease', *Brain*, 138(Pt 6), pp. 1722-37.
- Bales, K. R., Liu, F., Wu, S., Lin, S., Koger, D., DeLong, C., Hansen, J. C., Sullivan, P. M. and Paul, S. M. (2009) 'Human APOE isoform-dependent effects on brain beta-amyloid levels in PDAPP transgenic mice', *Journal of Neuroscience*, 29(21), pp. 6771-9.
- Bali, J., Gheinani, A. H., Zurbriggen, S. and Rajendran, L. (2012) 'Role of genes linked to sporadic Alzheimer's disease risk in the production of beta-amyloid peptides', *Proc Natl Acad Sci U S A*, 109(38), pp. 15307-11.
- Ballard, C. and Howard, R. (2006) 'Neuroleptic drugs in dementia: benefits and harm', *Nature Reviews Neuroscience*, 7(6), pp. 492-500.
- Balogh, E., Lengyel, Z., Emri, M., Szikszai, E., Esik, O., Kollár, J., Sikula, J., Trón, L. and Oláh, E. (2002) '[Cerebral glucose metabolism in Down syndrome using positron emission tomography]', *Orv Hetil*, 143(21 Suppl 3), pp. 1304-7.
- Barger, S. W. and Mattson, M. P. (1995) 'The secreted form of the Alzheimer's beta-amyloid precursor protein stimulates a membrane-associated guanylate cyclase', *Biochem J*, 311 ( Pt 1), pp. 45-7.
- Barnham, K. J. and Bush, A. I. (2008) 'Metals in Alzheimer's and Parkinson's diseases', *Curr Opin Chem Biol*, 12(2), pp. 222-8.
- Barnham, K. J., McKinstry, W. J., Multhaup, G., Galatis, D., Morton, C. J., Curtain, C. C., Williamson, N. A., White, A. R., Hinds, M. G., Norton, R. S., Beyreuther, K., Masters, C. L., Parker, M. W. and Cappai, R. (2003) 'Structure of the Alzheimer's disease amyloid precursor protein copper binding domain. A regulator of neuronal copper homeostasis', *Journal of Biological Chemistry*, 278(19), pp. 17401-7.
- Barone, E., Di Domenico, F., Sultana, R., Coccia, R., Mancuso, C., Perluigi, M. and Butterfield, D. A. (2012) 'Heme oxygenase-1 posttranslational modifications in the brain of subjects with Alzheimer disease and mild cognitive impairment', *Free Radic Biol Med*, 52(11-12), pp. 2292-301.
- Basi, G., Frigon, N., Barbour, R., Doan, T., Gordon, G., McConlogue, L., Sinha, S. and Zeller, M. (2003) 'Antagonistic effects of beta-site amyloid precursor protein-cleaving

enzymes 1 and 2 on beta-amyloid peptide production in cells', *J Biol Chem*, 278(34), pp. 31512-20.

Beach, T. G., Walker, R. and McGeer, E. G. (1989) 'Patterns of gliosis in Alzheimer's disease and aging cerebrum', *Glia*, 2(6), pp. 420-36.

Belyaev, N. D., Kellett, K. A., Beckett, C., Makova, N. Z., Revett, T. J., Nalivaeva, N. N., Hooper, N. M. and Turner, A. J. (2010) 'The transcriptionally active amyloid precursor protein (APP) intracellular domain is preferentially produced from the 695 isoform of APP in a {beta}-secretase-dependent pathway', *J Biol Chem*, 285(53), pp. 41443-54.

Belyaev, N. D., Nalivaeva, N. N., Makova, N. Z. and Turner, A. J. (2009) 'Nephrilysin gene expression requires binding of the amyloid precursor protein intracellular domain to its promoter: implications for Alzheimer disease', *EMBO Rep*, 10(1), pp. 94-100.

Benjannet, S., Elagoz, A., Wickham, L., Mamarbachi, M., Munzer, J. S., Basak, A., Lazure, C., Cromlish, J. A., Sisodia, S., Checler, F., Chretien, M. and Seidah, N. G. (2001) 'Post-translational processing of beta-secretase (beta-amyloid-converting enzyme) and its ectodomain shedding. The pro- and transmembrane/cytosolic domains affect its cellular activity and amyloid-beta production', *J Biol Chem*, 276(14), pp. 10879-87.

Bennett, B. D., Babu-Khan, S., Loeloff, R., Louis, J. C., Curran, E., Citron, M. and Vassar, R. (2000a) 'Expression analysis of BACE2 in brain and peripheral tissues', *J Biol Chem*, 275(27), pp. 20647-51.

Bennett, B. D., Denis, P., Haniu, M., Teplow, D. B., Kahn, S., Louis, J. C., Citron, M. and Vassar, R. (2000b) 'A furin-like convertase mediates propeptide cleavage of BACE, the Alzheimer's beta -secretase', *J Biol Chem*, 275(48), pp. 37712-7.

Bensadoun, J. C., Deglon, N., Tseng, J. L., Ridet, J. L., Zurn, A. D. and Aebischer, P. (2000) 'Lentiviral vectors as a gene delivery system in the mouse midbrain: cellular and behavioral improvements in a 6-OHDA model of Parkinson's disease using GDNF', *Exp Neurol*, 164(1), pp. 15-24.

Benzi, G., Pastoris, O., Marzatico, F., Villa, R. F., Dagani, F. and Curti, D. (1992) 'The mitochondrial electron transfer alteration as a factor involved in the brain aging', *Neurobiol Aging*, 13(3), pp. 361-8.

Berezovska, O., Lleo, A., Herl, L. D., Frosch, M. P., Stern, E. A., Bacskai, B. J. and Hyman, B. T. (2005) 'Familial Alzheimer's disease presenilin 1 mutations cause alterations in the conformation of presenilin and interactions with amyloid precursor protein', *Journal of Neuroscience*, 25(11), pp. 3009-17.

Berti, V., Osorio, R. S., Mosconi, L., Li, Y., De Santi, S. and de Leon, M. J. (2010) 'Early detection of Alzheimer's disease with PET imaging', *Neurodegener Dis*, 7(1-3), pp. 131-5.

Bhaskar, K., Yen, S. H. and Lee, G. (2005) 'Disease-related modifications in tau affect the interaction between Fyn and Tau', *J Biol Chem*, 280(42), pp. 35119-25.

Bhatia, R., Lin, H. and Lal, R. (2000) 'Fresh and globular amyloid beta protein (1-42) induces rapid cellular degeneration: evidence for AbetaP channel-mediated cellular toxicity', *Faseb Journal*, 14(9), pp. 1233-43.

Bhojak, T. J., DeKosky, S. T., Ganguli, M. and Kamboh, M. I. (2000) 'Genetic polymorphisms in the cathepsin D and interleukin-6 genes and the risk of Alzheimer's disease', *Neuroscience Letters*, 288(1), pp. 21-24.

Biedler, J. L., Roffler-Tarlov, S., Schachner, M. and Freedman, L. S. (1978) 'Multiple neurotransmitter synthesis by human neuroblastoma cell lines and clones', *Cancer Res*, 38(11 Pt 1), pp. 3751-7.

Billnitzer, A. J., Barskaya, I., Yin, C. and Perez, R. G. (2013) 'APP independent and dependent effects on neurite outgrowth are modulated by the receptor associated protein, RAP', *Journal of neurochemistry*, 124(1), pp. 123-132.

Bingham, E. M., Hopkins, D., Smith, D., Pernet, A., Hallett, W., Reed, L., Marsden, P. K. and Amiel, S. A. (2002) 'The role of insulin in human brain glucose metabolism: an 18fluoro-deoxyglucose positron emission tomography study', *Diabetes*, 51(12), pp. 3384-90.

Blalock, E. M., Geddes, J. W., Chen, K. C., Porter, N. M., Markesbery, W. R. and Landfield, P. W. (2004) 'Incipient Alzheimer's disease: microarray correlation analyses reveal major transcriptional and tumor suppressor responses', *Proc Natl Acad Sci U S A*, 101(7), pp. 2173-8.

Blázquez, E., Velázquez, E., Hurtado-Carneiro, V. and Ruiz-Albusac, J. M. (2014) 'Insulin in the brain: its pathophysiological implications for States related with central insulin resistance, type 2 diabetes and Alzheimer's disease', *Front Endocrinol (Lausanne)*, 5, pp. 161.

Blessed, G., Tomlinson, B. E. and Roth, M. (1968) 'The association between quantitative measures of dementia and of senile change in the cerebral grey matter of elderly subjects', *Br J Psychiatry*, 114(512), pp. 797-811.

Blurton-Jones, M., Kitazawa, M., Martinez-Coria, H., Castello, N. A., Muller, F. J., Loring, J. F., Yamasaki, T. R., Poon, W. W., Green, K. N. and LaFerla, F. M. (2009) 'Neural stem cells improve cognition via BDNF in a transgenic model of Alzheimer disease', *Proc Natl Acad Sci U S A*, 106(32), pp. 13594-9.

Bodovitz, S. and Klein, W. L. (1996) 'Cholesterol Modulates  $\beta$ -Secretase Cleavage of Amyloid Precursor Protein', *Journal of Biological Chemistry*, 271(8), pp. 4436-4440.

Bolanos, J. P., Almeida, A., Stewart, V., Peuchen, S., Land, J. M., Clark, J. B. and Heales, S. J. (1997) 'Nitric oxide-mediated mitochondrial damage in the brain: mechanisms and implications for neurodegenerative diseases', *J Neurochem*, 68(6), pp. 2227-40.

Boncrisiano, S., Calhoun, M. E., Kelly, P. H., Pfeifer, M., Bondolfi, L., Stalder, M., Phinney, A. L., Abramowski, D., Sturchler-Pierrat, C., Enz, A., Sommer, B., Staufenbiel, M. and Jucker, M. (2002) 'Cholinergic changes in the APP23 transgenic mouse model of cerebral amyloidosis', *J Neurosci*, 22(8), pp. 3234-43.

Borg, J. P., Ooi, J., Levy, E. and Margolis, B. (1996) 'The phosphotyrosine interaction domains of X11 and FE65 bind to distinct sites on the YENPTY motif of amyloid precursor protein', *Molecular and Cellular Biology*, 16(11), pp. 6229-41.

Bosman, G. J., Bartholomeus, I. G., de Man, A. J., van Kalmthout, P. J. and de Grip, W. J. (1991) 'Erythrocyte membrane characteristics indicate abnormal cellular aging in patients with Alzheimer's disease', *Neurobiol Aging*, 12(1), pp. 13-8.

Botelho, M. G., Wang, X., Arndt-Jovin, D. J., Becker, D. and Jovin, T. M. (2010) 'Induction of terminal differentiation in melanoma cells on downregulation of beta-amyloid precursor protein', *J Invest Dermatol*, 130(5), pp. 1400-10.

Bour, A., Little, S., Dodart, J. C., Kelche, C. and Mathis, C. (2004) 'A secreted form of the beta-amyloid precursor protein (sAPP695) improves spatial recognition memory in OF1 mice', *Neurobiol Learn Mem*, 81(1), pp. 27-38.

Bourre, J. M. (2010) 'Diet, Brain Lipids, and Brain Functions: Polyunsaturated Fatty Acids, Mainly Omega-3 Fatty Acids', in Lajtha, A., Tettamanti, G. & Goracci, G. (eds.) *Handbook of Neurochemistry and Molecular Neurobiology*: Springer US, pp. 409-441.

Braak, H. and Braak, E. (1991) 'Neuropathological staging of Alzheimer-related changes', *Acta Neuropathologica*, 82(4), pp. 239-59.

Braak, H. and Braak, E. (1995) 'Staging of Alzheimer's disease-related neurofibrillary changes', *Neurobiol Aging*, 16(3), pp. 271-8; discussion 278-84.

Braak, H., Braak, E. and Bohl, J. (1993) 'Staging of Alzheimer-related cortical destruction', *Eur Neurol*, 33, pp. 403 - 408.

Brand, M. D. and Nicholls, D. G. (2011) 'Assessing mitochondrial dysfunction in cells', *Biochem J*, 435(2), pp. 297-312.

Brewer, G. J., Torricelli, J. R., Evege, E. K. and Price, P. J. (1993) 'Optimized survival of hippocampal neurons in B27-supplemented Neurobasal, a new serum-free medium combination', *J Neurosci Res*, 35(5), pp. 567-76.

Brody, D. L., Magnoni, S., Schwetye, K. E., Spinner, M. L., Esparza, T. J., Stocchetti, N., Zipfel, G. J. and Holtzman, D. M. (2008) 'Amyloid- $\beta$  Dynamics Correlate with Neurological Status in the Injured Human Brain', *Science*, 321(5893), pp. 1221-1224.

Brookes, P. S., Levonen, A. L., Shiva, S., Sarti, P. and Darley-Usmar, V. M. (2002) 'Mitochondria: regulators of signal transduction by reactive oxygen and nitrogen species', *Free Radic Biol Med*, 33(6), pp. 755-64.

Brookes, P. S., Yoon, Y., Robotham, J. L., Anders, M. W. and Sheu, S. S. (2004) 'Calcium, ATP, and ROS: a mitochondrial love-hate triangle', *Am J Physiol Cell Physiol*, 287(4), pp. C817-33.

Brown, G. and Bal-Price, A. (2003) 'Inflammatory neurodegeneration mediated by nitric oxide, glutamate, and mitochondria', *Molecular Neurobiology*, 27(3), pp. 325-355.

Bruel, A., Cherqui, G., Columelli, S., Margelin, D., Roudier, M., Sinet, P. M., Prieur, M., Perignon, J. L. and Delabar, J. (1991) 'Reduced protein kinase C activity in sporadic Alzheimer's disease fibroblasts', *Neurosci Lett*, 133(1), pp. 89-92.

Brunden, K. R., Trojanowski, J. Q. and Lee, V. M. (2009) 'Advances in tau-focused drug discovery for Alzheimer's disease and related tauopathies', *Nat Rev Drug Discov*, 8(10), pp. 783-93.

Busciglio, J. and Yankner, B. A. (1995) 'Apoptosis and increased generation of reactive oxygen species in Down's syndrome neurons in vitro', *Nature*, 378(6559), pp. 776-9.

Butterfield, D. A., Howard, B., Yatin, S., Koppal, T., Drake, J., Hensley, K., Aksenov, M., Aksenova, M., Subramaniam, R., Varadarajan, S., Harris-White, M. E., Pedigo, N. W. and Carney, J. M. (1999) 'Elevated oxidative stress in models of normal brain aging and Alzheimer's disease', *Life Sci*, 65(18-19), pp. 1883-92.

Butterfield, D. A. and Lauderback, C. M. (2002) 'Lipid peroxidation and protein oxidation in Alzheimer's disease brain: potential causes and consequences involving amyloid beta-peptide-associated free radical oxidative stress', *Free Radic Biol Med*, 32(11), pp. 1050-60.

Buxbaum, J. (1998) 'Evidence that tumor necrosis factor alpha converting enzyme is involved in regulated alpha-secretase cleavage of the Alzheimer amyloid protein precursor', *J Biol Chem*, 273(43), pp. 27765 - 7.

Buxbaum, J. D., Koo, E. H. and Greengard, P. (1993) 'Protein phosphorylation inhibits production of Alzheimer amyloid beta/A4 peptide', *Proc Natl Acad Sci U S A*, 90(19), pp. 9195-8.

Calabrese, V., Sultana, R., Scapagnini, G., Guagliano, E., Sapienza, M., Bella, R., Kanski, J., Pennisi, G., Mancuso, C., Stella, A. M. and Butterfield, D. A. (2006) 'Nitrosative stress, cellular stress response, and thiol homeostasis in patients with Alzheimer's disease', *Antioxid Redox Signal*, 8(11-12), pp. 1975-86.

Calero, M., Rostagno, A., Frangione, B. and Ghiso, J. (2005) 'Clusterin and Alzheimer's disease', *Subcell Biochem*, 38, pp. 273-98.

Castello, M. A., Jeppson, J. D. and Soriano, S. (2014) 'Moving beyond anti-amyloid therapy for the prevention and treatment of Alzheimer's disease', *BMC Neurol*, 14, pp. 169.

Chance, B. and Williams, G. R. (1955) 'Respiratory enzymes in oxidative phosphorylation. I. Kinetics of oxygen utilization', *J Biol Chem*, 217(1), pp. 383-93.

Chartier-Harlin, M. C., Crawford, F., Houlden, H., Warren, A., Hughes, D., Fidani, L., Goate, A., Rossor, M., Roques, P., Hardy, J. and et al. (1991) 'Early-onset Alzheimer's disease caused by mutations at codon 717 of the beta-amyloid precursor protein gene', *Nature*, 353(6347), pp. 844-6.

Chen, C. and Xiao, S. F. (2011) 'Induced pluripotent stem cells and neurodegenerative diseases', *Neurosci Bull*, 27(2), pp. 107-14.

Chen, F., David, D., Ferrari, A. and Gotz, J. (2004) 'Posttranslational modifications of tau--role in human tauopathies and modeling in transgenic animals', *Curr Drug Targets*, 5(6), pp. 503-15.

Chen, G., Huang, L. D., Jiang, Y. M. and Manji, H. K. (1999) 'The mood-stabilizing agent valproate inhibits the activity of glycogen synthase kinase-3', *J Neurochem*, 72(3), pp. 1327-30.

Chen, M., Inestrosa, N. C., Ross, G. S. and Fernandez, H. L. (1995) 'Platelets are the primary source of amyloid beta-peptide in human blood', *Biochem Biophys Res Commun*, 213(1), pp. 96-103.

Chen, W. J., Goldstein, J. L. and Brown, M. S. (1990) 'NPXY, a sequence often found in cytoplasmic tails, is required for coated pit-mediated internalization of the low density lipoprotein receptor', *Journal of Biological Chemistry*, 265(6), pp. 3116-23.

- Chen, Y. and Dong, C. (2009) 'Aβ40 promotes neuronal cell fate in neural progenitor cells', *Cell Death Differ*, 16(3), pp. 386-94.
- Chen, Z. and Zhong, C. (2013) 'Decoding Alzheimer's disease from perturbed cerebral glucose metabolism: implications for diagnostic and therapeutic strategies', *Prog Neurobiol*, 108, pp. 21-43.
- Cheung, Y. T., Lau, W. K., Yu, M. S., Lai, C. S., Yeung, S. C., So, K. F. and Chang, R. C. (2009) 'Effects of all-trans-retinoic acid on human SH-SY5Y neuroblastoma as in vitro model in neurotoxicity research', *Neurotoxicology*, 30(1), pp. 127-35.
- Chin, J., Palop, J. J., Puolivali, J., Massaro, C., Bien-Ly, N., Gerstein, H., Searce-Levie, K., Masliah, E. and Mucke, L. (2005) 'Fyn kinase induces synaptic and cognitive impairments in a transgenic mouse model of Alzheimer's disease', *J Neurosci*, 25(42), pp. 9694-703.
- Choi, K. H., Basma, H., Singh, J. and Cheng, P. W. (2005) 'Activation of CMV promoter-controlled glycosyltransferase and beta-galactosidase glycozymes by butyrate, trichostatin A, and 5-aza-2'-deoxycytidine', *Glycoconj J*, 22(1-2), pp. 63-9.
- Ciani, E., Groneng, L., Voltattorni, M., Rolseth, V., Contestabile, A. and Paulsen, R. E. (1996) 'Inhibition of free radical production or free radical scavenging protects from the excitotoxic cell death mediated by glutamate in cultures of cerebellar granule neurons', *Brain Res*, 728(1), pp. 1-6.
- Citron, M., Oltersdorf, T., Haass, C., McConlogue, L., Hung, A. Y., Seubert, P., Vigo-Pelfrey, C., Lieberburg, I. and Selkoe, D. J. (1992) 'Mutation of the beta-amyloid precursor protein in familial Alzheimer's disease increases beta-protein production', *Nature*, 360(6405), pp. 672-4.
- Citron, M., Teplow, D. B. and Selkoe, D. J. (1995) 'Generation of amyloid beta protein from its precursor is sequence specific', *Neuron*, 14(3), pp. 661-70.
- Citron, M., Vigo-Pelfrey, C., Teplow, D. B., Miller, C., Schenk, D., Johnston, J., Winblad, B., Venizelos, N., Lannfelt, L. and Selkoe, D. J. (1994) 'Excessive production of amyloid beta-protein by peripheral cells of symptomatic and presymptomatic patients carrying the Swedish familial Alzheimer disease mutation', *Proc Natl Acad Sci U S A*, 91(25), pp. 11993-7.
- Citron, M., Westaway, D., Xia, W., Carlson, G., Diehl, T., Levesque, G., Johnson-wood, K., Lee, M., Seubert, P., Davis, A., Kholodenko, D., Motter, R., Sherrington, R., Perry, B., Yao, H., Strome, R., Lieberburg, I., Rommens, J., Kim, S., Schenk, D., Fraser, P., St George Hyslop, P. and Selkoe, D. J. (1997) 'Mutant presenilins of Alzheimer's disease increase production of 42-residue amyloid [beta]-protein in both transfected cells and transgenic mice', *Nature Medicine*, 3(1), pp. 67-72.
- Clark, R. F., Hutton, M., Fuldner, M., Froelich, S., Karran, E., Talbot, C., Crook, R., Lendon, C., Prihar, G., He, C., Korenblatt, K., Martinez, A., Wragg, M., Busfield, F., Behrens, M. I., Myers, A., Norton, J., Morris, J., Mehta, N., Pearson, C., Lincoln, S., Baker, M., Duff, K., Zehr, C., Perez-Tur, J., Houlden, H., Ruiz, A., Ossa, J., Lopera, F., Arcos, M., Madrigal, L., Collinge, J., Humphreys, C., Ashworth, A., Sarnes, S., Fox, N., Harvey, R., Kennedy, A., Roques, P., Cline, R. T., Phillips, C. A., Venter, J. C., Forsell, L., Axelman, K., Lilius, L., Johnston, J., Cowburn, R., Viitanen, M., Winblad, B., Kosik, K., Haltia, M., Poyhonen, M., Dickson, D., Mann, D., Neary, D., Snowden, J., Lantos, P., Lannfelt, L., Rossor, M., Roberts, G. W., Adams, M. D., Hardy, J. and Goate, A. (1995) 'The structure of the presenilin 1 (S182) gene and identification of six novel mutations in early onset AD families', *Nat Genet*, 11(2), pp. 219-222.
- Clarris, H. J., Cappai, R., Heffernan, D., Beyreuther, K., Masters, C. L. and Small, D. H. (1997) 'Identification of heparin-binding domains in the amyloid precursor protein of Alzheimer's disease by deletion mutagenesis and peptide mapping', *J Neurochem*, 68(3), pp. 1164-72.
- Clementi, M., Sampaolese, B., Triggiani, D., Tiezzi, A. and Giardina, B. (2013) 'S100b protects IMR-32 cells against Ab(1-42) induced neurotoxicity via modulation of apoptotic genes expression', *Advances in Alzheimer's Disease*, 2, pp. 9.
- Coburger, I., Dahms, S. O., Roeser, D., Gührs, K.-H., Hortschansky, P. and Than, M. E. (2013) 'Analysis of the Overall Structure of the Multi-Domain Amyloid Precursor Protein (APP)', *PLoS ONE*, 8(12), pp. e81926.

Cole, S. L. and Vassar, R. (2007a) 'The Alzheimer's disease beta-secretase enzyme, BACE1', *Molecular Neurodegeneration*, 2, pp. 22.

Cole, S. L. and Vassar, R. (2007b) 'The Alzheimer's disease beta-secretase enzyme, BACE1', *Mol Neurodegener*, 2, pp. 22.

Conti, A., Fabbrini, F., D'Agostino, P., Negri, R., Greco, D., Genesio, R., D'Armiento, M., Olla, C., Paladini, D., Zannini, M. and Nitsch, L. (2007) 'Altered expression of mitochondrial and extracellular matrix genes in the heart of human fetuses with chromosome 21 trisomy', *BMC Genomics*, 8, pp. 268.

Coon, K. D., Myers, A. J., Craig, D. W., Webster, J. A., Pearson, J. V., Lince, D. H., Zismann, V. L., Beach, T. G., Leung, D., Bryden, L., Halperin, R. F., Marlowe, L., Kaleem, M., Walker, D. G., Ravid, R., Heward, C. B., Rogers, J., Papassotiropoulos, A., Reiman, E. M., Hardy, J. and Stephan, D. A. (2007) 'A high-density whole-genome association study reveals that APOE is the major susceptibility gene for sporadic late-onset Alzheimer's disease', *J Clin Psychiatry*, 68(4), pp. 613-8.

Cornejo, V. H. and Hetz, C. (2013) 'The unfolded protein response in Alzheimer's disease', *Semin Immunopathol*, 35(3), pp. 277-92.

Cotman, C. W. and Su, J. H. (1996) 'Mechanisms of neuronal death in Alzheimer's disease', *Brain Pathol*, 6(4), pp. 493-506.

Cousins, S. L., Dai, W. and Stephenson, F. A. (2015) 'APLP1 and APLP2, members of the APP family of proteins, behave similarly to APP in that they associate with NMDA receptors and enhance NMDA receptor surface expression', *J Neurochem*, 133(6), pp. 879-85.

Crehan, H., Holton, P., Wray, S., Pocock, J., Guerreiro, R. and Hardy, J. (2012) 'Complement receptor 1 (CR1) and Alzheimer's disease', *Immunobiology*, 217(2), pp. 244-50.

Cruts, M., Theuns, J. and Van Broeckhoven, C. (2012) 'Locus-specific mutation databases for neurodegenerative brain diseases', *Hum Mutat*, 33(9), pp. 1340-4.

Cummings, J., Morstorf, T. and Zhong, K. (2014) 'Alzheimer's disease drug-development pipeline: few candidates, frequent failures', *Alzheimer's Research & Therapy*, 6(4), pp. 37.

Curti, D., Rognoni, F., Gasparini, L., Cattaneo, A., Paolillo, M., Racchi, M., Zani, L., Bianchetti, A., Trabucchi, M., Bergamaschi, S. and Govoni, S. (1997) 'Oxidative metabolism in cultured fibroblasts derived from sporadic Alzheimer's disease (AD) patients', *Neuroscience Letters*, 236(1), pp. 13-6.

Czech, C., Tremp, G. and Pradier, L. (2000) 'Presenilins and Alzheimer's disease: Biological functions and pathogenic mechanisms', *Progress in Neurobiology*, 60(4), pp. 363-384.

Daffner, K. R. (2010) 'Promoting successful cognitive aging: a comprehensive review', *J Alzheimers Dis*, 19(4), pp. 1101-22.

Daigle, I. and Li, C. (1993) 'apl-1, a Caenorhabditis elegans gene encoding a protein related to the human beta-amyloid protein precursor', *Proc Natl Acad Sci U S A*, 90(24), pp. 12045-9.

Davis, R. E., Miller, S., Herrnsstadt, C., Ghosh, S. S., Fahy, E., Shinobu, L. A., Galasko, D., Thal, L. J., Beal, M. F., Howell, N. and Parker, W. D. (1997a) 'Mutations in mitochondrial cytochrome c oxidase genes segregate with late-onset Alzheimer disease', *Proceedings of the National Academy of Sciences of the United States of America*, 94(9), pp. 4526-4531.

Davis, R. E., Miller, S., Herrnsstadt, C., Ghosh, S. S., Fahy, E., Shinobu, L. A., Galasko, D., Thal, L. J., Beal, M. F., Howell, N. and Parker, W. D., Jr. (1997b) 'Mutations in mitochondrial cytochrome c oxidase genes segregate with late-onset Alzheimer disease', *Proc Natl Acad Sci U S A*, 94(9), pp. 4526-31.

de Almeida, L. P., Zala, D., Aebischer, P. and Deglon, N. (2001) 'Neuroprotective effect of a CNTF-expressing lentiviral vector in the quinolinic acid rat model of Huntington's disease', *Neurobiol Dis*, 8(3), pp. 433-46.

De Jonghe, C., Esselens, C., Kumar-Singh, S., Craessaerts, K., Serneels, S., Checler, F., Annaert, W., Van Broeckhoven, C. and De Strooper, B. (2001) 'Pathogenic APP

mutations near the gamma-secretase cleavage site differentially affect Abeta secretion and APP C-terminal fragment stability', *Hum Mol Genet*, 10(16), pp. 1665-71.

De Jonghe, C., MarcCruts, Rogaeva, E. A., Tysoe, C., Singleton, A., Vanderstichele, H., Meschino, W., Dermaut, B., Vanderhoeven, I., Backhovens, H., Vanmechelen, E., Morris, C. M., Hardy, J., Rubinsztein, D. C., St George-Hyslop, P. H. and Van Broeckhoven, C. (1999) 'Aberrant Splicing in the Presenilin-1 Intron 4 Mutation Causes Presenile Alzheimer's Disease by Increased A $\beta$ 42 Secretion', *Human Molecular Genetics*, 8(8), pp. 1529-1540.

De Keulenaer, G. W., Chappell, D. C., Ishizaka, N., Nerem, R. M., Alexander, R. W. and Griendling, K. K. (1998) 'Oscillatory and steady laminar shear stress differentially affect human endothelial redox state: role of a superoxide-producing NADH oxidase', *Circ Res*, 82(10), pp. 1094-101.

de la Monte, S. M. and Wands, J. R. (2008) 'Alzheimer's Disease Is Type 3 Diabetes—Evidence Reviewed', *Journal of diabetes science and technology (Online)*, 2(6), pp. 1101-1113.

De Strooper, B., Beullens, M., Contreras, B., Levesque, L., Craessaerts, K., Cordell, B., Moechars, D., Bollen, M., Fraser, P., St. George-Hyslop, P. and Van Leuven, F. (1997) 'Phosphorylation, Subcellular Localization, and Membrane Orientation of the Alzheimer's Disease-associated Presenilins', *Journal of Biological Chemistry*, 272(6), pp. 3590-3598.

De Strooper, B., Saftig, P., Craessaerts, K., Vanderstichele, H., Guhde, G., Annaert, W., Von Figura, K. and Van Leuven, F. (1998) 'Deficiency of presenilin-1 inhibits the normal cleavage of amyloid precursor protein', *Nature*, 391(6665), pp. 387-90.

de Wert, G. and Mummery, C. (2003) 'Human embryonic stem cells: research, ethics and policy', *Hum Reprod*, 18(4), pp. 672-82.

Di, X., Yan, J., Zhao, Y., Zhang, J., Shi, Z., Chang, Y. and Zhao, B. (2010) 'L-theanine protects the APP (Swedish mutation) transgenic SH-SY5Y cell against glutamate-induced excitotoxicity via inhibition of the NMDA receptor pathway', *Neuroscience*, 168(3), pp. 778-86.

Dickson, D. W. (1997) 'The pathogenesis of senile plaques', *J Neuropathol Exp Neurol*, 56(4), pp. 321-39.

Dissen, G. A., Lomniczi, A., Neff, T. L., Hobbs, T. R., Kohama, S. G., Kroenke, C. D., Galimi, F. and Ojeda, S. R. (2009) 'In vivo manipulation of gene expression in non-human primates using lentiviral vectors as delivery vehicles', *Methods*, 49(1), pp. 70-7.

Dixon, S. J. and Stockwell, B. R. (2014) 'The role of iron and reactive oxygen species in cell death', *Nat Chem Biol*, 10(1), pp. 9-17.

Dringen, R. (2000) 'Metabolism and functions of glutathione in brain', *Prog Neurobiol*, 62(6), pp. 649-71.

Drubin, D. G., Feinstein, S. C., Shooter, E. M. and Kirschner, M. W. (1985) 'Nerve growth factor-induced neurite outgrowth in PC12 cells involves the coordinate induction of microtubule assembly and assembly-promoting factors', *J Cell Biol*, 101(5 Pt 1), pp. 1799-807.

Du, H., Guo, L. and Yan, S. S. (2012) 'Synaptic Mitochondrial Pathology in Alzheimer's Disease', *Antioxidants & Redox Signaling*, 16(12), pp. 1467-1475.

Duara, R., Lopez-Alberola, R. F., Barker, W. W., Loewenstein, D. A., Zatinsky, M., Eisdorfer, C. E. and Weinberg, G. B. (1993) 'A comparison of familial and sporadic Alzheimer's disease', *Neurology*, 43(7), pp. 1377-84.

Dubois, B., Feldman, H. H., Jacova, C., DeKosky, S. T., Barberger-Gateau, P., Cummings, J., Delacourte, A., Galasko, D., Gauthier, S., Jicha, G., Meguro, K., O'Brien, J., Pasquier, F., Robert, P., Rossor, M., Salloway, S., Stern, Y., Visser, P. J. and Scheltens, P. (2007) 'Research criteria for the diagnosis of Alzheimer's disease: revising the NINCDS-ADRDA criteria', *Lancet Neurology*, 6(8), pp. 734-746.

Duce, J. A., Tsatsanis, A., Cater, M. A., James, S. A., Robb, E., Wikke, K., Leong, S. L., Perez, K., Johanssen, T., Greenough, M. A., Cho, H.-H., Galatis, D., Moir, R. D., Masters, C. L., McLean, C., Tanzi, R. E., Cappai, R., Barnham, K. J., Ciccotosto, G. D., Rogers, J. T. and Bush, A. I. (2010a) 'An iron-export ferroxidase activity of  $\beta$ -amyloid protein precursor is inhibited by zinc in Alzheimer's Disease', *Cell*, 142(6), pp. 857-867.

Duce, J. A., Tsatsanis, A., Cater, M. A., James, S. A., Robb, E., Wikhe, K., Leong, S. L., Perez, K., Johanssen, T., Greenough, M. A., Cho, H. H., Galatis, D., Moir, R. D., Masters, C. L., McLean, C., Tanzi, R. E., Cappai, R., Barnham, K. J., Ciccotosto, G. D., Rogers, J. T. and Bush, A. I. (2010b) 'Iron-export ferroxidase activity of beta-amyloid precursor protein is inhibited by zinc in Alzheimer's disease', *Cell*, 142(6), pp. 857-67.

Duff, K., Eckman, C., Zehr, C., Yu, X., Prada, C. M., Perez-tur, J., Hutton, M., Buee, L., Harigaya, Y., Yager, D., Morgan, D., Gordon, M. N., Holcomb, L., Refolo, L., Zenk, B., Hardy, J. and Younkin, S. (1996) 'Increased amyloid-beta42(43) in brains of mice expressing mutant presenilin 1', *Nature*, 383(6602), pp. 710-3.

Dumanchin, C., Brice, A., Campion, D., Hannequin, D., Martin, C., Moreau, V., Agid, Y., Martinez, M., Clerget-Darpoux, F. and Frebourg, T. (1998) 'De novo presenilin 1 mutations are rare in clinically sporadic, early onset Alzheimer's disease cases. French Alzheimer's Disease Study Group', *J Med Genet*, 35(8), pp. 672-3.

Dysken, M. W., Sano, M., Asthana, S. and et al. (2014) 'Effect of vitamin e and memantine on functional decline in alzheimer disease: The team-ad va cooperative randomized trial', *JAMA*, 311(1), pp. 33-44.

Ebsen, H., Schröder, A., Kabelitz, D. and Janssen, O. (2013) 'Differential surface expression of ADAM10 and ADAM17 on human T lymphocytes and tumor cells', *PLoS One*, 8(10), pp. e76853.

Eckert, A., Hartmann, H., Forstl, H. and Muller, W. E. (1994) 'Alterations of intracellular calcium regulation during aging and Alzheimer's disease in nonneuronal cells', *Life Sci*, 55(25-26), pp. 2019-29.

Eggert, S., Paliga, K., Soba, P., Evin, G., Masters, C. L., Weidemann, A. and Beyreuther, K. (2004) 'The proteolytic processing of the amyloid precursor protein gene family members APLP-1 and APLP-2 involves alpha-, beta-, gamma-, and epsilon-like cleavages: modulation of APLP-1 processing by n-glycosylation', *J Biol Chem*, 279(18), pp. 18146-56.

Eikelenboom, P. and Veerhuis, R. (1996) 'The role of complement and activated microglia in the pathogenesis of Alzheimer's disease', *Neurobiol Aging*, 17(5), pp. 673-80.

Eketjall, S., Janson, J., Jeppsson, F., Svanhagen, A., Kolmodin, K., Gustavsson, S., Radesater, A. C., Eliason, K., Briem, S., Appelkvist, P., Niva, C., Berg, A. L., Karlstrom, S., Swahn, B. M. and Falting, J. (2013) 'AZ-4217: a high potency BACE inhibitor displaying acute central efficacy in different in vivo models and reduced amyloid deposition in Tg2576 mice', *J Neurosci*, 33(24), pp. 10075-84.

El Messari, S., Leloup, C., Quignon, M., Brisorgueil, M. J., Penicaud, L. and Arluison, M. (1998) 'Immunocytochemical localization of the insulin-responsive glucose transporter 4 (Glut4) in the rat central nervous system', *J Comp Neurol*, 399(4), pp. 492-512.

Elder, G. A., Gama Sosa, M. A. and De Gasperi, R. (2010) 'Transgenic Mouse Models of Alzheimer's Disease', *Mount Sinai Journal of Medicine: A Journal of Translational and Personalized Medicine*, 77(1), pp. 69-81.

Ellison, D. W., Beal, M. F., Mazurek, M. F., Bird, E. D. and Martin, J. B. (1986) 'A postmortem study of amino acid neurotransmitters in Alzheimer's disease', *Annals of Neurology*, 20(5), pp. 616-621.

Elshourbagy, N. A., Liao, W. S., Mahley, R. W. and Taylor, J. M. (1985) 'Apolipoprotein E mRNA is abundant in the brain and adrenals, as well as in the liver, and is present in other peripheral tissues of rats and marmosets', *Proceedings of the National Academy of Sciences of the United States of America*, 82(1), pp. 203-207.

Encinas, M., Iglesias, M., Liu, Y., Wang, H., Muhaisen, A., Ceña, V., Gallego, C. and Comella, J. X. (2000) 'Sequential Treatment of SH-SY5Y Cells with Retinoic Acid and Brain-Derived Neurotrophic Factor Gives Rise to Fully Differentiated, Neurotrophic Factor-Dependent, Human Neuron-Like Cells', *Journal of Neurochemistry*, 75(3), pp. 991-1003.

Epis, R., Marcello, E., Gardoni, F. and Di Luca, M. (2012) 'Alpha, beta-and gamma-secretases in Alzheimer's disease', *Front Biosci (Schol Ed)*, 4, pp. 1126-50.

Etcheberrigaray, R., Ito, E., Oka, K., Tofel-Grehl, B., Gibson, G. E. and Alkon, D. L. (1993) 'Potassium channel dysfunction in fibroblasts identifies patients with Alzheimer disease', *Proceedings of the National Academy of Sciences of the United States of America*, 90(17), pp. 8209-8213.

Evin, G. and Kenche, V. B. (2007) 'BACE inhibitors as potential therapeutics for Alzheimer's disease', *Recent Pat CNS Drug Discov*, 2(3), pp. 188-99.

Exley, C., House, E., Polwart, A. and Esiri, M. M. (2012) 'Brain burdens of aluminum, iron, and copper and their relationships with amyloid-beta pathology in 60 human brains', *J Alzheimers Dis*, 31(4), pp. 725-730.

Fang, B., Jia, L. and Jia, J. (2006) 'Chinese Presenilin-1 V97L mutation enhanced Abeta42 levels in SH-SY5Y neuroblastoma cells', *Neurosci Lett*, 406(1-2), pp. 33-7.

Farlow, M. R. (2004) 'NMDA receptor antagonists. A new therapeutic approach for Alzheimer's disease', *Geriatrics*, 59(6), pp. 22-7.

Farquhar, M. J., Gray, C. W. and Breen, K. C. (2003) 'The over-expression of the wild type or mutant forms of the presenilin-1 protein alters glycoprotein processing in a human neuroblastoma cell line', *Neuroscience Letters*, 346(1-2), pp. 53-6.

Farr, S. A., Poon, H. F., Dogrukol-Ak, D., Drake, J., Banks, W. A., Eyerman, E., Butterfield, D. A. and Morley, J. E. (2003) 'The antioxidants alpha-lipoic acid and N-acetylcysteine reverse memory impairment and brain oxidative stress in aged SAMP8 mice', *J Neurochem*, 84(5), pp. 1173-83.

Feng, X., Zhao, P., He, Y. and Zuo, Z. (2006) 'Allele-specific silencing of Alzheimer's disease genes: The amyloid precursor protein genes with Swedish or London mutations', *Gene*, 371(1), pp. 68-74.

Fischer, O. 1907. Miliare Nekrosen mit drusigen Wucherungen der Neurofibrillen, eine regelmässige Veränderung der Hirnrinde bei seniler Demenz. *Monatsschr Psychiat Neurol*.

Folstein, M. F., Folstein, S. E. and McHugh, P. R. (1975) "'Mini-mental state". A practical method for grading the cognitive state of patients for the clinician', *J Psychiatr Res*, 12(3), pp. 189-98.

Freude, K. K., Penjwini, M., Davis, J. L., LaFerla, F. M. and Blurton-Jones, M. (2011) 'Soluble amyloid precursor protein induces rapid neural differentiation of human embryonic stem cells', *J Biol Chem*, 286(27), pp. 24264-74.

Galloway, S., Jian, L., Johnsen, R., Chew, S. and Mamo, J. C. L. (2007) 'β-Amyloid or its precursor protein is found in epithelial cells of the small intestine and is stimulated by high-fat feeding', *Journal of Nutritional Biochemistry*, 18(4), pp. 279-284.

Games, D., Adams, D., Alessandrini, R., Barbour, R., Berthelette, P., Blackwell, C., Carr, T., Clemens, J., Donaldson, T., Gillespie, F. and et al. (1995) 'Alzheimer-type neuropathology in transgenic mice overexpressing V717F beta-amyloid precursor protein', *Nature*, 373(6514), pp. 523-7.

Garthwaite, J. (1991) 'Glutamate, nitric oxide and cell-cell signalling in the nervous system', *Trends in Neurosciences*, 14(2), pp. 60-67.

Gasparini, L., Racchi, M., Binetti, G., Trabucchi, M., Solerte, S. B., Alkon, D., Etcheberrigaray, R., Gibson, G., Blass, J., Paoletti, R. and Govoni, S. (1998) 'Peripheral markers in testing pathophysiological hypotheses and diagnosing Alzheimer's disease', *Faseb j*, 12(1), pp. 17-34.

Gatta, L. B., Albertini, A., Ravid, R. and Finazzi, D. (2002) 'Levels of beta-secretase BACE and alpha-secretase ADAM10 mRNAs in Alzheimer hippocampus', *Neuroreport*, 13(16), pp. 2031-3.

Georgopoulou, N., McLaughlin, M., McFarlane, I. and Breen, K. C. (2001) 'The role of post-translational modification in beta-amyloid precursor protein processing', *Biochem Soc Symp*, (67), pp. 23-36.

Ghiso, J., Rostagno, A., Gardella, J. E., Liem, L., Gorevic, P. D. and Frangione, B. (1992) 'A 109-amino-acid C-terminal fragment of Alzheimer's-disease amyloid precursor protein contains a sequence, -RHDS-, that promotes cell adhesion', *Biochem J*, 288 ( Pt 3), pp. 1053-9.

- Gibson, G., Martins, R., Blass, J. and Gandy, S. (1996) 'Altered oxidation and signal transduction systems in fibroblasts from Alzheimer patients', *Life Sci*, 59(5-6), pp. 477-89.
- Gibson, G. E., Sheu, K. F. and Blass, J. P. (1998) 'Abnormalities of mitochondrial enzymes in Alzheimer disease', *J Neural Transm (Vienna)*, 105(8-9), pp. 855-70.
- Gimenez-Cassina, A., Lim, F. and Diaz-Nido, J. (2006) 'Differentiation of a human neuroblastoma into neuron-like cells increases their susceptibility to transduction by herpesviral vectors', *J Neurosci Res*, 84(4), pp. 755-67.
- Giuffrida, M. L., Caraci, F., Pignataro, B., Cataldo, S., De Bona, P., Bruno, V., Molinaro, G., Pappalardo, G., Messina, A., Palmigiano, A., Garozzo, D., Nicoletti, F., Rizzarelli, E. and Copani, A. (2009) 'Beta-amyloid monomers are neuroprotective', *J Neurosci*, 29(34), pp. 10582-7.
- Glenner, G. G. and Wong, C. W. (1984a) 'Alzheimer's disease and Down's syndrome: Sharing of a unique cerebrovascular amyloid fibril protein', *Biochemical and Biophysical Research Communications*, 122(3), pp. 1131-1135.
- Glenner, G. G. and Wong, C. W. (1984b) 'Alzheimer's disease: initial report of the purification and characterization of a novel cerebrovascular amyloid protein', *Biochem Biophys Res Commun*, 120(3), pp. 885-90.
- Goate, A., Chartier-Harlin, M. C., Mullan, M., Brown, J., Crawford, F., Fidani, L., Giuffra, L., Haynes, A., Irving, N., James, L. and et al. (1991) 'Segregation of a missense mutation in the amyloid precursor protein gene with familial Alzheimer's disease', *Nature*, 349(6311), pp. 704-6.
- Godbolt, A. K., Beck, J. A., Collinge, J., Garrard, P., Warren, J. D., Fox, N. C. and Rossor, M. N. (2004) 'A presenilin 1 R278I mutation presenting with language impairment', *Neurology*, 63(9), pp. 1702-4.
- Golde, T. E., Estus, S., Usiak, M., Younkin, L. H. and Younkin, S. G. (1990) 'Expression of beta amyloid protein precursor mRNAs: recognition of a novel alternatively spliced form and quantitation in Alzheimer's disease using PCR', *Neuron*, 4(2), pp. 253-67.
- Goll, D. E., Thompson, V. F., Li, H., Wei, W. and Cong, J. (2003) 'The calpain system', *Physiol Rev*, 83(3), pp. 731-801.
- Gong, C. X. and Iqbal, K. (2008) 'Hyperphosphorylation of Microtubule-Associated Protein Tau: A Promising Therapeutic Target for Alzheimer Disease', *Current medicinal chemistry*, 15(23), pp. 2321-2328.
- Goodall, A. R., Danks, K., Walker, J. H., Ball, S. G. and Vaughan, P. F. (1997) 'Occurrence of two types of secretory vesicles in the human neuroblastoma SH-SY5Y', *J Neurochem*, 68(4), pp. 1542-52.
- Goodman, Y. and Mattson, M. P. (1994) 'Secreted forms of beta-amyloid precursor protein protect hippocampal neurons against amyloid beta-peptide-induced oxidative injury', *Exp Neurol*, 128(1), pp. 1-12.
- Gotz, J. (2001) 'Tau and transgenic animal models', *Brain Res Brain Res Rev*, 35(3), pp. 266-86.
- Gotz, J., Chen, F., van Dorpe, J. and Nitsch, R. M. (2001) 'Formation of neurofibrillary tangles in P301I tau transgenic mice induced by Abeta 42 fibrils', *Science*, 293(5534), pp. 1491-5.
- Gotz, J., Eckert, A., Matamales, M., Ittner, L. M. and Liu, X. (2011) 'Modes of Abeta toxicity in Alzheimer's disease', *Cell Mol Life Sci*, 68(20), pp. 3359-75.
- Gotz, J., Ittner, A. and Ittner, L. M. (2012) 'Tau-targeted treatment strategies in Alzheimer's disease', *Br J Pharmacol*, 165(5), pp. 1246-59.
- Gotz, J. and Ittner, L. M. (2008) 'Animal models of Alzheimer's disease and frontotemporal dementia', *Nat Rev Neurosci*, 9(7), pp. 532-44.
- Gouras, G. K., Almeida, C. G. and Takahashi, R. H. (2005) 'Intraneuronal A $\beta$  accumulation and origin of plaques in Alzheimer's disease', *Neurobiology of Aging*, 26(9), pp. 1235-1244.
- Gouras, G. K., Tsai, J., Naslund, J., Vincent, B., Edgar, M., Checler, F., Greenfield, J. P., Haroutunian, V., Buxbaum, J. D., Xu, H., Greengard, P. and Relkin, N. R. (2000)

'Intraneuronal A $\beta$ 42 accumulation in human brain', *American Journal of Pathology*, 156(1), pp. 15-20.

Govoni, S., Bergamaschi, S., Racchi, M., Battaini, F., Binetti, G., Bianchetti, A. and Trabucchi, M. (1993) 'Cytosol protein kinase C downregulation in fibroblasts from Alzheimer's disease patients', *Neurology*, 43(12), pp. 2581-6.

Gralle, M., Botelho, M. M., de Oliveira, C. L., Torriani, I. and Ferreira, S. T. (2002) 'Solution studies and structural model of the extracellular domain of the human amyloid precursor protein', *Biophys J*, 83(6), pp. 3513-24.

Gralle, M. and Ferreira, S. T. (2007) 'Structure and functions of the human amyloid precursor protein: the whole is more than the sum of its parts', *Progress in Neurobiology*, 82(1), pp. 11-32.

Green, D. R. and Reed, J. C. (1998) 'Mitochondria and apoptosis', *Science*, 281(5381), pp. 1309-12.

Griciuc, A., Serrano-Pozo, A., Parrado, A. R., Lesinski, A. N., Asselin, C. N., Mullin, K., Hooli, B., Choi, S. H., Hyman, B. T. and Tanzi, R. E. (2013) 'Alzheimer's disease risk gene CD33 inhibits microglial uptake of amyloid beta', *Neuron*, 78(4), pp. 631-43.

Grundke-Iqbal, I., Iqbal, K., Quinlan, M., Tung, Y. C., Zaidi, M. S. and Wisniewski, H. M. (1986) 'Microtubule-associated protein tau. A component of Alzheimer paired helical filaments', *J Biol Chem*, 261(13), pp. 6084-9.

Grynspan, F., Griffin, W. R., Cataldo, A., Katayama, S. and Nixon, R. A. (1997) 'Active site-directed antibodies identify calpain II as an early-appearing and pervasive component of neurofibrillary pathology in Alzheimer's disease', *Brain Research*, 763(2), pp. 145-58.

Guillozet, A. L., Smiley, J. F., Mash, D. C. and Mesulam, M. M. (1997) 'Butyrylcholinesterase in the life cycle of amyloid plaques', *Ann Neurol*, 42(6), pp. 909-18.

Gulbins, E., Dreschers, S. and Bock, J. (2003) 'Role of mitochondria in apoptosis', *Exp Physiol*, 88(1), pp. 85-90.

Guo, L., Du, H., Yan, S., Wu, X., McKhann, G. M., Chen, J. X. and Yan, S. S. (2013) 'Cyclophilin D Deficiency Rescues Axonal Mitochondrial Transport in Alzheimer's Neurons', *Plos One*, 8(1), pp. e54914.

Haapasalo, A. and Kovacs, D. M. (2011) 'The many substrates of presenilin/gamma-secretase', *J Alzheimers Dis*, 25(1), pp. 3-28.

Haass, C., Hung, A. Y., Schlossmacher, M. G., Teplow, D. B. and Selkoe, D. J. (1993) 'beta-Amyloid peptide and a 3-kDa fragment are derived by distinct cellular mechanisms', *Journal of Biological Chemistry*, 268(5), pp. 3021-3024.

Haass, C., Koo, E. H., Mellon, A., Hung, A. Y. and Selkoe, D. J. (1992a) 'Targeting of cell-surface beta-amyloid precursor protein to lysosomes: alternative processing into amyloid-bearing fragments', *Nature*, 357(6378), pp. 500-3.

Haass, C., Lemere, C. A., Capell, A., Citron, M., Seubert, P., Schenk, D., Lannfelt, L. and Selkoe, D. J. (1995) 'The Swedish mutation causes early-onset Alzheimer's disease by [beta]-secretase cleavage within the secretory pathway', *Nature Medicine*, 1(12), pp. 1291-1296.

Haass, C. and Mandelkow, E. (2010) 'Fyn-tau-amyloid: a toxic triad', *Cell*, 142(3), pp. 356-8.

Haass, C., Schlossmacher, M. G., Hung, A. Y., Vigo-Pelfrey, C., Mellon, A., Ostaszewski, B. L., Lieberburg, I., Koo, E. H., Schenk, D., Teplow, D. B. and et al. (1992b) 'Amyloid beta-peptide is produced by cultured cells during normal metabolism', *Nature*, 359(6393), pp. 322-5.

Haass, C. and Selkoe, D. J. (2007) 'Soluble protein oligomers in neurodegeneration: lessons from the Alzheimer's amyloid beta-peptide', *Nat Rev Mol Cell Biol*, 8(2), pp. 101-12.

Hamid, R., Kilger, E., Willem, M., Vassallo, N., Kostka, M., Bornhovd, C., Reichert, A. S., Kretzschmar, H. A., Haass, C. and Herms, J. (2007) 'Amyloid precursor protein intracellular domain modulates cellular calcium homeostasis and ATP content', *Journal of Neurochemistry*, 102(4), pp. 1264-75.

Hammad, S. M., Ranganathan, S., Loukinova, E., Twal, W. O. and Argraves, W. S. (1997) 'Interaction of apolipoprotein J-amyloid beta-peptide complex with low density lipoprotein receptor-related protein-2/megalin. A mechanism to prevent pathological accumulation of amyloid beta-peptide', *J Biol Chem*, 272(30), pp. 18644-9.

Hansson, C. A., Frykman, S., Farmery, M. R., Tjernberg, L. O., Nilsberth, C., Pursglove, S. E., Ito, A., Winblad, B., Cowburn, R. F., Thyberg, J. and Ankarcrona, M. (2004) 'Nicastrin, presenilin, APH-1, and PEN-2 form active gamma-secretase complexes in mitochondria', *Journal of Biological Chemistry*, 279(49), pp. 51654-60.

Hansson, O., Zetterberg, H., Buchhave, P., Londos, E., Blennow, K. and Minthon, L. (2006) 'Association between CSF biomarkers and incipient Alzheimer's disease in patients with mild cognitive impairment: a follow-up study', *The Lancet Neurology*, 5(3), pp. 228-234.

Hardy, J. and Selkoe, D. J. (2002) 'The amyloid hypothesis of Alzheimer's disease: progress and problems on the road to therapeutics', *Science*, 297(5580), pp. 353-6.

Harold, D., Abraham, R., Hollingworth, P., Sims, R., Gerrish, A., Hamshere, M. L., Pahwa, J. S., Moskvina, V., Dowzell, K., Williams, A., Jones, N., Thomas, C., Stretton, A., Morgan, A. R., Lovestone, S., Powell, J., Proitsi, P., Lupton, M. K., Brayne, C., Rubinsztein, D. C., Gill, M., Lawlor, B., Lynch, A., Morgan, K., Brown, K. S., Passmore, P. A., Craig, D., McGuinness, B., Todd, S., Holmes, C., Mann, D., Smith, A. D., Love, S., Kehoe, P. G., Hardy, J., Mead, S., Fox, N., Rossor, M., Collinge, J., Maier, W., Jessen, F., Schurmann, B., van den Bussche, H., Heuser, I., Kornhuber, J., Wiltfang, J., Dichgans, M., Frolich, L., Hampel, H., Hull, M., Rujescu, D., Goate, A. M., Kauwe, J. S. K., Cruchaga, C., Nowotny, P., Morris, J. C., Mayo, K., Sleegers, K., Bettens, K., Engelborghs, S., De Deyn, P. P., Van Broeckhoven, C., Livingston, G., Bass, N. J., Gurling, H., McQuillin, A., Gwilliam, R., Deloukas, P., Al-Chalabi, A., Shaw, C. E., Tsolaki, M., Singleton, A. B., Guerreiro, R., Muhleisen, T. W., Nothen, M. M., Moebus, S., Jockel, K.-H., Klopp, N., Wichmann, H. E., Carrasquillo, M. M., Pankratz, V. S., Younkin, S. G., Holmans, P. A., O'Donovan, M., Owen, M. J. and Williams, J. (2009) 'Genome-wide association study identifies variants at CLU and PICALM associated with Alzheimer's disease', *Nat Genet*, 41(10), pp. 1088-1093.

Harrison, S. M., Harper, A. J., Hawkins, J., Duddy, G., Grau, E., Pugh, P. L., Winter, P. H., Shilliam, C. S., Hughes, Z. A., Dawson, L. A., Gonzalez, M. I., Upton, N., Pangalos, M. N. and Dingwall, C. (2003) 'BACE1 (beta-secretase) transgenic and knockout mice: identification of neurochemical deficits and behavioral changes', *Mol Cell Neurosci*, 24(3), pp. 646-55.

Harry, G. J., Billingsley, M., Bruinink, A., Campbell, I. L., Classen, W., Dorman, D. C., Galli, C., Ray, D., Smith, R. A. and Tilson, H. A. (1998) 'In vitro techniques for the assessment of neurotoxicity', *Environ Health Perspect*, 106 Suppl 1, pp. 131-58.

Hartley, C. L., Johnston, H. B., Nicol, S., Chan, K. M., Baines, A. J., Anderton, B. H. and Thomas, S. M. (1996) 'Phenotypic morphology and the expression of cytoskeletal markers during long-term differentiation of human SH-SY5Y neuroblastoma cells', *Toxicol In Vitro*, 10(5), pp. 539-50.

Hartley, R. S., Margulis, M., Fishman, P. S., Lee, V. M. and Tang, C. M. (1999) 'Functional synapses are formed between human NTERa2 (NT2N, hNT) neurons grown on astrocytes', *J Comp Neurol*, 407(1), pp. 1-10.

Hartman, R. E., Laurer, H., Longhi, L., Bales, K. R., Paul, S. M., McIntosh, T. K. and Holtzman, D. M. (2002) 'Apolipoprotein E4 influences amyloid deposition but not cell loss after traumatic brain injury in a mouse model of Alzheimer's disease', *Journal of Neuroscience*, 22(23), pp. 10083-7.

Hashimoto, Y., Niikura, T., Ito, Y. and Nishimoto, I. (2000) 'Multiple mechanisms underlie neurotoxicity by different types of Alzheimer's disease mutations of amyloid precursor protein', *J Biol Chem*, 275(44), pp. 34541-51.

Haynes, C. M. and Ron, D. (2010) 'The mitochondrial UPR - protecting organelle protein homeostasis', *J Cell Sci*, 123(Pt 22), pp. 3849-55.

He, X., Cooley, K., Chung, C. H., Dashti, N. and Tang, J. (2007) 'Apolipoprotein receptor 2 and X11 alpha/beta mediate apolipoprotein E-induced endocytosis of

amyloid-beta precursor protein and beta-secretase, leading to amyloid-beta production', *Journal of Neuroscience*, 27(15), pp. 4052-60.

Herl, L., Thomas, A. V., Lill, C. M., Banks, M., Deng, A., Jones, P. B., Spoelgen, R., Hyman, B. T. and Berezovska, O. (2009) 'Mutations in amyloid precursor protein affect its interactions with presenilin/gamma-secretase', *Mol Cell Neurosci*, 41(2), pp. 166-74.

Herzog, V., Kirfel, G., Siemes, C. and Schmitz, A. (2004) 'Biological roles of APP in the epidermis', *Eur J Cell Biol*, 83(11-12), pp. 613-24.

Hill, E. J., Jiménez-González, C., Tarczyk, M., Nagel, D. A., Coleman, M. D. and Parri, H. R. (2012) 'NT2 Derived Neuronal and Astrocytic Network Signalling', *Plos One*, 7(5), pp. e36098.

Hill, E. J., Nagel, D. A., O'Neil, J. D., Torr, E., Woehrling, E. K., Devitt, A. and Coleman, M. D. (2013) 'Effects of lithium and valproic acid on gene expression and phenotypic markers in an NT2 neurosphere model of neural development', *PLoS One*, 8(3), pp. e58822.

Hill, E. J., Woehrling, E. K., Prince, M. and Coleman, M. D. (2008) 'Differentiating human NT2/D1 neurospheres as a versatile in vitro 3D model system for developmental neurotoxicity testing', *Toxicology*, 249(2-3), pp. 243-50.

Hippius, H. and Neundörfer, G. (2003) 'The discovery of Alzheimer's disease', *Dialogues in Clinical Neuroscience*, 5(1), pp. 101-108.

Hoe, H. S., Wessner, D., Beffert, U., Becker, A. G., Matsuoka, Y. and Rebeck, G. W. (2005) 'F-spondin interaction with the apolipoprotein E receptor ApoE2 affects processing of amyloid precursor protein', *Mol Cell Biol*, 25(21), pp. 9259-68.

Hofman, A., Ott, A., Breteler, M. M., Bots, M. L., Slooter, A. J., van Harskamp, F., van Duijn, C. N., Van Broeckhoven, C. and Grobbee, D. E. (1997) 'Atherosclerosis, apolipoprotein E, and prevalence of dementia and Alzheimer's disease in the Rotterdam Study', *Lancet*, 349(9046), pp. 151-4.

Hong, M. S., Hong, S. J., Barhoumi, R., Burghardt, R. C., Donnelly, K. C., Wild, J. R., Venktraj, V. and Tiffany-Castiglioni, E. (2003) 'Neurotoxicity induced in differentiated SK-N-SH-SY5Y human neuroblastoma cells by organophosphorus compounds', *Toxicology and Applied Pharmacology*, 186(2), pp. 110-118.

Howard, R., McShane, R., Lindsay, J., Ritchie, C., Baldwin, A., Barber, R., Burns, A., Denning, T., Findlay, D., Holmes, C., Hughes, A., Jacoby, R., Jones, R., Jones, R., McKeith, I., Macharouthu, A., O'Brien, J., Passmore, P., Sheehan, B., Juszcak, E., Katona, C., Hills, R., Knapp, M., Ballard, C., Brown, R., Banerjee, S., Onions, C., Griffin, M., Adams, J., Gray, R., Johnson, T., Bentham, P. and Phillips, P. (2012) 'Donepezil and Memantine for Moderate-to-Severe Alzheimer's Disease', *New England Journal of Medicine*, 366(10), pp. 893-903.

Hoyer, S. (1991) 'Abnormalities of glucose metabolism in Alzheimer's disease', *Ann N Y Acad Sci*, 640, pp. 53-8.

Hoyos Flight, M. (2007) 'Containing the excitement', *Nat Rev Neurosci*, 8(7), pp. 492-493.

Hsiao, K., Chapman, P., Nilsen, S., Eckman, C., Harigaya, Y., Younkin, S., Yang, F. and Cole, G. (1996) 'Correlative memory deficits, Abeta elevation, and amyloid plaques in transgenic mice', *Science*, 274(5284), pp. 99-102.

Hu, B. Y., Weick, J. P., Yu, J., Ma, L. X., Zhang, X. Q., Thomson, J. A. and Zhang, S. C. (2010) 'Neural differentiation of human induced pluripotent stem cells follows developmental principles but with variable potency', *Proc Natl Acad Sci U S A*, 107(9), pp. 4335-40.

Huang, H. C., Tang, D., Xu, K. and Jiang, Z. F. (2014) 'Curcumin attenuates amyloid-beta-induced tau hyperphosphorylation in human neuroblastoma SH-SY5Y cells involving PTEN/Akt/GSK-3beta signaling pathway', *J Recept Signal Transduct Res*, 34(1), pp. 26-37.

Huang, Y., Liu, X. Q., Wyss-Coray, T., Brecht, W. J., Sanan, D. A. and Mahley, R. W. (2001) 'Apolipoprotein E fragments present in Alzheimer's disease brains induce neurofibrillary tangle-like intracellular inclusions in neurons', *Proceedings of the National Academy of Sciences*, 98(15), pp. 8838-8843.

Huang, Y. and Wang, K. K. (2001) 'The calpain family and human disease', *Trends Mol Med*, 7(8), pp. 355-62.

Hussain, I., Powell, D., Howlett, D. R., Tew, D. G., Meek, T. D., Chapman, C., Gloger, I. S., Murphy, K. E., Southan, C. D., Ryan, D. M., Smith, T. S., Simmons, D. L., Walsh, F. S., Dingwall, C. and Christie, G. (1999) 'Identification of a novel aspartic protease (Asp 2) as beta-secretase', *Mol Cell Neurosci*, 14(6), pp. 419-27.

Hutton, M. and Hardy, J. (1997) 'The presenilins and Alzheimer's disease', *Human Molecular Genetics*, 6(10), pp. 1639-46.

Ignatius, M. J., Gebicke-Härter, P. J., Skene, J. H., Schilling, J. W., Weisgraber, K. H., Mahley, R. W. and Shooter, E. M. (1986) 'Expression of apolipoprotein E during nerve degeneration and regeneration', *Proceedings of the National Academy of Sciences of the United States of America*, 83(4), pp. 1125-1129.

Imhof, A., Charnay, Y., Vallet, P. G., Aronow, B., Kovari, E., French, L. E., Bouras, C. and Giannakopoulos, P. (2006) 'Sustained astrocytic clusterin expression improves remodeling after brain ischemia', *Neurobiol Dis*, 22(2), pp. 274-83.

International, A. d. (2013) *Dementia Statistics*. Available at: <http://www.alz.co.uk/research/statistics>.

Israel, M. A., Yuan, S. H., Bardy, C., Reyna, S. M., Mu, Y., Herrera, C., Hefferan, M. P., Van Gorp, S., Nazor, K. L., Boscolo, F. S., Carson, C. T., Laurent, L. C., Marsala, M., Gage, F. H., Remes, A. M., Koo, E. H. and Goldstein, L. S. (2012) 'Probing sporadic and familial Alzheimer's disease using induced pluripotent stem cells', *Nature*, 482(7384), pp. 216-20.

Ittner, L. M., Ke, Y. D., Delerue, F., Bi, M., Gladbach, A., van Eersel, J., Wolfing, H., Chieng, B. C., Christie, M. J., Napier, I. A., Eckert, A., Staufenbiel, M., Hardeman, E. and Gotz, J. (2010) 'Dendritic function of tau mediates amyloid-beta toxicity in Alzheimer's disease mouse models', *Cell*, 142(3), pp. 387-97.

Iwatsubo, T., Odaka, A., Suzuki, N., Mizusawa, H., Nukina, N. and Ihara, Y. (1994) 'Visualization of A beta 42(43) and A beta 40 in senile plaques with end-specific A beta monoclonals: evidence that an initially deposited species is A beta 42(43)', *Neuron*, 13(1), pp. 45-53.

Jahromi, S. R., Togha, M., Fesharaki, S. H., Najafi, M., Moghadam, N. B., Kheradmand, J. A., Kazemi, H. and Gorji, A. (2011) 'Gastrointestinal adverse effects of antiepileptic drugs in intractable epileptic patients', *Seizure*, 20(4), pp. 343-346.

Jain, V., Langham, M. C. and Wehrli, F. W. (2010) 'MRI estimation of global brain oxygen consumption rate', *Journal of Cerebral Blood Flow and Metabolism: Official Journal of the International Society of Cerebral Blood Flow and Metabolism*, 30(9), pp. 1598-1607.

Jamsa, A., Hasslund, K., Cowburn, R. F., Backstrom, A. and Vasange, M. (2004) 'The retinoic acid and brain-derived neurotrophic factor differentiated SH-SY5Y cell line as a model for Alzheimer's disease-like tau phosphorylation', *Biochem Biophys Res Commun*, 319(3), pp. 993-1000.

Jankowsky, J. L., Fadale, D. J., Anderson, J., Xu, G. M., Gonzales, V., Jenkins, N. A., Copeland, N. G., Lee, M. K., Younkin, L. H., Wagner, S. L., Younkin, S. G. and Borchelt, D. R. (2004) 'Mutant presenilins specifically elevate the levels of the 42 residue beta-amyloid peptide in vivo: evidence for augmentation of a 42-specific gamma secretase', *Hum Mol Genet*, 13(2), pp. 159-70.

Joachim, C. L., Mori, H. and Selkoe, D. J. (1989) 'Amyloid beta-protein deposition in tissues other than brain in Alzheimer's disease', *Nature*, 341(6239), pp. 226-30.

Jonsson, T., Atwal, J. K., Steinberg, S., Snaedal, J., Jonsson, P. V., Bjornsson, S., Stefansson, H., Sulem, P., Gudbjartsson, D., Maloney, J., Hoyte, K., Gustafson, A., Liu, Y., Lu, Y., Bhangale, T., Graham, R. R., Huttenlocher, J., Bjornsdottir, G., Andreassen, O. A., Jonsson, E. G., Palotie, A., Behrens, T. W., Magnusson, O. T., Kong, A., Thorsteinsdottir, U., Watts, R. J. and Stefansson, K. (2012) 'A mutation in APP protects against Alzheimer's disease and age-related cognitive decline', *Nature*, 488(7409), pp. 96-9.

Jorgensen, P., Bus, C., Pallisgaard, N., Bryder, M. and Jorgensen, A. L. (1996) 'Familial Alzheimer's disease co-segregates with a Met146Ile substitution in presenilin-1', *Clin Genet*, 50(5), pp. 281-6.

Kadowaki, H., Nishitoh, H., Urano, F., Sadamitsu, C., Matsuzawa, A., Takeda, K., Masutani, H., Yodoi, J., Urano, Y., Nagano, T. and Ichijo, H. (2005) 'Amyloid [beta] induces neuronal cell death through ROS-mediated ASK1 activation', *Cell Death Differ*, 12(1), pp. 19-24.

Kagan, V. E., Kisin, E. R., Kawai, K., Serinkan, B. F., Osipov, A. N., Serbinova, E. A., Wolinsky, I. and Shvedova, A. A. (2002) 'Toward mechanism-based antioxidant interventions: lessons from natural antioxidants', *Ann N Y Acad Sci*, 959, pp. 188-98.

Kang, J., Lemaire, H.-G., Unterbeck, A., Salbaum, J. M., Masters, C. L., Grzeschik, K.-H., Multhaup, G., Beyreuther, K. and Muller-Hill, B. (1987) 'The precursor of Alzheimer's disease amyloid A4 protein resembles a cell-surface receptor', *Nature*, 325(6106), pp. 733-736.

Kang, J. and Muller-Hill, B. (1990) 'Differential splicing of Alzheimer's disease amyloid A4 precursor RNA in rat tissues: PreA4(695) mRNA is predominantly produced in rat and human brain', *Biochem Biophys Res Commun*, 166(3), pp. 1192-200.

Kaplan, D. R., Matsumoto, K., Lucarelli, E. and Thiele, C. J. (1993) 'Induction of TrkB by retinoic acid mediates biologic responsiveness to BDNF and differentiation of human neuroblastoma cells. Eukaryotic Signal Transduction Group', *Neuron*, 11(2), pp. 321-31.

Katzman, R. (1993) 'Education and the prevalence of dementia and Alzheimer's disease', *Neurology*, 43(1), pp. 13-20.

Kazmi, M. (2013) 'AL amyloidosis', *Medicine*, 41(5), pp. 299-301.

Ke, Y. D., Suchowerska, A. K., van der Hoven, J., De Silva, D. M., Wu, C. W., van Eersel, J., Ittner, A. and Ittner, L. M. (2012) 'Lessons from Tau-Deficient Mice', *International Journal of Alzheimer's Disease*, 2012, pp. 8.

Keil, U., Bonert, A., Marques, C. A., Scherping, I., Weyermann, J., Strosznajder, J. B., Muller-Spahn, F., Haass, C., Czech, C., Pradier, L., Muller, W. E. and Eckert, A. (2004) 'Amyloid beta-induced changes in nitric oxide production and mitochondrial activity lead to apoptosis', *J Biol Chem*, 279(48), pp. 50310-20.

Kelly, B. L. and Ferreira, A. (2006) 'beta-Amyloid-induced dynamin 1 degradation is mediated by N-methyl-D-aspartate receptors in hippocampal neurons', *Journal of Biological Chemistry*, 281(38), pp. 28079-89.

Kennedy, A. M., Newman, S. K., Frackowiak, R. S., Cunningham, V. J., Roques, P., Stevens, J., Neary, D., Bruton, C. J., Warrington, E. K. and Rossor, M. N. (1995) 'Chromosome 14 linked familial Alzheimer's disease. A clinico-pathological study of a single pedigree', *Brain*, 118 ( Pt 1), pp. 185-205.

Kessing, L. V., Sondergard, L., Forman, J. L. and Andersen, P. K. (2008) 'Lithium treatment and risk of dementia', *Arch Gen Psychiatry*, 65(11), pp. 1331-5.

Khan, U. A., Liu, L., Provenzano, F. A., Berman, D. E., Profaci, C. P., Sloan, R., Mayeux, R., Duff, K. E. and Small, S. A. (2014a) 'Molecular drivers and cortical spread of lateral entorhinal cortex dysfunction in preclinical Alzheimer's disease', *Nature Neuroscience*, 17(2), pp. 304-311.

Khan, U. A., Liu, L., Provenzano, F. A., Berman, D. E., Profaci, C. P., Sloan, R., Mayeux, R., Duff, K. E. and Small, S. A. (2014b) 'Molecular drivers and cortical spread of lateral entorhinal cortex dysfunction in preclinical Alzheimer's disease', *Nat Neurosci*, 17(2), pp. 304-311.

Khurana, R., Coleman, C., Ionescu-Zanetti, C., Carter, S. A., Krishna, V., Grover, R. K., Roy, R. and Singh, S. (2005) 'Mechanism of thioflavin T binding to amyloid fibrils', *J Struct Biol*, 151(3), pp. 229-38.

Kim, W. and Hecht, M. H. (2006) 'Generic hydrophobic residues are sufficient to promote aggregation of the Alzheimer's A $\beta$ 42 peptide', *Proceedings of the National Academy of Sciences*, 103(43), pp. 15824-15829.

Kim, Y. J., Dubey, P., Ray, P., Gambhir, S. S. and Witte, O. N. (2004) 'Multimodality imaging of lymphocytic migration using lentiviral-based transduction of a tri-fusion reporter gene', *Mol Imaging Biol*, 6(5), pp. 331-40.

Klages, N., Zufferey, R. and Trono, D. (2000) 'A stable system for the high-titer production of multiply attenuated lentiviral vectors', *Mol Ther*, 2(2), pp. 170-6.

Klegeris, A., Walker, D. G. and McGeer, P. L. (1997) 'Regulation of glutamate in cultures of human monocytic THP-1 and astrocytoma U-373 MG cells', *J Neuroimmunol*, 78(1-2), pp. 152-61.

Klunk, W. E., Engler, H., Nordberg, A., Wang, Y., Blomqvist, G., Holt, D. P., Bergstrom, M., Savitcheva, I., Huang, G. F., Estrada, S., Ausen, B., Debnath, M. L., Barletta, J., Price, J. C., Sandell, J., Lopresti, B. J., Wall, A., Koivisto, P., Antoni, G., Mathis, C. A. and Langstrom, B. (2004) 'Imaging brain amyloid in Alzheimer's disease with Pittsburgh Compound-B', *Annals of Neurology*, 55(3), pp. 306-19.

Koechling, T., Lim, F., Hernandez, F. and Avila, J. (2010) 'Neuronal Models for Studying Tau Pathology', *International Journal of Alzheimer's Disease*, 2010.

Kondo, T., Asai, M., Tsukita, K., Kutoku, Y., Ohsawa, Y., Sunada, Y., Imamura, K., Egawa, N., Yahata, N., Okita, K., Takahashi, K., Asaka, I., Aoi, T., Watanabe, A., Watanabe, K., Kadoya, C., Nakano, R., Watanabe, D., Maruyama, K., Hori, O., Hibino, S., Choshi, T., Nakahata, T., Hioki, H., Kaneko, T., Naitoh, M., Yoshikawa, K., Yamawaki, S., Suzuki, S., Hata, R., Ueno, S.-i., Seki, T., Kobayashi, K., Toda, T., Murakami, K., Irie, K., Klein, William L., Mori, H., Asada, T., Takahashi, R., Iwata, N., Yamanaka, S. and Inoue, H. (2013) 'Modeling Alzheimer's Disease with iPSCs Reveals Stress Phenotypes Associated with Intracellular A $\beta$  and Differential Drug Responsiveness', *Cell Stem Cell*, 12(4), pp. 487-496.

Konig, G., Monning, U., Czech, C., Prior, R., Banati, R., Schreiter-Gasser, U., Bauer, J., Masters, C. L. and Beyreuther, K. (1992) 'Identification and differential expression of a novel alternative splice isoform of the beta A4 amyloid precursor protein (APP) mRNA in leukocytes and brain microglial cells', *J Biol Chem*, 267(15), pp. 10804-9.

Koryakina, A., Aeberhard, J., Kiefer, S., Hamburger, M. and Küenzi, P. (2009) 'Regulation of secretases by all-trans-retinoic acid', *FEBS J*, 276(9), pp. 2645-55.

Koudinov, A., Matsubara, E., Frangione, B. and Ghiso, J. (1994) 'The soluble form of Alzheimer's amyloid beta protein is complexed to high density lipoprotein 3 and very high density lipoprotein in normal human plasma', *Biochem Biophys Res Commun*, 205(2), pp. 1164 - 1171.

Kovalevich, J. and Langford, D. (2013) 'Considerations for the use of SH-SY5Y neuroblastoma cells in neurobiology', *Methods Mol Biol*, 1078, pp. 9-21.

Kristiansen, M. and Ham, J. (2014) 'Programmed cell death during neuronal development: the sympathetic neuron model', *Cell Death Differ*, 21(7), pp. 1025-1035.

Krystal, J. H. (1987) 'Positron Emission Tomography and Autoradiography: Principles and Applications for the Brain and Heart', *The Yale Journal of Biology and Medicine*, 60(2), pp. 202-202.

Kuchibhotla, K. V., Lattarulo, C. R., Hyman, B. T. and Bacskai, B. J. (2009) 'Synchronous hyperactivity and intercellular calcium waves in astrocytes in Alzheimer mice', *Science*, 323(5918), pp. 1211-5.

Kuentzel, S. L., Ali, S. M., Altman, R. A., Greenberg, B. D. and Raub, T. J. (1993) 'The Alzheimer beta-amyloid protein precursor/protease nexin-II is cleaved by secretase in a trans-Golgi secretory compartment in human neuroglioma cells', *Biochemical Journal*, 295(Pt 2), pp. 367-378.

Kuhn, P. H., Wang, H., Dislich, B., Colombo, A., Zeitschel, U., Ellwart, J. W., Kremmer, E., Rossner, S. and Lichtenthaler, S. F. (2010) 'ADAM10 is the physiologically relevant, constitutive alpha-secretase of the amyloid precursor protein in primary neurons', *Embo j*, 29(17), pp. 3020-32.

Kumar, U., Dunlop, D. M. and Richardson, J. S. (1994) 'Mitochondria from Alzheimer's fibroblasts show decreased uptake of calcium and increased sensitivity to free radicals', *Life Sci*, 54(24), pp. 1855-60.

Kunau, W. H., Dommès, V. and Schulz, H. (1995) 'beta-oxidation of fatty acids in mitochondria, peroxisomes, and bacteria: a century of continued progress', *Progress in Lipid Research*, 34(4), pp. 267-342.

Kurt, M. A., Davies, D. C. and Kidd, M. (1997) 'Paired helical filament morphology varies with intracellular location in Alzheimer's disease brain', *Neurosci Lett*, 239(1), pp. 41-4.

Kwok, J. B., Taddei, K., Hallupp, M., Fisher, C., Brooks, W. S., Broe, G. A., Hardy, J., Fulham, M. J., Nicholson, G. A., Stell, R., St George Hyslop, P. H., Fraser, P. E., Kakulas, B., Clarnette, R., Relkin, N., Gandy, S. E., Schofield, P. R. and Martins, R. N. (1997) 'Two novel (M233T and R278T) presenilin-1 mutations in early-onset Alzheimer's disease pedigrees and preliminary evidence for association of presenilin-1 mutations with a novel phenotype', *Neuroreport*, 8(6), pp. 1537-42.

L'Hernault, S. W. and Arduengo, P. M. (1992) 'Mutation of a putative sperm membrane protein in *Caenorhabditis elegans* prevents sperm differentiation but not its associated meiotic divisions', *Journal of Cell Biology*, 119(1), pp. 55-68.

LaFerla, F. M. (2002) 'Calcium dyshomeostasis and intracellular signalling in Alzheimer's disease', *Nature Reviews Neuroscience*, 3(11), pp. 862-872.

Lambert, J. C., Schraen-Maschke, S., Richard, F., Fievet, N., Rouaud, O., Berr, C., Dartigues, J. F., Tzourio, C., Alperovitch, A., Buee, L. and Amouyel, P. (2009) 'Association of plasma amyloid beta with risk of dementia The prospective Three-City Study', *Neurology*, 73(11), pp. 847-853.

Lammich, S., Kojro, E., Postina, R., Gilbert, S., Pfeiffer, R., Jasionowski, M., Haass, C. and Fahrenholz, F. (1999) 'Constitutive and regulated alpha-secretase cleavage of Alzheimer's amyloid precursor protein by a disintegrin metalloprotease', *Proc Natl Acad Sci U S A*, 96(7), pp. 3922-7.

Lancu, I. and Olmer, A. (2006) '[The minimal state examination--an up-to-date review]', *Harefuah*, 145(9), pp. 687-90, 701.

Landau, S. M., Breault, C., Joshi, A. D., Pontecorvo, M., Mathis, C. A., Jagust, W. J. and Mintun, M. A. (2013) 'Amyloid-beta imaging with Pittsburgh compound B and florbetapir: comparing radiotracers and quantification methods', *Journal of Nuclear Medicine*, 54(1), pp. 70-7.

Larson, E. B., Wang, L., Bowen, J. D., McCormick, W. C., Teri, L., Crane, P. and Kukull, W. (2006) 'Exercise is associated with reduced risk for incident dementia among persons 65 years of age and older', *Ann Intern Med*, 144(2), pp. 73-81.

Lazarov, O., Morfini, G. A., Lee, E. B., Farah, M. H., Szodrai, A., DeBoer, S. R., Koliatsos, V. E., Kins, S., Lee, V. M., Wong, P. C., Price, D. L., Brady, S. T. and Sisodia, S. S. (2005) 'Axonal transport, amyloid precursor protein, kinesin-1, and the processing apparatus: revisited', *Journal of Neuroscience*, 25(9), pp. 2386-95.

Le, W. D., Colom, L. V., Xie, W. J., Smith, R. G., Alexianu, M. and Appel, S. H. (1995) 'Cell death induced by beta-amyloid 1-40 in MES 23.5 hybrid clone: the role of nitric oxide and NMDA-gated channel activation leading to apoptosis', *Brain Res*, 686(1), pp. 49-60.

Lee, M. R., Lee, D., Shin, S. K., Kim, Y. H. and Choi, C. Y. (2008a) 'Inhibition of APP intracellular domain (AICD) transcriptional activity via covalent conjugation with Nedd8', *Biochem Biophys Res Commun*, 366(4), pp. 976-81.

Lee, V. M. and Andrews, P. W. (1986) 'Differentiation of NTERA-2 clonal human embryonal carcinoma cells into neurons involves the induction of all three neurofilament proteins', *Journal of Neuroscience*, 6(2), pp. 514-21.

Lee, Y. H., Tharp, W. G., Maple, R. L., Nair, S., Permana, P. A. and Pratley, R. E. (2008b) 'Amyloid precursor protein expression is upregulated in adipocytes in obesity', *Obesity*, 16(7), pp. 1493-1500.

Lengyel, Z., Balogh, E., Emri, M., Szikszai, E., Kollár, J., Sikula, J., Esik, O., Trón, L. and Oláh, E. (2006) 'Pattern of increased cerebral FDG uptake in Down syndrome patients', *Pediatr Neurol*, 34(4), pp. 270-5.

Levy-Lahad, E., Wasco, W., Poorkaj, P., Romano, D. M., Oshima, J., Pettingell, W. H., Yu, C. E., Jondro, P. D., Schmidt, S. D., Wang, K. and et al. (1995) 'Candidate gene for the chromosome 1 familial Alzheimer's disease locus', *Science*, 269(5226), pp. 973-7.

Lewis, J., Dickson, D. W., Lin, W. L., Chisholm, L., Corral, A., Jones, G., Yen, S. H., Sahara, N., Skipper, L., Yager, D., Eckman, C., Hardy, J., Hutton, M. and McGowan, E.

(2001) 'Enhanced neurofibrillary degeneration in transgenic mice expressing mutant tau and APP', *Science*, 293(5534), pp. 1487-91.

Li, Q. X., Berndt, M. C., Bush, A. I., Rumble, B., Mackenzie, I., Friedhuber, A., Beyreuther, K. and Masters, C. L. (1994) 'Membrane-associated forms of the beta A4 amyloid protein precursor of Alzheimer's disease in human platelet and brain: surface expression on the activated human platelet', *Blood*, 84(1), pp. 133-42.

Li, Q. X., Fuller, S. J., Beyreuther, K. and Masters, C. L. (1999) 'The amyloid precursor protein of Alzheimer disease in human brain and blood', *J Leukoc Biol*, 66(4), pp. 567-74.

Li, S., Jin, M., Koeglsperger, T., Shepardson, N. E., Shankar, G. M. and Selkoe, D. J. (2011) 'Soluble Aβ oligomers inhibit long-term potentiation through a mechanism involving excessive activation of extrasynaptic NR2B-containing NMDA receptors', *J Neurosci*, 31(18), pp. 6627-38.

Li, S., Rosenberg, J. E., Donjacour, A. A., Botchkina, I. L., Hom, Y. K., Cunha, G. R. and Blackburn, E. H. (2004) 'Rapid Inhibition of Cancer Cell Growth Induced by Lentiviral Delivery and Expression of Mutant-Template Telomerase RNA and Antitelomerase Short-Interfering RNA', *Cancer Research*, 64(14), pp. 4833-4840.

Li, X., Dang, S., Yan, C., Gong, X., Wang, J. and Shi, Y. (2013) 'Structure of a presenilin family intramembrane aspartate protease', *Nature*, 493(7430), pp. 56-61.

Li, Y., Zhou, W., Tong, Y., He, G. and Song, W. (2006) 'Control of APP processing and Aβ generation level by BACE1 enzymatic activity and transcription', *Faseb j*, 20(2), pp. 285-92.

Liao, F., Jiang, H., Srivatsan, S., Xiao, Q., Lefton, K. B., Yamada, K., Mahan, T. E., Lee, J.-M., Shaw, A. S. and Holtzman, D. M. (2015) 'Effects of CD2-associated protein deficiency on amyloid-β in neuroblastoma cells and in an APP transgenic mouse model', *Molecular Neurodegeneration*, 10, pp. 12.

Lidstrom, A. M., Bogdanovic, N., Hesse, C., Volkman, I., Davidsson, P. and Blennow, K. (1998) 'Clusterin (apolipoprotein J) protein levels are increased in hippocampus and in frontal cortex in Alzheimer's disease', *Exp Neurol*, 154(2), pp. 511-21.

Lin, M. T. and Beal, M. F. (2006) 'Alzheimer's APP mangles mitochondria', *Nature Medicine*, 12(11), pp. 1241-3.

Lindsay, J., Laurin, D., Verreault, R., Hebert, R., Helliwell, B., Hill, G. B. and McDowell, I. (2002) 'Risk factors for Alzheimer's disease: a prospective analysis from the Canadian Study of Health and Aging', *Am J Epidemiol*, 156(5), pp. 445-53.

Link, C. D. (2005) 'Invertebrate models of Alzheimer's disease', *Genes Brain and Behavior*, 4(3), pp. 147-56.

Lippa, C. F., Saunders, A. M., Smith, T. W., Swearer, J. M., Drachman, D. A., Ghetti, B., Nee, L., Pulaski-Salo, D., Dickson, D., Robitaille, Y., Bergeron, C., Crain, B., Benson, M. D., Farlow, M., Hyman, B. T., George-Hyslop, S. P., Roses, A. D. and Pollen, D. A. (1996) 'Familial and sporadic Alzheimer's disease: neuropathology cannot exclude a final common pathway', *Neurology*, 46(2), pp. 406-12.

Liu, B., Paton, J. F. and Kasparov, S. (2008) 'Viral vectors based on bidirectional cell-specific mammalian promoters and transcriptional amplification strategy for use in vitro and in vivo', *BMC Biotechnology*, 8, pp. 49-49.

Liu, F., Li, B., Tung, E. J., Grundke-Iqbal, I., Iqbal, K. and Gong, C. X. (2007) 'Site-specific effects of tau phosphorylation on its microtubule assembly activity and self-aggregation', *European Journal of Neuroscience*, 26(12), pp. 3429-36.

Livesey, F. J. (2012) 'Stem cell models of Alzheimer's disease and related neurological disorders', *Alzheimers Res Ther*, 4(6), pp. 44.

Lloret, A., Badia, M. C., Mora, N. J., Pallardo, F. V., Alonso, M. D. and Vina, J. (2009) 'Vitamin E paradox in Alzheimer's disease: it does not prevent loss of cognition and may even be detrimental', *J Alzheimers Dis*, 17(1), pp. 143-9.

Löffler, T., Flunkert, S., Taub, N., Schofield, E. L., Ward, M. A., Windisch, M. and Hutter-Paier, B. (2012) 'Stable Mutated tau441 Transfected SH-SY5Y Cells as Screening Tool for Alzheimer's Disease Drug Candidates', *Journal of Molecular Neuroscience*, 47(1), pp. 192-203.

Logan, A. C., Lutzko, C. and Kohn, D. B. (2002) 'Advances in lentiviral vector design for gene-modification of hematopoietic stem cells', *Current Opinion in Biotechnology*, 13(5), pp. 429-436.

Long, A. N., Owens, K., Schlappal, A. E., Kristian, T., Fishman, P. S. and Schuh, R. A. (2015) 'Effect of nicotinamide mononucleotide on brain mitochondrial respiratory deficits in an Alzheimer's disease-relevant murine model', *BMC Neurol*, 15, pp. 19.

Long, Z., Zheng, M., Zhao, L., Xie, P., Song, C., Chu, Y., Song, W. and He, G. (2013) 'Valproic acid attenuates neuronal loss in the brain of APP/PS1 double transgenic Alzheimer's disease mice model', *Curr Alzheimer Res*, 10(3), pp. 261-9.

Lopes, F. M., Schroder, R., da Frota, M. L., Jr., Zanotto-Filho, A., Muller, C. B., Pires, A. S., Meurer, R. T., Colpo, G. D., Gelain, D. P., Kapczinski, F., Moreira, J. C., Fernandes Mda, C. and Klamt, F. (2010) 'Comparison between proliferative and neuron-like SH-SY5Y cells as an in vitro model for Parkinson disease studies', *Brain Res*, 1337, pp. 85-94.

Lopez, O. L., Becker, J. T., Wahed, A. S., Saxton, J., Sweet, R. A., Wolk, D. A., Klunk, W. and Dekosky, S. T. (2009) 'Long-term effects of the concomitant use of memantine with cholinesterase inhibition in Alzheimer disease', *J Neurol Neurosurg Psychiatry*, 80(6), pp. 600-7.

Lorent, K., Overbergh, L., Moechars, D., De Strooper, B., Van Leuven, F. and Van den Berghe, H. (1995) 'Expression in mouse embryos and in adult mouse brain of three members of the amyloid precursor protein family, of the alpha-2-macroglobulin receptor/low density lipoprotein receptor-related protein and of its ligands apolipoprotein E, lipoprotein lipase, alpha-2-macroglobulin and the 40,000 molecular weight receptor-associated protein', *Neuroscience*, 65(4), pp. 1009-25.

Lott, I. T. and Head, E. (2001) 'Down syndrome and Alzheimer's disease: a link between development and aging', *Ment Retard Dev Disabil Res Rev*, 7(3), pp. 172-8.

Lustbader, J. W., Cirilli, M., Lin, C., Xu, H. W., Takuma, K., Wang, N., Caspersen, C., Chen, X., Pollak, S., Chaney, M., Trinchese, F., Liu, S., Gunn-Moore, F., Lue, L. F., Walker, D. G., Kuppusamy, P., Zewier, Z. L., Arancio, O., Stern, D., Yan, S. S. and Wu, H. (2004) 'ABAD directly links Abeta to mitochondrial toxicity in Alzheimer's disease', *Science*, 304(5669), pp. 448-52.

MacAskill, A. F. and Kittler, J. T. (2010) 'Control of mitochondrial transport and localization in neurons', *Trends Cell Biol*, 20(2), pp. 102-12.

Macdonald, I. R., DeBay, D. R., Reid, G. A., O'Leary, T. P., Jollymore, C. T., Mawko, G., Burrell, S., Martin, E., Bowen, C. V., Brown, R. E. and Darvesh, S. (2014) 'Early detection of cerebral glucose uptake changes in the 5XFAD mouse', *Curr Alzheimer Res*, 11(5), pp. 450-60.

Mahley, R. W. (1988) 'Apolipoprotein E: cholesterol transport protein with expanding role in cell biology', *Science*, 240(4852), pp. 622-30.

Mandybur, T. I. and Chuirazzi, C. C. (1990) 'Astrocytes and the plaques of Alzheimer's disease', *Neurology*, 40(4), pp. 635-9.

Mann, D. M., Yates, P. O. and Marcyniuk, B. (1984) 'Changes in nerve cells of the nucleus basalis of Meynert in Alzheimer's disease and their relationship to ageing and to the accumulation of lipofuscin pigment', *Mech Ageing Dev*, 25(1-2), pp. 189-204.

Mapstone, M., Cheema, A. K., Fiandaca, M. S., Zhong, X., Mhyre, T. R., MacArthur, L. H., Hall, W. J., Fisher, S. G., Peterson, D. R., Haley, J. M., Nazar, M. D., Rich, S. A., Berlau, D. J., Peltz, C. B., Tan, M. T., Kawas, C. H. and Federoff, H. J. (2014) 'Plasma phospholipids identify antecedent memory impairment in older adults', *Nat Med*, 20(4), pp. 415-8.

Marambaud, P., Shioi, J., Serban, G., Georgakopoulos, A., Sarnier, S., Nagy, V., Baki, L., Wen, P., Efthimiopoulos, S., Shao, Z., Wisniewski, T. and Robakis, N. K. (2002) 'A presenilin-1/gamma-secretase cleavage releases the E-cadherin intracellular domain and regulates disassembly of adherens junctions', *Embo j*, 21(8), pp. 1948-56.

Marambaud, P., Wen, P. H., Dutt, A., Shioi, J., Takashima, A., Siman, R. and Robakis, N. K. (2003) 'A CBP binding transcriptional repressor produced by the PS1/epsilon-cleavage of N-cadherin is inhibited by PS1 FAD mutations', *Cell*, 114(5), pp. 635-45.

Marcinkiewicz, M. and Seidah, N. G. (2000) 'Coordinated expression of beta-amyloid precursor protein and the putative beta-secretase BACE and alpha-secretase ADAM10 in mouse and human brain', *J Neurochem*, 75(5), pp. 2133-43.

Mark, L. P., Prost, R. W., Ulmer, J. L., Smith, M. M., Daniels, D. L., Strottmann, J. M., Brown, W. D. and Hacein-Bey, L. (2001) 'Pictorial Review of Glutamate Excitotoxicity: Fundamental Concepts for Neuroimaging', *American Journal of Neuroradiology*, 22(10), pp. 1813-1824.

Markesbery, W. R., Leung, P. K. and Butterfield, D. A. (1980) 'Spin label and biochemical studies of erythrocyte membranes in Alzheimer's disease', *Journal of the Neurological Sciences*, 45(2-3), pp. 323-30.

Martinou, J. C. and Green, D. R. (2001) 'Breaking the mitochondrial barrier', *Nat Rev Mol Cell Biol*, 2(1), pp. 63-7.

Masliah, E., Mallory, M., Hansen, L., Alford, M., DeTeresa, R., Terry, R., Baudier, J. and Saitoh, T. (1992) 'Localization of amyloid precursor protein in GAP43-immunoreactive aberrant sprouting neurites in Alzheimer's disease', *Brain Res*, 574(1-2), pp. 312-6.

Masters, C. L., Simms, G., Weinman, N. A., Multhaup, G., McDonald, B. L. and Beyreuther, K. (1985) 'Amyloid plaque core protein in Alzheimer disease and Down syndrome', *Proc Natl Acad Sci U S A*, 82(12), pp. 4245-9.

Mathews, P. M., Jiang, Y., Schmidt, S. D., Grbovic, O. M., Mercken, M. and Nixon, R. A. (2002) 'Calpain activity regulates the cell surface distribution of amyloid precursor protein. Inhibition of calpains enhances endosomal generation of beta-cleaved C-terminal APP fragments', *Journal of Biological Chemistry*, 277(39), pp. 36415-24.

Matsubara, E., Frangione, B. and Ghiso, J. (1995) 'Characterization of apolipoprotein J-Alzheimer's A beta interaction', *J Biol Chem*, 270(13), pp. 7563-7.

Mattson, M. P. (2000) 'Apoptosis in neurodegenerative disorders', *Nat Rev Mol Cell Biol*, 1(2), pp. 120-9.

Mattson, M. P. (2004) 'Pathways towards and away from Alzheimer's disease', *Nature*, 430(7000), pp. 631-9.

Mattson, M. P., Guo, Z. H. and Geiger, J. D. (1999) 'Secreted form of amyloid precursor protein enhances basal glucose and glutamate transport and protects against oxidative impairment of glucose and glutamate transport in synaptosomes by a cyclic GMP-mediated mechanism', *J Neurochem*, 73(2), pp. 532-7.

May, P. C., Lampert-Etchells, M., Johnson, S. A., Poirier, J., Masters, J. N. and Finch, C. E. (1990) 'Dynamics of gene expression for a hippocampal glycoprotein elevated in Alzheimer's disease and in response to experimental lesions in rat', *Neuron*, 5(6), pp. 831-9.

McGowan, E., Eriksen, J. and Hutton, M. (2006) 'A decade of modeling Alzheimer's disease in transgenic mice', *Trends in Genetics*, 22(5), pp. 281-289.

McIntosh, A. R., Cabeza, R. E. and Lobaugh, N. J. (1998) 'Analysis of neural interactions explains the activation of occipital cortex by an auditory stimulus', *J Neurophysiol*, 80(5), pp. 2790-6.

Medina, D. X., Caccamo, A. and Oddo, S. (2011) 'Methylene blue reduces A $\beta$  levels and rescues early cognitive deficit by increasing proteasome activity', *Brain pathology (Zurich, Switzerland)*, 21(2), pp. 140-149.

Mei, Z., Situ, B., Tan, X., Zheng, S., Zhang, F., Yan, P. and Liu, P. (2010) 'Cryptotanshinone upregulates alpha-secretase by activation PI3K pathway in cortical neurons', *Brain Research*, 1348, pp. 165-73.

Melino, G., Thiele, C. J., Knight, R. A. and Piacentini, M. (1997) 'Retinoids and the control of growth/death decisions in human neuroblastoma cell lines', *J Neurooncol*, 31(1-2), pp. 65-83.

Membrez, M., Hummler, E., Beermann, F., Haefliger, J. A., Savioz, R., Pedrazzini, T. and Thorens, B. (2006) 'GLUT8 is dispensable for embryonic development but influences hippocampal neurogenesis and heart function', *Mol Cell Biol*, 26(11), pp. 4268-76.

Mesulam, M. (2004) 'The cholinergic lesion of Alzheimer's disease: pivotal factor or side show?', *Learn Mem*, 11(1), pp. 43-9.

Miller, B. and Cummings, J. (2007) *The Human Frontal Lobes: Functions and Disorders*. New York and London: The Guildford Press, p. 68-77.

Mills, J. and Reiner, P. B. (1999) 'Regulation of Amyloid Precursor Protein Cleavage', *Journal of Neurochemistry*, 72(2), pp. 443-460.

Minniti, A. N., Rebolledo, D. L., Grez, P. M., Fadic, R., Aldunate, R., Volitakis, I., Cherny, R. A., Opazo, C., Masters, C., Bush, A. I. and Inestrosa, N. C. (2009) 'Intracellular amyloid formation in muscle cells of Abeta-transgenic *Caenorhabditis elegans*: determinants and physiological role in copper detoxification', *Molecular Neurodegeneration*, 4, pp. 2.

Minoshima, S., Giordani, B., Berent, S., Frey, K. A., Foster, N. L. and Kuhl, D. E. (1997) 'Metabolic reduction in the posterior cingulate cortex in very early Alzheimer's disease', *Ann Neurol*, 42(1), pp. 85-94.

Misko, T. P., Radeke, M. J. and Shooter, E. M. (1987) 'Nerve growth factor in neuronal development and maintenance', *J Exp Biol*, 132, pp. 177-90.

Miura, T., Yamamiya, C., Sasaki, M., Suzuki, K. and Takeuchi, H. (2002) 'Binding mode of Congo Red to Alzheimer's amyloid  $\beta$ -peptide studied by UV Raman spectroscopy', *Journal of Raman Spectroscopy*, 33(7), pp. 530-535.

Miyakawa, T. and Uehara, Y. (1979) 'Observations of amyloid angiopathy and senile plaques by the scanning electron microscope', *Acta Neuropathologica*, 48(2), pp. 153-156.

Moechars, D., Dewachter, I., Lorent, K., Reverse, D., Baekelandt, V., Naidu, A., Tesseur, I., Spittaels, K., Haute, C. V., Checler, F., Godaux, E., Cordell, B. and Van Leuven, F. (1999) 'Early phenotypic changes in transgenic mice that overexpress different mutants of amyloid precursor protein in brain', *J Biol Chem*, 274(10), pp. 6483-92.

Mohamet, L., Miazga, N. J. and Ward, C. M. (2014) 'Familial Alzheimer's disease modelling using induced pluripotent stem cell technology', *World Journal of Stem Cells*, 6(2), pp. 239-247.

Monning, U., Sandbrink, R., Weidemann, A., Banati, R. B., Masters, C. L. and Beyreuther, K. (1995) 'Extracellular matrix influences the biogenesis of amyloid precursor protein in microglial cells', *J Biol Chem*, 270(13), pp. 7104-10.

Montine, T. J., Neely, M. D., Quinn, J. F., Beal, M. F., Markesbery, W. R., Roberts, L. J. and Morrow, J. D. (2002) 'Lipid peroxidation in aging brain and Alzheimer's disease', *Free Radic Biol Med*, 33(5), pp. 620-6.

Morales, R., Moreno-Gonzalez, I. and Soto, C. (2013) 'Cross-Seeding of Misfolded Proteins: Implications for Etiology and Pathogenesis of Protein Misfolding Diseases', *PLoS Pathogens*, 9(9), pp. e1003537.

Moreira, P. I., Carvalho, C., Zhu, X., Smith, M. A. and Perry, G. (2010) 'Mitochondrial dysfunction is a trigger of Alzheimer's disease pathophysiology', *Biochim Biophys Acta*, 1802(1), pp. 2-10.

Morgan, C., Colombres, M., Nunez, M. T. and Inestrosa, N. C. (2004a) 'Structure and function of amyloid in Alzheimer's disease', *Prog Neurobiol*, 74(6), pp. 323-49.

Morgan, C., Colombres, M., Nunez, M. T. and Inestrosa, N. C. (2004b) 'Structure and function of amyloid in Alzheimer's disease', *Progress in Neurobiology*, 74(6), pp. 323-49.

Morgan, K. (2011) 'The three new pathways leading to Alzheimer's disease', *Neuropathology and Applied Neurobiology*, 37(4), pp. 353-357.

Moriyoshi, K., Richards, L. J., Akazawa, C., O'Leary, D. D. and Nakanishi, S. (1996) 'Labeling neural cells using adenoviral gene transfer of membrane-targeted GFP', *Neuron*, 16(2), pp. 255-60.

Morley, J. E., Armbrecht, H. J., Farr, S. A. and Kumar, V. B. (2012) 'The senescence accelerated mouse (SAMP8) as a model for oxidative stress and Alzheimer's disease', *Biochim Biophys Acta*, 1822(5), pp. 650-6.

Mosconi, L. (2005) 'Brain glucose metabolism in the early and specific diagnosis of Alzheimer's disease. FDG-PET studies in MCI and AD', *Eur J Nucl Med Mol Imaging*, 32(4), pp. 486-510.

Mosconi, L., De Santi, S., Li, J., Tsui, W. H., Li, Y., Boppana, M., Laska, E., Rusinek, H. and de Leon, M. J. (2008a) 'Hippocampal hypometabolism predicts cognitive decline from normal aging', *Neurobiol Aging*, 29(5), pp. 676-92.

Mosconi, L., Perani, D., Sorbi, S., Herholz, K., Nacmias, B., Holthoff, V., Salmon, E., Baron, J. C., De Cristofaro, M. T., Padovani, A., Borroni, B., Franceschi, M., Bracco, L. and Pupi, A. (2004) 'MCI conversion to dementia and the APOE genotype: a prediction study with FDG-PET', *Neurology*, 63(12), pp. 2332-40.

Mosconi, L., Pupi, A. and De Leon, M. J. (2008b) 'Brain glucose hypometabolism and oxidative stress in preclinical Alzheimer's disease', *Ann N Y Acad Sci*, 1147, pp. 180-95.

Mosconi, L., Tsui, W., Murray, J., McHugh, P., Li, Y., Williams, S., Pirraglia, E., Glodzik, L., De Santi, S., Vallabhajosula, S. and de Leon, M. J. (2012) 'Maternal age affects brain metabolism in adult children of mothers affected by Alzheimer's disease', *Neurobiol Aging*, 33(3), pp. 624.e1-9.

Mu, Y. and Gage, F. (2011) 'Adult hippocampal neurogenesis and its role in Alzheimer's disease', *Molecular Neurodegeneration*, 6(1), pp. 85.

Mullan, M., Crawford, F., Axelman, K., Houlden, H., Lilius, L., Winblad, B. and Lannfelt, L. (1992) 'A pathogenic mutation for probable Alzheimer's disease in the APP gene at the N-terminus of beta-amyloid', *Nat Genet*, 1(5), pp. 345-7.

Muller, T., Concannon, C. G., Ward, M. W., Walsh, C. M., Tirniceriu, A. L., Tribl, F., Kogel, D., Prehn, J. H. and Egensperger, R. (2007) 'Modulation of gene expression and cytoskeletal dynamics by the amyloid precursor protein intracellular domain (AICD)', *Mol Biol Cell*, 18(1), pp. 201-10.

Mullis, K., Faloona, F., Scharf, S., Saiki, R., Horn, G. and Erlich, H. (1986) 'Specific enzymatic amplification of DNA in vitro: the polymerase chain reaction', *Cold Spring Harb Symp Quant Biol*, 51 Pt 1, pp. 263-73.

Muratore, C. R., Rice, H. C., Srikanth, P., Callahan, D. G., Shin, T., Benjamin, L. N., Walsh, D. M., Selkoe, D. J. and Young-Pearse, T. L. (2014) 'The familial Alzheimer's disease APPV717I mutation alters APP processing and Tau expression in iPSC-derived neurons', *Human Molecular Genetics*, 23(13), pp. 3523-36.

Nagy, Z., Esiri, M. M., LeGris, M. and Matthews, P. M. (1999) 'Mitochondrial enzyme expression in the hippocampus in relation to Alzheimer-type pathology', *Acta Neuropathol*, 97(4), pp. 346-54.

Naj, A. C. and Jun, G. and Beecham, G. W. and Wang, L.-S. and Vardarajan, B. N. and Buross, J. and Gallins, P. J. and Buxbaum, J. D. and Jarvik, G. P. and Crane, P. K. and Larson, E. B. and Bird, T. D. and Boeve, B. F. and Graff-Radford, N. R. and De Jager, P. L. and Evans, D. and Schneider, J. A. and Carrasquillo, M. M. and Ertekin-Taner, N. and Younkin, S. G. and Cruchaga, C. and Kauwe, J. S. K. and Nowotny, P. and Kramer, P. and Hardy, J. and Huentelman, M. J. and Myers, A. J. and Barmada, M. M. and Demirci, F. Y. and Baldwin, C. T. and Green, R. C. and Rogava, E. and George-Hyslop, P. S. and Arnold, S. E. and Barber, R. and Beach, T. and Bigio, E. H. and Bowen, J. D. and Boxer, A. and Burke, J. R. and Cairns, N. J. and Carlson, C. S. and Carney, R. M. and Carroll, S. L. and Chui, H. C. and Clark, D. G. and Corneveaux, J. and Cotman, C. W. and Cummings, J. L. and DeCarli, C. and DeKosky, S. T. and Diaz-Arrastia, R. and Dick, M. and Dickson, D. W. and Ellis, W. G. and Faber, K. M. and Fallon, K. B. and Farlow, M. R. and Ferris, S. and Frosch, M. P. and Galasko, D. R. and Ganguli, M. and Gearing, M. and Geschwind, D. H. and Ghetti, B. and Gilbert, J. R. and Gilman, S. and Giordani, B. and Glass, J. D. and Growdon, J. H. and Hamilton, R. L. and Harrell, L. E. and Head, E. and Honig, L. S. and Hulette, C. M. and Hyman, B. T. and Jicha, G. A. and Jin, L.-W. and Johnson, N. and Karlawish, J. and Karydas, A. and Kaye, J. A. and Kim, R. and Koo, E. H. and Kowall, N. W. and Lah, J. J. and Levey, A. I. and Lieberman, A. P. and Lopez, O. L. and Mack, W. J. and Marson, D. C. and Martiniuk, F. and Mash, D. C. and Masliah, E. and McCormick, W. C. and McCurry, S. M. and McDavid, A. N. and McKee, A. C. and Mesulam, M. and Miller, B. L. and Miller, C. A. and Miller, J. W. and Parisi, J. E. and Perl, D. P. and Peskind, E. and Petersen, R. C. and Poon, W. W. and Quinn, J. F. and Rajbhandary, R. A. and Raskind, M. and Reisberg, B. and Ringman, J. M. and Roberson, E. D. and

Rosenberg, R. N. and Sano, M. and Schneider, L. S. and Seeley, W. and Shelanski, M. L. and Slifer, M. A. and Smith, C. D. and Sonnen, J. A. and Spina, S. and Stern, R. A. and Tanzi, R. E. and Trojanowski, J. Q. and Troncoso, J. C. and Van Deerlin, V. M. and Vinters, H. V. and Vonsattel, J. P. and Weintraub, S. and Welsh-Bohmer, K. A. and Williamson, J. and Woltjer, R. L. and Cantwell, L. B. and Dombroski, B. A. and Beekly, D. and Lunetta, K. L. and Martin, E. R. and Kamboh, M. I. and Saykin, A. J. and Reiman, E. M. and Bennett, D. A. and Morris, J. C. and Montine, T. J. and Goate, A. M. and Blacker, D. and Tsuang, D. W. and Hakonarson, H. and Kukull, W. A. and Foroud, T. M. and Haines, J. L. and Mayeux, R. and Pericak-Vance, M. A. and Farrer, L. A. and Schellenberg, G. D. (2011) 'Common variants at MS4A4/MS4A6E, CD2AP, CD33 and EPHA1 are associated with late-onset Alzheimer's disease', *Nat Genet*, 43(5), pp. 436-441.

Naldini, L., Blomer, U., Gage, F. H., Trono, D. and Verma, I. M. (1996) 'Efficient transfer, integration, and sustained long-term expression of the transgene in adult rat brains injected with a lentiviral vector', *Proc Natl Acad Sci U S A*, 93(21), pp. 11382-8.

Namba, Y., Tomonaga, M., Kawasaki, H., Otomo, E. and Ikeda, K. (1991) 'Apolipoprotein E immunoreactivity in cerebral amyloid deposits and neurofibrillary tangles in Alzheimer's disease and kuru plaque amyloid in Creutzfeldt-Jakob disease', *Brain Research*, 541(1), pp. 163-6.

Neill, D., Hughes, D., Edwardson, J. A., Rima, B. K. and Allsop, D. (1994) 'Human IMR-32 neuroblastoma cells as a model cell line in Alzheimer's disease research', *J Neurosci Res*, 39(4), pp. 482-93.

Nguyen, T. L. X., Kim, C. K., Cho, J.-H., Lee, K.-H. and Ahn, J.-Y. (2010) 'Neuroprotection signaling pathway of nerve growth factor and brain-derived neurotrophic factor against staurosporine induced apoptosis in hippocampal H19-7 cells', *Exp Mol Med*, 42, pp. 583-595.

Nicholson, R. M., Kusne, Y., Nowak, L. A., LaFerla, F. M., Reiman, E. M. and Valla, J. (2010) 'Regional cerebral glucose uptake in the 3xTG model of Alzheimer's disease highlights common regional vulnerability across AD mouse models', *Brain Res*, 1347, pp. 179-85.

Nixon, R. A. (2003) 'The calpains in aging and aging-related diseases', *Ageing Res Rev*, 2(4), pp. 407-18.

Nixon, R. A. (2005) 'Endosome function and dysfunction in Alzheimer's disease and other neurodegenerative diseases', *Neurobiology of Aging*, 26(3), pp. 373-382.

Noh, H. and Seo, H. (2014) 'Age-dependent effects of valproic acid in Alzheimer's disease (AD) mice are associated with nerve growth factor (NGF) regulation', *Neuroscience*, 266, pp. 255-65.

Nunan, J. and Small, D. H. (2000) 'Regulation of APP cleavage by  $\alpha$ -,  $\beta$ - and  $\gamma$ -secretases', *FEBS Letters*, 483(1), pp. 6-10.

Nuutinen, T., Suuronen, T., Kauppinen, A. and Salminen, A. (2009) 'Clusterin: a forgotten player in Alzheimer's disease', *Brain Research Reviews*, 61(2), pp. 89-104.

Nuutinen, T., Suuronen, T., Kauppinen, A. and Salminen, A. (2010) 'Valproic acid stimulates clusterin expression in human astrocytes: Implications for Alzheimer's disease', *Neuroscience Letters*, 475(2), pp. 64-68.

O'Carroll, R. and Ebmeier, K. (1995) 'Education and prevalence of Alzheimer's disease and vascular dementia. Premorbid ability influences measures used to identify dementia', *BMJ*, 311(6997), pp. 125-6.

O'Brien, R. J. and Wong, P. C. (2011) 'Amyloid Precursor Protein Processing and Alzheimer's Disease', *Annual review of neuroscience*, 34, pp. 185-204.

Obregon, D., Hou, H., Deng, J., Giunta, B., Tian, J., Darlington, D., Shahaduzzaman, M., Zhu, Y., Mori, T., Mattson, M. P. and Tan, J. (2012) 'Soluble amyloid precursor protein- $\alpha$  modulates  $\beta$ -secretase activity and amyloid- $\beta$  generation', *Nat Commun*, 3, pp. 777.

Odelstad, L., Pahlman, S., Nilsson, K., Larsson, E., Lackgren, G., Johansson, K. E., Hjerten, S. and Grotte, G. (1981) 'Neuron-specific enolase in relation to differentiation in human neuroblastoma', *Brain Res*, 224(1), pp. 69-82.

Ohi, Y., Qin, H., Hong, C., Blouin, L., Polo, J. M., Guo, T., Qi, Z., Downey, S. L., Manos, P. D., Rossi, D. J., Yu, J., Hebrok, M., Hochedlinger, K., Costello, J. F., Song, J. S. and Ramalho-Santos, M. (2011) 'Incomplete DNA methylation underlies a transcriptional memory of somatic cells in human iPS cells', *Nat Cell Biol*, 13(5), pp. 541-549.

Ohsawa, I., Takamura, C. and Kohsaka, S. (2001) 'Fibulin-1 binds the amino-terminal head of  $\beta$ -amyloid precursor protein and modulates its physiological function', *Journal of Neurochemistry*, 76(5), pp. 1411-1420.

Ohsawa, I., Takamura, C., Morimoto, T., Ishiguro, M. and Kohsaka, S. (1999) 'Amino-terminal region of secreted form of amyloid precursor protein stimulates proliferation of neural stem cells', *Eur J Neurosci*, 11(6), pp. 1907-13.

Oikawa, D., Akai, R., Tokuda, M. and Iwawaki, T. (2012) 'A transgenic mouse model for monitoring oxidative stress', *Sci Rep*, 2, pp. 229.

Orrenius, S., Gogvadze, V. and Zhivotovsky, B. (2007) 'Mitochondrial oxidative stress: implications for cell death', *Annu Rev Pharmacol Toxicol*, 47, pp. 143-83.

Owen, J. B. and Butterfield, D. A. (2010) 'Measurement of oxidized/reduced glutathione ratio', *Methods Mol Biol*, 648, pp. 269-77.

Oyarce, A. M. and Fleming, P. J. (1991) 'Multiple forms of human dopamine beta-hydroxylase in SH-SY5Y neuroblastoma cells', *Arch Biochem Biophys*, 290(2), pp. 503-10.

Påhlman, S., Ruusala, A.-I., Abrahamsson, L., Mattsson, M. E. K. and Esscher, T. (1984) 'Retinoic acid-induced differentiation of cultured human neuroblastoma cells: a comparison with phorbol ester-induced differentiation', *Cell Differentiation*, 14(2), pp. 135-144.

Pahlman, S., Ruusala, A. I., Abrahamsson, L., Mattsson, M. E. and Esscher, T. (1984) 'Retinoic acid-induced differentiation of cultured human neuroblastoma cells: a comparison with phorbol ester-induced differentiation', *Cell Differ*, 14(2), pp. 135-44.

Pani, A., Dessi, S., Diaz, G., La Colla, P., Abete, C., Mulas, C., Angius, F., Cannas, M. D., Orru, C. D., Cocco, P. L., Mandas, A., Putzu, P., Laurenzana, A., Cellai, C., Costanza, A. M., Bavazzano, A., Mocali, A. and Paoletti, F. (2009) 'Altered cholesterol ester cycle in skin fibroblasts from patients with Alzheimer's disease', *J Alzheimers Dis*, 18(4), pp. 829-41.

Pant, S., Sharma, M., Patel, K., Caplan, S., Carr, C. M. and Grant, B. D. (2009) 'AMPH-1/Amphiphysin/Bin1 functions with RME-1/Ehd1 in endocytic recycling', *Nat Cell Biol*, 11(12), pp. 1399-410.

Papassotiropoulos, A., Bagli, M., Jessen, F., Bayer, T. A., Maier, W., Rao, M. L. and Heun, R. (1999) 'A genetic variation of the inflammatory cytokine interleukin-6 delays the initial onset and reduces the risk for sporadic Alzheimer's disease', *Annals of Neurology*, 45(5), pp. 666-668.

Parent, A. T. and Thinakaran, G. (2010) 'Modeling Presenilin-Dependent Familial Alzheimer's Disease: Emphasis on Presenilin Substrate-Mediated Signaling and Synaptic Function', *International Journal of Alzheimer's Disease*, 2010, pp. 11.

Park, I.-H., Zhao, R., West, J. A., Yabuuchi, A., Huo, H., Ince, T. A., Lerou, P. H., Lensch, M. W. and Daley, G. Q. (2008a) 'Reprogramming of human somatic cells to pluripotency with defined factors', *Nature*, 451(7175), pp. 141-146.

Park, I. H., Zhao, R., West, J. A., Yabuuchi, A., Huo, H., Ince, T. A., Lerou, P. H., Lensch, M. W. and Daley, G. Q. (2008b) 'Reprogramming of human somatic cells to pluripotency with defined factors', *Nature*, 451(7175), pp. 141-6.

Park, S. Y. and Ferreira, A. (2005) 'The generation of a 17 kDa neurotoxic fragment: an alternative mechanism by which tau mediates beta-amyloid-induced neurodegeneration', *J Neurosci*, 25(22), pp. 5365-75.

Parker, W. D., Jr., Filley, C. M. and Parks, J. K. (1990) 'Cytochrome oxidase deficiency in Alzheimer's disease', *Neurology*, 40(8), pp. 1302-3.

Pasinetti, G. M., Johnson, S. A., Oda, T., Rozovsky, I. and Finch, C. E. (1994) 'Clusterin (SGP-2): a multifunctional glycoprotein with regional expression in astrocytes and neurons of the adult rat brain', *J Comp Neurol*, 339(3), pp. 387-400.

Pastorino, L. and Lu, K. P. (2006) 'Pathogenic mechanisms in Alzheimer's disease', *European Journal of Pharmacology*, 545(1), pp. 29-38.

Patergnani, S., Suski, J. M., Agnoletto, C., Bononi, A., Bonora, M., De Marchi, E., Giorgi, C., Marchi, S., Missiroli, S., Poletti, F., Rimessi, A., Duszynski, J., Wieckowski, M. R. and Pinton, P. (2011) 'Calcium signaling around Mitochondria Associated Membranes (MAMs)', *Cell Commun Signal*, 9, pp. 19.

Pellegrino, M. W., Nargund, A. M. and Haynes, C. M. (2013) 'Signaling the mitochondrial unfolded protein response', *Biochim Biophys Acta*, 1833(2), pp. 410-6.

Perlmutter, L. S., Siman, R., Gall, C., Seubert, P., Baudry, M. and Lynch, G. (1988) 'The ultrastructural localization of calcium-activated protease "calpain" in rat brain', *Synapse*, 2(1), pp. 79-88.

Perry, E. K., Tomlinson, B. E., Blessed, G., Bergmann, K., Gibson, P. H. and Perry, R. H. (1978) 'Correlation of cholinergic abnormalities with senile plaques and mental test scores in senile dementia', *Br Med J*, 2(6150), pp. 1457-9.

Peterson, C., Gibson, G. E. and Blass, J. P. (1985) 'Altered calcium uptake in cultured skin fibroblasts from patients with Alzheimer's disease', *N Engl J Med*, 312(16), pp. 1063-5.

Peterson, C. and Goldman, J. E. (1986) 'Alterations in calcium content and biochemical processes in cultured skin fibroblasts from aged and Alzheimer donors', *Proc Natl Acad Sci U S A*, 83(8), pp. 2758-62.

Petratos, S., Li, Q.-X., George, A. J., Hou, X., Kerr, M. L., Unabia, S. E., Hatzinisiriou, I., Maksel, D., Aguilar, M.-I. and Small, D. H. (2008) *The  $\beta$ -amyloid protein of Alzheimer's disease increases neuronal CRMP-2 phosphorylation by a Rho-GTP mechanism.*

Pickering-Brown, S., Baker, M., Yen, S. H., Liu, W. K., Hasegawa, M., Cairns, N., Lantos, P. L., Rossor, M., Iwatsubo, T., Davies, Y., Allsop, D., Furlong, R., Owen, F., Hardy, J., Mann, D. and Hutton, M. (2000) 'Pick's disease is associated with mutations in the tau gene', *Annals of Neurology*, 48(6), pp. 859-67.

Pietrzik, C. U., Hoffmann, J., Stöber, K., Chen, C. Y., Bauer, C., Otero, D. A., Roch, J. M. and Herzog, V. (1998) 'From differentiation to proliferation: the secretory amyloid precursor protein as a local mediator of growth in thyroid epithelial cells', *Proc Natl Acad Sci U S A*, 95(4), pp. 1770-5.

Pleasure, S. J., Page, C. and Lee, V. M. (1992) 'Pure, postmitotic, polarized human neurons derived from NTera 2 cells provide a system for expressing exogenous proteins in terminally differentiated neurons', *J Neurosci*, 12(5), pp. 1802-15.

Plucinska, K., Crouch, B., Koss, D., Robinson, L., Siebrecht, M., Riedel, G. and Platt, B. (2014) 'Knock-in of human BACE1 cleaves murine APP and reiterates Alzheimer-like phenotypes', *J Neurosci*, 34(32), pp. 10710-28.

Pocernich, C. B. and Butterfield, D. A. (2012) 'Elevation of glutathione as a therapeutic strategy in Alzheimer disease', *Biochimica et Biophysica Acta (BBA) - Molecular Basis of Disease*, 1822(5), pp. 625-630.

Ponte, P., DeWhitt, P. G., Schilling, J., Miller, J., Hsu, D., Greenberg, B., Davis, K., Wallace, W., Lieberburg, I., Fuller, F. and Cordell, B. (1988) 'A new A4 amyloid mRNA contains a domain homologous to serine proteinase inhibitors', *Nature*, 331(6156), pp. 525-527.

Poon, S., Easterbrook-Smith, S. B., Rybchyn, M. S., Carver, J. A. and Wilson, M. R. (2000) 'Clusterin is an ATP-independent chaperone with very broad substrate specificity that stabilizes stressed proteins in a folding-competent state', *Biochemistry*, 39(51), pp. 15953-60.

Postina, R., Schroeder, A., Dewachter, I., Bohl, J., Schmitt, U., Kojro, E., Prinzen, C., Endres, K., Hiemke, C., Blessing, M., Flamez, P., Dequenne, A., Godaux, E., van Leuven, F. and Fahrenholz, F. (2004) 'A disintegrin-metalloproteinase prevents amyloid plaque formation and hippocampal defects in an Alzheimer disease mouse model', *J Clin Invest*, 113(10), pp. 1456-64.

Powers, E. T. and Powers, D. L. (2008) 'Mechanisms of protein fibril formation: nucleated polymerization with competing off-pathway aggregation', *Biophysical Journal*, 94(2), pp. 379-91.

Prasanthi, J. R., Huls, A., Thomasson, S., Thompson, A., Schommer, E. and Ghribi, O. (2009) 'Differential effects of 24-hydroxycholesterol and 27-hydroxycholesterol on beta-amyloid precursor protein levels and processing in human neuroblastoma SH-SY5Y cells', *Mol Neurodegener*, 4, pp. 1.

Presgraves, S., Ahmed, T., Borwege, S. and Joyce, J. (2003) 'Terminally differentiated SH-SY5Y cells provide a model system for studying neuroprotective effects of dopamine agonists', *Neurotoxicity Research*, 5(8), pp. 579-598.

Price, D. L. and Sisodia, S. S. (1998) 'Mutant genes in familial Alzheimer's disease and transgenic models', *Annu Rev Neurosci*, 21, pp. 479-505.

Price, D. L., Tanzi, R. E., Borchelt, D. R. and Sisodia, S. S. (1998) 'Alzheimer's disease: genetic studies and transgenic models', *Annu Rev Genet*, 32, pp. 461-93.

Price, J. L. and Morris, J. C. (1999) 'Tangles and plaques in nondemented aging and "preclinical" Alzheimer's disease', *Ann Neurol*, 45(3), pp. 358-68.

Prihar, G., Fuldner, R. A., Perez-Tur, J., Lincoln, S., Duff, K., Crook, R., Hardy, J., Philips, C. A., Venter, C., Talbot, C., Clark, R. F., Goate, A., Li, J., Potter, H., Karran, E., Roberts, G. W., Hutton, M. and Adams, M. D. (1996) 'Structure and alternative splicing of the presenilin-2 gene', *Neuroreport*, 7(10), pp. 1680-4.

Puig, K. L. and Combs, C. K. (2013) 'Expression and function of APP and its metabolites outside the central nervous system', *Experimental Gerontology*, 48(7), pp. 608-611.

Puig, K. L., Floden, A. M., Adhikari, R., Golovko, M. Y. and Combs, C. K. (2012a) 'Amyloid Precursor Protein and Proinflammatory Changes Are Regulated in Brain and Adipose Tissue in a Murine Model of High Fat Diet-Induced Obesity', *PLoS ONE*, 7(1), pp. e30378.

Puig, K. L., Swigost, A. J., Zhou, X., Sens, M. A. and Combs, C. K. (2012b) 'Amyloid precursor protein expression modulates intestine immune phenotype', *J Neuroimmune Pharmacol*, 7(1), pp. 215-30.

Qian, S., Jiang, P., Guan, X.-M., Singh, G., Trumbauer, M. E., Yu, H., Chen, H. Y., Van der Ploeg, L. H. T. and Zheng, H. (1998) 'Mutant Human Presenilin 1 Protects presenilin 1 Null Mouse against Embryonic Lethality and Elevates A $\beta$ 1-42/43 Expression', *Neuron*, 20(3), pp. 611-617.

Qiang, L., Fujita, R., Yamashita, T., Angulo, S., Rhinn, H., Rhee, D., Doege, C., Chau, L., Aubry, L., Vanti, W. B., Moreno, H. and Abeliovich, A. (2011) 'Directed conversion of Alzheimer's disease patient skin fibroblasts into functional neurons', *Cell*, 146(3), pp. 359-71.

Quinn, J. F., Bussiere, J. R., Hammond, R. S., Montine, T. J., Henson, E., Jones, R. E. and Stackman, R. W. (2007) 'Chronic dietary alpha-lipoic acid reduces deficits in hippocampal memory of aged Tg2576 mice', *Neurobiol Aging*, 28(2), pp. 213-25.

Rademakers, R., Cruts, M. and van Broeckhoven, C. (2004) 'The role of tau (MAPT) in frontotemporal dementia and related tauopathies', *Hum Mutat*, 24(4), pp. 277-95.

Raha, S. and Robinson, B. H. (2000) 'Mitochondria, oxygen free radicals, disease and ageing', *Trends in Biochemical Sciences*, 25(10), pp. 502-8.

Ramamoorthy, M., Sykora, P., Scheibye-Knudsen, M., Dunn, C., Kasmer, C., Zhang, Y., Becker, K. G., Croteau, D. L. and Bohr, V. A. (2012) 'Sporadic Alzheimer disease fibroblasts display an oxidative stress phenotype', *Free Radical Biology and Medicine*, 53(6), pp. 1371-1380.

Rapoport, M., Dawson, H. N., Binder, L. I., Vitek, M. P. and Ferreira, A. (2002) 'Tau is essential to beta -amyloid-induced neurotoxicity', *Proc Natl Acad Sci U S A*, 99(9), pp. 6364-9.

Ray, P. D., Huang, B.-W. and Tsuji, Y. (2012a) 'Reactive oxygen species (ROS) homeostasis and redox regulation in cellular signaling', *Cellular Signalling*, 24(5), pp. 981-990.

Ray, P. D., Huang, B. W. and Tsuji, Y. (2012b) 'Reactive oxygen species (ROS) homeostasis and redox regulation in cellular signaling', *Cell Signal*, 24(5), pp. 981-90.

Readnower, R. D., Sauerbeck, A. D. and Sullivan, P. G. (2011) 'Mitochondria, Amyloid  $\beta$ , and Alzheimer's Disease', *Int J Alzheimers Dis*, 2011, pp. 104545.

Reiman, E. M., Chen, K., Alexander, G. E., Caselli, R. J., Bandy, D., Osborne, D., Saunders, A. M. and Hardy, J. (2004) 'Functional brain abnormalities in young adults at genetic risk for late-onset Alzheimer's dementia', *Proc Natl Acad Sci U S A*, 101(1), pp. 284-9.

Reinhard, C., Hebert, S. S. and De Strooper, B. (2005) 'The amyloid-beta precursor protein: integrating structure with biological function', *Embo j*, 24(23), pp. 3996-4006.

Reiniger, L., Lukic, A., Linehan, J., Rudge, P., Collinge, J., Mead, S. and Brandner, S. (2011) 'Tau, prions and A $\beta$ : the triad of neurodegeneration', *Acta Neuropathologica*, 121(1), pp. 5-20.

Reisberg, B., Doody, R., Stoffler, A., Schmitt, F., Ferris, S. and Mobius, H. J. (2003) 'Memantine in moderate-to-severe Alzheimer's disease', *N Engl J Med*, 348(14), pp. 1333-41.

Richardson, J. A. and Burns, D. K. (2002) 'Mouse models of Alzheimer's disease: a quest for plaques and tangles', *ILAR J*, 43(2), pp. 89-99.

Ritchie, K. and Lovestone, S. (2002) 'The dementias', *Lancet*, 360(9347), pp. 1759-66.

Roberson, E. D., Scarce-Levie, K., Palop, J. J., Yan, F., Cheng, I. H., Wu, T., Gerstein, H., Yu, G. Q. and Mucke, L. (2007) 'Reducing endogenous tau ameliorates amyloid beta-induced deficits in an Alzheimer's disease mouse model', *Science*, 316(5825), pp. 750-4.

Roberts, S. B., Ripellino, J. A., Ingalls, K. M., Robakis, N. K. and Felsenstein, K. M. (1994) 'Non-amyloidogenic cleavage of the beta-amyloid precursor protein by an integral membrane metalloendopeptidase', *Journal of Biological Chemistry*, 269(4), pp. 3111-6.

Robinson, D. M. and Keating, G. M. (2006) 'Memantine: a review of its use in Alzheimer's disease', *Drugs*, 66(11), pp. 1515-34.

Rogaev, E. I., Sherrington, R., Rogaeva, E. A., Levesque, G., Ikeda, M., Liang, Y., Chi, H., Lin, C., Holman, K., Tsuda, T. and et al. (1995) 'Familial Alzheimer's disease in kindreds with missense mutations in a gene on chromosome 1 related to the Alzheimer's disease type 3 gene', *Nature*, 376(6543), pp. 775-8.

Rogaev, E. I., Sherrington, R., Wu, C., Levesque, G., Liang, Y., Rogaeva, E. A., Ikeda, M., Holman, K., Lin, C., Lukiw, W. J., de Jong, P. J., Fraser, P. E., Rommens, J. M. and St George-Hyslop, P. (1997) 'Analysis of the 5' sequence, genomic structure, and alternative splicing of the presenilin-1 gene (PSEN1) associated with early onset Alzheimer disease', *Genomics*, 40(3), pp. 415-24.

Rogers, J. T., Randall, J. D., Cahill, C. M., Eder, P. S., Huang, X., Gunshin, H., Leiter, L., McPhee, J., Sarang, S. S., Utsuki, T., Greig, N. H., Lahiri, D. K., Tanzi, R. E., Bush, A. I., Giordano, T. and Gullans, S. R. (2002) 'An iron-responsive element type II in the 5'-untranslated region of the Alzheimer's amyloid precursor protein transcript', *Journal of Biological Chemistry*, 277(47), pp. 45518-28.

Roh, Jee H. and Holtzman, David M. (2012) 'Stealth Attack: Plaque-Specific Antibody Allows for Efficient A $\beta$  Removal without Side Effects', *Neuron*, 76(5), pp. 859-861.

Roizen, N. J. and Patterson, D. (2003) 'Down's syndrome', *The Lancet*, 361(9365), pp. 1281-1289.

Romanowska, M., Evans, A., Kellock, D., Bray, S. E., McLean, K., Donandt, S. and Foerster, J. (2009) 'Wnt5a exhibits layer-specific expression in adult skin, is upregulated in psoriasis, and synergizes with type 1 interferon', *PLoS One*, 4(4), pp. e5354.

Ross, R. A., Spengler, B. A. and Biedler, J. L. (1983) 'Coordinate morphological and biochemical interconversion of human neuroblastoma cells', *J Natl Cancer Inst*, 71(4), pp. 741-7.

Rossjohn, J., Cappai, R., Feil, S. C., Henry, A., McKinstry, W. J., Galatis, D., Hesse, L., Multhaup, G., Beyreuther, K., Masters, C. L. and Parker, M. W. (1999) 'Crystal structure of the N-terminal, growth factor-like domain of Alzheimer amyloid precursor protein', *Nat Struct Mol Biol*, 6(4), pp. 327-331.

Rottenberg, H. and Scarpa, A. (1974) 'Calcium uptake and membrane potential in mitochondria', *Biochemistry*, 13(23), pp. 4811-4817.

Rovelet-Lecrux, A., Hannequin, D., Raux, G., Le Meur, N., Laquerriere, A., Vital, A., Dumanchin, C., Feuillet, S., Brice, A., Vercelletto, M., Dubas, F., Frebourg, T. and Campion, D. (2006) 'APP locus duplication causes autosomal dominant early-onset Alzheimer disease with cerebral amyloid angiopathy', *Nat Genet*, 38(1), pp. 24-6.

Rowe, C. C., Ng, S., Ackermann, U., Gong, S. J., Pike, K., Savage, G., Cowie, T. F., Dickinson, K. L., Maruff, P., Darby, D., Smith, C., Woodward, M., Merory, J., Tochon-Danguy, H., O'Keefe, G., Klunk, W. E., Mathis, C. A., Price, J. C., Masters, C. L. and Villemagne, V. L. (2007) 'Imaging beta-amyloid burden in aging and dementia', *Neurology*, 68(20), pp. 1718-25.

Saharan, S. and Mandal, P. K. (2014) 'The emerging role of glutathione in Alzheimer's disease', *J Alzheimers Dis*, 40(3), pp. 519-29.

Saitoh, T., Sundsmo, M., Roch, J.-M., Kimura, N., Cole, G., Schubert, D., Oltersdorf, T. and Schenk, D. B. (1989) 'Secreted form of amyloid  $\beta$  protein precursor is involved in the growth regulation of fibroblasts', *Cell*, 58(4), pp. 615-622.

Sancheti, H., Akopian, G., Yin, F., Brinton, R. D., Walsh, J. P. and Cadenas, E. (2013) 'Age-dependent modulation of synaptic plasticity and insulin mimetic effect of lipoic acid on a mouse model of Alzheimer's disease', *Plos One*, 8(7), pp. e69830.

Sanchez Martin, C., Diaz-Nido, J. and Avila, J. (1998) 'Regulation of a site-specific phosphorylation of the microtubule-associated protein 2 during the development of cultured neurons', *Neuroscience*, 87(4), pp. 861-70.

Sandbrink, R., Masters, C. L. and Beyreuther, K. (1996) 'APP gene family. Alternative splicing generates functionally related isoforms', *Ann N Y Acad Sci*, 777, pp. 281-7.

Sano, M., Ernesto, C., Thomas, R. G., Klauber, M. R., Schafer, K., Grundman, M., Woodbury, P., Growdon, J., Cotman, C. W., Pfeiffer, E., Schneider, L. S. and Thal, L. J. (1997) 'A controlled trial of selegiline, alpha-tocopherol, or both as treatment for Alzheimer's disease. The Alzheimer's Disease Cooperative Study', *N Engl J Med*, 336(17), pp. 1216-22.

Santos, R. X., Correia, S. C., Wang, X., Perry, G., Smith, M. A., Moreira, P. I. and Zhu, X. (2010) 'A synergistic dysfunction of mitochondrial fission/fusion dynamics and mitophagy in Alzheimer's disease', *Journal of Alzheimers Disease*, 20 Suppl 2, pp. S401-12.

Sarkanen, J.-R., Nykky, J., Siikanen, J., Selinummi, J., Ylikomi, T. and Jalonen, T. O. (2007) 'Cholesterol supports the retinoic acid-induced synaptic vesicle formation in differentiating human SH-SY5Y neuroblastoma cells', *Journal of Neurochemistry*, 102(6), pp. 1941-1952.

Sarti, P., Forte, E., Mastronicola, D., Giuffre, A. and Arese, M. (2012) 'Cytochrome c oxidase and nitric oxide in action: molecular mechanisms and pathophysiological implications', *Biochim Biophys Acta*, 1817(4), pp. 610-9.

Sayre, L. M., Zelasko, D. A., Harris, P. L., Perry, G., Salomon, R. G. and Smith, M. A. (1997) '4-Hydroxynonenal-derived advanced lipid peroxidation end products are increased in Alzheimer's disease', *J Neurochem*, 68(5), pp. 2092-7.

Scarmeas, N., Luchsinger, J. A., Schupf, N., Brickman, A. M., Cosentino, S., Tang, M. X. and Stern, Y. (2009) 'Physical Activity, Diet, and Risk of Alzheimer Disease', *JAMA : the journal of the American Medical Association*, 302(6), pp. 627-637.

Scarmeas, N., Stern, Y., Tang, M.-X., Mayeux, R. and Luchsinger, J. A. (2006) 'Mediterranean Diet and Risk for Alzheimer's Disease', *Annals of neurology*, 59(6), pp. 912-921.

Schedin-Weiss, S., Winblad, B. and Tjernberg, L. O. (2014) 'The role of protein glycosylation in Alzheimer disease', *FEBS Journal*, 281(1), pp. 46-62.

Scheuner, D., Eckman, C., Jensen, M., Song, X., Citron, M., Suzuki, N., Bird, T. D., Hardy, J., Hutton, M., Kukull, W., Larson, E., Levy-Lahad, E., Viitanen, M., Peskind, E., Poorkaj, P., Schellenberg, G., Tanzi, R., Wasco, W., Lannfelt, L., Selkoe, D. and Younkin, S. (1996a) 'Secreted amyloid beta-protein similar to that in the senile plaques of Alzheimer's disease is increased in vivo by the presenilin 1 and 2 and APP mutations linked to familial Alzheimer's disease', *Nat Med*, 2(8), pp. 864-70.

Scheuner, D., Eckman, C., Jensen, M., Song, X., Citron, M., Suzuki, N., Bird, T. D., Hardy, J., Hutton, M., Kukull, W., Larson, E., Levy-Lahad, L., Viitanen, M., Peskind, E.,

Poorkaj, P., Schellenberg, G., Tanzi, R., Wasco, W., Lannfelt, L., Selkoe, D. and Younkin, S. (1996b) 'Secreted amyloid [beta]-protein similar to that in the senile plaques of Alzheimer's disease is increased in vivo by the presenilin 1 and 2 and APP mutations linked to familial Alzheimer's disease', *Nature Medicine*, 2(8), pp. 864-870.

Schneider, L., Giordano, S., Zelickson, B. R., M, S. J., G, A. B., Ouyang, X., Fineberg, N., Darley-USmar, V. M. and Zhang, J. (2011a) 'Differentiation of SH-SY5Y cells to a neuronal phenotype changes cellular bioenergetics and the response to oxidative stress', *Free Radic Biol Med*, 51(11), pp. 2007-17.

Schneider, L., Giordano, S., Zelickson, B. R., S. Johnson, M., A. Benavides, G., Ouyang, X., Fineberg, N., Darley-USmar, V. M. and Zhang, J. (2011b) 'Differentiation of SH-SY5Y cells to a neuronal phenotype changes cellular bioenergetics and the response to oxidative stress', *Free Radical Biology and Medicine*, 51(11), pp. 2007-2017.

Schoch, S., Cibelli, G. and Thiel, G. (1996) 'Neuron-specific gene expression of synapsin I. Major role of a negative regulatory mechanism', *J Biol Chem*, 271(6), pp. 3317-23.

Seeman, P. and Seeman, N. (2011) 'Alzheimer's disease:  $\beta$ -amyloid plaque formation in human brain', *Synapse*, 65(12), pp. 1289-1297.

Segal, D. J. and McCoy, E. E. (1974) 'Studies on Down's syndrome in tissue culture. I. Growth rates and protein contents of fibroblast cultures', *J Cell Physiol*, 83(1), pp. 85-90.

Selkoe, D. J. (1998) 'The cell biology of beta-amyloid precursor protein and presenilin in Alzheimer's disease', *Trends Cell Biol*, 8(11), pp. 447-53.

Selkoe, D. J. (2001a) 'Alzheimer's disease results from the cerebral accumulation and cytotoxicity of amyloid beta-protein', *Journal of Alzheimers Disease*, 3(1), pp. 75-80.

Selkoe, D. J. (2001b) 'Alzheimer's disease: genes, proteins, and therapy', *Physiol Rev*, 81(2), pp. 741-66.

Selkoe, D. J. and Wolfe, M. S. (2007) 'Presenilin: running with scissors in the membrane', *Cell*, 131(2), pp. 215-21.

Senechal, Y., Kelly, P. H. and Dev, K. K. (2008) 'Amyloid precursor protein knockout mice show age-dependent deficits in passive avoidance learning', *Behav Brain Res*, 186(1), pp. 126-32.

Seoposengwe, K., van Tonder, J. and Steenkamp, V. (2013) 'In vitro neuroprotective potential of four medicinal plants against rotenone-induced toxicity in SH-SY5Y neuroblastoma cells', *BMC Complementary and Alternative Medicine*, 13(1), pp. 353.

Serrano-Pozo, A., Frosch, M. P., Masliah, E. and Hyman, B. T. (2011) 'Neuropathological Alterations in Alzheimer Disease', *Cold Spring Harbor Perspectives in Medicine*, 1(1), pp. a006189.

Shen, J., Bronson, R. T., Chen, D. F., Xia, W., Selkoe, D. J. and Tonegawa, S. (1997) 'Skeletal and CNS Defects in Presenilin-1-Deficient Mice', *Cell*, 89(4), pp. 629-639.

Sherer, T., Betarbet, R., Testa, C., Seo, B., Richardson, J., Kim, J., Miller, G., Yagi, T., Matsuno-Yagi, A. and JT, G. (2003) 'Mechanism of toxicity in rotenone models of Parkinson's disease', *J Neurosci*, 23, pp. 10756 - 10764.

Sherrington, R., Rogaev, E. I., Liang, Y., Rogaeva, E. A., Levesque, G., Ikeda, M., Chi, H., Lin, C., Li, G., Holman, K., Tsuda, T., Mar, L., Foncin, J. F., Bruni, A. C., Montesi, M. P., Sorbi, S., Rainero, I., Pinessi, L., Nee, L., Chumakov, I., Pollen, D., Brookes, A., Sanseau, P., Polinsky, R. J., Wasco, W., Da Silva, H. A. R., Haines, J. L., Pericak-Vance, M. A., Tanzi, R. E., Roses, A. D., Fraser, P. E., Rommens, J. M. and St George-Hyslop, P. H. (1995) 'Cloning of a gene bearing missense mutations in early-onset familial Alzheimer's disease', *Nature*, 375(6534), pp. 754-760.

Shi, Y., Kirwan, P., Smith, J., MacLean, G., Orkin, S. H. and Livesey, F. J. (2012a) 'A Human Stem Cell Model of Early Alzheimer's Disease Pathology in Down Syndrome', *Science Translational Medicine*.

Shi, Y., Kirwan, P., Smith, J., Robinson, H. P. C. and Livesey, F. J. (2012b) 'Human cerebral cortex development from pluripotent stem cells to functional excitatory synapses', *Nat Neurosci*, 15(3), pp. 477-486.

Shin, J., Yu, S. B., Yu, U. Y., Jo, S. A. and Ahn, J. H. (2010) 'Swedish mutation within amyloid precursor protein modulates global gene expression towards the pathogenesis of Alzheimer's disease', *BMB Rep*, 43(10), pp. 704-9.

Shipton, O. A., Leitz, J. R., Dworzak, J., Acton, C. E., Tunbridge, E. M., Denk, F., Dawson, H. N., Vitek, M. P., Wade-Martins, R., Paulsen, O. and Vargas-Caballero, M. (2011) 'Tau protein is required for amyloid {beta}-induced impairment of hippocampal long-term potentiation', *Journal of Neuroscience*, 31(5), pp. 1688-92.

Siedlak, S. L., Casadesus, G., Webber, K. M., Pappolla, M. A., Atwood, C. S., Smith, M. A. and Perry, G. (2009) 'Chronic antioxidant therapy reduces oxidative stress in a mouse model of Alzheimer's disease', *Free radical research*, 43(2), pp. 156-164.

Siemes, C., Quast, T., Klein, E., Bieber, T., Hooper, N. M. and Herzog, V. (2004) 'Normalized Proliferation of Normal and Psoriatic Keratinocytes by Suppression of sAPP[alpha]-Release', *J Investig Dermatol*, 123(3), pp. 556-563.

Silva, D. F., Selfridge, J. E., Lu, J., E, L., Roy, N., Huffles, L., Burns, J. M., Michaelis, E. K., Yan, S., Cardoso, S. M. and Swerdlow, R. H. (2013) 'Bioenergetic flux, mitochondrial mass and mitochondrial morphology dynamics in AD and MCI cybrid cell lines', *Human Molecular Genetics*, 22(19), pp. 3931-3946.

Siman, R., Card, J. P. and Davis, L. G. (1990) 'Proteolytic processing of beta-amyloid precursor by calpain I', *Journal of Neuroscience*, 10(7), pp. 2400-11.

Simpson, P. B., Bacha, J. I., Palfreyman, E. L., Woollacott, A. J., McKernan, R. M. and Kerby, J. (2001) 'Retinoic Acid-Evoked Differentiation of Neuroblastoma Cells Predominates over Growth Factor Stimulation: An Automated Image Capture and Quantitation Approach to Neuritogenesis', *Analytical Biochemistry*, 298(2), pp. 163-169.

Sims, N. R., Finegan, J. M. and Blass, J. P. (1987) 'Altered metabolic properties of cultured skin fibroblasts in Alzheimer's disease', *Annals of Neurology*, 21(5), pp. 451-7.

Singleton, A. B., Hall, R., Ballard, C. G., Perry, R. H., Xuereb, J. H., Rubinsztein, D. C., Tysoe, C., Matthews, P., Cordell, B., Kumar-Singh, S., De Jonghe, C., Cruts, M., van Broeckhoven, C. and Morris, C. M. (2000) 'Pathology of early-onset Alzheimer's disease cases bearing the Thr113-114ins presenilin-1 mutation', *Brain*, 123 Pt 12, pp. 2467-74.

Sisodia, S. S., Koo, E. H., Hoffman, P. N., Perry, G. and Price, D. L. (1993) 'Identification and transport of full-length amyloid precursor proteins in rat peripheral nervous system', *Journal of Neuroscience*, 13(7), pp. 3136-42.

Skovronsky, D. M., Fath, S., Lee, V. M. and Milla, M. E. (2001) 'Neuronal localization of the TNFalpha converting enzyme (TACE) in brain tissue and its correlation to amyloid plaques', *J Neurobiol*, 49(1), pp. 40-6.

Smith, M. A., Kutty, R. K., Richey, P. L., Yan, S. D., Stern, D., Chader, G. J., Wiggert, B., Petersen, R. B. and Perry, G. (1994) 'Heme oxygenase-1 is associated with the neurofibrillary pathology of Alzheimer's disease', *The American Journal of Pathology*, 145(1), pp. 42-47.

Smith, M. A., Richey Harris, P. L., Sayre, L. M., Beckman, J. S. and Perry, G. (1997) 'Widespread peroxynitrite-mediated damage in Alzheimer's disease', *J Neurosci*, 17(8), pp. 2653-7.

Snyder, S. W., Lador, U. S., Wade, W. S., Wang, G. T., Barrett, L. W., Matayoshi, E. D., Huffaker, H. J., Krafft, G. A. and Holzman, T. F. (1994) 'Amyloid-beta aggregation: selective inhibition of aggregation in mixtures of amyloid with different chain lengths', *Biophysical Journal*, 67(3), pp. 1216-28.

Sommer, G., Kralisch, S., Lipfert, J., Weise, S., Krause, K., Jessnitzer, B., Lössner, U., Blüher, M., Stumvoll, M. and Fasshauer, M. (2009) 'Amyloid precursor protein expression is induced by tumor necrosis factor  $\alpha$  in 3T3-L1 adipocytes', *Journal of Cellular Biochemistry*, 108(6), pp. 1418-1422.

Sprecher, C. A., Grant, F. J., Grimm, G., O'Hara, P. J., Norris, F., Norris, K. and Foster, D. C. (1993) 'Molecular cloning of the cDNA for a human amyloid precursor protein homolog: Evidence for a multigene family', *Biochemistry*, 32(17), pp. 4481-4486.

Sproul, A. A., Jacob, S., Pre, D., Kim, S. H., Nestor, M. W., Navarro-Sobrino, M., Santa-Maria, I., Zimmer, M., Aubry, S., Steele, J. W., Kahler, D. J., Dranovsky, A.,

Arancio, O., Crary, J. F., Gandy, S. and Noggle, S. A. (2014) 'Characterization and molecular profiling of PSEN1 familial Alzheimer's disease iPSC-derived neural progenitors', *PLoS One*, 9(1), pp. e84547.

Stadelmann, C., Deckwerth, T. L., Srinivasan, A., Bancher, C., Bruck, W., Jellinger, K. and Lassmann, H. (1999) 'Activation of caspase-3 in single neurons and autophagic granules of granulovacuolar degeneration in Alzheimer's disease. Evidence for apoptotic cell death', *Am J Pathol*, 155(5), pp. 1459-66.

Steinberg, S., Stefansson, H., Jonsson, T., Johannsdottir, H., Ingason, A., Helgason, H., Sulem, P., Magnusson, O. T., Gudjonsson, S. A., Unnsteinsdottir, U., Kong, A., Helisalimi, S., Soininen, H., Lah, J. J., DemGene, Aarsland, D., Fladby, T., Ulstein, I. D., Djurovic, S., Sando, S. B., White, L. R., Knudsen, G.-P., Westlye, L. T., Selbaek, G., Giegling, I., Hampel, H., Hiltunen, M., Levey, A. I., Andreassen, O. A., Rujescu, D., Jonsson, P. V., Bjornsson, S., Snaedal, J. and Stefansson, K. (2015) 'Loss-of-function variants in ABCA7 confer risk of Alzheimer's disease', *Nat Genet*, advance online publication.

Steiner, H., Capell, A., Pesold, B., Citron, M., Kloetzel, P. M., Selkoe, D. J., Romig, H., Mendla, K. and Haass, C. (1998) 'Expression of Alzheimer's Disease-associated Presenilin-1 Is Controlled by Proteolytic Degradation and Complex Formation', *Journal of Biological Chemistry*, 273(48), pp. 32322-32331.

Stellato, F., Menestrina, G., Serra, M., Potrich, C., Tomazzolli, R., Meyer-Klaucke, W. and Morante, S. (2006) 'Metal binding in amyloid  $\beta$ -peptides shows intra- and inter-peptide coordination modes', *European Biophysics Journal*, 35(4), pp. 340-351.

Stoll, S., Hartmann, H., Cohen, S. A. and Müller, W. E. (1993) 'The potent free radical scavenger alpha-lipoic acid improves memory in aged mice: putative relationship to NMDA receptor deficits', *Pharmacol Biochem Behav*, 46(4), pp. 799-805.

Strittmatter, W. J., Saunders, A. M., Schmechel, D., Pericak-Vance, M., Enghild, J., Salvesen, G. S. and Roses, A. D. (1993) 'Apolipoprotein E: high-avidity binding to beta-amyloid and increased frequency of type 4 allele in late-onset familial Alzheimer disease', *Proceedings of the National Academy of Sciences of the United States of America*, 90(5), pp. 1977-1981.

Stutzbach, L. D., Xie, S. X., Naj, A. C., Albin, R., Gilman, S., Lee, V. M., Trojanowski, J. Q., Devlin, B., Schellenberg, G. D. and Group, P. G. S. (2013) 'The unfolded protein response is activated in disease-affected brain regions in progressive supranuclear palsy and Alzheimer's disease', *Acta Neuropathol Commun*, 1, pp. 31.

Sultana, R., Piroddi, M., Galli, F. and Butterfield, D. A. (2008) 'Protein levels and activity of some antioxidant enzymes in hippocampus of subjects with amnesic mild cognitive impairment', *Neurochem Res*, 33(12), pp. 2540-6.

Swerdlow, R. H., Golbe, L. I., Parks, J. K., Cassarino, D. S., Binder, D. R., Grawey, A. E., Litvan, I., Bennett, J. P., Jr., Wooten, G. F. and Parker, W. D. (2000) 'Mitochondrial dysfunction in cybrid lines expressing mitochondrial genes from patients with progressive supranuclear palsy', *J Neurochem*, 75(4), pp. 1681-4.

Tagliavini, F., Giaccone, G., Frangione, B. and Bugiani, O. (1988) 'Preamyloid deposits in the cerebral cortex of patients with Alzheimer's disease and nondemented individuals', *Neuroscience Letters*, 93(2-3), pp. 191-6.

Tait, S. W. and Green, D. R. (2012) 'Mitochondria and cell signalling', *J Cell Sci*, 125(Pt 4), pp. 807-15.

Takagane, K., Nojima, J., Mitsuhashi, H., Suo, S., Yanagihara, D., Takaiwa, F., Urano, Y., Noguchi, N. and Ishiura, S. (2015) 'Abeta induces oxidative stress in senescence-accelerated (SAMP8) mice', *Biosci Biotechnol Biochem*, pp. 1-7.

Takahashi, K. and Yamanaka, S. (2006a) 'Induction of Pluripotent Stem Cells from Mouse Embryonic and Adult Fibroblast Cultures by Defined Factors', *Cell*, 126(4), pp. 663-676.

Takahashi, K. and Yamanaka, S. (2006b) 'Induction of pluripotent stem cells from mouse embryonic and adult fibroblast cultures by defined factors', *Cell*, 126(4), pp. 663-76.

- Takano, T., Sahara, N., Yamanouchi, Y. and Mori, H. (1997) 'Assignment of Alzheimer's presenilin-2 (PS-2) gene to 1q42.1 by fluorescence in situ hybridization', *Neuroscience Letters*, 221(2-3), pp. 205-7.
- Takebayashi, M., Hayashi, T. and Su, T. P. (2002) 'Nerve growth factor-induced neurite sprouting in PC12 cells involves sigma-1 receptors: implications for antidepressants', *J Pharmacol Exp Ther*, 303(3), pp. 1227-37.
- Takeda, M., Nishimura, T., Hariguchi, S., Tatebayashi, Y., Tanaka, T., Tanimukai, S. and Tada, K. (1991) 'Study of cytoskeletal proteins in fibroblasts cultured from familial Alzheimer's disease', *Acta Neurologica Scandinavica*, 84(5), pp. 416-420.
- Takeda, M., Tanaka, M., Kudo, T., Nakamura, Y., Tada, K. and Nishimura, T. (1990) 'Changes in adhesion efficiency and vimentin distribution of fibroblasts from familial Alzheimer's disease patients', *Acta Neurol Scand*, 82(4), pp. 238-44.
- Talantova, M., Sanz-Blasco, S., Zhang, X., Xia, P., Akhtar, M. W., Okamoto, S., Dziejczapolski, G., Nakamura, T., Cao, G., Pratt, A. E., Kang, Y. J., Tu, S., Molokanova, E., McKercher, S. R., Hires, S. A., Sason, H., Stouffer, D. G., Buczynski, M. W., Solomon, J. P., Michael, S., Powers, E. T., Kelly, J. W., Roberts, A., Tong, G., Fang-Newmeyer, T., Parker, J., Holland, E. A., Zhang, D., Nakanishi, N., Chen, H. S., Wolosker, H., Wang, Y., Parsons, L. H., Ambasadhan, R., Masliah, E., Heinemann, S. F., Pina-Crespo, J. C. and Lipton, S. A. (2013) 'Abeta induces astrocytic glutamate release, extrasynaptic NMDA receptor activation, and synaptic loss', *Proc Natl Acad Sci U S A*, 110(27), pp. E2518-27.
- Tamaoka, A., Odaka, A., Ishibashi, Y., Usami, M., Sahara, N., Suzuki, N., Nukina, N., Mizusawa, H., Shoji, S., Kanazawa, I. and et al. (1994) 'APP717 missense mutation affects the ratio of amyloid beta protein species (A beta 1-42/43 and a beta 1-40) in familial Alzheimer's disease brain', *J Biol Chem*, 269(52), pp. 32721-4.
- Tanaka, S., Shiojiri, S., Takahashi, Y., Kitaguchi, N., Ito, H., Kameyama, M., Kimura, J., Nakamura, S. and Ueda, K. (1989) 'Tissue-specific expression of three types of  $\beta$ -protein precursor mRNA: Enhancement of protease inhibitor-harboring types in Alzheimer's disease brain', *Biochemical and Biophysical Research Communications*, 165(3), pp. 1406-1414.
- Tanzi, R. E. and Hyman, B. T. (1991) 'Alzheimer's mutation', *Nature*, 350(6319), pp. 564.
- Tarczylyuk, M. A., Nagel, D. A., Rhein Parri, H., Tse, E. H., Brown, J. E., Coleman, M. D. and Hill, E. J. (2015) 'Amyloid beta 1-42 induces hypometabolism in human stem cell-derived neuron and astrocyte networks', *J Cereb Blood Flow Metab*.
- Tatebayashi, Y., Takeda, M., Kashiwagi, Y., Okochi, M., Kurumadani, T., Sekiyama, A., Kanayama, G., Hariguchi, S. and Nishimura, T. (1995) 'Cell-cycle-dependent abnormal calcium response in fibroblasts from patients with familial Alzheimer's disease', *Dementia*, 6(1), pp. 9-16.
- Taylor, C. J., Ireland, D. R., Ballagh, I., Bourne, K., Marechal, N. M., Turner, P. R., Bilkey, D. K., Tate, W. P. and Abraham, W. C. (2008a) 'Endogenous secreted amyloid precursor protein-alpha regulates hippocampal NMDA receptor function, long-term potentiation and spatial memory', *Neurobiology of Disease*, 31(2), pp. 250-60.
- Taylor, C. J., Ireland, D. R., Ballagh, I., Bourne, K., Marechal, N. M., Turner, P. R., Bilkey, D. K., Tate, W. P. and Abraham, W. C. (2008b) 'Endogenous secreted amyloid precursor protein-alpha regulates hippocampal NMDA receptor function, long-term potentiation and spatial memory', *Neurobiol Dis*, 31(2), pp. 250-60.
- Tebar, F., Bohlander, S. K. and Sorkin, A. (1999) 'Clathrin assembly lymphoid myeloid leukemia (CALM) protein: localization in endocytic-coated pits, interactions with clathrin, and the impact of overexpression on clathrin-mediated traffic', *Mol Biol Cell*, 10(8), pp. 2687-702.
- Teipel, S., Heinsen, H., Amaro Jr, E., Grinberg, L. T., Krause, B. and Grothe, M. (2014) 'Cholinergic basal forebrain atrophy predicts amyloid burden in Alzheimer's disease', *Neurobiology of Aging*, 35(3), pp. 482-491.
- Tesco, G., Latorraca, S., Piersanti, P., Piacentini, S., Amaducci, L. and Sorbi, S. (1992) 'Alzheimer skin fibroblasts show increased susceptibility to free radicals', *Mechanisms of Ageing and Development*, 66(2), pp. 117-20.

Texido, L., Martin-Satue, M., Alberdi, E., Solsona, C. and Matute, C. (2011) 'Amyloid beta peptide oligomers directly activate NMDA receptors', *Cell Calcium*, 49(3), pp. 184-90.

Thambisetty, M., An, Y., Nalls, M., Sojkova, J., Swaminathan, S., Zhou, Y., Singleton, A. B., Wong, D. F., Ferrucci, L., Saykin, A. J. and Resnick, S. M. (2013) 'Effect of complement CR1 on brain amyloid burden during aging and its modification by APOE genotype', *Biol Psychiatry*, 73(5), pp. 422-8.

Theuns, J., Marjaux, E., Vandenbulcke, M., Van Laere, K., Kumar-Singh, S., Bormans, G., Brouwers, N., Van den Broeck, M., Vennekens, K., Corsmit, E., Cruts, M., De Strooper, B., Van Broeckhoven, C. and Vandenberghe, R. (2006) 'Alzheimer dementia caused by a novel mutation located in the APP C-terminal intracytosolic fragment', *Hum Mutat*, 27(9), pp. 888-96.

Thinakaran, G., Borchelt, D. R., Lee, M. K., Slunt, H. H., Spitzer, L., Kim, G., Ratovitsky, T., Davenport, F., Nordstedt, C., Seeger, M., Hardy, J., Levey, A. I., Gandy, S. E., Jenkins, N. A., Copeland, N. G., Price, D. L. and Sisodia, S. S. (1996) 'Endoproteolysis of presenilin 1 and accumulation of processed derivatives in vivo', *Neuron*, 17(1), pp. 181-90.

Thinakaran, G. and Koo, E. H. (2008) 'Amyloid precursor protein trafficking, processing, and function', *Journal of Biological Chemistry*, 283(44), pp. 29615-9.

Thrash, J. C., Boyd, A., Huggett, M. J., Grote, J., Carini, P., Yoder, R. J., Robbertse, B., Spatafora, J. W., Rappe, M. S. and Giovannoni, S. J. (2011) 'Phylogenomic evidence for a common ancestor of mitochondria and the SAR11 clade', *Sci. Rep.*, 1.

Tretter, L. and Adam-Vizi, V. (2005) 'Alpha-ketoglutarate dehydrogenase: a target and generator of oxidative stress', *Philos Trans R Soc Lond B Biol Sci*, 360(1464), pp. 2335-45.

Turner, P. R., O'Connor, K., Tate, W. P. and Abraham, W. C. (2003) 'Roles of amyloid precursor protein and its fragments in regulating neural activity, plasticity and memory', *Progress in Neurobiology*, 70(1), pp. 1-32.

Ueda, K., Cole, G., Sundsmo, M., Katzman, R. and Saitoh, T. (1989) 'Decreased adhesiveness of Alzheimer's disease fibroblasts: is amyloid beta-protein precursor involved?', *Annals of Neurology*, 25(3), pp. 246-51.

Valenti, D., Manente, G. A., Moro, L., Marra, E. and Vacca, R. A. (2011) 'Deficit of complex I activity in human skin fibroblasts with chromosome 21 trisomy and overproduction of reactive oxygen species by mitochondria: involvement of the cAMP/PKA signalling pathway', *Biochem J*, 435(3), pp. 679-88.

van Bebber, F., Paquet, D., Hruscha, A., Schmid, B. and Haass, C. (2010) 'Methylene blue fails to inhibit Tau and polyglutamine protein dependent toxicity in zebrafish', *Neurobiol Dis*, 39(3), pp. 265-71.

van der Blik, A. M., Shen, Q. and Kawajiri, S. (2013) 'Mechanisms of mitochondrial fission and fusion', *Cold Spring Harb Perspect Biol*, 5(6).

Van Nostrand, W. E., Melchor, J. P., Keane, D. M., Saporito-Irwin, S. M., Romanov, G., Davis, J. and Xu, F. (2002) 'Localization of a fibrillar amyloid beta-protein binding domain on its precursor', *J Biol Chem*, 277(39), pp. 36392-8.

Varghese, M., Zhao, W., Wang, J., Cheng, A., Qian, X., Chaudhry, A., Ho, L. and Pasinetti, G. (2011) 'Mitochondrial bioenergetics is defective in presymptomatic Tg2576 AD Mice', *Translational Neuroscience*, 2(1), pp. 1-5.

Vassar, R. (2005) 'beta-Secretase, APP and Abeta in Alzheimer's disease', *Subcell Biochem*, 38, pp. 79-103.

Vassar, R., Bennett, B. D., Babu-Khan, S., Kahn, S., Mendiaz, E. A., Denis, P., Teplow, D. B., Ross, S., Amarante, P., Loeloff, R., Luo, Y., Fisher, S., Fuller, J., Edenson, S., Lile, J., Jarosinski, M. A., Biere, A. L., Curran, E., Burgess, T., Louis, J. C., Collins, F., Treanor, J., Rogers, G. and Citron, M. (1999) 'Beta-secretase cleavage of Alzheimer's amyloid precursor protein by the transmembrane aspartic protease BACE', *Science*, 286(5440), pp. 735-41.

Vestling, M., Cedazo-Minguez, A., Adem, A., Wiehager, B., Racchi, M., Lannfelt, L. and Cowburn, R. F. (1999) 'Protein kinase C and amyloid precursor protein processing in

skin fibroblasts from sporadic and familial Alzheimer's disease cases', *Biochim Biophys Acta*, 1453(3), pp. 341-50.

Villemagne, V. L., Furumoto, S., Fodero-Tavoletti, M. T., Mulligan, R. S., Hodges, J., Harada, R., Yates, P., Piguet, O., Pejoska, S., Dore, V., Yanai, K., Masters, C. L., Kudo, Y., Rowe, C. C. and Okamura, N. (2014) 'In vivo evaluation of a novel tau imaging tracer for Alzheimer's disease', *European Journal of Nuclear Medicine and Molecular Imaging*, 41(5), pp. 816-26.

von Arnim, C. A., Kinoshita, A., Peltan, I. D., Tangredi, M. M., Herl, L., Lee, B. M., Spoelgen, R., Hshieh, T. T., Ranganathan, S., Battey, F. D., Liu, C. X., Bacskai, B. J., Sever, S., Irizarry, M. C., Strickland, D. K. and Hyman, B. T. (2005) 'The low density lipoprotein receptor-related protein (LRP) is a novel beta-secretase (BACE1) substrate', *J Biol Chem*, 280(18), pp. 17777-85.

Vossel, K. A., Zhang, K., Brodbeck, J., Daub, A. C., Sharma, P., Finkbeiner, S., Cui, B. and Mucke, L. (2010) 'Tau Reduction Prevents A $\beta$ -Induced Defects in Axonal Transport', *Science*, 330(6001), pp. 198.

Walgren, J. L., Amani, Z., McMillan, J. M., Locher, M. and Buse, M. G. (2004) 'Effect of R(+)-alpha-lipoic acid on pyruvate metabolism and fatty acid oxidation in rat hepatocytes', *Metabolism*, 53(2), pp. 165-73.

Walls, K. C., Coskun, P., Gallegos-Perez, J. L., Zadourian, N., Freude, K., Rasool, S., Blurton-Jones, M., Green, K. N. and LaFerla, F. M. (2012a) 'Swedish Alzheimer mutation induces mitochondrial dysfunction mediated by HSP60 mislocalization of amyloid precursor protein (APP) and beta-amyloid', *Journal of Biological Chemistry*, 287(36), pp. 30317-27.

Walls, K. C., Coskun, P., Gallegos-Perez, J. L., Zadourian, N., Freude, K., Rasool, S., Blurton-Jones, M., Green, K. N. and LaFerla, F. M. (2012b) 'Swedish Alzheimer Mutation Induces Mitochondrial Dysfunction Mediated by HSP60 Mislocalization of Amyloid Precursor Protein (APP) and Beta-Amyloid', *The Journal of Biological Chemistry*, 287(36), pp. 30317-30327.

Walsh, D. M., Minogue, A. M., Sala Frigerio, C., Fadeeva, J. V., Wasco, W. and Selkoe, D. J. (2007) 'The APP family of proteins: similarities and differences', *Biochem Soc Trans*, 35(Pt 2), pp. 416-20.

Wang, H. F., Tan, L., Hao, X. K., Jiang, T., Tan, M. S., Liu, Y., Zhang, D. Q. and Yu, J. T. (2015a) 'Effect of EPHA1 genetic variation on cerebrospinal fluid and neuroimaging biomarkers in healthy, mild cognitive impairment and Alzheimer's disease cohorts', *J Alzheimers Dis*, 44(1), pp. 115-23.

Wang, P., Yang, G., Mosier, D. R., Chang, P., Zaidi, T., Gong, Y. D., Zhao, N. M., Dominguez, B., Lee, K. F., Gan, W. B. and Zheng, H. (2005) 'Defective neuromuscular synapses in mice lacking amyloid precursor protein (APP) and APP-like protein 2', *Journal of Neuroscience*, 25(5), pp. 1219-1225.

Wang, R., Chen, S., Liu, Y., Diao, S., Xue, Y., You, X., Park, E. A. and Liao, F. F. (2015b) 'All-trans-retinoic Acid Reduces BACE1 Expression under Inflammatory Conditions via Modulation of Nuclear Factor  $\kappa$ B (NF $\kappa$ B) Signaling', *J Biol Chem*, 290(37), pp. 22532-42.

Wang, S., Song, P. and Zou, M. H. (2012) 'AMP-activated protein kinase, stress responses and cardiovascular diseases', *Clinical Science*, 122(12), pp. 555-573.

Wang, X., Su, B., Lee, H. G., Li, X., Perry, G., Smith, M. A. and Zhu, X. (2009a) 'Impaired balance of mitochondrial fission and fusion in Alzheimer's disease', *J Neurosci*, 29(28), pp. 9090-103.

Wang, X., Su, B., Lee, H. G., Li, X., Perry, G., Smith, M. A. and Zhu, X. (2009b) 'Impaired balance of mitochondrial fission and fusion in Alzheimer's disease', *Journal of Neuroscience*, 29(28), pp. 9090-103.

Wang, X., Wang, W., Li, L., Perry, G., Lee, H. G. and Zhu, X. (2014a) 'Oxidative stress and mitochondrial dysfunction in Alzheimer's disease', *Biochim Biophys Acta*, 1842(8), pp. 1240-7.

Wang, X., Wang, Z., Chen, Y., Huang, X., Hu, Y., Zhang, R., Ho, M. S. and Xue, L. (2014b) 'FoxO mediates APP-induced AICD-dependent cell death', *Cell Death Dis*, 5, pp. e1233.

Wang, X. F. and Cynader, M. S. (2000) 'Astrocytes provide cysteine to neurons by releasing glutathione', *J Neurochem*, 74(4), pp. 1434-42.

Wang, Y. and Ha, Y. (2004) 'The X-ray structure of an antiparallel dimer of the human amyloid precursor protein E2 domain', *Mol Cell*, 15(3), pp. 343-53.

Waring, S. C. and Rosenberg, R. N. (2008) 'Genome-wide association studies in Alzheimer disease', *Arch Neurol*, 65(3), pp. 329-34.

Wasco, W., Bupp, K., Magendantz, M., Gusella, J. F., Tanzi, R. E. and Solomon, F. (1992) 'Identification of a mouse brain cDNA that encodes a protein related to the Alzheimer disease-associated amyloid beta protein precursor', *Proc Natl Acad Sci U S A*, 89(22), pp. 10758-62.

Weber, G. F. (1999) 'Final common pathways in neurodegenerative diseases: regulatory role of the glutathione cycle', *Neurosci Biobehav Rev*, 23(8), pp. 1079-86.

Weggen, S. and Beher, D. (2012) 'Molecular consequences of amyloid precursor protein and presenilin mutations causing autosomal-dominant Alzheimer's disease', *Alzheimers Res Ther*, 4(2), pp. 9.

Wegiel, J. and Wisniewski, H. M. (1990) 'The complex of microglial cells and amyloid star in three-dimensional reconstruction', *Acta Neuropathol*, 81(2), pp. 116-24.

Werb, Z. and Yan, Y. (1998) 'A cellular striptease act', *Science*, 282(5392), pp. 1279-80.

Weskamp, G., Cai, H., Brodie, T. A., Higashyama, S., Manova, K., Ludwig, T. and Blobel, C. P. (2002) 'Mice lacking the metalloprotease-disintegrin MDC9 (ADAM9) have no evident major abnormalities during development or adult life', *Molecular and Cellular Biology*, 22(5), pp. 1537-44.

Westermarck, P., Benson, M. D., Buxbaum, J. N., Cohen, A. S., Frangione, B., Ikeda, S.-I., Masters, C. L., Merlini, G., Saraiva, M. J. and Sipe, J. D. (2007) 'A primer of amyloid nomenclature', *Amyloid*, 14(3), pp. 179-183.

Weuve, J., Kang, J. H., Manson, J. E., Breteler, M. M., Ware, J. H. and Grodstein, F. (2004) 'Physical activity, including walking, and cognitive function in older women', *Jama*, 292(12), pp. 1454-61.

Willem, M., Garratt, A. N., Novak, B., Citron, M., Kaufmann, S., Rittger, A., DeStrooper, B., Saftig, P., Birchmeier, C. and Haass, C. (2006) 'Control of peripheral nerve myelination by the beta-secretase BACE1', *Science*, 314(5799), pp. 664-6.

Wilson, R. S., Li, Y., Aggarwal, N. T., Barnes, L. L., McCann, J. J., Gilley, D. W. and Evans, D. A. (2004) 'Education and the course of cognitive decline in Alzheimer disease', *Neurology*, 63(7), pp. 1198-202.

Winblad, B., Mobius, H. J. and Stoffler, A. (2002) 'Glutamate receptors as a target for Alzheimer's disease--are clinical results supporting the hope?', *J Neural Transm Suppl*, (62), pp. 217-25.

Wischik, C. and Staff, R. (2009) 'Challenges in the conduct of disease-modifying trials in AD: practical experience from a phase 2 trial of Tau-aggregation inhibitor therapy', *J Nutr Health Aging*, 13(4), pp. 367-9.

Wisniewski, T. and Frangione, B. (1992) 'Apolipoprotein E: a pathological chaperone protein in patients with cerebral and systemic amyloid', *Neuroscience Letters*, 135(2), pp. 235-8.

Woehrling, E. K., Hill, E. J. and Coleman, M. D. (2007) 'Development of a neurotoxicity test-system, using human post-mitotic, astrocytic and neuronal cell lines in co-culture', *Toxicol In Vitro*, 21(7), pp. 1241-6.

Wollmer, M. A. (2010) 'Cholesterol-related genes in Alzheimer's disease', *Biochimica et Biophysica Acta (BBA) - Molecular and Cell Biology of Lipids*, 1801(8), pp. 762-773.

Wong, H. K., Sakurai, T., Oyama, F., Kaneko, K., Wada, K., Miyazaki, H., Kurosawa, M., De Strooper, B., Saftig, P. and Nukina, N. (2005) 'beta Subunits of voltage-gated sodium channels are novel substrates of beta-site amyloid precursor protein-cleaving enzyme (BACE1) and gamma-secretase', *J Biol Chem*, 280(24), pp. 23009-17.

Wong, P. C., Zheng, H., Chen, H., Becher, M. W., Sirinathsinghji, D. J. S., Trumbauer, M. E., Chen, H. Y., Price, D. L., Van der Ploeg, L. H. T. and Sisodia, S. S. (1997) 'Presenilin 1 is required for Notch 1 and Dll1 expression in the paraxial mesoderm', *Nature*, 387(6630), pp. 288-292.

- Wray, S. and Lewis, P. A. (2010) 'A tangled web - tau and sporadic Parkinson's disease', *Front Psychiatry*, 1, pp. 150.
- Xie, H. R., Hu, L. S. and Li, G. Y. (2010) 'SH-SY5Y human neuroblastoma cell line: in vitro cell model of dopaminergic neurons in Parkinson's disease', *Chin Med J (Engl)*, 123(8), pp. 1086-92.
- Xue, Y., Lee, S. and Ha, Y. (2011) 'Crystal structure of amyloid precursor-like protein 1 and heparin complex suggests a dual role of heparin in E2 dimerization', *Proceedings of the National Academy of Sciences*, 108(39), pp. 16229-16234.
- Xun, Z., Lee, D. Y., Lim, J., Canaria, C. A., Barnebey, A., Yanonne, S. M. and McMurray, C. T. (2012) 'Retinoic acid-induced differentiation increases the rate of oxygen consumption and enhances the spare respiratory capacity of mitochondria in SH-SY5Y cells', *Mech Ageing Dev*, 133(4), pp. 176-85.
- Yagi, T., Ito, D., Okada, Y., Akamatsu, W., Nihei, Y., Yoshizaki, T., Yamanaka, S., Okano, H. and Suzuki, N. (2011) 'Modeling familial Alzheimer's disease with induced pluripotent stem cells', *Human Molecular Genetics*.
- Yamatsuji, T., Matsui, T., Okamoto, T., Komatsuzaki, K., Takeda, S., Fukumoto, H., Iwatsubo, T., Suzuki, N., Asami-Odaka, A., Ireland, S., Kinane, T. B., Giambarella, U. and Nishimoto, I. (1996) 'G protein-mediated neuronal DNA fragmentation induced by familial Alzheimer's disease-associated mutants of APP', *Science*, 272(5266), pp. 1349-52.
- Yan, P. K., Mei, Z. R., Situ, B., Tan, X. P., Zheng, S. M., Zhang, F. Y. and Liu, P. Q. (2010) 'Cryptotanshinone upregulates alpha-secretase by activation PI3K pathway in cortical neurons', *Brain Research*, 1348, pp. 165-173.
- Yan, R., Munzner, J. B., Shuck, M. E. and Bienkowski, M. J. (2001) 'BACE2 functions as an alternative alpha-secretase in cells', *J Biol Chem*, 276(36), pp. 34019-27.
- Yanamandra, K., Kfoury, N., Jiang, H., Mahan, Thomas E., Ma, S., Maloney, Susan E., Wozniak, David F., Diamond, Marc I. and Holtzman, David M. (2013) 'Anti-Tau Antibodies that Block Tau Aggregate Seeding In Vitro Markedly Decrease Pathology and Improve Cognition In Vivo', *Neuron*, 80(2), pp. 402-414.
- Yang, T.-T., Hsu, C.-T. and Kuo, Y.-M. (2009) 'Amyloid precursor protein, heat-shock proteins, and Bcl-2 form a complex in mitochondria and modulate mitochondria function and apoptosis in N2a cells', *Mechanisms of Ageing and Development*, 130(9), pp. 592-601.
- Yankner, B. A., Duffy, L. K. and Kirschner, D. A. (1990) 'Neurotrophic and neurotoxic effects of amyloid beta protein: reversal by tachykinin neuropeptides', *Science*, 250(4978), pp. 279-82.
- Yao, J., Du, H., Yan, S., Fang, F., Wang, C., Lue, L. F., Guo, L., Chen, D., Stern, D. M., Gunn Moore, F. J., Xi Chen, J., Arancio, O. and Yan, S. S. (2011) 'Inhibition of amyloid-beta (A $\beta$ ) peptide-binding alcohol dehydrogenase-A $\beta$  interaction reduces A $\beta$  accumulation and improves mitochondrial function in a mouse model of Alzheimer's disease', *Journal of Neuroscience*, 31(6), pp. 2313-20.
- Yao, J., Irwin, R. W., Zhao, L., Nilsen, J., Hamilton, R. T. and Brinton, R. D. (2009a) 'Mitochondrial bioenergetic deficit precedes Alzheimer's pathology in female mouse model of Alzheimer's disease', *Proc Natl Acad Sci U S A*, 106(34), pp. 14670-5.
- Yao, J., Irwin, R. W., Zhao, L., Nilsen, J., Hamilton, R. T. and Brinton, R. D. (2009b) 'Mitochondrial bioenergetic deficit precedes Alzheimer's pathology in female mouse model of Alzheimer's disease', *Proceedings of the National Academy of Sciences*.
- Yao, J., Taylor, M., Davey, F., Ren, Y., Aiton, J., Coote, P., Fang, F., Chen, J. X., Yan, S. D. and Gunn-Moore, F. J. (2007) 'Interaction of amyloid binding alcohol dehydrogenase/A $\beta$  mediates up-regulation of peroxiredoxin II in the brains of Alzheimer's disease patients and a transgenic Alzheimer's disease mouse model', *Mol Cell Neurosci*, 35(2), pp. 377-82.
- Yoshikai, S.-i., Sasaki, H., Doh-ura, K., Furuya, H. and Sakaki, Y. (1990) 'Genomic organization of the human amyloid beta-protein precursor gene', *Gene*, 87(2), pp. 257-263.
- Young, J. E., Boulanger-Weill, J., Williams, D. A., Woodruff, G., Buen, F., Revilla, A. C., Herrera, C., Israel, M. A., Yuan, S. H., Edland, S. D. and Goldstein, L. S. (2015)

'Elucidating Molecular Phenotypes Caused by the SORL1 Alzheimer's Disease Genetic Risk Factor Using Human Induced Pluripotent Stem Cells', *Cell Stem Cell*, 16(4), pp. 373-85.

Yu, G., Nishimura, M., Arawaka, S., Levitan, D., Zhang, L., Tandon, A., Song, Y. Q., Rogaeva, E., Chen, F., Kawarai, T., Supala, A., Levesque, L., Yu, H., Yang, D. S., Holmes, E., Milman, P., Liang, Y., Zhang, D. M., Xu, D. H., Sato, C., Rogaeve, E., Smith, M., Janus, C., Zhang, Y., Aebbersold, R., Farrer, L. S., Sorbi, S., Bruni, A., Fraser, P. and St George-Hyslop, P. (2000) 'Nicastrin modulates presenilin-mediated notch/glp-1 signal transduction and betaAPP processing', *Nature*, 407(6800), pp. 48-54.

Yusuf, M., Leung, K., Morris, K. and Volpi, E. (2013) 'Comprehensive cytogenomic profile of the in vitro neuronal model SH-SY5Y', *neurogenetics*, 14(1), pp. 63-70.

Zhang, H., Ma, Q., Zhang, Y.-w. and Xu, H. (2012a) 'Proteolytic processing of Alzheimer's  $\beta$ -amyloid precursor protein', *Journal of Neurochemistry*, 120, pp. 9-21.

Zhang, J., Cao, Q., Li, S., Lu, X., Zhao, Y., Guan, J. S., Chen, J. C., Wu, Q. and Chen, G. Q. (2013) '3-Hydroxybutyrate methyl ester as a potential drug against Alzheimer's disease via mitochondria protection mechanism', *Biomaterials*, 34(30), pp. 7552-62.

Zhang, J., Nuebel, E., Wisidagama, D. R. R., Setoguchi, K., Hong, J. S., Van Horn, C. M., Imam, S. S., Vergnes, L., Malone, C. S., Koehler, C. M. and Teitell, M. A. (2012b) 'Measuring energy metabolism in cultured cells, including human pluripotent stem cells and differentiated cells', *Nature protocols*, 7(6), pp. 10.1038/nprot.2012.048.

Zhang, M. (1990) '[Prevalence study on dementia and Alzheimer disease]', *Zhonghua Yi Xue Za Zhi*, 70(8), pp. 424-8, 30.

Zhang, W., Arteaga, J., Cashion, D. K., Chen, G., Gangadharmath, U., Gomez, L. F., Kasi, D., Lam, C., Liang, Q., Liu, C., Mocharla, V. P., Mu, F., Sinha, A., Szardenings, A. K., Wang, E., Walsh, J. C., Xia, C., Yu, C., Zhao, T. and Kolb, H. C. (2012c) 'A highly selective and specific PET tracer for imaging of tau pathologies', *J Alzheimers Dis*, 31(3), pp. 601-12.

Zhang, Y.-w., Thompson, R., Zhang, H. and Xu, H. (2011) 'APP processing in Alzheimer's disease', *Molecular Brain*, 4(1), pp. 3.

Zhang, Z., Nadeau, P., Song, W., Donoviel, D., Yuan, M., Bernstein, A. and Yankner, B. A. (2000) 'Presenilins are required for gamma-secretase cleavage of beta-APP and transmembrane cleavage of Notch-1', *Nat Cell Biol*, 2(7), pp. 463-5.

Zhao, W.-Q. and Townsend, M. (2009) 'Insulin resistance and amyloidogenesis as common molecular foundation for type 2 diabetes and Alzheimer's disease', *Biochimica et Biophysica Acta (BBA) - Molecular Basis of Disease*, 1792(5), pp. 482-496.

Zheng, H. and Koo, E. H. (2006a) 'The amyloid precursor protein: beyond amyloid', *Molecular Neurodegeneration*, 1, pp. 5.

Zheng, H. and Koo, E. H. (2006b) 'The amyloid precursor protein: beyond amyloid', *Mol Neurodegener*, 1, pp. 5.

Zheng, L., Calvo-Garrido, J., Hallbeck, M., Hultenby, K., Marcusson, J., Cedazo-Minguez, A. and Terman, A. (2013) 'Intracellular localization of amyloid-beta peptide in SH-SY5Y neuroblastoma cells', *J Alzheimers Dis*, 37(4), pp. 713-33.

Zimmermann, K. C. and Green, D. R. (2001) 'How cells die: Apoptosis pathways', *Journal of Allergy and Clinical Immunology*, 108(4, Supplement), pp. S99-S103.

Zubenko, G., Wusylko, M., Cohen, B., Boller, F. and Teply, I. (1987) 'Family study of platelet membrane fluidity in Alzheimer's disease', *Science*, 238(4826), pp. 539-542.

Zufferey, R., Nagy, D., Mandel, R. J., Naldini, L. and Trono, D. (1997) 'Multiply attenuated lentiviral vector achieves efficient gene delivery in vivo', *Nat Biotechnol*, 15(9), pp. 871-5.

## 7.0 Appendices

### 7.1 Sequencing for Pittsburgh/ jAPP695 in pcDNA3.1

Sample	Primer	Construct	Comment
1	Pcdna 100- seq	EM3 DH5 mini	23-916
2	App 613 for	EM3 DH5 mini	correct
3	App1004	EM3 DH5 mini	G-T at 2124
4	PCDNA+70 rev	EM3 DH5 mini	g-t at 2124
5	Pcdna 100- seq	EM4 MTR mini	correct
6	App 613 for	EM4 MTR mini	correct
7	App1004	EM4 MTR mini	G – T at 2124
8	PCDNA+70 rev	EM4 MTR mini	G – T at 2124
9	Pcdna 100- seq	EM7 MTR mini	correct
10	App 613 for	EM7 MTR mini	correct
11	App1004	EM7 MTR mini	G – T at 2124
12	PCDNA+70 rev	EM7 MTR mini	G – T at 2124
13	HindIII primer (Ex apps alt for)	Franks APP donor plasmid	correct
14	App 613 for	Franks APP donor plasmid	correct
15	App1004	Franks APP donor plasmid	G -> T at 2124
16	APP 1545	Franks APP donor plasmid	G -> T at 2124
17	APP2040 for	Franks APP donor plasmid	Ok, did not get sequence until at 2290, after mutation
18	App165 rev	Franks APP donor plasmid	Unrecognised
19	APP695rev	Franks APP donor plasmid	1150-1923
20	Ex apps alt for	Pittsburgh APP donor plasmid	25-834 , downstream mismatching
21	App 613 for	Pittsburgh APP donor plasmid	Upstream sequence does not match, 883- 1568
22	App1004	Pittsburgh APP donor plasmid	1050-2092
23	APP 1545	Pittsburgh APP donor plasmid	1579-2361
24	APP2040 for	Pittsburgh APP donor plasmid	2081- end of gene
25	App165 rev	Pittsburgh APP donor plasmid	Mismatching
26	APP695rev	Pittsburgh APP donor plasmid	1071-2049

## 7.2 Gel extraction



### 7.3 PCR Purification



## 7.4 QIAGEN Miniprep protocol



## 7.5 Transfection of COS7 with Lipofectamine LTX



Astron University

Illustration removed for copyright restrictions

## 7.5 PierceNet BCA protein assay



## 7.6 Antibodies for Western blotting

Antibody	Dilution	Company
Mouse anti-APP695	1:2000	Invitrogen
Mouse anti- A $\beta$ (6E10)	1:1000	Covance
Rabbit anti- $\beta$ actin	1:1000	Sigma Aldrich
Goat anti-rabbit HRP	1:5000	Dako
Rabbit anti-mouse HRP	1:5000	Cell Signalling

## 7.7 Recipe for making buffers (Western blotting)

10x Tris buffered saline (TBS): Trizma base (Sigma)  
NaCl  
Make up to final volume of 1L distilled water  
Adjust pH to 8.0 with 6N HCl

10% Tween: 5ml Tween-20  
45ml distilled water

TBS-T (1L): 100ml 10x TBS  
10ml 10% Tween  
890ml distilled water

10x Transfer buffer (TB): 72.08g Glycine (Sigma)  
15.52g Trizma base (Sigma)  
5g SDS (Sigma)

Dissolve in 1L distilled water

## 7.8 DNA/ Protein Ladder sizing

### PageRuler Prestained Protein Ladder



## 7.9 List of primers used

Purpose	Annealing temp (°C)	Primer
Sequencing of the pcDNA3 plasmid	-	pcDNA -100 seq <b>5' CAAATGGGCGGTAGGCG 3'</b> pcDNA+70 <b>5' GGTCAAGGAAGGCACGG 3'</b>
Sequencing the donor plasmids	-	APP2040 <b>5' CGGCTACGAAAATCCAACC 3'</b> APP165 Rev <b>5' GGTTTTGGTCCCTGATGG 3'</b>
Sequencing the APP gene	-	APP613 <b>5' GACTCGGATGTCTGGTGG 3'</b> APP1004 <b>5' TGAGAGAATGGGAAGAGGC 3'</b> APP 1545 <b>5' TCAGTTACGGAAACGATGC 3'</b>
Introducing 5' HindIII RS	55	Ex Alt APP for <b>5'TCCCAAGCTTGCCACCATGCTGCCCGGT TTGGC 3'</b>
Introducing 3' XbaI RS		APP695rev <b>5' AGCTTCTAGACTAGTTCTGCATCTGCTCAA A 3'</b>
Introducing the Swedish mutations	55	SweAPP695 rev <b>5' TCGGAATTCTGCATCCAGATTCCTTC 3'</b>
PCR of APP for entry into pCR8	66	APP P8 TOPO For G <b>5' TTGCCACCATGCTGCCCG 3'</b> APP 8 Rev 3 STOP <b>5' CTAGTTAAGACTAGTTCTGCATCTGCTC 3'</b>
PCR of SYN1 for entry into pENTR5'		Syn1 pentr5 For g <b>5'AGGCGGTATCCTGCAGAGGG 3'</b> Syn1 pentr Rev <b>5' GATCCCTGCGCTCTCAGG 3'</b>
Colony screening of pcDNA3/ pcDNA3.1	55	BGH REV <b>5' TAGAAGGCACAGTCGAGG 3'</b> T7 promoter <b>5'TTAATACGACTCACTATAGGG 3'</b>
Colony screening of pLenti6.4 constructs	55	pLenti6.4 for seq <b>5' GATTGGGGGGTACAGTGC 3'</b> WPRE Rev SQ <b>5' CCACATAGCGTAAAAGGAGC 3'</b>
Colony screening of pCR8/ pENTR5' vectors		M13 For (-20) <b>5' GTAAAACGACGGCCAGT 3'</b> M13 Rev <b>5' AACAGCTATGACCATG 3'</b>

## 7.10 Recombination of TOPO vector into final destination vector



## 7.11 293FT resurrection and culture





Illustration removed for copyright restrictions

## 7.12 Lenti-X GoStix



### 7.13 QuickTiter Lentivirus Titer test (Lentivirus-associated HIV p24)



## 7.14 A $\beta$ 1-42 ELISA





Illustration removed for copyright restrictions